

City Research Online

City St George's, University of London

Citation: Field, G. J. (1973). The elastohydrodynamic behaviour of rubber seals under conditions of reciprocating motion. (Unpublished Doctoral thesis, The City University)

This is the accepted version of the paper.

This version of the publication may differ from the final published version. To cite this item please consult the publisher's version.

Permanent repository link: https://openaccess.city.ac.uk/id/eprint/38367/

Copyright and Reuse: Copyright and Moral Rights remain with the author(s) and/or copyright holders. Copies of full items can be used for personal research or study, educational, or not-for-profit purposes without prior permission or charge, unless otherwise indicated, provided that the authors, title and full bibliographic details are credited, a hyperlink and/or URL is given for the original metadata page and the content is not changed in any way. For full details of reuse please refer to City Research Online policy.

City Research Online: http://openaccess.city.ac.uk/ publications@citystgeorges.ac.uk

The Elastohydrodynamic Behaviour of Rubber Seals under conditions of Reciprocating Motion

by George John Field

A thesis submitted for the
Degree of Doctor of Philosophy

Department of Mechanical Engineering,
The City University, London

August 1973

THE CITY UNIVERSITY LIBRARY,
ST. JOHN STREET, LONDON, E.C.1.

SUMMARY

The literature survey on reciprocating seals revealed a considerable lack of data relating to the film thickness of the lubricant film under such a seal and the work described is an attempt to remedy this. Significant progress towards this end has been achieved both experimentally and theoretically.

Two experimental approaches were used, the first using optical interferometry to study the film formation between a rubber pad specimen and a reciprocating glass plate, the second a reciprocating seal test rig on which the film thickness and pressure in the lubricant film could be measured under conditions typical of those experienced in a hydraulic jack.

The theoretical approach again took two forms. The first using the 'inverse' solution of Reynold's equation, did not provide a unique solution to the problem, but allowed a rapid estimate of the effect on the film profile of small changes in the pressure profile. By suitably modifying a measured film profile, film profiles typical of those measured could be obtained. In the second approach a stable solution was obtained for the elasticity and Reynold's equations. Variables such as rubber hardness, sealed pressure and speed were studied in this approach.

The results, which are presented in Imperial Units, show that in general the outstroke film thickness is thicker than the instroke and hence seals will inherently leak and the measured values of friction are considerably higher than expected from the measured film thickness profiles.

The elastohydrodynamic behaviour of reciprocating rubber seals is shown to be complex and dependent on many factors, many of which relate to the seal material itself, which cannot be directly controlled.

ACKNOWLEDGEMENTS

I would like to express my thanks to my many colleagues who have been directly or indirectly connected with the work of this thesis. I am grateful to the Director of Research, BHRA Fluid Engineering for the facilities provided by the Association, and also to Dr. B. S. Nau, my external supervisor for his advice, collaboration in the theoretical evaluations and suggestions for the experimental program. Thanks must also go to [redacted] for their practical assistance, moral support and encouragement, to [redacted] for many helpful discussions and advice on computing problems, to [redacted] and [redacted] for solutions to many problems of instrumentation and the workshop staff for the manufacture of various parts in the experimental apparatus.

Thanks must also go to [redacted], my internal supervisor for his advice and encouragement throughout the project.

My wife should also be thanked for her acceptance of many lonely evenings and her practical assistance in collating the manuscript.

The work was carried out with the financial support of [redacted] Ministry of Defence under contract number KS/1/0574/CB43AC and I wish to express my thanks for this and the continued interest and technical advice throughout the project of [redacted]

NOTATION

a_1	=	a constant, $6\zeta U$
a_2	=	a constant, $a_1 I_1(\ell) - (P_o - P_1) / I_2(\ell)$
a_{ij}	=	coefficients in eq. L7, Appendix L.
A	=	elasticity equation constant, $2(1+\nu)/b^2$
b'	=	axial length of rectangular section seal.
b	=	radial thickness of seal
b_1	=	axial distance along seal from atmospheric edge to point where $dp/dx = 0$
B	=	elasticity equation constant, Ab/E.
C	=	capacitance
d	=	finite difference mesh size, d_n is value on R. H. S. of node n.
dp/dx	=	pressure gradient along the seal contact.
D	=	diameter of shaft or bore of cylinder.
E	=	Young's modulus.
E'	=	effective modulus of rubber/disc contact, $2E/\nu^2$.
F	=	radial shear stress in the seal.
G'	=	rubber shear modulus
G	=	variable in the 'inverse' form of Reynold's equation, $h^{*2}/6\zeta U \times dp/dx$.
h	=	oil film thickness.
h*	=	oil film thickness where $dp/dx = 0$
H	=	variable in the 'inverse' form of Reynold's equation, h/h^*
$\overline{H}$	=	dimensionless film thickness, h/b
i	=	subscript, instroke.
i, j, k	=	indexing constants.
ℓ	=	axial length of seal.
L	=	total seal leakage.
L_1	=	a constant, $6\zeta U\ell R/(Eb^2)$
L_2	=	a constant, $\ell R a_2/(Eb^2)$
n, N	=	node labels
o	=	subscript, outstroke.
P	=	oil film pressure.

P_s, P_1 = system pressure

P_o, P_a = external or atmospheric pressure

P' = interference pressure

P_r = total radial load on seal.

P_d = hydrodynamic film pressure

P_{st} = hydrostatic film pressure

P^* = oil film pressure where $dp/dx = 0$.

$\overline{P}$ = dimensionless film pressure, $PA\ell^2/E$

q = seal leakage for unit circumference

Q = seal internal stress normal to the sliding face.

$\overline{Q}$ = dimensionless internal stress, $QA\ell^2/E$

Q_i = interference stress

Q_s = stress due to P_s transmitted through seal

r = P'/P_s

R = dimensionless constant, $A\ell^2$

R′ = radius of rubber surface

sf = specific friction, seal friction force / contact area.

S = net stress on the seal sliding face $S = Q - P$

S_1 = see figure 2.8, p. 23.

u = fluid velocity in x direction.

U = seal sliding speed.

w = load per unit width.

x = coordinate parallel to axis of seal, zero at high pressure end of seal.

X = dimensionless coordinate, x/ℓ.

y = coordinate normal to axis of seal.

Z = number of nodes.

ζ = fluid viscosity

λ = limiting value of convergence in Gauss-Seidel iteration.

μ = coefficient of friction.

ω = relaxation factor $\omega > 1$ for elasticity eq. and < 1 for the main iteration loop.

ϕ = angle between the assumed film profile and the shaft.

GLOSSARY

Back-up clearance (BUC):	radial clearance between piston and cylinder on the low pressure side of the seal.
Breakout friction:	the friction force required to initiate movement of the seal.
Couette flow:	the fluid flow through a clearance or a bearing caused by the relative motion of the two surfaces.
Groove fill:	the percentage volume of the seal groove occupied by the seal.
Instroke:	the reverse of the outstroke
IRHD:	International Rubber Hardness Degrees
I.S.P.:	interseal pressure.
Outstroke:	the stroke of a seal in which a point on the sliding metal surface, when passing the seal, moves from a high to a low pressure.
Piston seal:	the seal preventing leakage past the piston of a hydraulic jack. The dynamic sealing takes place on the outside diameter of the seal.
Poiseuille flow:	the flow through a clearance or bearing caused by a pressure gradient across the clearance or existing in the fluid.
Rod or gland seal:	the seal on the rod of a hydraulic jack preventing leakage to atmosphere. The dynamic sealing takes place on the inside diameter of the seal.
Stress relaxation:	the decrease with time of the stress in a rubber seal with the seal maintained at a constant strain.
Pumping stroke:	outstroke.
Motoring stroke:	instroke.

METRICATION (S.I. Units)

1. Speed

$1\ in/s = 5\ ft/min = 2.5 \times 10^{-2}\ m/s$

$20\ ft/min = 0.1\ m/s$

2. Pressure

$1\ lbf/in^2 = 6.89\ kN/m^2$

$15\ lbf/in^2 = 1\ bar = 10^5\ N/m^2$

$1000\ lbf/in^2 = 6.89\ MN/m^2$

3. Viscosity

$1\ reyn\ (lbfs/in^2 = 6.89\ kNs/m^2$

$10^{-6}\ reyn = 6.89 \times 10^{-3}\ Ns/m^2$

$1\ cPoise = 10^{-3}\ Ns/m^2$

4. Film thickness

$1\ microinch = 2.5 \times 10^{-2}$ micrometre (micron)

$40\ microinches = 1$ micrometre (micron)

5. Specific-friction, Young's Modulus, seal stress

$1\ lbf/in^2 = 6.89\ kN/m^2$

6. Linear measurements

$1\ in = 2.5 \times 10^{-2}\ m.$

$0.010\ in = 2.5 \times 10^{-4}\ m$

$= 0.25\ mm.$

CONTENTS

Summary		i
Acknowledgements		ii
Notation		iii
Glossary, metrication		v
Chapter 1	Introduction to Reciprocating Seals	1
Chapter 2	Literature Survey	5
2.1.	Introduction	6
2.2.	Work before 1950	8
2.3.	Literature between 1951 and 1960	17
2.4.	Literature between 1961 and 1963	21
2.5.	Literature of 1964/65	22
2.6.	Literature of 1966/67	29
2.7.	Literature of 1968/69	36
2.8.	Additional work at BHRA Fluid Engineering	51
2.9.	Discussion of reviews	54
2.9.1.	Seal leakage	55
2.9.2.	Seal friction	58
2.9.3.	Film thickness	61
2.10.	Conclusions	63
2.11.	Scope of the present work	64
2.12.	Methods of attaining the experimental aims of section 2.11.	65
Chapter 3	An Interferometric Study	66
3.1.	Design and development	67
3.1.1.	Introduction	67
3.1.2.	Use of white light fringes	68
3.1.3.	Conditions necessary to form interference fringes	69
3.1.4.	Specimen manufacture	73
3.1.5.	Optical systems	74
3.1.6.	Calibration of white light fringes	79
3.1.7.	Mechanical details of the rig	79
3.1.8.	Photographic techniques	84
3.2.	Results	87
3.2.1.	General observations	87
3.2.2.	Observations of static 'bubbles' in the contact area	88
3.2.3.	The propogation of disturbance in the film	89
3.2.4.	Transverse 'black' lines	94
3.2.5.	The effect of specimen edge	96
3.2.6.	A study of the residual film	99
3.2.7.	The effect of viscosity and speed on the film thickness and friction	100
3.2.8.	Stick-slip behaviour	109
3.2.9.	The effect of short stroke lengths	109
3.2.10.	Application of a pressure differential	117
3.2.11.	Ciné film	118
3.3.	Discussion	118

Chapter 4	Instrumented Seal Study	120
4.1.	Design and development of test rig	121
4.1.1.	Introduction	121
4.1.2.	General layout	121
4.1.3.	Pressure vessel design and transducer mountings	123
4.1.4.	Seal carrier and shaft	125
4.1.5.	Seals	125
4.1.6.	Fluid	127
4.1.7.	Controlled variables	127
4.1.8.	Dependent variables	129
4.1.9.	Recording and processing of results	133
4.1.10.	Details of experimental procedure	136
4.2.	Results	138
4.2.1.	Preliminary tests	138
4.2.2.	Film profiles	142
4.2.3.	Seal friction	156
4.2.4.	Seal leakage	162
4.2.5.	Circumferential film thickness variations	166
4.2.6.	Variations in film thickness and friction through the stroke	168
4.2.7.	The effect of fluid viscosity	172
4.2.8.	The effect of seal hardness	176
4.2.9.	The effect of seal interference	181
4.2.10.	The effect of back-up clearance	191
4.2.11.	The effect of seal edge profile	197
4.2.12.	Alternating sealed pressures	203
4.2.13.	Repeatability	204
4.3.	Discussion	205
Chapter 5	A Theoretical Approach	214
5.1.	Introduction	215
5.1.1.	The 'inverse' form of Reynold's equation	215
5.1.2.	Solution of the EHL problem	217
5.1.3.	The stress balance in the seal	217
5.1.4.	Seal types	219
5.2.	Derivation of seal profiles using the 'inverse' form of Reynold's equation	220
5.2.1.	Derivation of the outstroke film profile	223
5.2.2.	Derivation of the instroke film profile	231
5.3.	An elastohydrodynamic approach	237
5.3.1.	Mathematical formulation of the problem	238
5.3.2.	Numerical solution	239
5.3.3.	Results	247
5.4.	Discussion	257
Chapter 6	Discussion	262
Chapter 7	Conclusions	270
Chapter 8	Future requirements	274

References		277
Appendices		281
A	Escape of Liquid from a Trapped Bubble via a Thin Film	282
B	Absorption Equation for a Trapped Liquid Bubble	283
C	Speed of Propagation of Disturbances	284
D	Physical Properties of Seal Materials	285
E	Capacitance Method of Film Thickness Measurement	286
F	Error Analysis of Film Thickness Measurement	293
G	Pressurised Rayleigh Step Bearing Analogy	296
H	Specific Friction of an Annulus having Relative Motion of the two Surfaces and Subject to a Pressure Differential	302
I	Derivation of 'Inverse' Form of Reynold's Lubrication Equation	304
J	Derivation of the Lubrication Equation	306
K	Derivation of the Elasticity Equation	308
L	Variable Mesh Finite Difference Formulation of the Elasticity Equation	310
M	Input Data used for Program Development	312
N	Flow Chart and Notation for "EHD Mk II" Program	313
Published Papers		315

CHAPTER 1

INTRODUCTION - RUBBER SEALS FOR RECIPROCATING MOTION

A seal is a machine element devised to separate two fluids. The seal may be static as in the case of gaskets or dynamic for use on rotating or reciprocating shafts. The dynamic seal forms the most difficult sealing problem due to the two conflicting requirements of any such seal.

1. the leakage, from the sealed medium to the atmosphere over many hours of operation, should be zero

2. the friction of the seal should be zero.

Zero leakage is not attainable and small leakages are generally acceptable. The achievement of this entails that the two surfaces forming the seal should be in intimate contact throughout their life.

As for leakage, zero friction is unattainable and some friction must be accepted but this should be as low as possible as many seals, in a large process plant for instance, could result in considerable loss of energy. High values of friction will also result in execessive heating of the seal elements and housing necessitating additional cooling facilities. The achievement of low friction values depends on providing either materials with a low coefficient of friction or a complete hydrodynamic film between the two moving surfaces.

The two conditions of low leakage and low friction conflict and the present 'art' of seal design which applies to all types of dynamic seal is to balance leakage against friction to provide an acceptable compromise.

The moulded elastomeric sealing ring used for reciprocating duties owes its existence to two factors, the development of synthetic elastomers resistant to mineral oils and the use of hydraulic power in aircraft control systems, earth moving and many other industries.

In view of this vast upsurge in the use of elastomer seals for hydraulic machinery, it is surprising that the actual sealing mechanism is so little understood. Throughout the years much research and development work has been applied to the problem of seals and many different designs and types have been proposed in which various elastomers and plastics moulded to various geometries have been used. These designs have been developed with specific applications in mind, and rely on previous experience and empirical relationships based on measurements of friction and leakage only, and hence without any precise knowledge of the

fundamental processes which control the leakage, friction and wear of the seals.

These methods have led to success in many cases but it is still impossible to formulate suitable seal designs, on a sound basis, even if the specific requirements of the seal are known, and the cost of seal failure through poor design can be high.

Some typical examples of this can be found in reference 17 in which two users of seals, one the R.A.F. and the other British European Airways (B.E.A.), report on the cost and problems of seal failures. The R.A.F. reports that seal defects on four types of aircraft during 1965 totalled 94 cases and extrapolation to the whole fleet of the R.A.F. amounts to 378 cases per year, where these range from serious defects to complete system failure. B.E.A. show that in a fleet of 20 aircraft of one type, seal failures cost £27,000 per year and an examination of the records shows that 35% of all unscheduled removals of hydraulic components are due to seal failures, this being typical of that found in many industries.

However, the experience of seal manufacturers and BHRA Fluid Engineering shows that many failures may not be due solely to faulty seal design, as it is commonly found that the design of equipment is finalised before sufficient or, in some cases, any attention has been paid to the most important aspect of the design the problems of sealing. Other seal failures can be due to wrong assembly or damage to the seal during storage or installation.

The temperature and pressure requirements of supersonic aircraft and space vehicles currently being developed are stretching the available seal designs and materials to the limit, and although new materials obviously help to meet the increasingly stringent requirements, a better understanding of the sealing mechanism would enable designs to proceed with confidence and optimal designs to be arrived at.

This present lack of understanding is due to the fact that the mathematics and mechanics of the sealing problem are complex and are further complicated by the unpredictable behaviour of the elastomer from which the seals are made.

This material, when compared to metals, has a very low value of

Young's modulus and deflections upto 300% can be achieved under low stress, the Poisson ratio is almost 0.5 and hence the material transmits pressure as would a fluid. The general properties change with age, exposure to weather, ozone and radiation and the material swells when immersed in the sealed fluid giving a reduction in hardness. Being of a viscoelastic nature it suffers from permanent set, in that when released from a given strain it never fully recovers to its original shape. Conversely when under a given strain, the stress in the material gradually reduces with time (stress relaxation) and hence from the seal point of view, the sealing ability reduces with time. Unfortunately it possesses a high coefficient of friction when sliding in the dry condition over almost any other material and has a low thermal conductivity leading to poor dissipation of the heat created by the high friction.

It can be seen therefore that the mathematical problem of calculating the film thickness during the elastohydrodynamic lubrication of rubber seals for reciprocating motion is complicated by the non-linear and time dependent properties of the material itself.

But in spite of these disadvantages rubber will continue to be used for seals for many years because of its one great advantage, its elasticity, which allows deformation and perfect sealing to be achieved under very low contact stresses.

CHAPTER 2

A SURVEY OF LITERATURE

2.1. INTRODUCTION

The literature associated with reciprocating seals for hydraulic applications dates mainly from the work of White and Denny (53) published in 1947. The upsurge in hydraulic machinery using such seals depended on the development of synthetic elastomers capable of resisting mineral oils and these were first formed just prior to World War II. Original work was done to develop various seal geometries which would provide satisfactory operation over the relatively low pressures provided by the hydraulic pumps available. The work of White and Denny is an early attempt in a line of continued experimental development of reciprocating seals to cope with the ever increasing temperatures and pressures.

The urgent need for seals to operate satisfactorily with these environmental conditions led to experimental rather than theoretical development as the need for practical seals outstripped the necessary theoretical knowledge of the sealing action. This is shown fairly conclusively in the literature in which approximately 80% is devoted to experimental work. The experimental work, therefore, was devoted to measurements solely of leakage, friction and wear, these being the most important variables in relation to the working life of the seals. The lubrication process itself was obviously of interest, and this is clear from the attempts of White and Denny to estimate the film thickness of seals, and their development of a simple theory based on their assumed film profile, however, due to the technical difficulties of measuring the film thickness of working seals and the need for rapid development of acceptable seals, attempts to measure film thickness were not of the greatest importance.

However, current aircraft and space projects are calling for seals to operate beyond even the best currently available seals and materials and a better understanding of the seal problem has become necessary. This is shown in the upsurge of the number of papers on reciprocating seals presented at the international conferences organised by BHRA Fluid Engineering. It is a fact also that many articles written for the popular engineering press are simply abstractions from manufacturers catalogues and as such are just indicating the lack of knowledge that the manufacturers themselves have of the sealing process.

The literature survey presented here covers the majority of relevant papers and articles that have appeared since the publication of the work of White and Denny(53).

A great deal of experimental work on reciprocating seals has been conducted on 'O' rings although this section of ring is very rarely used in a reciprocating mode apart from some low pressure applications in the pneumatic field. At the end of the World War II, pressures in hydraulic equipment rarely exceeded 1000 lbf /in^2 and since the sealing mechanism was not wholly understood, 'O' rings were considered to be sufficient. However, as pressure increased, new types of seal such as T seals, D seals, and composite seals were developed to cope with higher pressures. The ring of rectangular cross section has been used by the aircraft industry for many years, but the published literature on these appears to be confined to reports published by BHRA Fluid Engineering. No doubt many commercial firms have records of a great deal of work, particularly experimental, but unfortunately the majority of this is unavailable.

Recently the interest in the reciprocating 'O' ring has been due to the development of elastohydrodynamic lubrication theory, which is a modified form of the theory of hydrodynamic lubrication first formulated by Reynolds(46) in 1886 which assumes that the solid boundaries of the lubricant film do not deform. The successful operation of heavily loaded contacts such as those occurring in gear teeth, could not be predicted from the Reynolds theory and the assumption of rigid boundaries had to be removed. The first successful solution to the elastohydrodynamic problem relied on a shape of contact which could be formed easily during experiments and which was also amenable to theoretical evaluation, and was of circular or parabolic form. An equation of the form suggested by Timoshenko and Goodier (52) can be used in conjunction with Hertz's analysis of solid bodies in contact to determine the deflection of the boundaries of the fluid film. For hard materials such as steel pressures in the fluid film are high enough to affect the viscosity of the fluid and this too, is usually taken into account.

With the added possibility of using EHL theory to determine the film thickness profiles, experiments again turned to the circular section used in the theory, which was represented in seals research by the simple 'O' ring in a reciprocating mode. Several recent attempts have been made to measure film thickness and pressure profiles under 'O' rings and correlate the results with theoretical work. However, much of the theory is invalidated by an assumption basic to the theory of elasticity, that the deflections are small relative to the dimensions of the body in question. This is true for the theory when applied to metals, but is not true when applied to rubbers in which strains of 50% in compression and 300% in tension are perfectly feasible.

2.2. WORK BEFORE 1950

White and Denny (53)

One of the earliest and most comprehensive references to many types of hydraulic seal was that of White and Denny (53). The work reported was conducted in the period 1944-1946, when very little was understood of the sealing mechansim. A number of test rigs and methods were used to elucidate various phenomena including the leakage and frictional behaviour of seals, the distortion of various types of seal under pressure, the extrusion of the seal, the interference pressure and the film thickness to be expected, where the latter was estimated from experiments in which a simulated seal on a rotating glass disc was used.

Determination of strain and extrusion

One of the earliest objectives of this work was to determine the distortion under pressure of rectangular section rings and this was achieved in two ways. In the first method an enlarged cross-section of a seal was clamped between glass plates, and when pressurised the seal section effectively had a pressure differential across it and deformed to a shape typical of that of rectangular section rings, that is the face seeing the pressure formed only a slight curve whilst the portion adjacent to the back-up clearance was extruded into the clearance (figure 2.1). In the second method however, a glass cylinder was used to enable the strains in the contacting surface to be evaluated, these being determined from the measured displacement after pressurising of lines marked onto the

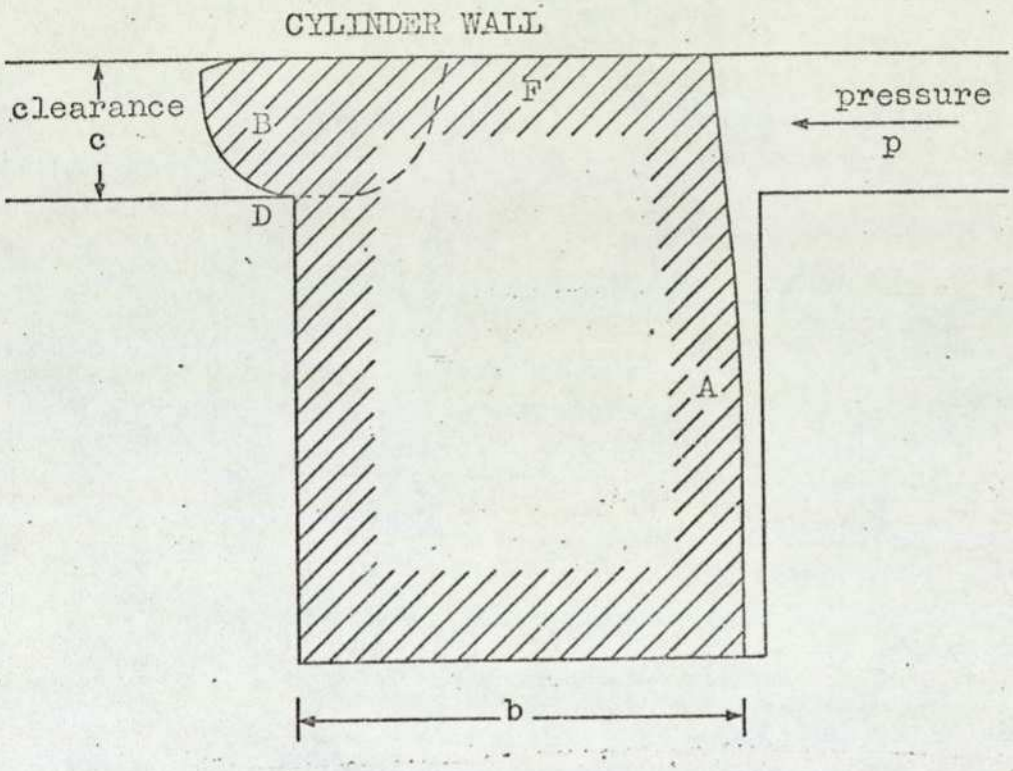


Fig. 2.1 The effect of pressure on a square section seal (White and Denny, ref. 53, fig. 17)

seal before assembly. Results showed that although the strain at the pressure side of the seal was fairly small, at the extruded portion it exceeded 55% in some cases. Because a glass cylinder was used the pressures were fairly low and in order to get an idea of the amount of extrusion occurring at higher pressures, a different method was used and it was shown that the extrusion appeared to extend for up to six times the extrusion clearance, thus showing the severe condition a seal must withstand. An interesting point here is that the ratio did not change for clearances down to 0.005 inches and this behaviour must, therefore, be expected to occur for clearances less than this. This means that although the back-up clearance can be reduced to a minimum the strains in the seal will still be the same although concentrated in a smaller volume and seal damage is therefore just as likely to occur.

The interference pressure between the seal and the cylinder is also of importance and a method was devised to measure this in a static condition. A typical profile of the interference pressure is shown in figure 2.2 where it is apparent that severe extrusion has occurred, and it is interesting to note that the interference force exerted on the wall of the cylinder extends almost a third of the way along the extruded portion of the seal. The shape of the extruded portion in this figure is purely speculative for although the extent of the extrusion had been measured, the actual shape was not. For the case of simple extrusion where the ratio of the extrusion/clearance is around unity the true shape for a square seal edge is as shown in figure 2.3. The work of Field and Nau (19), (20) and (21) indicates that the shape of the extruded portion of a seal is important as regards the formation of a film on the instroke of the seal.

Seal friction

White and Denny (53) found in many tests that the friction force was directly proportional to pressure, the force increasing with increasing pressure, but that the absolute value and the rate of increase with pressure depended to a great extent on the material of the seal, the fluids and the cylinder surface finishes. Coefficients of friction for seals are of somewhat doubtful value since the true normal load is generally

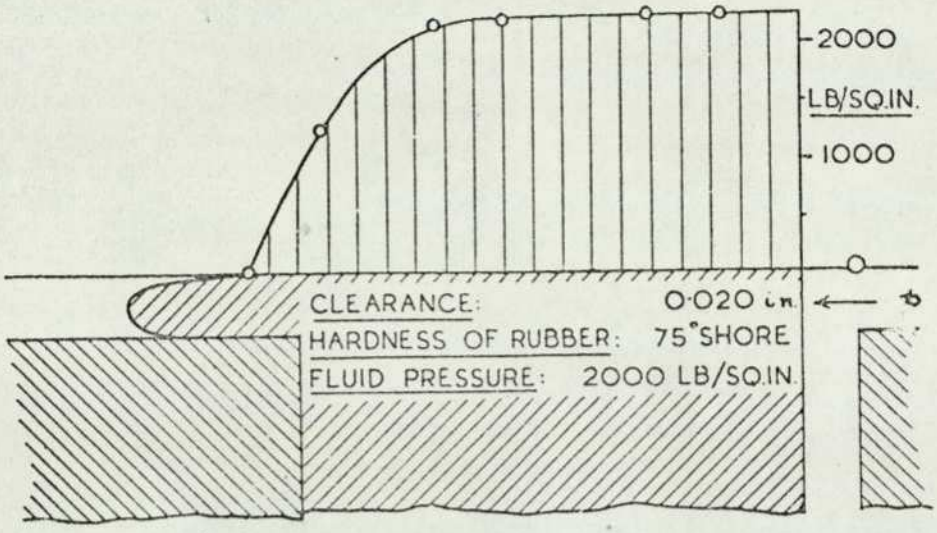
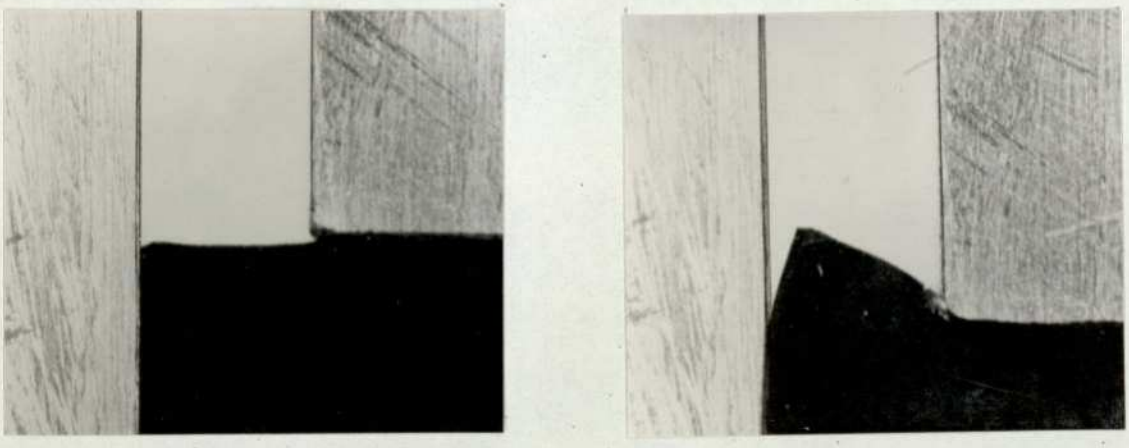


Fig. 2. 2 The contact pressure across the working face of a square section seal (White and Denny, ref. 53, fig. 34)



Unpressurised Pressurised

Fig. 2. 3 The extrusion profile of a square section seal (Field and Nau, ref. 19, fig. 12)

unknown. The radial stress is a combination of two stresses, the pressure and the initial interference stress. A number of interference stresses were measured and appeared to correlate fairly well with the equation:

$$\text{interference stress} = \frac{E \cdot \Delta b}{b} \qquad (2.1)$$

A value of Young's Modulus for rubbers is difficult to determine as it depends to a great extent on the previous life of the elastomer and attempts by Nau (38) to measure the modulus by various methods indicated that a wide range of values could be obtained for one material. However, apparent values were taken by White and Denny and a coefficient of friction was calculated as follows:

$$\mu = \frac{\text{friction force of one ring}}{\text{contact area} \times (P_s + P')} \qquad (2.2)$$

The interference stress, P', calculated by means of Hookes Law is low, because the value of Young's Modulus for rubbers is low, and in view of the indeterminate nature of the latter variable, sufficient accuracy in calculating the coefficient of friction can be achieved simply by dividing the specific friction, defined as the seal friction force per unit contact area, by the sealed pressure. The absolute values of the coefficients were sufficiently low to indicate the existence of a hydrodynamic film, even at pressure up to 3000 lbf/in^2. A criticism of White and Denny (53) and other workers is that the nature of the rig used resulted in the friction of two seals being measured, one seal on an instroke, the other on an outstroke and thus only a mean friction was recorded. Furthermore, the rig only allowed friction to be measured on one stroke of the piston. However, the important point here is that the results indicated that even rectangular section rings appeared to operate under both hydrodynamic and boundary lubrication conditions rather than by dry contact, specific friction values being of the order of 20-60lbf/in^2 for all fluids, figure 2.4 shows typical values of friction against pressure for various fluids.

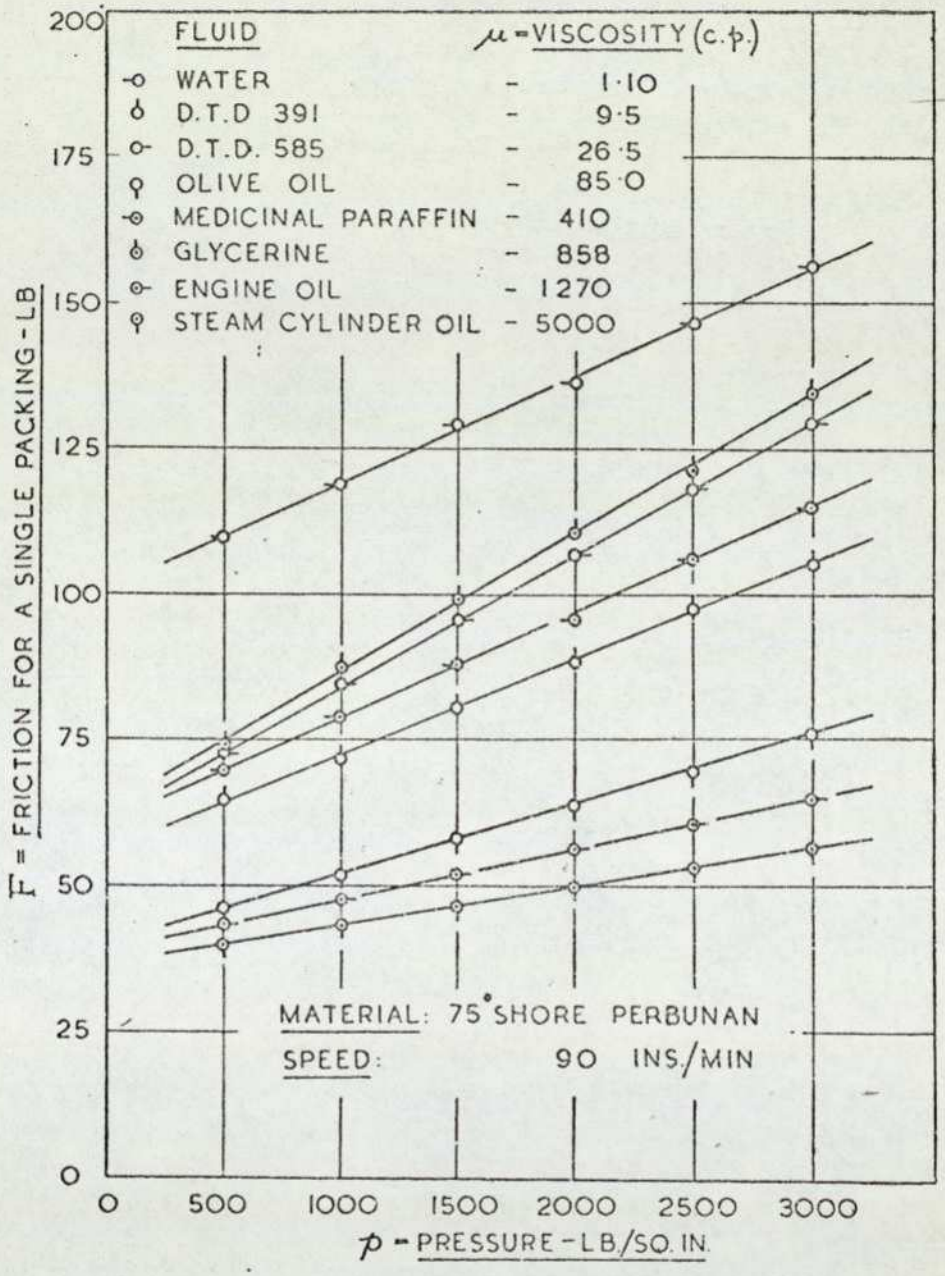


Fig. 2.4 The effect on the friction of a seal of the working fluid. (White and Denny, ref. 53, fig. 53)

A number of tests using various fluids including a very viscous steam cylinder oil gave friction values which decreased with an initial increase in speed but increased steadily from a minimum value as the speed continued to rise, as would be expected with complete hydrodynamic lubrication. The general form is given in figure 2.5. An interesting point is that in some of these tests, although the friction indicated that the lubrication was hydrodynamic, the leakage was essentially zero. This condition would not be impossible for a seal under constant pressure since the instroke and the outstroke film thicknesses could be the same.

Film thickness measurements

By using an enlarged model seal and collecting the leakage that passed it, calculations were made of the film thickness, and these agreed well with a theoretical equation for film thickness derived from Reynold's equation, by assuming a double tapered film profile and a parabolic pressure profile over the seal contact area. The form of the equation was as follows:

$$h = \frac{Ub'}{P_s (16.2 + 38\ r.)} \qquad (2.3)$$

Several tests were conducted to determine the film thickness at which the change from hydrodynamic to boundary lubrication occurred and indicated that this was of the order of 200 micro inches, a value which appears to be high in view of the fact that the rubber pads were run against a glass plate which would have had a very smooth surface of less than 1 micro inch CLA.

'O' Rings

Several experiments were conducted with reciprocating 'O' rings and it was shown that provided the contact area could be determined the friction force appeared to be of the same order as that of the rectangular section packings.

Cheyney, Mueller and Duval (7)

The authors conducted numerous tests on 'O' rings to determine typical friction values and to evaluate the effect of various parameters on the friction. The speeds were generally low being below 25 ft/min. while the pressures were up to 1500 lbf/in^2. An interesting point is

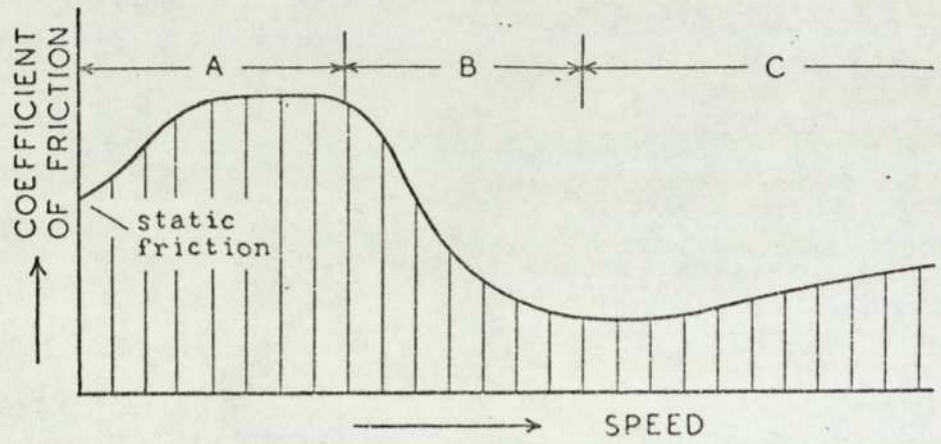


Fig. 2.5 General curve of the coefficient friction against speed. (White and Denny, ref. 53, fig. 55)

that this work measured the friction of a single seal. This was achieved by using a close fitting bush at one end of the housing and supplying sufficient fluid to allow for the leakage past the bush. This represents an improvement on the method of White and Denny (53) since it admits the possibility that friction values for the instrokes and the outstrokes may be different. In the authors' comments more information is supplied on the friction of each stroke. The pressure on the test seal was always applied and the friction recorded was that of an instroke everytime. The outstroke friction was not recorded, as a severe stick-slip phenomenon was encountered and this was thought to be 'unworthy of analysis'. This was a great pity as the stick-slip phenomena has been experimentally evaluated to some extent, in a seal situation, by Nau (39) and shown to be a function of temperature (or viscosity) and speed. A change of either of these might have caused smooth operation and provided an insight into the lubrication process of the 'O' rings.

The instroke friction would normally be expected to be higher than the outstroke friction since the atmospheric side of the rod seal would not normally be flooded with oil and boundary friction in this case would be more likely to occur. This appears to be confirmed by the results which indicate that friction was nominally constant throughout the speed range although the graphs show the friction force extrapolated to zero at zero speed.

Other tests showed that the "squeeze" or interference had no effect on the dynamic friction, but the breakout friction increased with increased interference. The authors do not state precisely when or how the friction values were recorded and this would be particularly important in the case of the breakout friction, which would depend to a great extent on the time spent at rest. These results indicated scatter of $\pm$ 30% in the breakout friction.

Friction is shown to be related linearly with the pressure,friction increasing with increased pressure, as was found by White and Denny (53) although the specific friction values were slightly lower. The data shown also indicates considerable scatter in the dynamic friction. In some cases this reached +100%, - 50% of the mean friction. The final variable

tested, was that of surface finish which was varied between 2 micro-inches CLA and 30 micro-inches CLA and showed that friction increased with the rougher surfaces as would be expected for a seal operating under boundary conditions.

2.3. LITERATURE BETWEEN 1951 and 1960

There appears to be very little work relating to reciprocating seals published between 1951 and 1960. Two reports were the results of further experimental work by Denny (10 and 11), and a third a theoretical analysis of the lubrication of reciprocating seals by Nau and Turnbull (41).

Denny (10 and 11)

References 10 and 11 deal with leakage and friction characteristics of various types of U and V seals reference (10) giving experimental data for 15 different types of single ring seals. The characteristics of each were similar but the actual values recorded varied considerably. The friction did not appear to depend on the shaft speed which is consistent with the findings of Cheyney, Mueller and Duval (7) in their experiments with 'O' rings, and suggests that the mode of lubrication was the same in both cases. This is again suggested in the results of the pressure on friction where Denny (10) found that the friction was directly proportional to the pressure that is $F = F_o + \alpha P_s$ where F_o is the friction force at zero pressure and is entirely due to the initial interference force, and α is a constant.

Leakage was found to increase with pressure up to 1000 lbf/in^2 but thereafter remained fairly constant up to 4000 lbf/in^2, the highest pressure tested. An interesting point is that the leakage could be controlled by alternating the sealed pressure between zero and system pressure and indicated that in fact negative leakage is possible in some cases as shown in figure 2.6.

An extension of the above work is reported by Denny (11) in which multiples of U and V rings were used in place of the single rings. In general the results were similar to those given in reference 10 in that leakage still increased linearly with pressure up to 1000 lbf/in^2 above which the leakage remained constant. A very important point mentioned

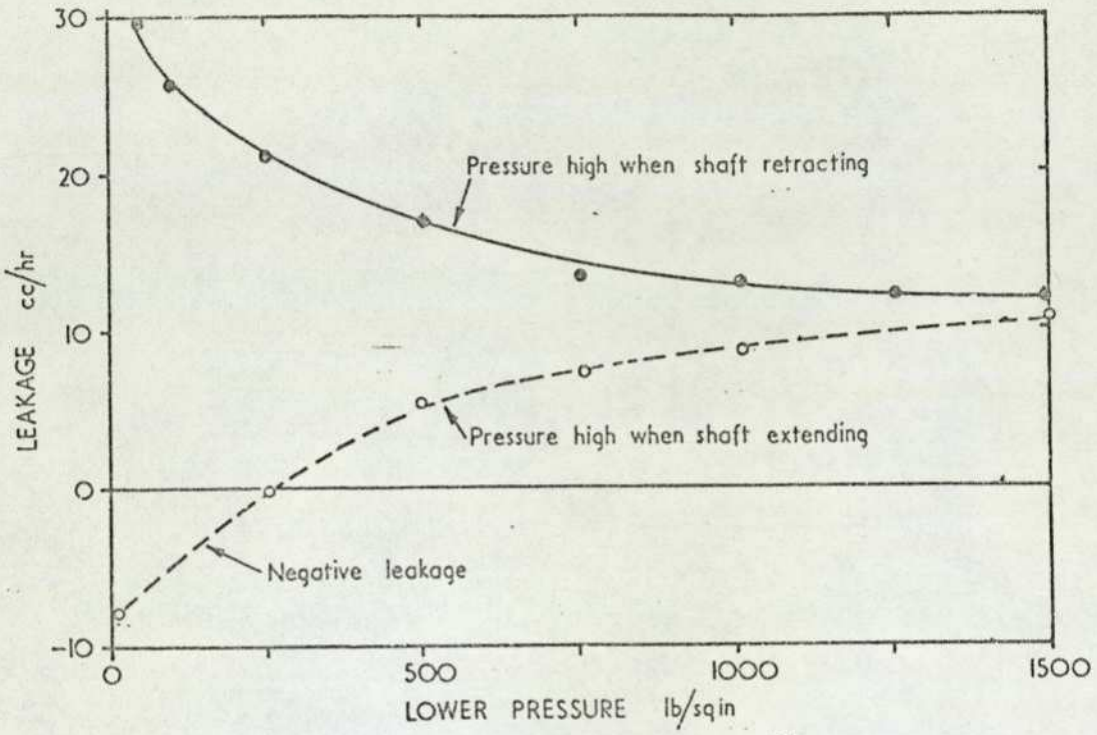


Fig. 2. 6 The effect on seal leakage of an alternating system pressure. (Denny, ref. 10, fig. 12a)

in this report concerns the relationship between leakage and speed. It was shown experimentally that leakage increased as the square of the speed that is $q \propto U^2$, the result being obtained with a constant system pressure.

As mentioned in reference 10 the leakage could be drastically increased by operating the seal in the mode normally found on rod glands of jacks, that is a low sealed pressure on an outstroke and a high sealed pressure on the instroke. The explanation given by Denny is that the observed leakage depends on the difference between the film thickness on the outstroke and the film thickness on the instroke. During the outstroke the pressure is low and hence a thick film of oil is taken out on the rod, figure 2.7. The reverse is true on the instroke and not all the oil taken out is returned. The difference is termed leakage. By reversing the phase of the pressure that is high pressure for the outstroke and vice versa, negative leakage could be obtained.

Nau and Turnbull (41)

In 1960 Nau and Turnbull (41) published a simplified analysis of the lubrication characteristics of reciprocating seals. Unlike White and Denny (53) they did not assume any particular film profile. Rather, they assumed a seal deflection proportional to the film pressure, neglecting shear stress in the seal material. The material was assumed to deflect according to Hooke's Law and thus

$$h = \frac{Pb}{E} \qquad (2.4)$$

Using this and Reynold's equation the author managed to obtain a non-dimensional equation for the leakage of a square section seal, which appeared to correlate well with experiments in that leakage was proportional to viscosity and speed squared. However, a major fault in the theory is apparent and concerns the use of Hooke's Law as stated. The seal material here, an elastomer, has a Poisson ratio of 0.5 and hence transmits the sealed pressure on a fluid. Therefore, the available pressure at any point through the seal contact to deflect the seal would be the film pressure minus the seal contact stress. This includes shear stress in the material. The equation:

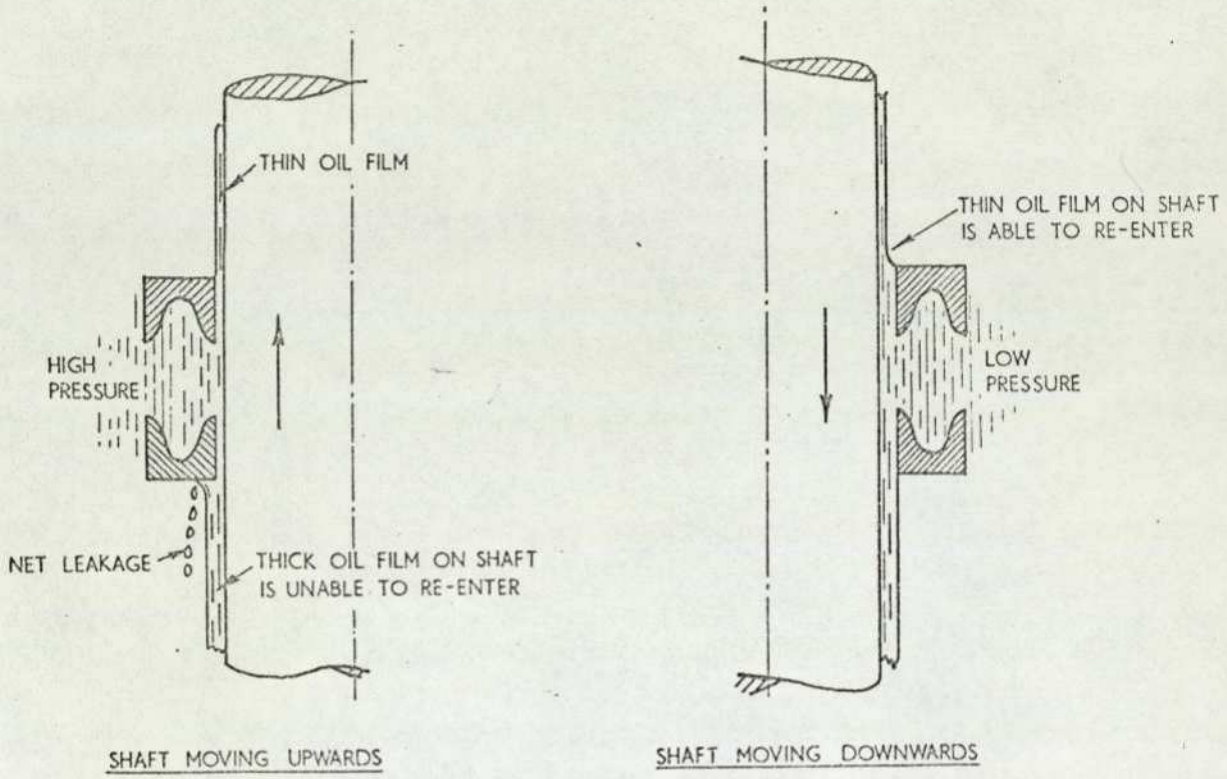


Fig. 2.7 Mechanism of seal leakage: lower seal leaks, upper seal does not. (Denny, ref. 10, fig. 15)

$$h = \frac{(P - Q)b}{E} \qquad (2.5)$$

gives a much better estimate of the seal deflection provided that the values of P and Q are known throughout the contact between the seal and sliding surface. In general though this is not so.

2.4. LITERATURE BETWEEN 1961-1963

Iwanami and Tikamori (28)

In 1961, BHRA organised the First International Conference on Fluid Sealing and whilst many papers were presented only one by Iwanami and Tikamori (28) related directly to reciprocating seals. They presented some results of a simple theoretical analysis and experimental leakage values for the reciprocating 'O' ring. Their experimental apparatus was similar to that used by other workers consisting of a pressure vessel containing the two test seals through which a rod was reciprocated with a sinusoidal motion by means of crank arrangement. By assuming a linearly tapered wedge they obtained a theoretical solution for the leakage which showed that: $q \propto \zeta U^2$, but found experimentally that the relationship was of the form $q \propto \zeta^{1.5} U^2$. The discrepancy in the exponent of viscosity ζ, was said to be due to the viscosity of oil increasing with pressure whereas their theoretical assessment assumed a constant viscosity. The maximum pressure used in the experimental work was 1500 lbf/in^2 and if the change of viscosity with pressure is taken into account it would have increased approximately 20%*. Whilst this may have

* From Dowson and Higginson 'The fundamentals of roller gear lubrication, elastohydrodynamic lubrication' p 143 the change of viscosity with pressure can be written: $\zeta = \zeta_o e^{\alpha p}$ where ζ_o = viscosity at atmospheric pressure α is an experimentally determined constant, the value of which for oils is approximately 2.5×10^{-9} cm^2/dyne.

for 1000 lbf/in^2 $\zeta = \zeta_o \times e^{2.5 \times 10^{-9} \times 6.8 \times 10^7} = \zeta_o e^{.17}$

$= \zeta_o \times 1.185$

i.e. an 18.5% increase in viscosity.

affected the empirical equation for tests conducted at the maximum pressure, it would have been unlikely to affect results at much lower pressures, and therefore the exponent of viscosity should be a function of pressure, being 1 at zero pressure and increasing to 1.5 at 1500lbf/in^2. This fact has not been reported by other workers, but due to the low pressures seals are used for the change of viscosity with pressure has been ignored. It could, however, be significant bearing in mind the 20% increase in the viscosity and the soft nature of the seal material.

The authors also present data giving the influence of pressure on the leakage and as mentioned by other workers leakage appears to increase with pressure but begins to level off as the pressure nears 1500 lbf/in^2.

As the maximum speeds during the tests were quite high that is around 100 ft/min it can be assumed that the seals were lubricated hydrodynamically. The authors results show that the leakage increases as the hardness of the elastomer used decreases, it is interesting to speculate whether the increased leakage was the result of an increase in the mean film thickness or due simply to an increase in the difference in the film thicknesses obtained for the outstroke and the instroke.

2.5. LITERATURE 1964/65

In 1964 the Second International Conference on Fluid Sealing was organised by BHRA Fluid Engineering, and whilst the majority of papers were still concerned with rotating seals, there was a significant increase of interest in reciprocating seals.

Müller (34), (35)

Müller's theoretical work appears to be based to some extent on that of White and Denny (53) in that Reynold's equation has been applied to a form of double wedge film profile. White and Denny, by extending the film profile, in a straight line, down to the axis, figure 2.8 obtained h in terms of b_1,ϕ and S_1 . Substituting this into Reynold's equation enabled a direct integration to be carried out to obtain the pressure profile. Müller modified this approach by not assuming that the change in slope occurred where the pressure gradient was zero and thereby eliminated one unknown from the equation of White and Denny, but

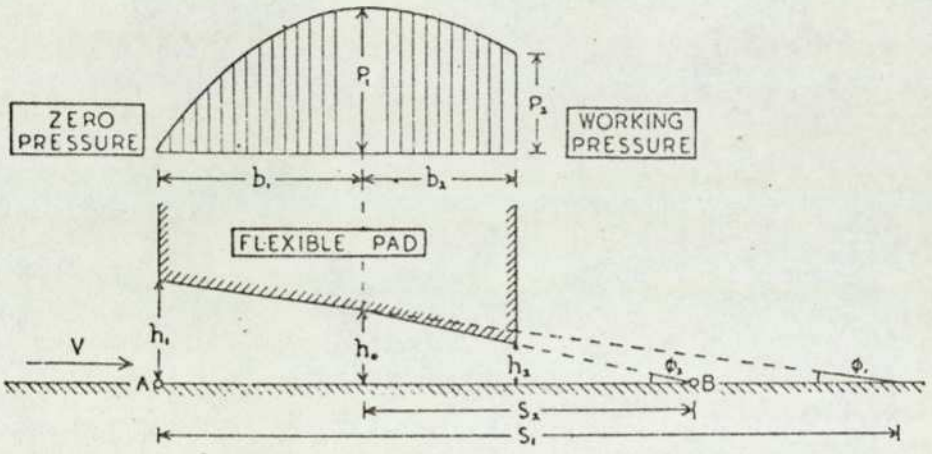


Fig. 2.8 Assumed film and pressure profile for the theoretical evaluation. (White and Denny, ref. 53 appendix II)

introduced another one, ℓ, the distance along the seal where the pressure in the film equalled the system pressure, figure 2.9. Müllers equation for film thickness was thus:

$$h^* = \left(\frac{\zeta U \ell}{(P^* - P_s)}\right)^{0.5} \propto \qquad \text{where } \propto = f(a, \ell) \tag{2.6}$$

Because h^* is the film thickness where the pressure gradient is zero the leakage can be calculated as follows:

$$q = \frac{\pi D U h^*}{2} \tag{2.7}$$

substituting for h^* we have:

$$q = \frac{\pi}{2} \propto D U \left(\frac{\zeta U \ell}{(P^* - P_s)}\right)^{0.5} \tag{2.8}$$

applicable for the instrokes and the outstrokes.

The above equation relates to the leakage for each stroke, but the net leakage is defined as the outstroke minus the instroke leakage, thus

$$q_{net} = q_{out} - q_{in} \tag{2.9}$$

Müller shows that the net leakage, q_{net}, can be shown to be related in the following way to viscosity and speed:

$$q_{net} \propto \left(\frac{\zeta U \ell}{P^* - P_s}\right)^{0.5}$$

Thus, $$q_{net} \propto (\zeta U)^{0.5}$$

The experimental leakage results, shown in figure 2.10 confirm his theoretical results and indicate that operation of the seals was in the hydrodynamic regime. Müller goes on to develop equations for the instroke and outstroke frictions of a seal using the above equation for h^* and these also contain the term $(\zeta U)^{0.5}$.

Müller's experimental work included measuring the friction of a single seal for both the instroke and the outstroke, by using a loading device which measured the friction force plus the end load on the rod due to the sealed pressure, the latter being assumed to be constant for

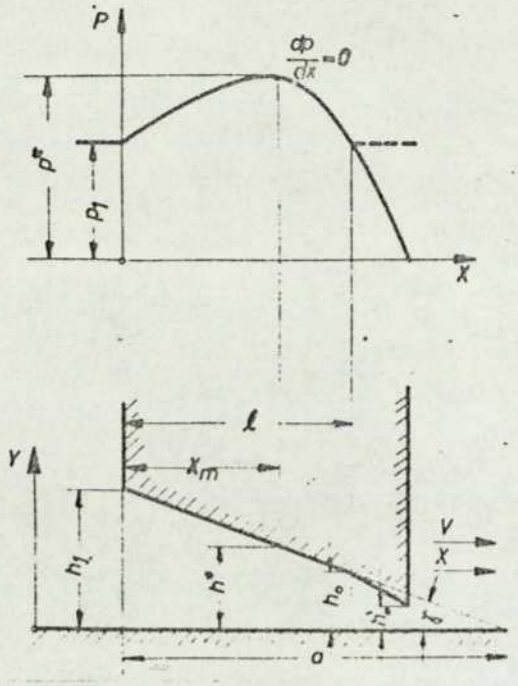


Fig. 2.9 Assumed film and pressure profile for the theoretical evaluation, (Müller, ref. 34, fig. 2)

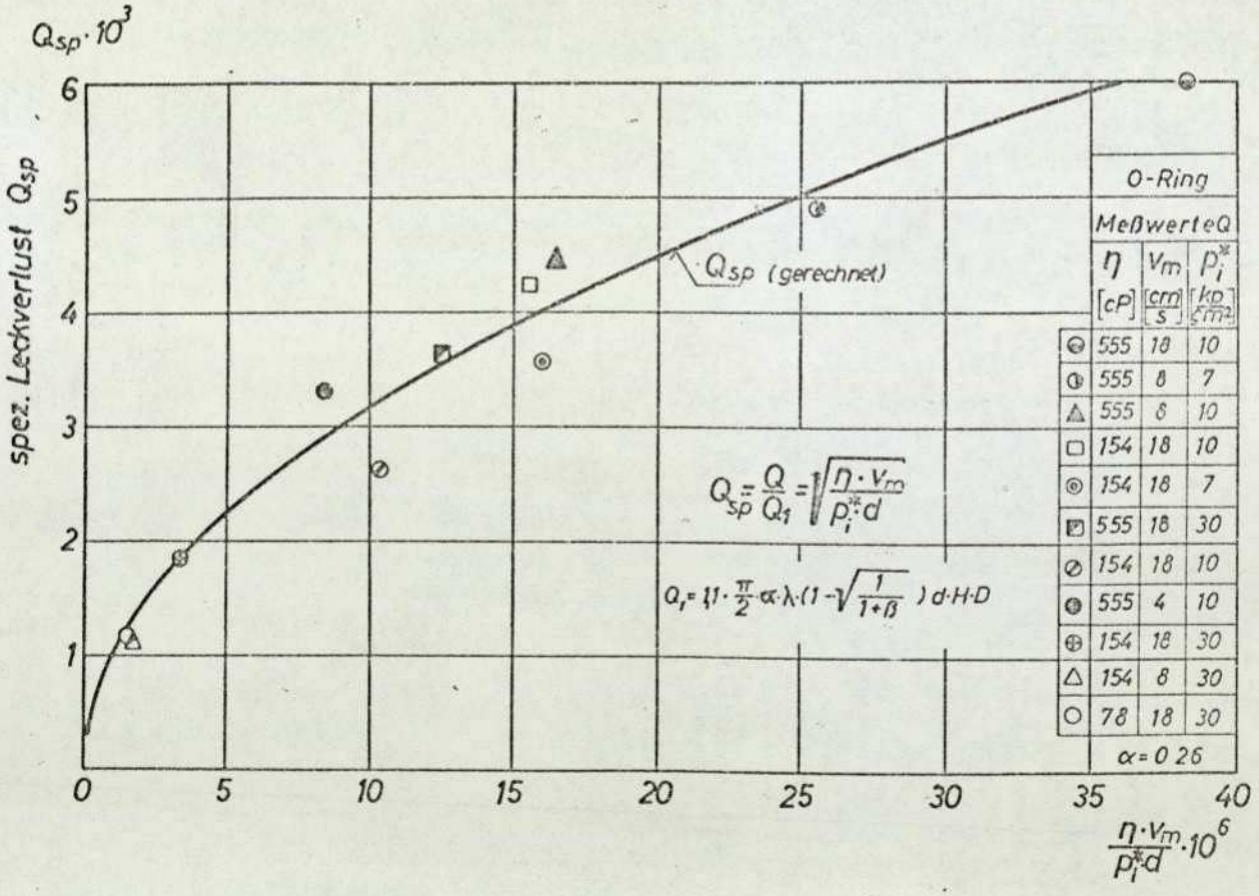


Fig. 2.10 Relationship between leakage and a characteristic factor. (Müller, ref. 35, fig. 36)

both strokes. The friction values are therefore the difference of two relatively large values and this is likely to lead to inaccuracies. The system pressure may also have changed due to the rod reducing the volume available to the sealed oil. However, this may have been controlled. Müller gives a friction trace obtained from this rig and the main details are shown in figure 2.11. The different friction force on each stroke can clearly be seen, there being a low friction for the outstroke in which sufficient oil is available to form a hydrodynamic film, but the return or instroke shows much higher values indicating a change at point (2) to boundary lubrication in spite of the fact that these are 'O' and quad rings being tested, in which a good entry profile on the seal exists for the instroke. However, examination of the rig used by Müller shows that the test rod was vertical with the sealed oil above the seal and therefore it is possible that oil which leaked on the outstroke, drained away from the seal causing a deficiency of oil for the return stroke. If the sealed oil had been below the seal the outside of the seal may well have been flooded and the friction values would then have shown a different result. Pressure distributions under 'O' rings and quad rings were achieved in a similar manner to that of White and Denny (53) by supplying pressurised oil to a small slot under the sealing area of the seal. By gradually increasing the pressure, the interference pressure could be detected at the point where the seal lifted off the surface and leakage became apparent. By traversing the slot across the seal the pressure distribution under the seal could be plotted. Obviously this method only allows static measurement of the pressure distribution, but in view of the very small pressure required to form a film (about 1 lbf/in^2), the static pressure would be very close to the pressure distribution measured under dynamic conditions. Some variation in the pressure distribution under dynamic conditions may arise due to the fact that the friction force produces a shearing stress at the rubber surface, though this would probably be very low.

Kambayashi and Ishiwata (29)

Kambayashi and Ishiwata presented some experimental data on reciprocating lip seals. The controlled variables were temperature,

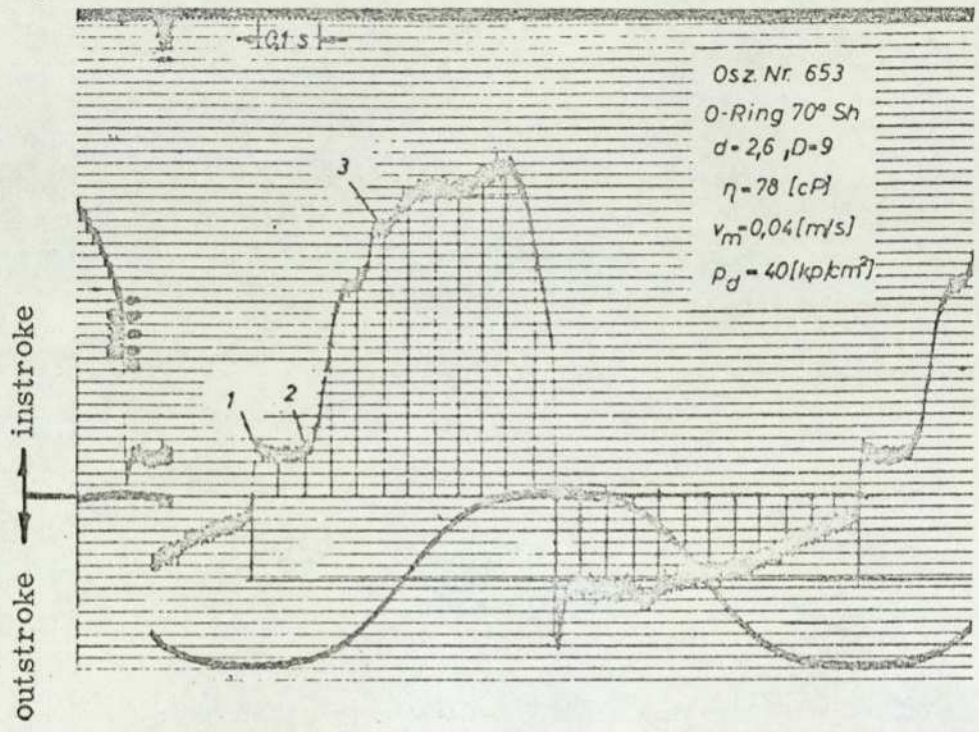


Fig. 2.11 Friction trace showing the variation in seal friction between instroke and outstroke. (Muller, ref. 35, fig. 39)

covering a range from 25°C to 100°C, sealed pressures up to 45 lbf/in^2 which is very low for general hydraulic seals and speeds from 10-15 ft/min. These results, plotted non-dimensionally against $G \left(= \frac{U \pi D}{P_r} \right)$, show that boundary lubrication is in evidence for values of G below 1.5×10^4 with hydrodynamic lubrication occurring at values higher than this.

O'Donoghue and Lawrie (42)

O'Donoghue and Lawrie (42) used two new techniques to study the mechanism of lubrication of U type seals used in automobile brake and clutch cylinders, and is one of the first papers to describe a qualitative assessment of the film thickness under a reciprocating seal.

The first method used a conducting rubber for the seal and the resistance between the seal and the shaft was measured, infinite resistance indicating a full fluid film and zero resistance indicating partial film lubrication. The second method was to reciprocate the seals in a glass cylinder and by using suitable lighting techniques, the oil film could be made visible. A ciné film was made of the oil film and whilst both methods only gave a qualitative indication it was shown that a fluid film definitely existed. The film thickness could be seen to be low under high friction conditions that existed during the pumping stroke and large for the motoring stroke. The conditions tested were pressures from 0-500 lbf/in^2 and speeds from 4 to 10 ft/min. A number of tests indicated the presence of boundary lubrication.

Cnops (8)

Cnops used a number of cup type elastomeric seals to study experimentally the friction and leakage of reciprocating seals. Some theoretical evaluation of the lubricating mechanism is given using mainly empirical relationships and the theoretical results are presented only in a qualitative manner as he regards the results as being influenced by too many factors to be accurate.

Nau (36)

Nau ran a number of tests to verify Denny's (10) empirical relationship $q \propto \frac{2}{3} U^2$ over a wider range of viscosity and used tap water and deionised water to achieve this end. The seals were U seals of elastomers and leathers. The leather seals seemed to be best in this application, probably due to the wax contained in the leather which acted

as a lubricant. Rubber seals exhibited very high friction due to the film thickness, assumed to be proportional to the viscosity, being of the order of 1 micro-inch thus indicating that boundary lubrication existed. However, in spite of the high friction the leakage rates were in reasonable agreement with those given by the above relationship.

Blok and Koens (3)

By imparting a sinusoidal oscillating motion to a circular specimen of rubber and pressing a piece of glass onto its curved surface Blok and Koens were able to simulate the action of a reciprocating 'O' ring seal. Interference fringes were used to measure the film thickness and optical problems were solved by wrapping the circular section of the 'O' ring with metal foil to improve the reflectivity. They obtained monochromatic fringes of the contact and this allowed them to obtain the general film shape, the shapes given are typical of elastohydrodynamic lubrication having a relatively constant film thickness throughout much of the contact with a prounced 'nip' at the exit. The technique is interesting but in effect the action is of rolling rather than sliding, and, of course, there can be no pressure drop across the seal. Monochromatic fringes allow only the difference in film thickness to be obtained between adjacent dark fringes and the actual film shape must be inferred from a knowledge of the possible profile. Because of this, the absolute value of the film thickness is not known unless intimate contact occurs between the rubber and the glass somewhere in the contact area, or the fringes are actually counted as the film gradually builds up. The method can, therefore, be very susceptible to error unless great care is taken, but is nevertheless a very powerful method of obtaining accurate film profiles. The authors present a qualitative picture of the film profile throughout a complete cycle shown in figure 2.12 which clearly shows the changing shape of the film as the motion changes in speed and direction.

2.6. LITERATURE OF 1966/67

In 1967 the Third International Conference on Fluid Sealing was organised by BHRA Fluid Engineering and a review of the papers presented on reciprocating seals reveals the changing emphasis in the general research approach to seals, in that all four papers were mainly

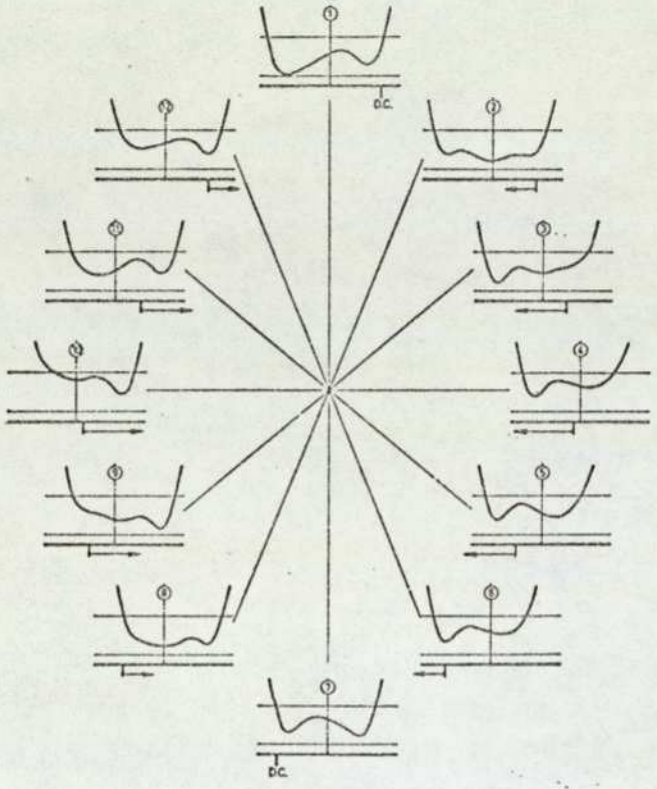


Fig. 2.12 Twelve successive phases during the cycle of a 'breathing' film. (Blok and Koens, ref. 3, fig. S7-4)

theoretical attempts to apply the 'inverse' elastohydrodynamic approach to the problem of reciprocating seals.

Dowson and Swales (14)

Dowson and Swales applied EHL theory not directly to seals, but to a 'soft' elastic contact rather than the 'hard contacts' normally developed in the lubrication of gear teeth and ball and roller bearings. A solution of Hertz's equations to other than a circular or parabolic contact becomes extremely difficult and for this reason the interest in the 'O' ring lubrication problem again becomes of interest. In this paper an iterative method has been used, based on Reynold's equation and the usual equation for elastic deflection as given in their paper. For light loads this procedure is sufficient and this paper presents theoretical values of film thickness for a parabolic profile having a zero pressure drop across it. Minimum film thickness values vary from a limited low value of 190 micro-inches to values around 1200 micro-inches. It is difficult to compare these values with practical seals, but Müller (34) in fact quotes film thickness values of around 100 micro-inches and this reduction below that calculated above, may be due to the pressure differential across the seal changing the contact pressure distribution through the seal from that of a pure Hertzian contact.

The equation mentioned above for the elastic deflection of the ring material only applies to deflections which are small in relation to the radius used and Theyse (51) points out that this hardly ever applies to working seals. However, Dowson and Swales state that their results are for lightly loaded contacts and in fact to create a reliable seal only very small interferences are required.

Hooke, Lines and O'Donoghue (26 and 27)

Hooke, Lines and O'Donoghue present an extension to their original solution to the 'O' ring lubrication problem in answer to criticisms by Blok, Theyse and Swales (45) on the inlet condition to the seals. The original analysis by Hooke, Lines and O'Donoghue showed an infinite pressure gradient at the entrance to the lubricated contact.

The original paper, using the elasticity equations of

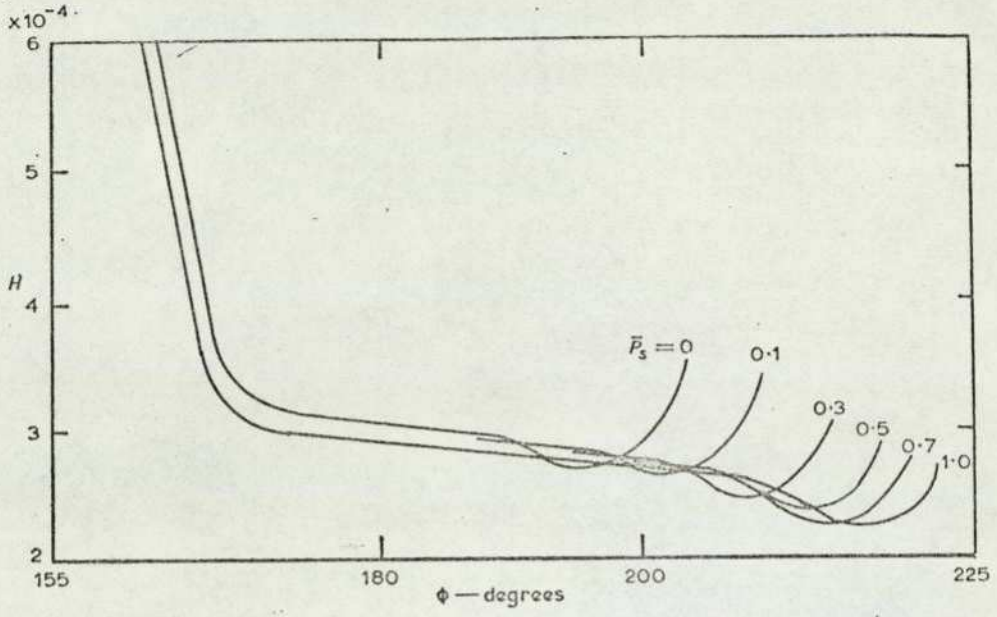
Milne-Thompson*, used iterative techniques to determine the shape and pressure distributions of an 'O' ring in a square groove, with a pressure differential across the ring. A knowledge of the pressure profile at the contact then allowed the shape of the film to be calculated.

Reference 26 of Hooke, Lines and O'Donoghue gives several film shapes calculated for 'O' ring seals, figures 2.13a and b. It is interesting to note that for the pumping stroke (the outstroke) the sealed pressure does not have much effect on the film thickness although the extent of the seal contact increases as the sealed pressure is increased. The profiles show the typical EHL shape and the values of film thickness are similar to those measured by Nau (37) being around 300 micro-inches. On the motoring stroke (the instroke) the film shapes are similar, but reversed, and show a notable decrease with increasing pressure down to 150 micro-inches due, the authors state, to the fluid being dragged across the seal against the fluid pressure. It must be remembered here from a practical point of view that the authors are dealing with a piston seal and as such both sides of the seal will be in a flooded condition. This would give rise to different instroke films than would be found in a rod seal where the atmospheric side of the seal would not in general be flooded.

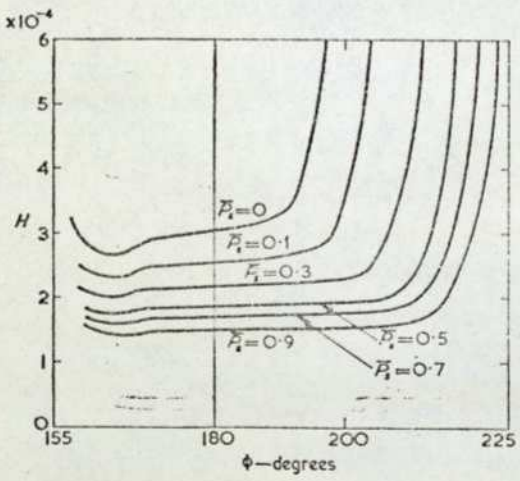
The operation of hydraulic jack seals is complex and a consideration of the direction of the pressure differential and the stroke direction is enlightening. For the case of a single piston seal, in the form of an 'O' ring, two possibilities exist, that of a single acting piston seal and that of a double acting piston seal. The double acting piston seal 'sees' identical conditions no matter which way the piston is moving and is therefore continually on an instroke. Therefore, according to the theory of Hooke, Lines and O'Donoghue, the net leakage past the piston must be zero, providing the speed is constant for both strokes.

For the single acting seal the conditions are slightly different for in this case the stroke during which the pressure is applied is an instroke whilst the other is in effect the same stroke with a nominally zero

* Milne-Thompson, L. M. Plane elastic systems. 1960. 117, (Springer Verlag, Berlin).



(a) pumping stroke (outstroke)



(b) motoring stroke (instroke)

Fig. 2.13 Variation of calculated film thickness with pressure. (Hooke, Lines and O'Donoghue, ref. 26, figs. 36 and 37)

pressure differential, an external force providing the returning force required to operate against the tank pressure and the pipe resistance. The leakage will therefore be proportional to the difference between h* at system pressure and h* at zero pressure. The report shows that for this stroke, pressure has a profound effect, and a net leakage must ensue. For this application in a practical actuator, there is no outstroke and the leakage cannot be defined as stated,

$$q = \frac{\pi D U}{2} (h^*_o - h^*_i) \qquad (2.10)$$

Similar considerations given to the rod seal lead to the same conclusions.

The net leakage from the piston or the rod gland is not easy to calculate, and in order to achieve it the operating conditions of the seal need to be clearly specified. However, once this has been done, the results of this paper could be used to calculate the leakage, if it is assumed that both sides of the seal are flooded at all times.

The effect of speed and viscosity on the leakage can be obtained from the theoretical result for film thickness:

$$h^* \propto (\zeta U)^{0.5} \qquad (2.11)$$

The Couette leakage can, therefore, be represented by

$$q \propto \zeta^{0.5} U^{1.5} \qquad (2.12)$$

and can be compared with the experimental results of other workers.

Hirano (24)

The paper by Hirano applies the inverse approach to the EHL problem and includes frictional heating effects as well as time dependant effects caused by a sinusoidal velocity throughout the stroke. As a pressure profile, Hirano assumes in this paper a parabolic form initially but later uses a sinusoidal profile to obtain film shapes. The results formed are shown graphically.

Theyse (51)

Theyse discusses in great detail the inverse approach to the elastohydrodynamic lubrication problem related to seals generally and assumes to start with that all seals must leak to prevent wear of the surfaces which depends onthe minimum film thickness. However, the design of the seal must be such that the inevitable leakage is minimised.

Theyse points out early on in the paper that the elasticity equation normally used in EHL analysis cannot be applied to elastomeric surfaces because the equation relies on the assumption that the deformations are small in relation to the body itself a condition which is rarely true for seals which may be compressed radially by up to 20%.

In conclusion, Theyse states that providing the pressure reaches a maximum at some point and that $h = {}^{3}/_{2}\, h^{*}$ at some other point in the contact, then a stable film will follow. These conditions may be produced by suitably shaping either the seal or the housing. He does not suggest any way in which the film shape can be verified experimentally. However, Theyse compares his theoretical treatment with some experimental results obtained by optical interference methods by Koens, Hammerschlag and Liem (31) for a free 'O' ring, presumably operating without a pressure differential on a reciprocating rod and found that the pressure profile determined from the measured film profile did not agree very well with the expected pressure profile and states that the reason for this was that the fluid 'slipped' at the bounding surfaces of the film. This point is raised in the discussion of the paper and Theyse points out that this condition can occur where the surfaces are not 'wetted' and cites as an example the case of a liquid such as mercury on glass. The possibility of slip between the fluid and the seal used in these experiments, is debatable, and cannot be confirmed or denied without specific experiments to show what does occur, but it would appear from the discussion that slip between the fluid and the seal would be very unlikely. The other possible explanation of the discrepancy between the measured and calculated pressure profiles could be misinterpretation of the interference fringes in the experimental work, which has been mentioned before in the discussion of reference (3).

2.7. LITERATURE OF 1968/1969

Nau (38) and (39)

During the period 1963-1966 much experimental work was conducted by BHRA Fluid Engineering on the friction and leakage characteristics of square section seals having various forms of construction and the results are published in (38) and (39). Much of the previous experimental work conducted by Denny et alia had concentrated on 'O' rings and commercially available seals of which few were of similar geometry or construction and therefore not open to direct comparison. The tests carried out by Nau were thus designed to determine the effects of different forms of construction on the same section of seal. Speeds were to 50 ft/min with pressure to 3000 lbf/in^2 and each seal was tested for approximately 5000 hrs.

Over these long test periods it was noticed that the square law relating leakage and speed propounded by Denny (11) did not appear to hold. Friction also appeared to be fairly random with time, and frequent stops caused even more erratic behaviour. It was also found that the repeatability of tests was very poor. Figure 2.14 shows some typical results, the friction and leakage being the mean values over 50 hr periods, for the three pressures 1000, 2000 and 3000 lbf/in^2. The erratic behaviour of the results can clearly be seen, in particular stopping and starting the rig appeared to cause an immediate rise in friction which then gradually decreased. These results are for a rubberised fabric square section ring sealing mineral oil and the friction values are the mean of an outstroke and an instroke.

The friction rose almost linearly with pressure and the lowest friction was always accompanied by the highest leakage and vice versa. This fact is well known. The design of a seal must always therefore be a compromise between friction and leakage.

Due to the unrepeatability of the results the original intention of the tests, to determine the effects of various forms of seal construction, had to be abandoned. The main conclusions from the paper appear to be that Denny's (11) empirical formula for leakage and speed does not apply to long term tests and the random fluctuations throughout the tests indicate

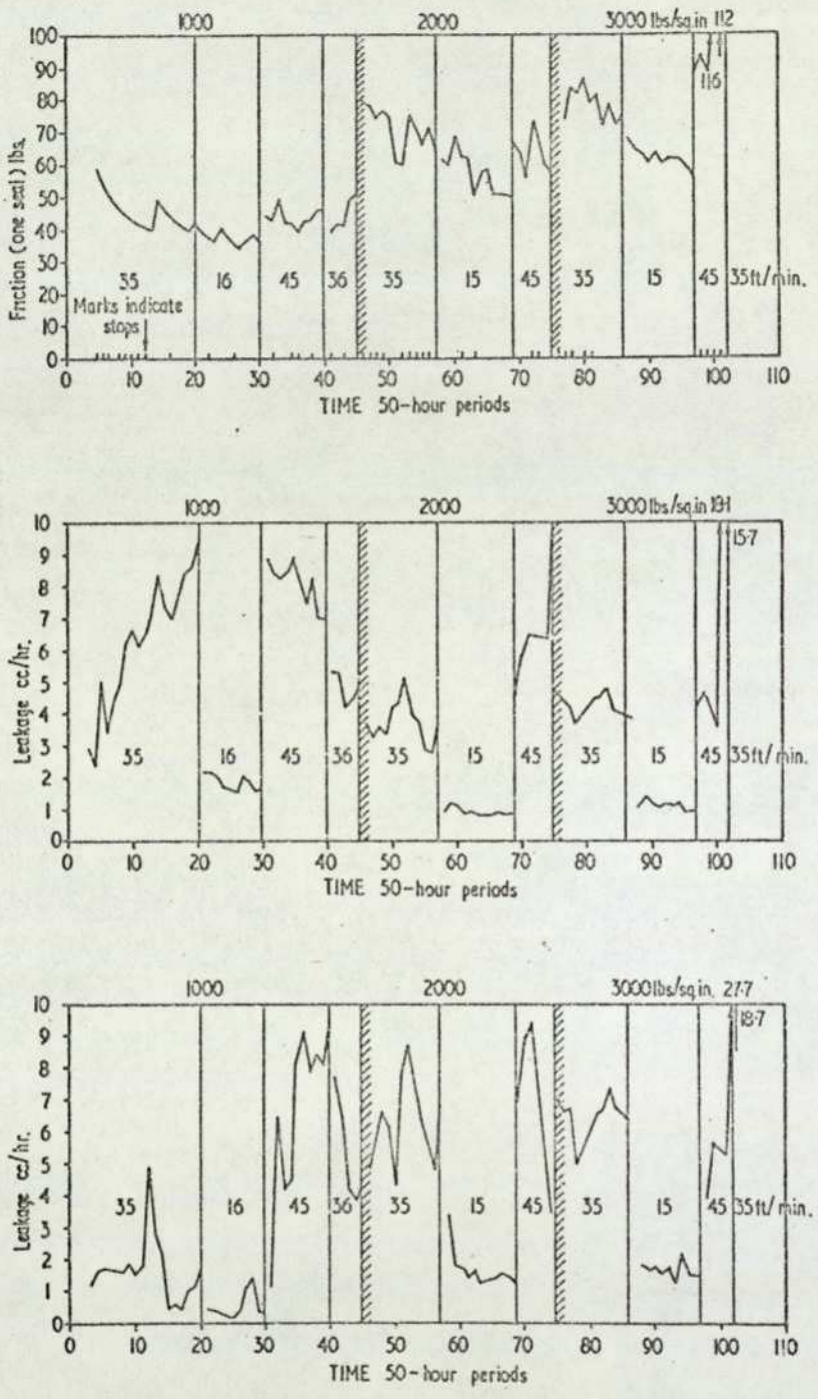


Fig. 2.14 Examples of the fluctuating leakage and friction of a rubberised fabric seal. (Nau, ref. 38, fig. 15)

that either (a) all the variables were not controlled or (b) those that were, had not been controlled accurately enough. The least controlled variables are those of the elastomer itself particularly in these long term tests, where oil absorption, stress relaxation and creep of the rubber occur. Although some regard is given to the film thickness it is still one of the extremely important dependent variables in seal experimental work about which little is known.

Reference 38 gave details of experiments by Nau on square section seals and an analysis of the results including the results of additional tests are given in reference 39. It is shown that the friction values of the rubber obtained with lubricated seals, give qualitatively similar results to those obtained for dry unlubricated contacts. It shows that the friction coefficient rises to a maximum due to adhesion between the rubber specimen and the track and then decreases. A second peak in the curve occurs at a slightly higher speed when rough surfaces are used. This is due to hysteresis losses caused by deformation of the asperities in the rubber surface. However, quantitatively the values of friction under lubricated conditions are lower by two orders of magnitude than those for dry contact. The peak due to the adhesive friction is shown to be rationalised by the Williams, Landel and Ferry transformation which relies on the glass transition point of the elastomer. For normal seal materials the maximum coefficient of friction can be shown to lie within the speed and temperature ranges likely to occur in general hydraulic systems.

Because the friction appears to be due to adhesion between the rubber and the rod or cylinder bore material the seal must be in intimate contact with the shaft or cylinder and therefore leakage would appear to be unlikely. Nau, however, actually measured the leakage of these seals.

By plotting the ratio of the kinetic friction coefficients μ/μ_0 against the ratio P_s/E, figure 2.15, Nau obtained a similar result to that of Denny (9) who had worked at very low speeds with lubricated pad specimens to prevent hydrodynamic lubrication. The shape of the curve can be explained by assuming that the rubber surface is composed of microasperities. At low values of P_s/E the asperities are only partially

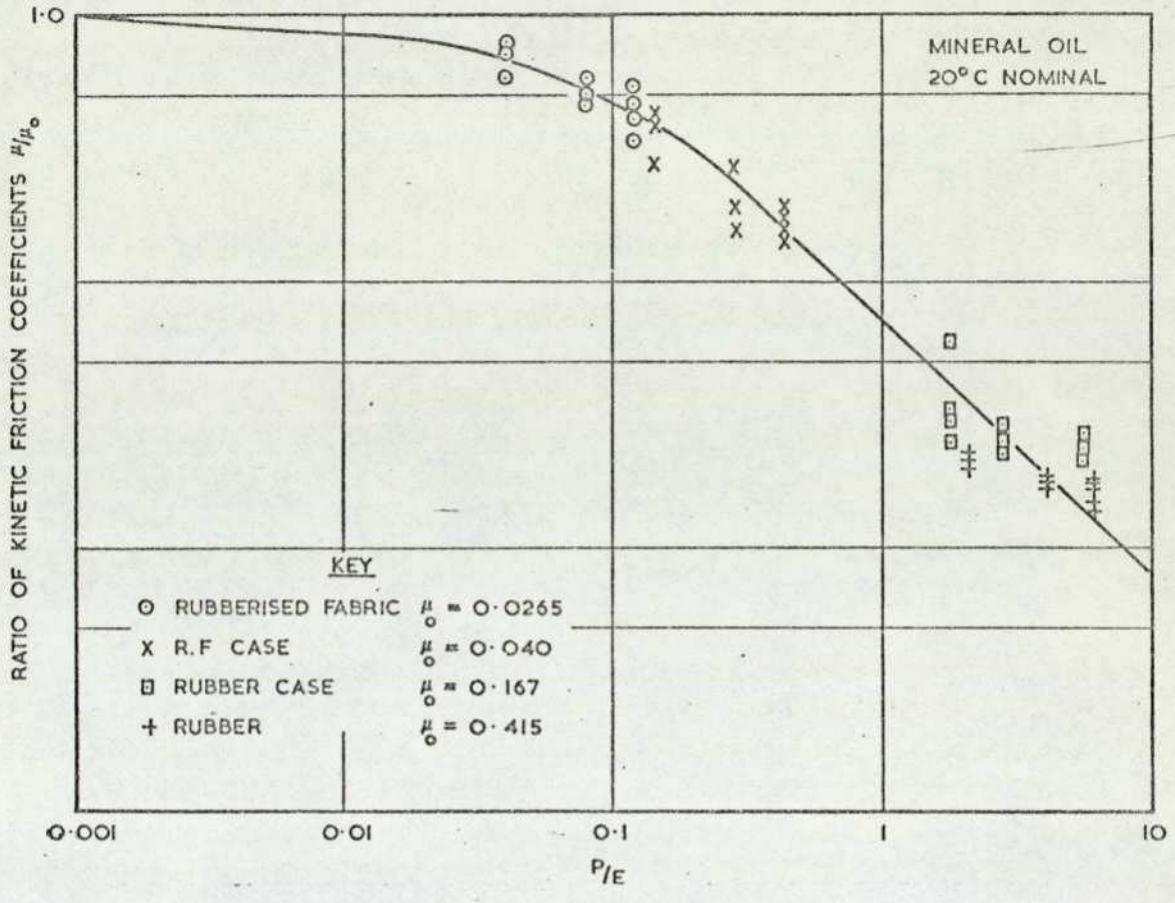


Fig. 2.15 The kinetic friction coefficient of a seal as a function of the sealed pressure for different forms of construction. (Nau, ref. 39, fig. 4)

flattened, but as the ratio P_s/E increases they are progressively flattened until the maximum possible area of rubber is in contact with the steel surface. At this point the friction force remains constant, the friction coefficient therefore decreases as the pressure increases.

Nau's results for the effect of speed on the kinetic friction over a speed range of 1 to 105 ft/min. are given in figure 2.16 which shows that the friction coefficient increases slightly for speeds up to 10 ft/min, above which the coefficient falls, the slope of the graph being -0.5 showing that $\mu \propto U^{-0.5}$. At a speed of 90 ft/min. the slope changes to +0.5, and $\mu \propto U^{0.5}$; this suggests that the seal was hydrodynamically lubricated. However, after correcting the data of figure 2.16 for viscosity and temperature effects, figure 2.17 is obtained in which the hydrodynamic portion of figure 2.16 is eliminated. Thus over the majority of the speed range Nau shows that:

$$\mu \propto (\zeta U)^{-0.5} \qquad (2.13)$$

Nau also shows that, after suitable corrections for the frictional heating effect, the leakage followed the law proposed by Denny (10) $q \propto \zeta U^2$, but that each combination of materials had generally different leakage values. In an attempt to reduce the scatter of the data he correlated it in terms of the parameter $(\zeta U^2 P_s^{0.5}/E^{0.25})$, figure 2.18. However, this is obviously not the correct parameter as it has the dimensions $F^{1.25}T^{-1}L^{-0.5}$ rather than L^3T^{-1} (leakage) and indicates some error in the experimental work or the effect of other variables as yet uncontrolled.

Figure 2.19 indicates the effect of P_s/E on the leakage rate and shows that for values of P_s/E greater than 0.1, the leakage is proportional to $P_s/E^{0.5}$. It is interesting to note that the friction transition region of the curve occurs at a P_s/E of 0.1 which corresponds, in figure 2.15, to the region where the friction force is constant due to the complete flattening of the microasperities.

A number of tests were conducted by Nau to determine the static or breakout friction. These indicated that the static friction increases slowly with time to a maximum value of friction corresponding to that

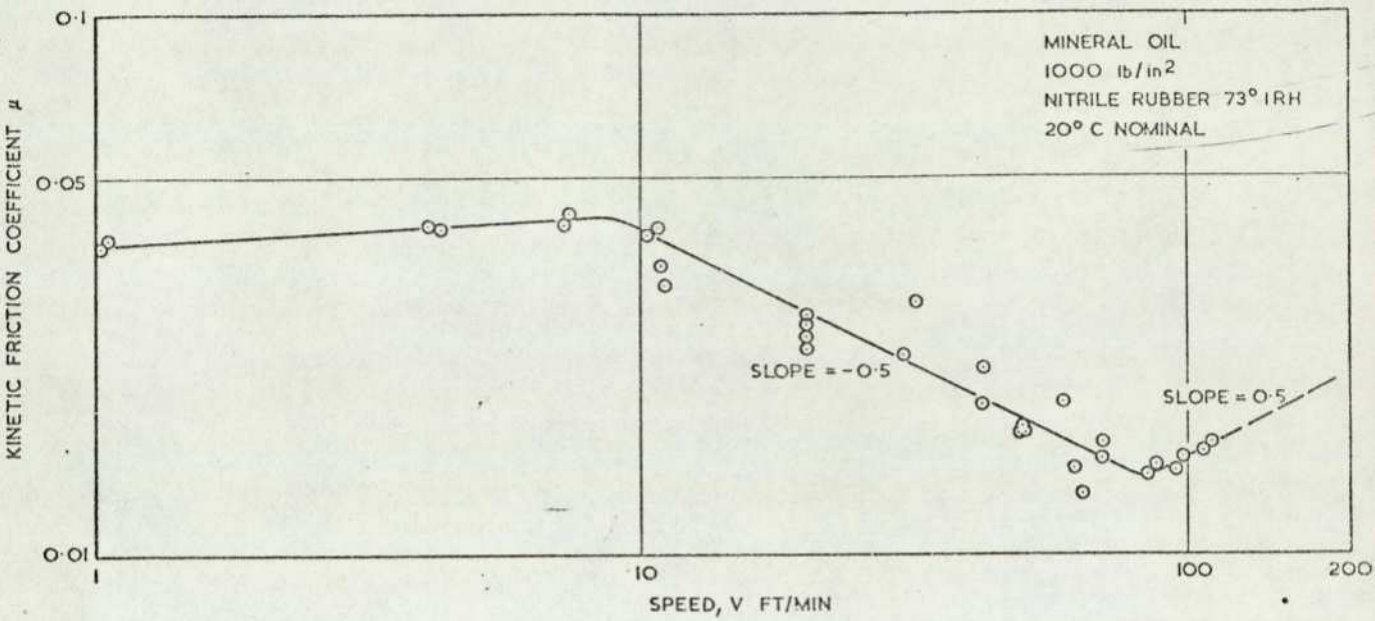


Fig. 2.16 The kinetic friction coefficient as a function of speed. (Nau, ref. 39, fig. 6)

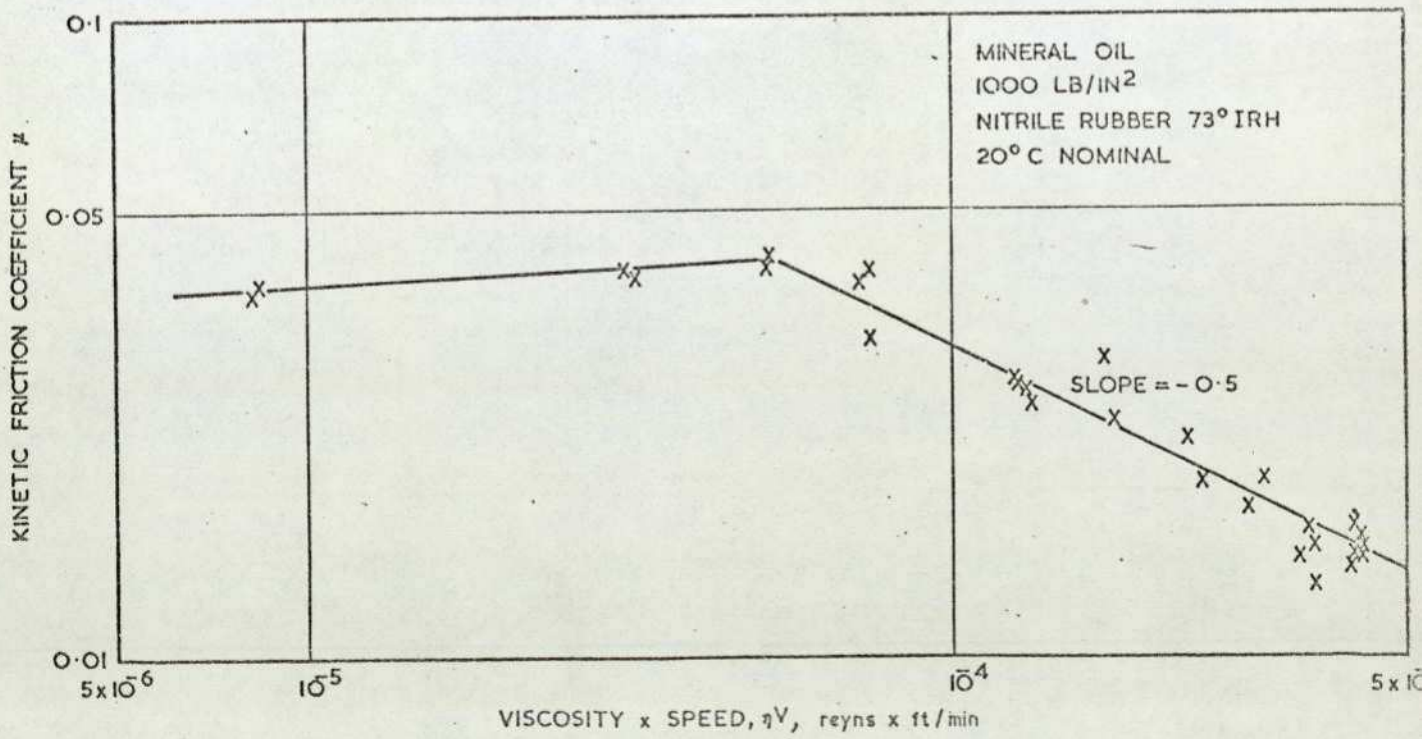


Fig. 2.17 The data from figure 2.16 compensated for viscosity variations caused by frictional heating. (Nau, ref. 39, fig. 8)

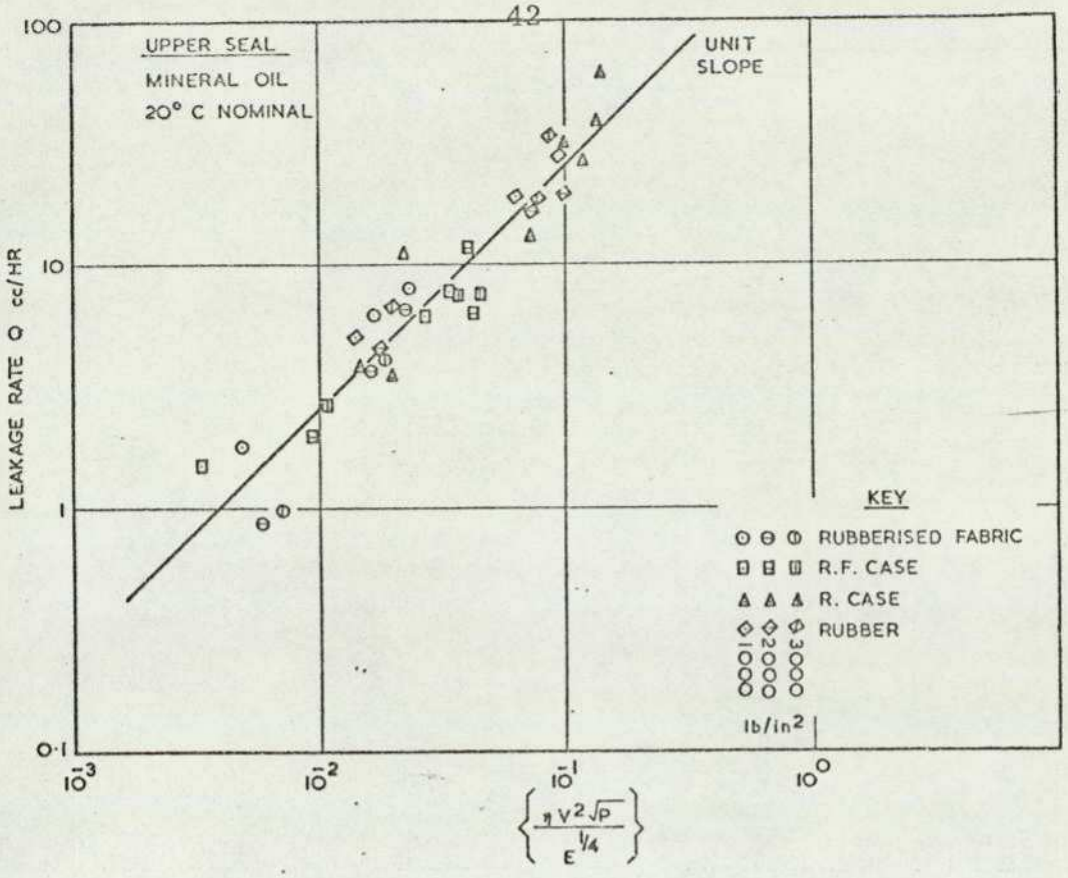


Fig. 2.18 The correlation of seal leakage with the experimental variables. (Nau, ref. 39, fig. 12)

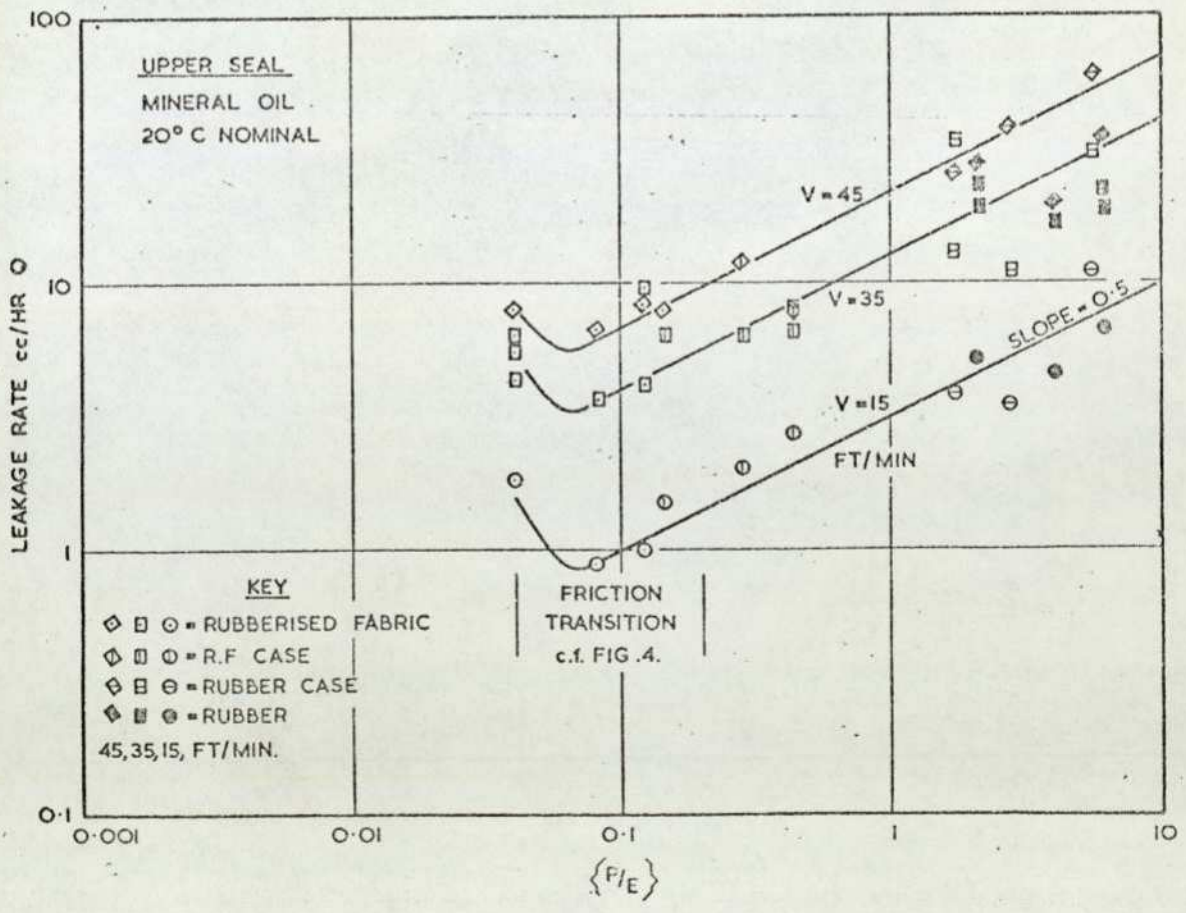


Fig. 2.19 The dependence of seal leakage rate (Q) on the sealed pressure. (Nau, ref. 39, fig. 10)

obtained with a dry contact and found that the friction correlated well with the quantity $\log_e Et/\gamma$, where t is the time at rest.

There appears a contradiction in the work reported by Nau in that the friction is shown to be fairly high, possibly boundary, whilst considerable leakage still occurs. The test method used utilised two seals with pressurised fluid between them and for any one stroke of the shaft one seal 'sees' an instroke whilst the other 'sees' an outstroke, the recorded friction being averaged between the two seals. Since the two seals are working under somewhat different conditions, the average friction will only represent a qualitative measurement of the friction and is unlikely to give a picture of the true state of affairs.

Lang (32) and (33)

Lang provides a great deal of data for the friction of 'O' rings and 'U' rings and provides in reference 32 several empirical formulae for determining the maximum friction, the static friction and the friction coefficient. However, the pressure and speed range over which he has operated is fairly small being 0-700 lbf/in^2 and 0-6 ft/min respectively. The friction is again measured and taken to be the average of two seals, one on an instroke, the other on an outstroke but Lang states that the mean value for the two seals does not complicate the assessment of the seals since their behaviour under the different friction shear stress is basically the same.

In his results, Lang shows that the friction/speed curve has the same shape as a Stribeck curve figure 2.20 the friction/speed curve for a plain journal bearing. Thus for the range in which there is hydrodynamic lubrication, friction = $C\,(U)^{0.5}$. He also states that the friction should be higher on an instroke - presumably because there will be no oil available to provide an hydrodynamic film.

Where the seal operates with a pressure differential Lang shows that the friction increases with increasing pressure at all speeds, for both 'O' and 'U' rings. Typical values for 'O' rings of 2 inch bore were 10 to 120 lbf per ring giving a specific friction between 10 and 120 lbf/in^2. These values appear to be very high when compared to specific frictions measured by other workers. Nau (38), for example, using square

section rings recorded a maximum specific friction of 30 lbf/in^2 at a sealed pressure of 3000 lbf/in^2 and a speed of 45 ft/min.

The results show, as expected, that in general leakage and friction are inversely proportional to each other. Also leakage decreases with increasing temperature due to the reduction in the viscosity of the oil. However, this statement must only refer to a particular case where Couette flow is predominant, the leakage then depending purely on the film thickness which would be expected to decrease as the viscosity decreased. For thicker films where Poiseuille flow would also be important, a reduced viscosity may result in an increased leakage.

Leakage is shown to be directly proportional to the speed over the range tested compared with the results of Nau and Denny which showed that $q \propto \frac{1}{2} U^2$ and Müllers theoretical and experimental results which showed that the seals operated hydrodynamically and that $q \propto (\frac{1}{2} U)^{0.5}$. However, comparing the speed ranges of Lang's results, figure 2.20 with those of Müller, figure 2.10, the discrepancy in their formulae for leakage against speed can be found. The full Stribeck curve obtained by Lang shows that hydrodynamic lubrication of the seals occurs for speeds above 25 mm/sec. (5 ft/min) but most of the work was conducted at speeds below this. Müllers results however, covered a much wider speed range and figure 2.10 refers to speeds between 40 mm/sec. and 180 mm/sec. (10 to 35 ft/min) which according to Lang was completely in the hydrodynamic range. Thus for a seal operating hydrodynamically, $q \propto (\frac{1}{2} U)^{0.5}$ but for seals not in this range, $q \propto U$. Both of the above reports used 'O' ring seals and the results can be compared to the results of Denny and Nau who used various lip seals and rectangular section seals over a wider range of viscosities and speed and who showed that $q \propto \frac{1}{2} U^2$ indicating a mode of operation involving a combination of both hydrodynamic and boundary lubrication.

Lang also states that leakage/stroke at constant speed is directly proportional to stroke length but his graph of figure 2.21 does not pass through the origin. It is suggested that this is caused by slight pumping action due to the ring rolling in its groove. This statement of the effect of stroke length on leakage is misleading in that leakge is

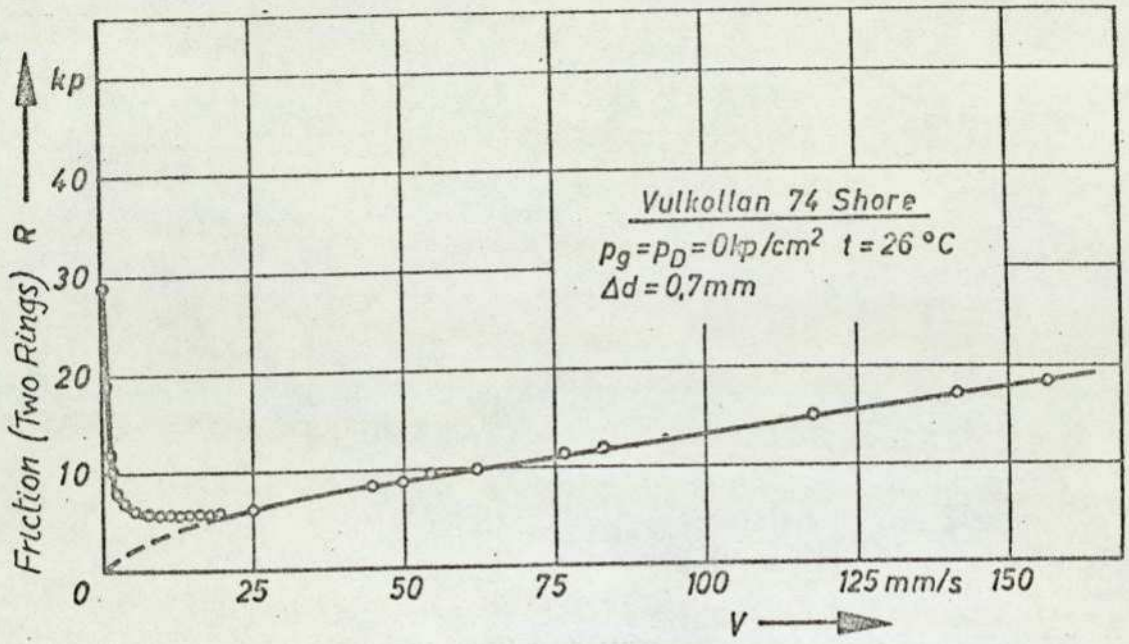


Fig. 2. 20 The relationship between the friction of two 'O' ring seals against speed. (Lang, ref. 33, fig. 16)

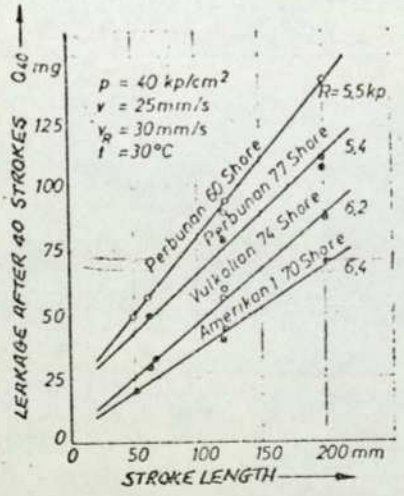


Fig. 2. 21 Seal leakage as a function of the stroke length. (Lan, ref. 32, fig. 21)

normally measured as a volume per unit time and if the stroke length is increased at constant speed, then the cycle time must increase, the leakage per unit time thus remaining constant. However, as stated, the results lead to an important conclusion in that the straight line result obtained gives a strong indication that the film shape is stable throughout the stroke length. This fact was true for all the rubbers tested.

Lang utilises the leakage volume/stroke to calculate values of film thickness and shows that the calculated film is up to 16 micro-inches thick. This value appears to be somewhat low in view of the stated surface finish of the rod of 100 micro-inches CLA and does not compare well with the results of other workers in the field. However, in comparison with Müllers (34), (35) results it has been shown that Lang was working in the boundary and mixed lubrication regime and this could account for the low film thickness and the high friction values.

Dowson and Swales (15)

Dowson and Swales at the same conference presented experimental work in which attempts had been made to measure the film thickness of a simulated seal. The experimental apparatus consisted of a rotating disc 2 feet in diameter with a box containing an enlarged model of the seal, pressed onto the top of the disc. The seal model was so arranged that a small pressure differential, up to 150 lbf/in^2, could be applied. As the disc rotated the model seal 'saw' a continuous in or outstroke. The apparatus did not simulate precisely a seal situation because the simulated interference force determined the effective backup clearance of the seal and because of this, interference force and backup clearance were not independent as would be the case in a true seal.

However, the purpose of the apparatus was to measure the film thickness and pressure profile under a lubricated sliding rubber pad. The film thickness was measured using a capacitance transducer of 0.036 inches in diameter and a 2 MHz frequency demodulation system. A piezo type pressure transducer was used to determine the pressure profile, the diameter of the sensing piston was 0.059 inches. Both signals were passed to the instrumentation via mercury slip rings

and the authors stated that this caused a great deal of trouble and could account for a considerable amount of the 'noise' shown on the film thickness trace. The pressure signal was also troublesome due to the very high impedance required between the signal and earth at the slip rings, a requirement of the piezo type of transducer.

The results for a cylindrical rubber specimen, used to simulate an 'O' ring shows typical EHL profiles figure 2.22 with values of minimum film thickness varying from 600 micro-inches at 80 lbf/in load to 1200 micro-inches at 2.5 lbf/in load. A square section ring gave values an order of magnitude less than this the minimum film thickness being in the range 30-200 micro-inches and the authors state that the probe was less accurate in this the film region. The thinner films experienced with the square section rings may have been due to the leading edge of the seal forming a poor inlet profile as compared to the cylindrical inlet profile of the 'O' ring specimens.

However, the results clearly indicate that the film thickness on the extending stroke was thicker than that on the retracting stroke under the conditions tested.

A criticism of the presentation of this paper is that many of the film thickness profiles are shown with an inverted non-linear axis for the film thickness. This makes interpretation of the results very difficult.

Typical graphs of the minimum film thickness against speed and pressure are shown in figure 2.23a, b and c. It can be seen that for a square section seal h_{min} increases with speed but tends to level out at the maximum speeds shown, and decreases with increasing pressure although the authors state that in general application of the pressure alone does not greatly affect the film thickness because the seal stress and the film pressure increase in proportion. An empirical formula for the minimum film thickness was obtained and shows a number of changes, mainly in the indexes of the non-dimensional parameters used, when compared with established EHL theory for 'hard' contacts. The empirical equation is given as:

$$h_{min} = \frac{1.7\,(\tfrac{1}{2}U)^{.57}R'^{.56}}{w^{.13} \times E'^{.44}} \qquad (2.13)$$

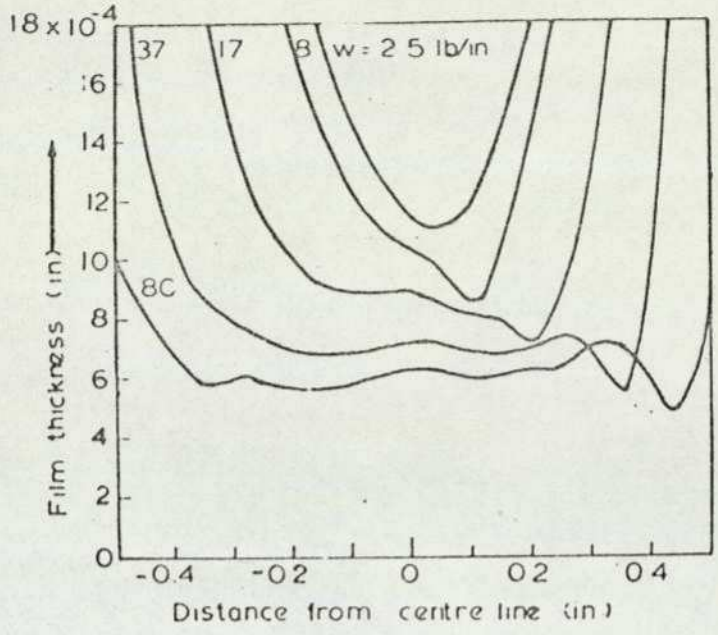


Fig. 2.22 The measured film profiles of a soft sliding cylinder. (Dowson and Swales, ref. 15, fig. 5)

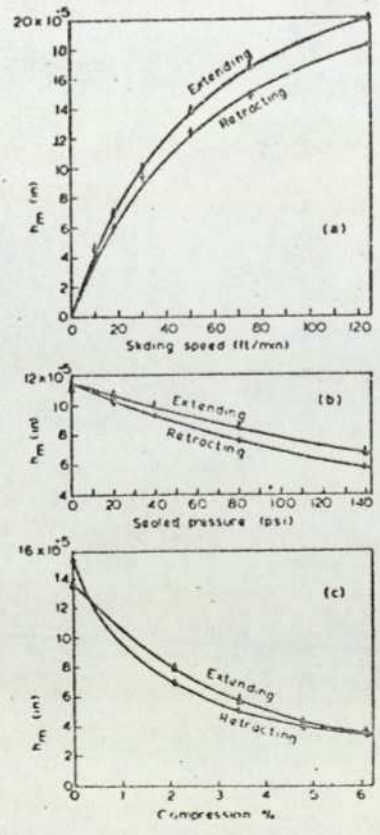


Fig. 2.23 Variation of measured film thickness for a square section seal. (Dowson and Swales, ref. 15, fig. 10)

Thus assuming only Couette flow, the leakage using the above equation can be written as $q \propto \zeta^{0.57} U^{1.57}$ and compared with the various indices of Müller, Lang, Denny and Nau. However, the Couette leakage can only be calculated from the film thickness, h^*, in the film, where the pressure gradient is zero, and this value is not necessarily related to the minimum film thickness in the same way as is assumed in this paper. The stated relationship between leakage, viscosity and speed may therefore be in error. A further criticism, mentioned in the discussion is that the proposed relationship is based on a unidirectional Couette flow whereas the actual seal leakage would be the difference between the outstroke leakage and the instroke leakage, which is not the same thing.

Roberts and Swales (47)

An attempt to measure film thickness, again in a simulated 'O' ring situation, was reported by Roberts and Swales in which optical interference between a glass plate and the rubber surface was used. The authors used monochromatic light of wavelength 5461 Å and a silicone fluid of 1025 cp viscosity. As mentioned before, monochromatic fringes do not give an absolute measure of film thickness unless a reference is known at some point. The authors overcame this obstacle by counting the fringes at one point as the glass slide was started from rest. This then gave a reference point from which to determine the film shape and the absolute film thickness.

The results again showed the typical EHL film profiles shown in figure 2.24, but the experimental results did not agree well with the theoretical values. Further examination revealed that some of the discrepancy could be accounted for by the fact that due to the contact not being fully flooded, the pressure did not start to build up until well into the flooded region. The rest of the error was assumed to be due to end leakage along the cylinder.

The work shows that normal EHL theory appears to give reasonable prediction of film thickness for high loads and slow speeds for soft elastic solids. This was the aim of this work, therefore a pressure differential was not applied to the specimen. With a pressure differential the normal

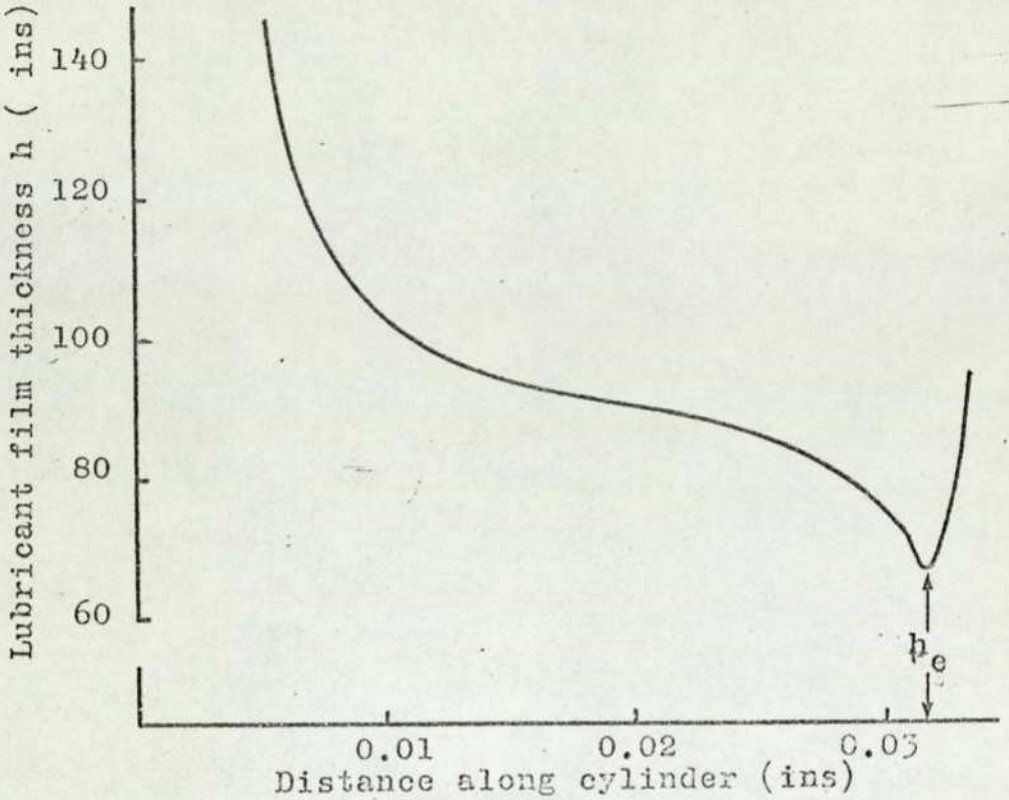


Fig. 2.24 Typical film profile deduced from an interferogram for a soft sliding cylinder. (Roberts and Swales, ref. 47, fig. 4)

load would not be known precisely and, further, the fluid viscosity in a typical seal situation would be much less than that used in these experiments. However, for the highest loads the film thickness was of the order of 100 micro-inches which agrees well with previous predictions of typical seal films by other workers.

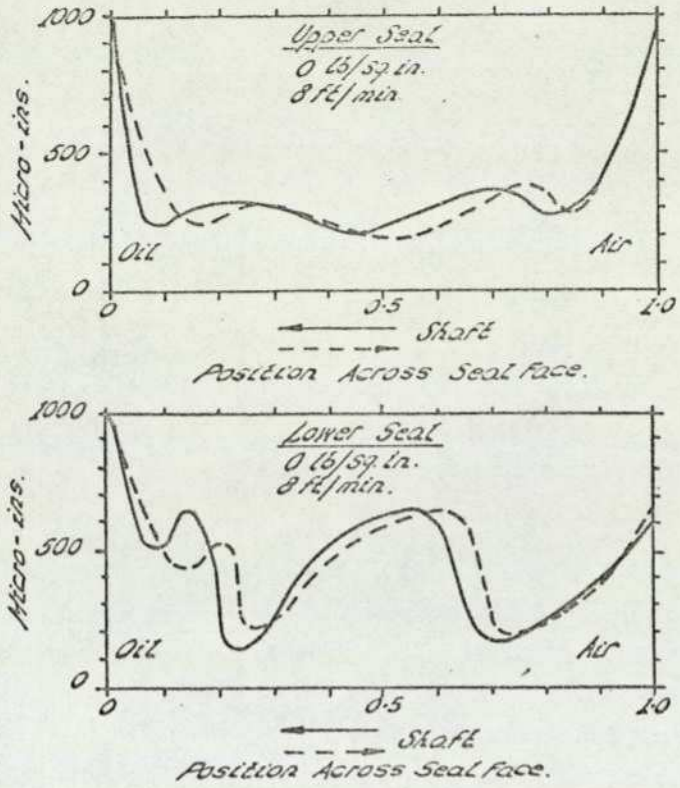
2.8. ADDITIONAL WORK AT BHRA FLUID ENGINEERING

During the period 1960 to 1969, much experimental work on reciprocating seals had been conducted at the BHRA Fluid Engineering Laboratories, and some of the work has already been reviewed in references (12), (36), (38), (39) and (41). However, the bi-annual progress reports produced by BHRA provide additional information not available in these reports.

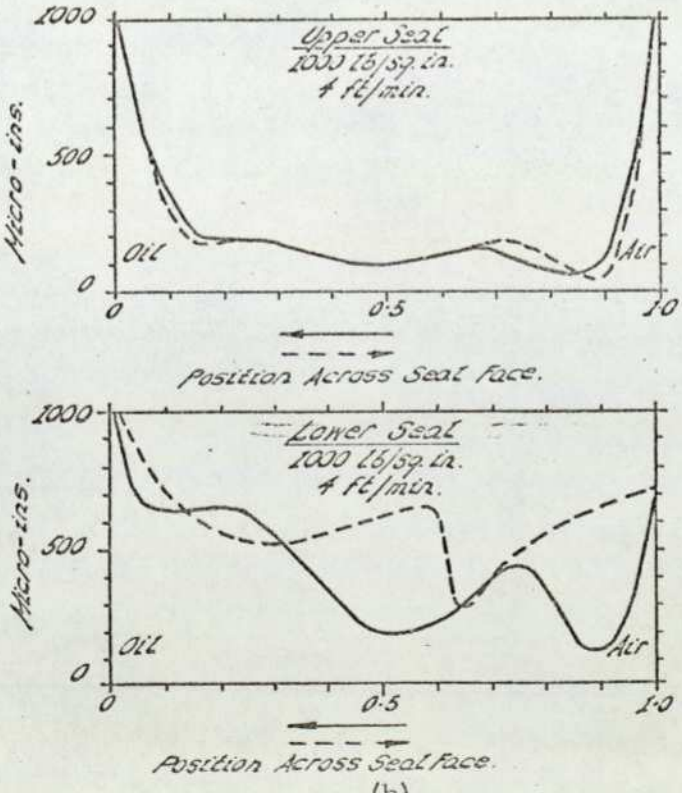
Reference (22) indicates that Nau and Turnbull's theoretical analysis of the reciprocating seal problem (41) was severely criticised on the points mentioned in the review and Fisher (22) formulated a more refined approach to the elastic deformation of the seal incorporating a term to cover the shear stress in the elastomer. Atempts to solve this elasticity equation simultaneously with Reynold's equation for the lubricated rectangular section seal contact led to complete failure and proposals were put forward to measure the film thickness.

Nau (37) gives preliminary results of the attempts to measure the seal film thickness proposed in reference (22) and some idea of the film profiles obtained can be seen in figure 2.25a and b. A capacitive method was used in conjunction with a conductive rubber seal of rectangular section. This work was the first attempt to measure the film thickness of a seal in a typical seal situation and results were obtained for pressures up to 3000 lbf/in^2. In any system designed to measure the film thickness in a seal contact, some compromise must be expected and in this case the seals were of a hard rubber (approximately 90 IRHD) and the circular probe was 0.080 inches diameter giving a seal length/probe diameter ratio of 4.6. This ratio is fairly small and would tend to average the film thickness over a significant length of the seal, small spikes or peaks in the film profile not being detectable.

When this work was conducted in 1965 it was thought that the seal



(a)



(b)

Fig. 2. 25 Typical measured film profiles for a reciprocating rectangular section seal. (Nau, ref. 37, figs. 2, 3, 4, 5)

profile would have been an approximately linear tapered wedge or a shape typical of elastohydrodynamic lubrication. The reported findings, however, indicated a complex film shape of a possible undulating nature and figure 2.25a and b shows examples of the film profiles for unpressurised and pressurised square section seals. For the unpressurised seal, the film thickness appears to be fairly large at 300 micro-inches, considering the slow speed of 8 ft/min. and the profile of the upper and lower seals are completely different even though they were made in the same mould. It is interesting to note that the seal surface appears to be dragged in the direction of motion of the shaft for instroke and outstroke and this may be a frictional effect.

On pressurising the seal, it can be seen that the film thickness has decreased to around 100 micro-inches for the upper seal, but has in fact increased for the lower seal and this is unaccounted for. Whether this phenomena was typical is not mentioned, and therefore may be taken to be a particular case.

The profiles of the upper seal for unpressurised and pressurised conditions, bear some qualitative resemblance with each other but those of the lower seal are completely different and may indicate a somewhat unstable film shape.

In reply to the discussion by Theyse of reference (26), Hooke, Lines and O'Donoghue say that in order for a film to form under a square section ring, there must be a small but finite radius at the corners of the sliding surfaces of the seal. In fact they state that the value of this radius will determine the film thickness throughout the contact. This may account for the difference between the film shapes of the upper and lower seals. However, where pressure is applied to the seal, extrusion of the seal will occur and in general will tend to form a smooth inlet profile as shown in figure 2.3 and the seal edge will not be so important. Generally then the outstroke film shape should be different from the instroke film shape. This can be seen to some extent in the film shapes of the lower seal, but not in those of the upper seal, where, although the film shapes are shifted axially for the different strokes, the general shape and mean film thickness appear to be the same.

Due to the poor resolution of the probe, the film profiles lacked the fineness of detail that would have been liked. For this reason attempts were made to increase the effective length of the seal by fitting two seals in the place of one and increasing the groove length. This in fact would not have improved the resolution to a great extent because the radial thickness of the unit would still have been the same and the seal stress profile would have been modified. However, the attempts failed because high friction was encountered and traced via the film thickness measurements to a build-up of pressure between each pair of seals causing severe extrusion both to atmosphere and into the system pressure. This phenomena has been termed 'interseal pressure' and has been studied by the present author (19), (20) and (21). Basically interseal pressure is caused by 'negative' leakage of the seals, possible when Couette flow alone is in operation.

2.9. DISCUSSION OF REVIEWS

This review has covered the majority of relevant papers, on reciprocating seals to be published since that of White and Denny (53) and has shown generally that the major portion of the published literature has been devoted to experimental rather than theoretical work. Experimentally the work has been spread over a number of different designs of reciprocating seal of which, in the earlier and the later reports the 'O' ring appears to be the most common. This would have been expected in the earlier reports when 'O' rings were being used in hydraulic jacks, but recent seals would not be of this form (due to the inherent faults associated with reciprocating 'O' rings), and the current interest is due to the emergence of elastohydrodynamic lubrication theory. Denny published two reports (10) and (11) on various commercial lip seals, used singly and in multiples, and several reports from BHRA have dealt with rectangular section seals, but apart from these there is a noticeable lack of literature covering the more commonly used commercial squeeze type seals. The work of Nau (38) used square section rings simply as a basic form to evaluate the effects of different forms of construction on the sealing qualities, but may equally well have utilised a circular form of ring.

It can be seen also from the experimental work that effort has been allotèd to measurements of seal friction and leakage, the mechanism of sealing being almost disregarded in many cases. This may have been due, in many instances, to the need for seals in practical applications outstripping the necessary development of suitable theories of sealing or technical means of measuring the film shapes.

Early theoretical work was based on the assumption that the film shape would be of a linearly tapered wedge form, allowing the seal behaviour to be analytically investigated using Reynold's equation. The experiment work of Nau (37) shows that this is definitely not the case. More recent work has used the inverse method of solving Reynold's equation based on the fact that the dynamic pressure distribution through the seal under dynamic conditions will be that of the static profile. O'Donoghue et alia, (23), (26) and (27) managed to solve these equations for certain conditions in the case of 'O' rings. Hirano et alia (24) and (25) using the inverse approach assumed various pressure profiles and calculated film shapes from Reynold's equation involving a time dependant term to allow for a varying velocity throughout the stroke.

2.9.1. Seal leakage

Reciprocating seals must of necessity operate in a completely different mode to rotating seals in that a stable film shape cannot be of continuous duration because the direction of the velocity must change at the end of the stroke. At some point therefore the velocity must be zero and at this point film collapse could occur. The film profile then, will, in general, have to reform each time the velocity changes direction and for each stroke the film shape may be different. The net leakage of any reciprocating seal must be the difference between the oil passing the seal on the outstroke and that returning on the instroke and therefore to be precise it is necessary to know how much oil passes the seal at each stroke. For instance, in discussing the leakage of a rod gland seal, (the leakage of a piston seal is generally of less importance), the conditions of each stroke must be specified, as in some cases the rod may be extended for long periods of time, in which any oil passing the seal during the outstroke has a chance to drain away from the seal and

cannot therefore be returned to the oil system on the instroke. The net result would be a higher apparent leakage than if the rod was continuously reciprocated. As another example, it may be desirable in dusty environments to make attempts to positively prevent any oil passing back into the system in order to prevent contamination of the system fluid. In certain circumstances, again Denny (10) shows that alternating system pressures can cause negative leakage, showing that it is not even necessary for leakage to occur from a high to a low pressure, and this is confirmed in the work of Field and Nau (19), (20) and (21) which showed that pressure can build up between an unvented pair of seals to such an extent that the seals fail by extrusion into the system pressure.

All these various mechanisms could possibly be observed on a single jack, depending on its attitude. Thus in a jack extending vertically upwards the outer edge of the seal is always likely to be flooded by the leakage which will be less than that of a jack extending vertically downwards, where the leaked oil can drain away.

Denny's result for negative leakage depended on an alternating system pressure where, during the outstroke, the sealed pressure was high, resulting in a thin film of oil passing under the seal and on the instroke the pressure was low giving a thick inlet film, the net result being an inward flow of oil. This situation, however, would never arise in a practical situation and the pressure in the jack would be in the opposite sense, that is, high on the instroke, and would therefore lead to a thick outlet film and a thin film giving a high positive leakage, which is undesirable.

It can be shown then that leakage of a rod gland seal can range from negative to positive depending on many practical conditions and in order to determine the leakage, these conditions must be specified.

The experimentally measured leakage of seals has been conducted in a similar way throughout the literature. In this, the seal is usually continually pressurised during the instroke and the outstroke, and the leakage per unit time is taken over a number of continuous full cycles of the rod or piston. The results have then generally been related to the viscosity of the sealed fluid, and the mean speed of reciprocation of the shaft. In these experiments leakage has rarely been negative or zero.

Assuming the experimental values are relative to the practical jack, a number of different relationships with viscosity and speed have been proposed. Thus, the original relationship of Denny (10) later confirmed by Nau (36) shows that for a wide range of viscosity and speed

$$q \propto \zeta U^2 \tag{2.14}$$

This relationship applied to many types of 'U' lip seals and also to square section rings, although Nau later mentions that it did not hold for long term tests.

Müller (34) and Lang (33) both using 'O' rings obtained different results. From the friction recordings of the two papers, it is fairly obvious that Lang (33) was operating in a fully boundary or a mixed lubrication regime and obtained the relationship

$$q \propto \zeta U \tag{2.15}$$

The 'O' rings of Müller (34) however operating at a higher speed showed friction results indicating full hydrodynamic lubrication and obtained the result, derived theoretically as well, that

$$q \propto (\zeta U)^{0.5} \tag{2.16}$$

A further relationship obtained experimentally by Iwanami and Tikamari (28) showed:

$$q \propto \zeta^{1.5} U^2 \tag{2.17}$$

Dowson and Swales (15) on measuring the film thickness under a simulated 'O' ring derived an equation for the minimum film thickness showing:

$$h_{min} \propto (\zeta U)^{.57} \tag{2.18}$$

Assuming Couette flow, leakage can be calculated as

$$q \propto \frac{Uh}{2} \tag{2.19}$$

$$\therefore \quad q \propto \zeta^{0.57} U^{1.57} \tag{2.20}$$

There are thus five relationships between leakage, viscosity and speed all supported by experimental evidence, three obtained using the same basic form of ring, the 'O' ring.

These various results are due in some instances to the form of the lubrication film, boundary of hydrodynamic, and appear at present to be dependent to a great extent on the type of seal used, and the form of the test equipment. As shown in the previous section many factors will affect the leakage of a practical jack and in view of this, it would be difficult to reliably apply any of the above equations to a practical situation.

In view of these comments it is obvious that the leakage must depend on the film thickness throughout both strokes. Theoretically leakage has been calculated by White and Denny (53), Müller (34) and Hooke, Lines and O'Donoghue (26) but all have assumed hydrodynamic lubrication on both strokes.

2.9.2. Seal friction

Whereas the leakage of piston seals is generally not quite as important as the leakage of a gland seal, the importance of seal friction is probably reversed in that both piston and gland seals combine to provide the overall friction, and the greatest proportion of this would be derived from the piston seal, the friction being proportional to the contact area of the seals.

Again similar reasoning to that of the leakage phenomena can show that friction will also depend to a great extent on the conditions prevailing at the practical jack situation. Thus, in theory a piston seal of a double acting jack should give the same value of friction on both strokes, but in practice this may not be the case. The gland seal on the other hand 'sees' a pressure for the instroke but generally the outstroke pressure would be low. The friction would therefore be expected to be different on the two strokes.

In general there can be two modes of lubrication causing seal friction. First, boundary lubrication, secondly hydrodynamic or elastohydrodynamic lubrication.

Boundary lubrication is characterised by the two contacting

surfaces being in intimate contact with perhaps some form of solid film between them, which may be a specific boundary lubricant such as stearic acid or an oxide film of the metal surface. Generally boundary lubrication is in evidence in low speed, highly loaded contacts and results in high values of friction.

Hydrodynamic or elastohydrodynamic lubrication is characteristic of surfaces which are in relative motion having a full fluid film separating them. In hydrodynamic lubrication the film profile is determined by the rigidity of the surfaces, whereas in elastohydrodynamic lubrication one or both surfaces may deflect elastically under the influence of the generated pressure in the fluid. These contacts usually can be recognised by the extremely low friction force, caused purely by the shearing of the fluid film. An example will illustrate the low friction values possible in a typical seal sealing hydraulic fluid of viscosity η, a speed of U and a film thickness of h.

Thus specific friction $= \frac{\eta U}{h}$

$\eta = 10^{-5}$ lbf sec/in^2

U = 10 ins/sec

h = 100 micro-inches

$= \underline{1 \text{ lbf/in}^2}$

For an 'O' ring seal on a two inch diameter shaft, the total friction would be of the order of 1 lbf, assuming a complete fluid film around the circumference of the seal.

The friction force then in general must be composed of either boundary lubrication or hydrodynamic lubrication, or a combination of the two. In view of the very low friction force which would be obtained for a complete hydrodynamic film, it seems very unlikely that this will ever occur. However, the leakage obtained with seals would not occur, were boundary lubrication the mode of lubrication. The answer appears to be a combination of the two, either as a function of the circumference, that is part hydrodynamic, resulting in a net leakage and part boundary giving the friction force, or a different friction on each stroke. If leakage occurs this must mean a thicker mean film on the outstroke than occurs on the instroke resulting in a low outstroke friction with a high instroke friction.

Along with leakage, friction has been the most commonly measured variable in seals research and development, because again it is a fairly easy variable to measure, and gives a fair indication of the type of lubrication prevailing. Practically it is an important variable and one which manufacturers are very reluctant to mention quantitatively, because of the very wide confidence limits necessary even for tests under nominally the same conditions. This fact has been demonstrated by Cheyney, Mueller and Duval (7) for 'O' rings and appears to be particularly bad for rectangular section rings, as shown by Nau (38).

For 'O' rings, Lang (32) and (33) shows that the friction curve against speed resembles a Stribeck curve in that at low speeds the friction decreases rapidly, but above 6 ft/min there is a gradual increase in friction with speed, where the seal is operating hydrodynamically. Lang's results generally appear to be in the region of boundary lubrication, whilst those of Müller (34) appear to be in the hydrodynamic region. Müller (34) also measured the friction of individual seals and showed a friction trace having a low friction for the outstroke and a transition to a high friction for the instroke as expected. The majority of reported data however has been based on a mean friction for two seals and thus cannot show the difference in friction force for each stroke.

Nau (39) shows that the mean friction values of two seals as a function of the sealed pressure follows, qualitatively at least, a similar form to that of the friction of dry pad specimens, although quantitatively the lubricated seal friction was much lower. Further, Nau (39) has explained the decreasing coefficient of friction with increasing pressure by means of the flattening of the asperities in the rubber. This explains the results obtained by other workers in which the friction force increases with increasing sealed pressure up to a particular value and then begins to level out to a constant value. This result would tend to indicate a boundary lubrication process. However, these results could be the result of using the mean friction force of two seals, one showing a high friction, the other a low friction.

Kambayashi and Ishiwata also measuring the friction of single seals by a similar method to that of Müller (34) show varying frictions for the instroke and the outstroke although in this case the sealed pressure obviously changed with the length of stroke. However, boundary lubrication was again in evidence.

2.9.3. Film thickness

In spite of the available friction data indicating boundary lubrication, leakage still occurs. The friction data then alone cannot indicate the true state of affairs in the reciprocating seal. The leakage of seals demands that there must be, at some stage throughout the cycle, a fluid film between the seal and the shaft or cylinder surface.

Whether this film exists evenly around the circumference of the seal and over how much of the stroke length, has yet to be determined.

However, discussion can possibly bring some insight into the magnitude of the film.

Assuming an annular lubricant film between the seal and shaft, an equation for the leakage can be written as:

$$q = \frac{h^3}{6\zeta U} \cdot \frac{dp}{dx} \pm \frac{Uh}{2} \qquad (2.22)$$

The first term of equation determines the Poiseuille leakage of the seal and in all cases must be from a high to a low pressure that is a positive leakage.

The second term relates to the leakage due to the relative motion of the seal and shaft. For an outstroke this will be positive, for an instroke, negative.

In general it can be assumed that the film thickness for each stroke is different, thus:

$$q_{out} = \frac{h^3}{6\zeta U} \cdot \frac{dp}{dx} + \frac{Uh}{2} \qquad (2.23)$$

$$q_{in} = \frac{h'^3}{6\zeta U} \cdot \frac{dp}{dx} - \frac{Uh'}{2} \qquad (2.24)$$

$$\therefore \quad q_{net} = q_{out} - q_{in} = \frac{1}{6\zeta U} \frac{dp}{dx} (h^3 + h'^3) + \frac{U}{2}(h - h') \qquad (2.25)$$

Assuming a constant film thickness throughout the cycle, the shear flow term disappears and the leakage must be entirely due to the pressure gradient and hence positive.

An example can be taken using a typical leakage value obtained by Nau (38) for rectangular section rings of 20 cc/hr.

For typical seal operating conditions, this leakage would be caused by a seal operating with a film thickness of 265 micro-inches.

The mean film thickness then based on measured leakage values may be of the order of tens to hundreds of micro-inches, a very thin film.

The film shape is generally unknown, although simple theoretical work has assumed a linearly tapered film. However, more recent indications are that the seal operates in some cases in an elasto-hydrodynamic mode and as such should exhibit a fairly constant film throughout the majority of the constant with a pronounced 'nip' at the trailing edge. This is shown fairly conclusively for 'O' rings in the work by Hooke, Lines and O'Donoghue (26) but has yet to be determined for rectangular section or commerical designs of seal, which are, practically, much more important.

The review has indicated a number of attempts to determine the film shape and thickness in a reciprocating seal and the majority have used simulation, in some cases without a pressure differential, but others have attempted to apply a very low pressure gradient. Thus Blok and Koens (3) and also Roberts and Swales (47) used a circular section simulation on an 'O' ring without a pressure gradient and used optical interference methods to determine film shape and thickness. Both obtained a typical elastohydrodynamic profile, with values of film thickness between 40 and 300 micro-inches.

Film thickness values for simulated seals with a small pressure differential have been obtained by White and Denny (53) and more recently by Dowson and Swales (14). White and Denny (53) measured the leakage of their simulated seal and from that calculated a mean film thickness. These were in fact higher, in the range of thousands of micro-inches, than would be expected in a practical seal.

Dowson and Swales (14) however, used electrical techniques to measure the film thickness and the pressure distribution under a simulated seal, with pressure differentials up to 150 lbf/in^2. Their values of film thickness range up to 1200 micro-inches, again fairly large for a practical seal.

Nau (37) on the other hand used electrical techniques to measure the film thickness of square section seals for speed up to 100 ft/min and pressure differentials to 4000 lbf/ins^2. The results here were encouraging in that film values were around 200-300 micro-inches as predicted in the previous section when calculated from the leakage of such seals. The film shapes obtained were very variable and did not give typical EHL shapes but appeared to be more of an undulating nature. However, the method of measuring the films appeared to be successful and demonstrated the possibility of measuring the film thickness of practical seals in their working environment. O'Donoghue and Lawrie (42) also qualitatively measured the lubricating film in typical seals by a tracer technique and showed conclusively that a film did exist.

2.10 CONCLUSIONS

Leakage and friction values for various seals have been published by many workers and show generally that whilst friction can be higher than would normally occur if full fluid film lubrication were in evidence, the seals still leak. It has been shown that seals operate at low speeds in a boundary lubrication mode and, at higher speeds this can change to hydrodynamic lubrication which would be more likely to lead to leakage.

Several attempts to understand this phenomena have been made by measuring or theoretically predicting the film shape and its thickness. However, theoretical evaluations necessarily maintain that the seal is fully hydrodynamic and whilst this appears to be the case at fairly high speeds for 'O' rings under low pressure, many examples can be quoted for seals obviously working in a boundary lubrication mode which again still leak. Experimental attempts to measure the film shape have led to some indications about the film formation but have mainly relied on optical techniques which necessitate very smooth surfaces unlike the usual seal surfaces or have been seal simulations able to withstand only

very small pressure differentials. This may lead to incorrect conclusions in regard to practical seals where pressure up to 6000 lbf/in^2 are being used. Only one attempt has been made to measure the film thickness of seals in their true working environment and these results whilst not giving the answer, were a step in the right direction.

In general friction and leakage have been measured as the mean of two strokes. However, work has shown that the friction of each stroke can be different. Leakage has been measured over a number of cycles and quoted as leakage per unit time, but there is every reason to suppose that the leakage on the outstroke is entirely independent of the leakage on the instroke and one equation to cover all seals is therefore not very meaningful. Film thickness measurements deemed essential in any fundamental work concerning bearings, has been for all practical purposes ignored in spite of the fact that it is only through a knowledge of the lubrication process that the operation of reciprocating seals can be improved.

In view of these arguments, it seems essential, if reciprocating rubber seals are to be improved both through decreased leakage and friction or extended life at higher temperatures and pressures, that fundamental knowledge of the lubricating process be pursued vigorously by experimental and theoretical means.

2.11. SCOPE OF THE PRESENT WORK

In view of the conclusions reached from the literature survey a number of aims need to be achieved in order to advance the present knowledge on the lubricating mechanism of reciprocating rubber seals. These are as follows:

1. Techniques to measure the film thickness and pressure in the fluid film between the seal and its mating surface must be improved and must be utilised to determine the effect of many variables, but most important those of speed and pressure, on the film thickness and pressure for a seal operating under typical conditions found in hydraulic jacks and rams. The equipment must be able to measure the film thicknesses within the range expected for both the instroke and the outstrokes and

must be sensitive enough to show the major variations in film thickness and pressure throughout the seal contact.

2. The friction of the seal needs to be measured separately for the instroke and the outstroke in order that these can be correlated with the measurements of the film profile obtained in objective (1) above.

3. In order that design data can be eventually presented a theoretical solution to the problem is essential.

2.12. METHODS OF ATTAINING THE EXPERIMENTAL AIMS OF SECTION 2.11

The main aim of the experimental work was to measure the thickness of the lubricant film thought to exist between the seal and its mating surface. This was achieved in two ways. The first, the subject of chapter 3 used the property of interference fringes to measure the lubricant film between a rubber pad specimen and a reciprocating glass plate. Although not being a strictly analogous situation to that of a seal it was thought that the advantage of such a method outweighed the disadvantage. In this test method, the complete area of contact can be seen and it is a simple matter to determine the effects of speed and load on the film. Later modifications enabled the friction of the specimen to be measured in order to correlate this with the film thickness.

The second method used, the subject of chapter 4 utilised capacitance and piezo transducers to measure the film thickness and pressure in the fluid film for a seal operating under typical conditions associated with hydraulic jacks. The method of capacitance measurement had been used previously by Nau but in the present work the resolution of the transducer was improved and a wider range of variables tested.

Both of the above methods required considerable development before they could be used for the aims of the present work.

CHAPTER 3

AN INTERFEROMETRIC STUDY

3.1. DESIGN AND DEVELOPMENT

3.1.1. Introduction

The interference phenomena of light waves have been known and used for many years. The principle is as follows: suppose that a wave, at a certain point and time, has an amplitude X and another wave at the same point and time has amplitude Y in the same plane, then by the Principle of Superposition the instantaneous displacement of the combined wave is the algebraic sum of the separate amplitudes, thus R=X+Y. This principle can be applied to measure the thickness of thin layers or films of transparent media. Consider a beam of light projected normally on to a film of oil floating on a water surface, two reflected beams result since part of the incident light is reflected from the air/oil interface and part from the oil/water interface. The remainder of the light continues into the water and is variously absorbed or scattered. The two reflected beams are in general no longer in phase although both emanated from the same source, one wave having travelled an extra distance equal to twice the thickness of the oil film. The reflected waves interfere and, if the amplitudes of both waves are in phase, appear as a bright spot, if out of phase the amplitudes cancel and the spot appears dark.

The development of the theory of elastohydrodynamic lubrication led to the need to accurately determine the film thicknesses in various types of contacts and many methods have been used. Recently, a number of workers (5) and (13) have used optical interferometry to study such contacts, particularly the heavily loaded contacts of ball bearings. Most methods of measuring film thickness such as those of capacitance and inductance transducers, allow the film thickness to be measured at a single point only, whereas interferometry gives a 'contour' map of the complete contact area at any instant of time and from this point of view has a major advantage over all other methods. A major disadvantage, however, is immediately obvious, one of the contacting surfaces must be transparent. Cameron and co-workers in studying the elastohydrodynamic lubrication of ball bearing contacts have used diamond as the transparent medium to allow very high contact stresses to be obtained. The transparent medium most generally used, however,

is glass or perspex and certain problems of reflectivity present themselves, that is, the steel ball normally reflects considerably more light than the glass/oil interface and interference fringes are therefore not visible. Several methods of obviating this problem have been used, such as high density glass, and vacuum deposited metal films on the glass to increase the reflectance of the glass/oil interface. In this way the experiments have been very successful in showing the true shape of elastohydrodynamic contacts. Roberts and Tabor (48) have used interferometry methods to study the film thickness between sliding rubber and glass surfaces with water as a lubricant. Much of the early work by Roberts was devoted to providing the correct conditions to enable the interference fringes to be seen and forming an optically smooth surface on the rubber. However, these problems were overcome and several interferograms have been published.

Blok and Koens (3) describe experiments with a low elastic modulus material in which interference fringes were used to determine the film profiles in an 'O' ring contact pattern. Kirk (30) used a perspex cylinder covered with aluminium foil to obtain interference fringes between two perspex materials.

In view of the success of the above workers it was decided that, in conjunction with the capacitance transducer measurements of film thickness on the instrumented reciprocating seal rig (chapter 4), the technique of optical interferometry could be used to determine the film thickness in a seal contact situation. This would complement the capacitance technique and allow a 'contour' map of the seal contact to be seen. This method would also enable the effect of the change of direction at the end of a stroke and very short stroke lengths on the film thickness to be determined; two conditions which cannot be studied using the capacitance transducer method.

3.1.2. Use of white light fringes

The majority of work adopting the interference phenomena as a measuring tool, uses monochromatic fringes, because the dark and light bands represent known changes in film thickness if the wavelength of the illuminating light is known. Monochromatic light is also

sufficiently coherent to enable fairly thick films to be evaluated. However, the major disadvantage from the point of view of the present work is that the fringes represent 'contour' lines of equal film thickness, which are not 'labelled'. It is therefore difficult to determine whether the film thickness at one dark fringe is thicker or thinner than at the next dark fringe unless the shape of the film is known intuitively. Also unless the absolute value of film thickness at some point in the film is known only changes in film thickness can be measured. This problem can be solved by starting at zero film thickness and counting the dark fringes at a point as the film builds up.

An alternative method to determine whether the film thickness is increasing or decreasing and also to obtain absolute values of film thickness is to use white light or preferably light having a few well defined spectral lines. When fringes are formed, each wavelength is seen as a particular colour and as the film thickness increases the colours overlap and combine to form unique colours representing absolute values of film thickness. The order in which the colours appear indicates whether the film is increasing or decreasing. Once the colours and film thicknesses have been calibrated the shape of the film and its absolute thickness can easily be deduced.

3.1.3. Conditions necessary to form interference fringes

Although interference fringes are theoretically simple to obtain, in practice a number of practical problems arise.

The main problems stem from the physical conditions imposed by the system, a lubricated contact between rubber and glass. In practice the amount of light reflected from the contacting surface of two transparent materials is dependent on the refractive indices of the two materials:

$$\% \text{ of light reflected} = \frac{(n_1 - n_2)^2}{(n_1 + n_2)^2} \times 100 \qquad (3.1)$$

where n_1 and n_2 are the refractive indices of the materials, forming the interface. In the case of the lubricated contact the important interface is that of the glass and oil which, because the refractive indices

of the materials are almost the same, reflects only about 0.005% of the incident light. In order to obtain interference fringes the oil/rubber interface must also reflect a similar amount, and the rubber surface must be optically smooth. There was a further problem in that the amount of light reflected at an air/glass interface is of the order of 4% and this would swamp any light reflected from the contact, making the interference fringes invisible. In order to obtain maximum colour definition it is also essential to reduce to a minimum any stray light in the optical system.

Considerable effort was required to solve the above problems and the solutions are discussed in the following sections

Counterfaces

A solution to the problem of reflection at the air/glass interface was supplied by Mr. A. D. Roberts of the Mechanical Engineering Department of Cambridge University. This involved the deposition of a coating of magnesium flouride (MgF2) on the front surface of the glass, the thickness of which would be a quarter of the wavelength of light and would have the effect of reducing the reflectivity of the glass surface. Similar coatings are used for lenses in cameras and optical equipment. A coating of magnesium flouride would however only be effective for one particular wavelength of light and double or triple layers were available commercially, which covered a wider part of the visible spectrum.

One of these was in fact used and several pieces of $\frac{1}{4}$ inch thick plate glass with non-reflective coatings were obtained. Because the thickness of the coating was only a quarter of the wavelength of light, it required exceptional care in cleaning, as very thin films of oil or finger prints altered the optical parameters of the coating, and its non-reflecting property was then lost. Careful cleaning in trichloroethylene was found to be the most successful method of dealing with the problem. The glass was first carefully cleaned with cotton wool soaked in trichloroethylene and then dipped into a bath of clean laboratory grade trichloroethylene. When removed the glass was left to dry freely. It was then carefully fitted to the rig ensuring that the cleaned surface was

not touched or smeared at all. Providing oil was not spilt over the surface it remained clean for long periods of time. Later experiments used a much thicker piece of 'Perspex' in place of the glass which eliminated the need for the non-reflective coating.

In order to find suitably smooth rubber surfaces a number of carbon filled rubbers were examined. One, a filled neoprene rubber, satisfied the smoothness criteria as well as could be expected, but when tried in the rig, it was found that the amount of reflected light was much greater than from the glass/oil interface, and the fringes were again swamped by the excess light.

In order to be certain that interference fringes could be obtained if the reflectivity at the oil/rubber interface could be reduced, an attempt was made to obtain fringes between two glass surfaces separated by an oil film, thus ensuring that the intensities of the two reflected beams were the same. The first glass/air surface had a non-reflecting coating, whilst the back surface of the second piece of glass was coated with a matt black paint to prevent reflection of the light transmitted through the lubricated contact. Using this method interference fringes were obtained with both air and oil between the glass plates and showed that if the reflection of the glass/oil and the oil/rubber interfaces could be made the same, interference fringes would be visible.

The possibility of using a transparent rubber and relying on the relative refractive indices of the oil and rubber to give reasonable reflectivity was then raised. Roberts at Cambridge had used unfilled gum rubber as the low modulus material, which is translucent and very soft but would not have been compatible with the mineral oil to be used for this investigation. However, a transparent silicone rubber, intended for potting electronic components, was found to be commercially available and attempts to obtain interference fringes with this material were successful.

The first samples tried were completely clear throughout, and considerable back scattering of the light passing through the oil contact occurred. The back surface of the specimen was therefore painted with matt black paint, as was the glass mentioned above. However, because

of the flexibility of the rubber the paint soon flaked off. New samples were then made in which only the first few millimetres of the specimen consisted of clear rubber, the remainder being composed of rubber loaded with carbon black, which had the same function, of absorbing stray light, as did the matt black paint. This worked successfully and was adopted for all specimens used.

The unfilled silicone rubber such used was very soft, around 40 IRHD, compared to a normal filled nitrile rubber of 70-80 IRHD and in order to increase the hardness of the rubber some specimens were made of clear polyurethane rubber, the hardness of which could be varied over a wide range. Hardnesses of 65 and 90 IRHD were obtained.

Fluids

The refractive index of the polyurethane rubber was higher than that of the silicone rubber and attempts to obtain interference fringes with mineral oil did not give very good results.

Of the many fluids considered, silicone fluid, having a refractive index of 1.4 was tried and gave excellent fringes with the polyurethane rubber, but none at all with the silicone rubber. This latter fact was understandable as the silicone fluid and rubber have the same refractive index. The silicone fluids used were Midland Silicones Ltd., type MS 200 with viscosities of 26, 65.5, 260 and 650 x 10^{-7} reyns (20, 50, 200, 500 cSt.).

Other fluids used were water and paraffin B.P., these being simple fluids with no surface active constituents.

Both the rubbers used gave satisfactory fringes with at least two of the above fluids and more comprehensive details of the fringe definition obtained with various rubber/fluid combinations are given in Table 3.1. It was found, however, that the best fringe definition was obtained with the following combinations

(i) plate glass/Tellus 27/silicone rubber

(ii) plate glass/Paraffin BP/silicone rubber

(iii) plate glass/silicone fluid/polyurethane rubber

Optical System	Reflect. air/glass%	Counterface		Reflect. glass/fluid%	Fluid		Reflect. fluid/rubber%	Rubber		Notes
		description	RI		description	RI		description	RI	
Mk I	0.5†	Plate glass + MLNR coating on air face	1.51	0.01	Tellus 27 (mineral oil)	1.48	0.01	Plate glass + matt black rear face	1.51	fringes visible
Mk I	0.5	Plate glass + MLNR coating on air face	1.51	0.01	Tellus 27 (mineral oil)	1.48	-	Neoprene moulded sheet	N	too much reflected light from rubber face
Mk I	0.5	Plate glass + MLNR coating on air face	1.51	4.41	Air	1.00	-	Neoprene moulded sheet	N	fringes visible
Mk I	0.5	Plate glass + MLNR coating on air face	1.51	0.01	Tellus 27 (mineral oil)	1.48	0.07	Silicone rubber*, 40 IRHD clear throughout	1.40	poor fringes
Mk I	0.5	Plate glass + MLNR coating on air face	1.51	0.01	Tellus 27 (mineral oil)	1.48	0.07	ditto plus matt black point on rear face	1.40	better fringes but paint flakes off
Mk II Mk III Mk III	0.5 4.40x	(a) as above (b) thick perspex (c) thick glass	1.51 1.49 1.51	0.01 0.001 0.01	Tellus 27 (mineral oil) Tellus 27 (mineral oil) Tellus 27 (mineral oil)	1.48 1.48 1.48	0.07 0.07 0.07	ditto, but carbon filler in rear of test piece (no paint)	1.40	fringes satisfactory
Mk II	0.5†	Plate glass + MLNR coating on air face	1.51	0.143	Silicone fluids	1.40	0.00	ditto, but carbon filler in rear of test piece (no paint)	1.40	no fringes
Mk II, III	0.5 4.40x 4.40x	(a) as above (b) thick perspex (c) thick glass	1.51 1.49 1.51	0.143 0.097 0.143	Silicone fluids Silicone fluids Silicone fluids	1.40 1.40 1.40	0.09 0.09 0.09	Polyurethane rubber ** 65 or 90 IRHD carbon filler in rear of test piece	1.488 1.488 1.488	fringes good
Mk II	0.5	Plate glass + MLNR coating on air face	1.51	0.01	Tellus 27 (mineral oil)	1.48	0.0007	Polyurethane rubber ** 65 or 90 IRHD carbon filler in rear of test	1.488	poor fringes
Mk II	0.5	Plate glass + MLNR coating on air face	1.51	0.402	Water	1.33	0.06	Silicone rubber as above	1.40	fringes visible
Mk II	0.5	Plate glass + MLNR coating on air face	1.51	0.018	Paraffin B.P.	1.47	0.047	Silicone rubber as above	1.40	fringes satisfactory
Mk II	0.5	Plate glass + MLNR coating on air face	1.51	0.018	Paraffin B.P.	1.47	0.0037	Polyurethane rubber as above	1.488	poor fringes
Mk II	0.5	Plate glass + MLNR coating on air face	1.60	0.152	Tellus 27 (mineral oil)	1.48	0.07	Silicone rubber as above	1.40	fringes satisfactory

TABLE 3.1 Counterface, fluid and rubber material combinations used during the test program.

* I.C.I. Ltd. "Silicoloid 202"; ** E.M.I. Ltd. "Feldex 984 B"; †Reflectivity of MLNR coating; x eliminated by Mk II system.
N = no value known; RI = refractive index; MLNR = multilayer non reflective; IRHD = International Rubber Hardness Degrees.

3.1.4. Specimen manufacture

The specimens made with square edges were moulded in a brass mould rigidly clamped to a glass plate. By this means the specimens acquired a sharply square edge having little or no flash and an optically smooth and flat front surface.

Experiments with the square edged specimens indicated the need for specimens having a tapered or chamfered edge and several methods were tried to achieve this. However, none of the methods was entirely satisfactory when judged in terms of the effect of the edge on the seal film profile. The major difficulty appeared in avoiding a micro-step at the junction between the chamfer and the seal face, which when the specimen was sliding produced similar effects to the square edge specimens. The methods of forming the chamfer were:-

(i) cutting at room temperature with a razor blade

(ii) grinding at room temperature

(iii) cutting at room temperature with a microtome

(iv) cutting at liquid nitrogen temperature with a microtome.

In order to achieve a smooth transition between an inlet edge curve and the flat face of the specimen, attempts were made to mould specimens having a radius of approximately 0.020 ins. on the leading and trailing edges. This required a considerable amount of experimentation before success was achieved.

The methods tried were:-

(i) a strip of thin, smooth PTFE film was fitted into the mould so as to cover two sides and the glass base of the mould. At the mould side/glass corner the PTFE formed a smooth curvature of the required radius. The disadvantage using this method was that the rubber leaked past the PTFE film during curing. Some satisfactory specimens were made however but the failure rate was high.

(ii) a mould was formed from a glass microscope slide by heating the slide and carefully bending it round a graphite former. The method was more effective than (i) but mould breakage was a problem and this was particularly so during the bending of the glass slide.

(iii) the final method was to manufacture a metal mould, form

ground and hand polished to the required section. The contact surface of the specimens made in this mould were not as flat as when the rubber was moulded against glass, but was acceptable. The mould and a specimen are shown in figure 3.1.

It was found that the silicone rubber was simple to mould and cure and because of the absence of solid particles in the rubber, it could be moulded against a glass surface to give a completely smooth and flat surface. The material was supplied by I.C.I. Limited, Nobel Division, Scotland and was designated Silcoloid 202. The mixed rubber was cured in an oven for 4 hours at a temperature of 150°C and it was found that leaving the moulds in the oven to cool slowly overnight eliminated a tendency for the flat surface, in contact with the glass, to warp. In filling the mould, clear rubber was first poured in until it was about $\frac{1}{8}$ inches thick over the surface of the glass. This was then partly cured before more silicone rubber loaded with carbon black was poured in until the mould was filled. The final specimen size was 10 mm square on the flat face, about 15 mm long, the first few millimetres of which were of clear rubber. After the curing cycle the specimens were easily removed from the moulds, no release agent being required.

Attempts at moulding the polyurethane samples in the laboratory were however less successful and after curing, all the specimens contained bubbles of gas making them useless for test purposes. This was in spite of strict adherence to the manufacturers instructions. However, specimens were obtained from EMI Electronics of Feltham who had had considerable experience with this material. These were most successful.

3.1.5. Optical systems

Interference fringes were to be obtained in an oil film between a reciprocating glass plate and a rubber specimen pressed against the glass.

Mk.I system: normal incidence lighting

The system initially used is shown in figure 3.2. Light from a 'point source' (mercury vapour lamp) was collimated by a lens system and projected onto a beam splitter. The beam splitter reflected a



Fig. 3.1 Rubber mould and uncut specimen

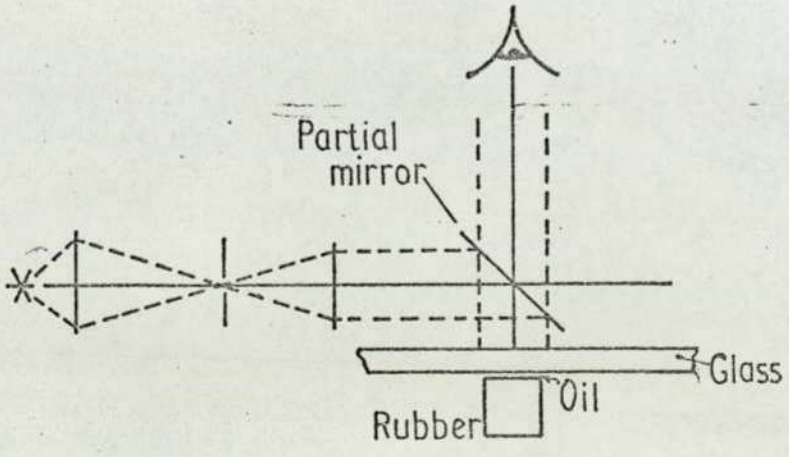


Fig. 3.2 Mk I optical system: using normal incidence lighting

proportion of the incident light onto the contact of interest to produce interference fringes in the oil film which were viewed through the beam splitter with the naked eye or with a microscope.

This method is successful where there is sufficient light available to allow for the losses in the beam splitter, this device being particularly inefficient as even a partial mirror reflects only 40% of the incident light, the remainder being transmitted and absorbed. This means that of the light available from the source only 40% is reflected on to the contact of interest and of this perhaps only 10% is reflected from the contact. The light then has to pass through the beam splitter again to be seen and of the light available only 40% is transmitted. The light available for viewing is thus of the order of 2% of that from the source. For situations where static or slow moving contacts are of interest this system gives excellent results.

Mk. II system - angled illumination

Because of the low intensity of light available using the beam splitter, exposure times for photographic recording of the fringes were of the order of 2-5 seconds, and obviously too long to obtain adequate sharpness under dynamic conditions.

As explained above, the majority of the light available from the lamp was lost by the beam splitter, and elimination of this device would enable much shorter exposure times to be achieved.

The modification of the system is shown in figure 3.3. It consisted of projecting the collimated beam of light from the high pressure mercury arc lamp on to the contact surface at an acute angle. The beam was then reflected at the same angle and could be easily viewed. This gave a significant increase in intensity and allowed photographic exposure times to be reduced to the order of 1/500 sec.

The modification to the system does introduce a small error in the final measurement of the film thickness and calculation of the error was achieved as follows:

A ray trace is shown in figure 3.4 and for oblique incidence of the light beam:

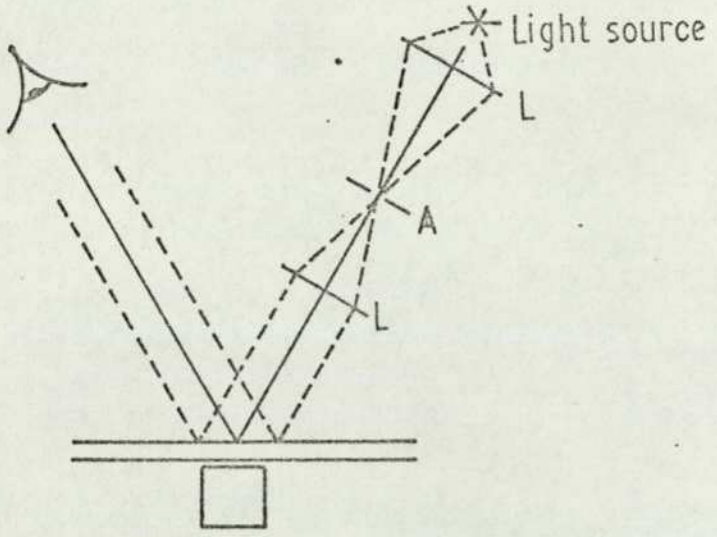


Fig. 3. 3 Mk II optical system: using an acute angle of incidence lighting

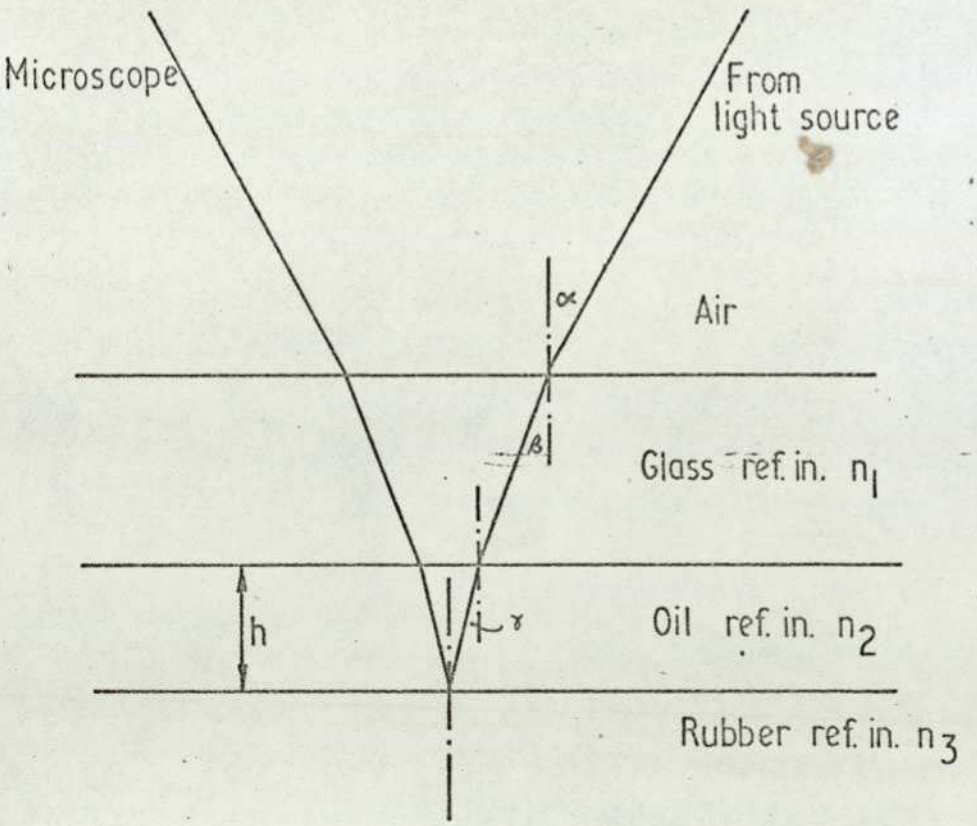


Fig. 3. 4 Ray diagram for Mk II optical system

at air/glass interface

$$n_1 \sin\alpha = n_2 \sin\beta$$

$$\therefore \sin\beta = \sin\alpha \cdot n_1/n_2 \qquad (3.2)$$

at glass/oil interface

$$n_2 \sin\beta = n_3 \sin\gamma$$

$$\therefore \sin\gamma = \sin\beta\ n_2/n_3 = \sin\alpha \times n_1/n_3 \qquad (3.3)$$

for a measured angle of incidence of α of 12°

$$\gamma = \sin^{-1}(\sin 12. \quad 1.0/1.5)$$

$$\gamma = 8^\circ$$

The percentage error introduced if this angle is neglected is:

$$100 \times \left\{\frac{1}{\cos\gamma} - 1\right\} \qquad (3.4)$$

$$= 100\ (\sec\gamma - 1)$$

$$= 0.98\%$$

which can safely be neglected.

Mk. III system - Köhler illumination with a thick glass plate

The original system of lenses used for collimating the light beam provided a larger area of light than was really necessary, but by changing to Köhler illumination, a system used for illuminating microscope specimens, both the area and shape of the light beam could be controlled. This enabled a squared shaped area of light, just covering the specimen to be projected and considerably reduced the amount of stray light. More important however it was realised that the reflected beam of light from the front glass surface was laterally displaced from the beams of interest reflected from the rubber/glass contact. This was an important discovery as it meant that by using a thicker glass plate the lateral

displacement of the two reflected beams could be increased to such an extent that the stray, unwanted beam could be made to miss the microscope objective completely. By this means the non-reflective coating on the front surface of the glass was rendered unnecessary, which saved the cost of the coating, improved tremendously the fringe definition and eliminated the need to carefully clean the glass surfaces. The final system adopted is shown in figure 3.5.

3.1.6. Calibration of white light fringes

Calibration of the white light interference fringes was simply achieved by photographing an arbitrary film shape illuminated firstly with monochromatic light and then with white light. For the present work the arbitrary film shape was formed by pressing a large radius lens against the glass surface. Illuminating the film shape with monochromatic light of known wavelength created black and white fringes in the contact, and these were photographed. Without changing the contact, a similar photograph was taken using white light.

Mapping of the contact shape was achieved by noting the spacing of the dark bands, which represented change in film thickness of half a wavelength of the monochromatic light used, the film thickness at the centre of the lens being assumed to be zero.

A similar exercise using the coloured photograph and noting the position of the various colours enabled a direct comparison to be made of film thicknesses and their representative colours.

A descriptive chart of the calibration is given in figure 3.6. showing the film thickness against the colour bands.

3.1.7. Mechanical details of the rig

Basic design

The rig decided upon for the optical experiments was basically very simple, consisting of a small specimen of rubber pressed against a reciprocating glass plate. The film thickness could be viewed by looking through the glass plate. A diagrammatic view of the rig is shown in figure 3.7.

The specimen of rubber was A held in a holder, B, attached to the slider C. A small pneumatic cylinder, D, was used to load the

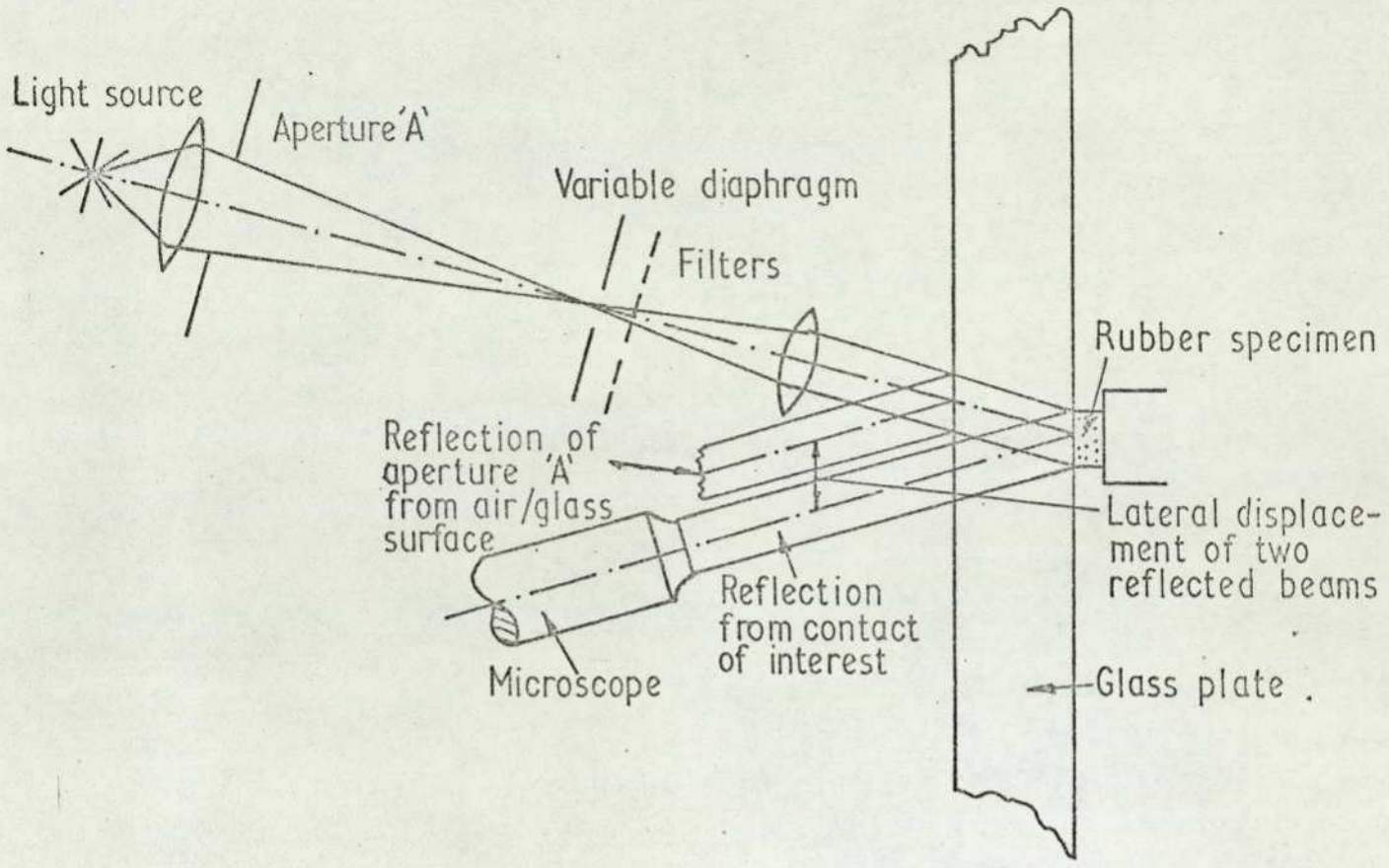


Fig. 3.5 Mk III optical system: using Kohler illumination in conjunction with a thick glass plate

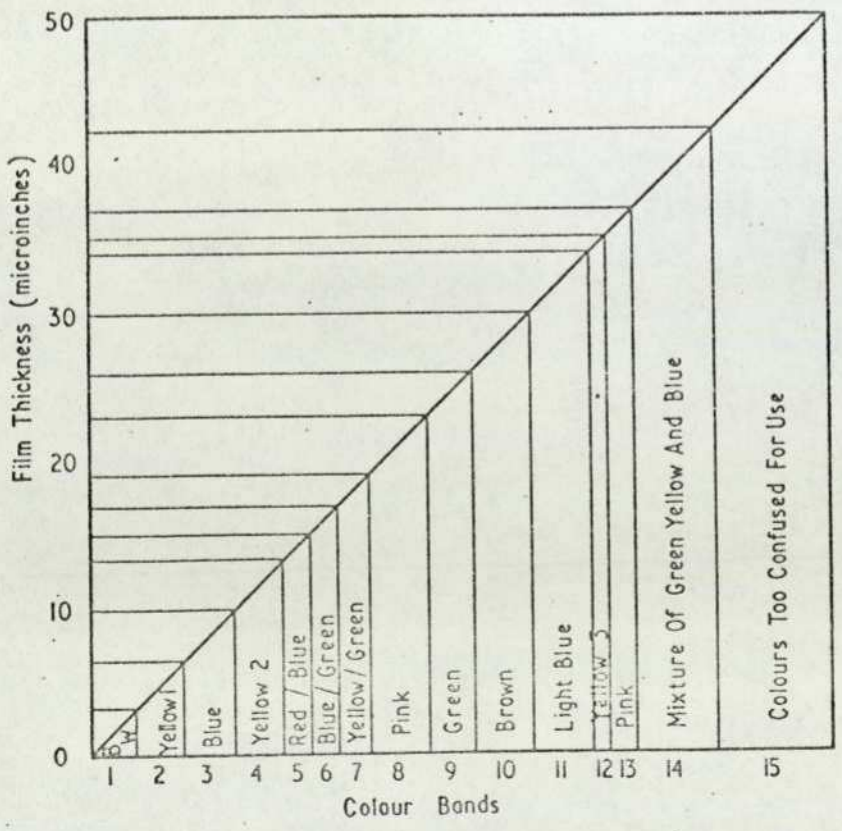


Fig. 3.6 Calibration of interference colours

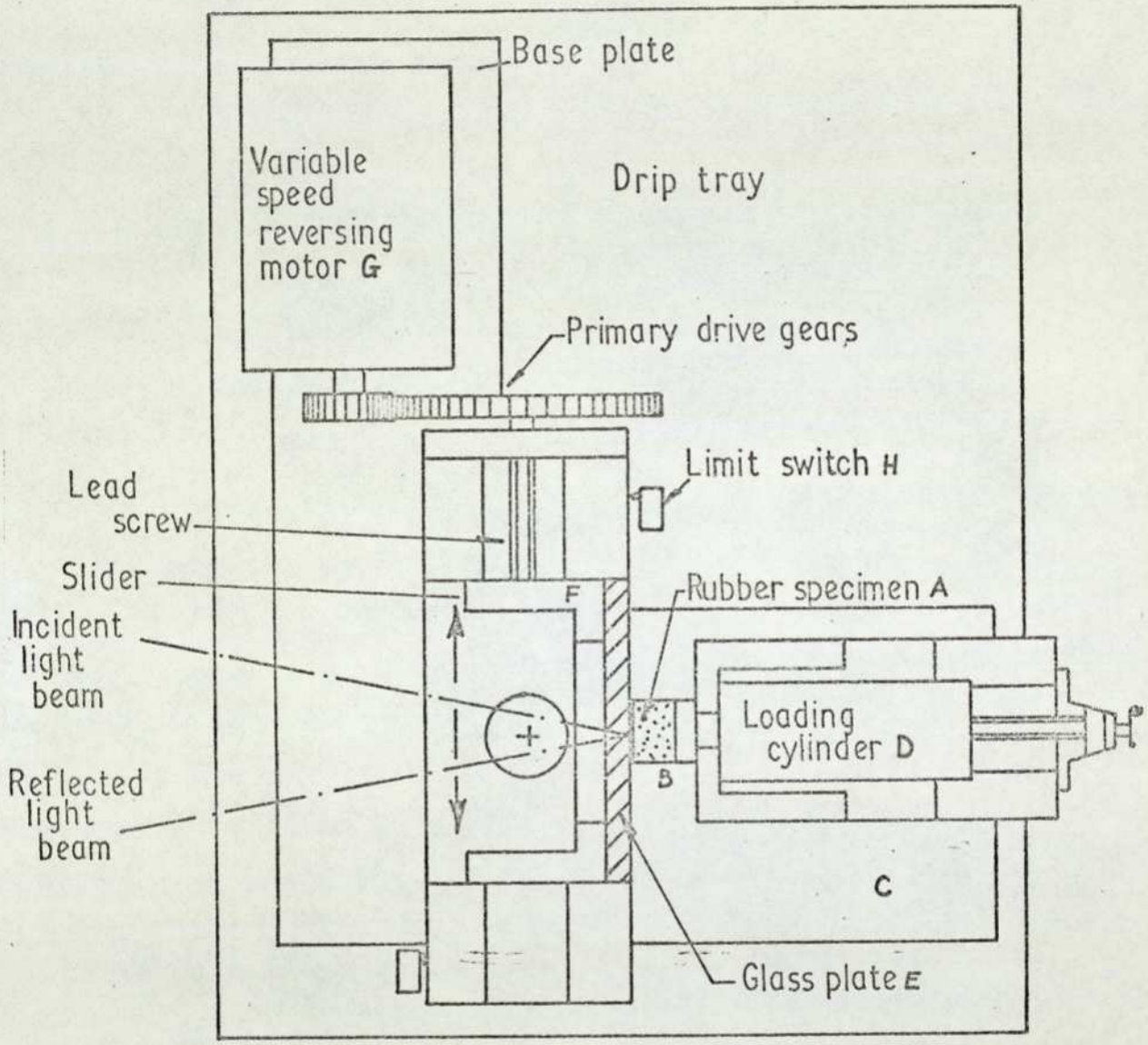


Fig. 3.7 Diagrammatic plan view of optical rig layout

specimen against the glass plate, E, which was clamped to a second slider, F, at right angles to the first. In order that the second slider had a smooth steady motion it was driven, via spur gears by a variable speed reversing motor, G. Suitably placed microswitches, H, enabled the motor to be reversed, the stroke length being approximately 4 inches. The speed of reciprocation was controlled via a tachogenerator in the feedback system of the motor speed controller and displayed on a suitable meter and was constant throughout the stroke. Basic variations in the speed could be obtained by the simple process of changing the driving gears between the spindle of the motor and the lead screw. The speeds used were in the range 0-5 ft/min., much slower than those of the instrumented rig, but early high speed tests had shown that it was impossible to view the film and note the changes in it at speeds in excess of this, without using high speed photographic techniques.

The two slides were mounted on a rigid base plate, the whole rig being placed in a large oil collecting tray.

Oil was originally fed to the contact area by means of a small pump but later tests using silicone fluid utilised a simple drip feed system.

The complete rig is shown in figure 3.8.

Measurement of friction

To enhance the usefulness of the optical rig by obtaining a correlation between film thickness and friction, later tests used a second specimen holder. The second design, shown in figure 3.9 mounts the specimen in a holder free to swing on two needle roller bearings. The specimen holder is restrained by means of a cantilevered beam and the deflection of the specimen holder, caused by the friction between the rubber and glass, is monitored by the linear displacement transducer, the measured displacement being directly proportional to the friction force. The total displacement is of the order of $\pm$ 0.005 ins. at the specimen, representing a specific friction of approximately $\pm$ 100 lbf/in^2.

Short stroke length operation

A modification to the rig consisted of adding a reed switch in addition to the two microswitches and a magnet attached to the

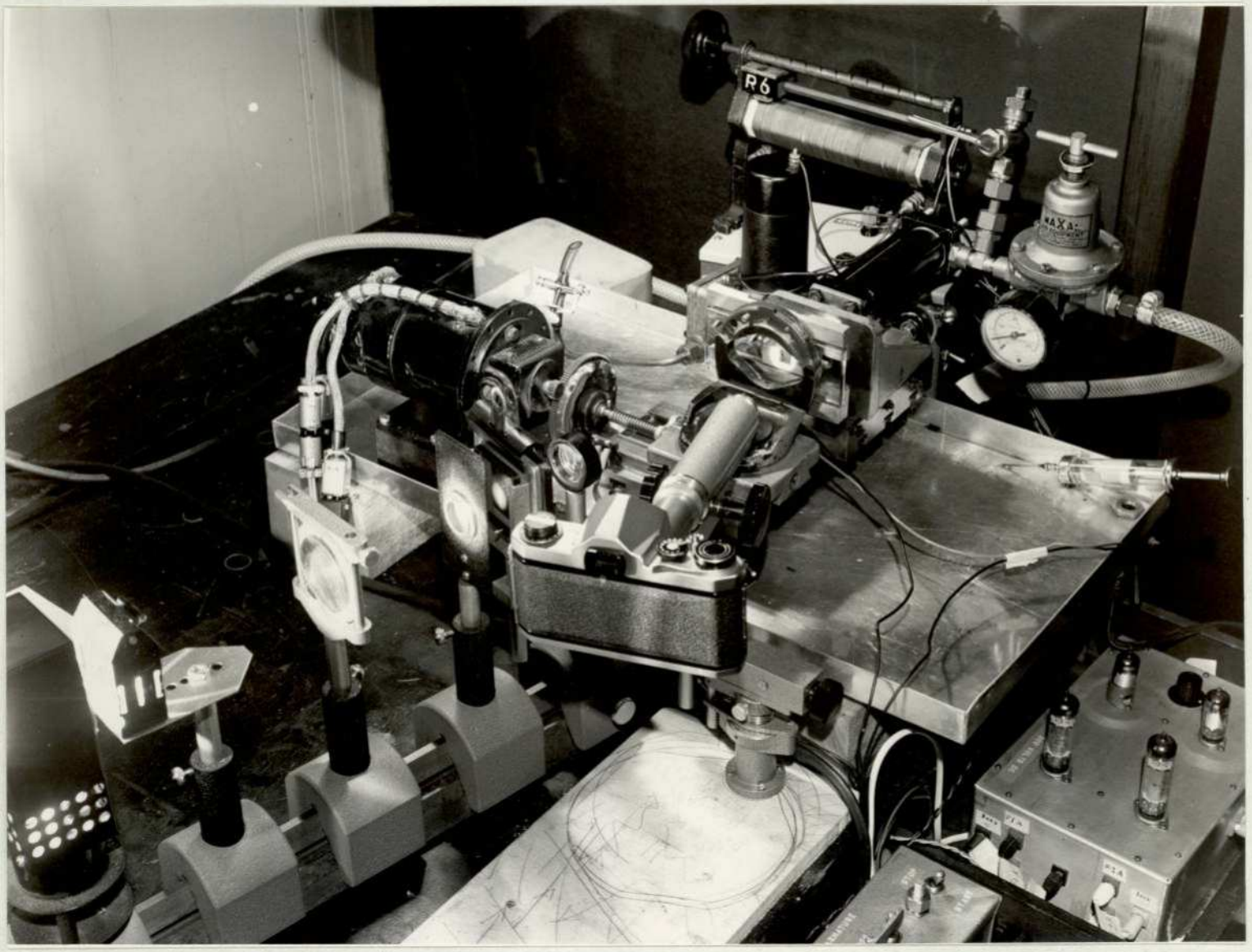


Fig. 3.8 Optical rig for interferometric study

reciprocating slide which enabled continuously variable stroke lengths to be achieved. A switch allowed a changeover between long strokes controlled by two microswitches to short strokes using one microswitch and the reed switch without stopping the reciprocation of the slider. The long stroke length was therefore used to form a steady fluid film between the specimen and the glass surface before switching to a short stroke cycle, enabling the effect of short strokes on a developed lubricant film to be studied.

3.1.8. Photographic techniques

The simulated seal in this rig was 1 cm. square on the sealing surface and the fringes could be seen with the naked eye but a magnified view could be obtained using a microscope. Initial tests were conducted using a standard travelling microscope, which could only traverse in one direction and a special microscope was later obtained which was capable of traversing in two dimensions and which also had a much greater range of magnification. This allowed small areas of the seal to be more closely examined. The microscope had a maximum magnification of x 45.

In order to study the interference fringes more closely, attempts were made to photograph the fringes using a Polaroid Land camera and these attempts used the Mk. I lighting system. The Polaroid camera allowed coloured photographs to be obtained almost immediately and greatly reduced the overall time required to develop suitable techniques, and to determine exposure times.

The first attempts proved a failure in that although the fringe definition and colour was very good when viewed with the naked eye, the coloured prints of the fringes generally had a blue cast over them. It was at first thought that this was due to the excess of blue and ultra-violet light in the source, the high pressure mercury vapour lamp. A range of filters of the ultra-violet and short wave-length cut-off types was tried but without success. The mercury light source was known to have an excess of ultra-violet and blue light and so these filters were incorporated permanently into the system.

In addition to these experiments using various filters, several

types of colour film were tried using a 35 mm camera with a through-the-lens light metering system, allowing correct exposure times to be obtained repeatedly even with large variations to the light system. The various films used were as follows:

(i) Agfacolor CT18 (50 ASA)

(ii) Ektachrome (160 ASA including push-processed film with a rating of 320 ASA)

(iii) Ansochrome (200 and 500 ASA).

All these attempts resulted in the same fault, a blue appearance throughout the photograph.

The next possibility was the light source, and a number of sources including xenon, tungsten filament and quartz iodine were tried but without success.

Throughout these attempts the exposure time for all of the films including the very high speed Ansochrome colour film had been of the order of 2-5 sec., which eliminated the possibility of recording the interference fringes under dynamic conditions. The Mk.II lighting system was then tried, and gave a much more intense beam of light through the microscope. With this system neutral density filters were required in the light beam before the fringes could be viewed with the naked eye. However, this state of affairs was ideal for the colour film as the exposure time could then be reduced by several orders of magnitude and correctly exposed film could be obtained with exposure times of the order of 1/500 second allowing fringes under dynamic conditions to be recorded. Also with this reduction of exposure time came the improvement in the colour definition of the film and satisfactory recording of the fringes could be achieved. An example of the coloured fringes is shown in figure 3.10.

In general, for photographic film the product of light intensity and exposure time is a constant and therefore doubling the light intensity will halve the exposure time. However, this 'reciprocity' law only relates to a certain range of exposure times between approximately 1/1000 of a second and 1 second. The times of 2-5 seconds required for the Mk.I lighting system were outside of this range. Colour film is

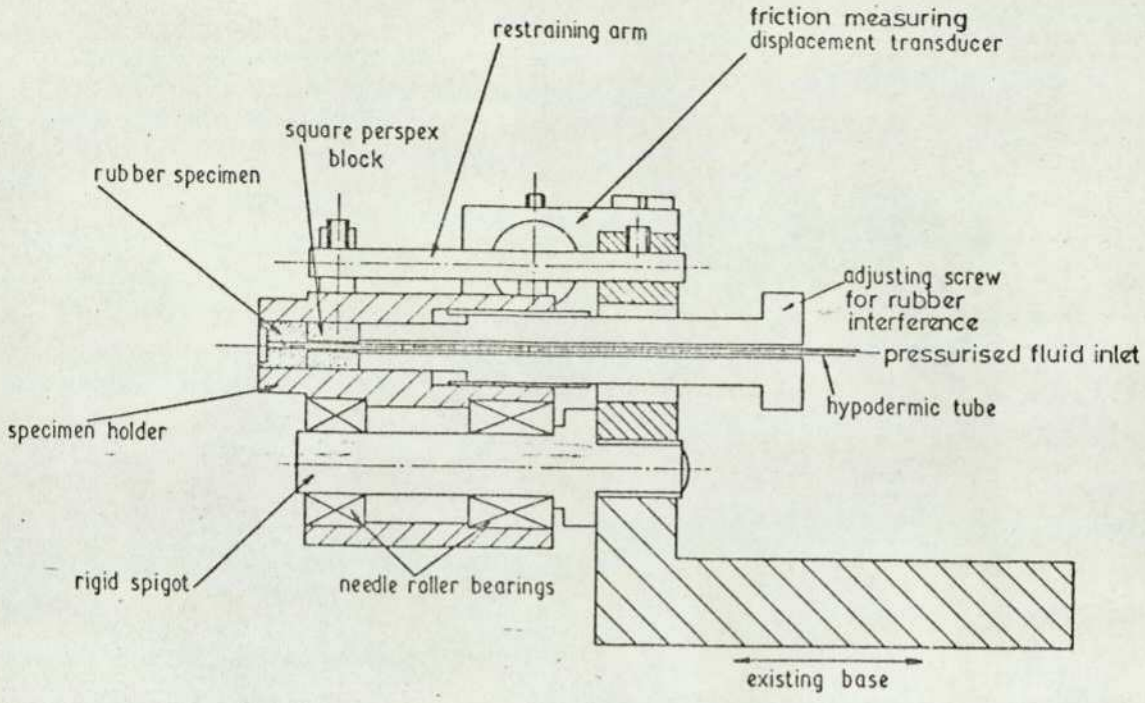


Fig. 3.9 Mk II specimen holder for the measurement of friction

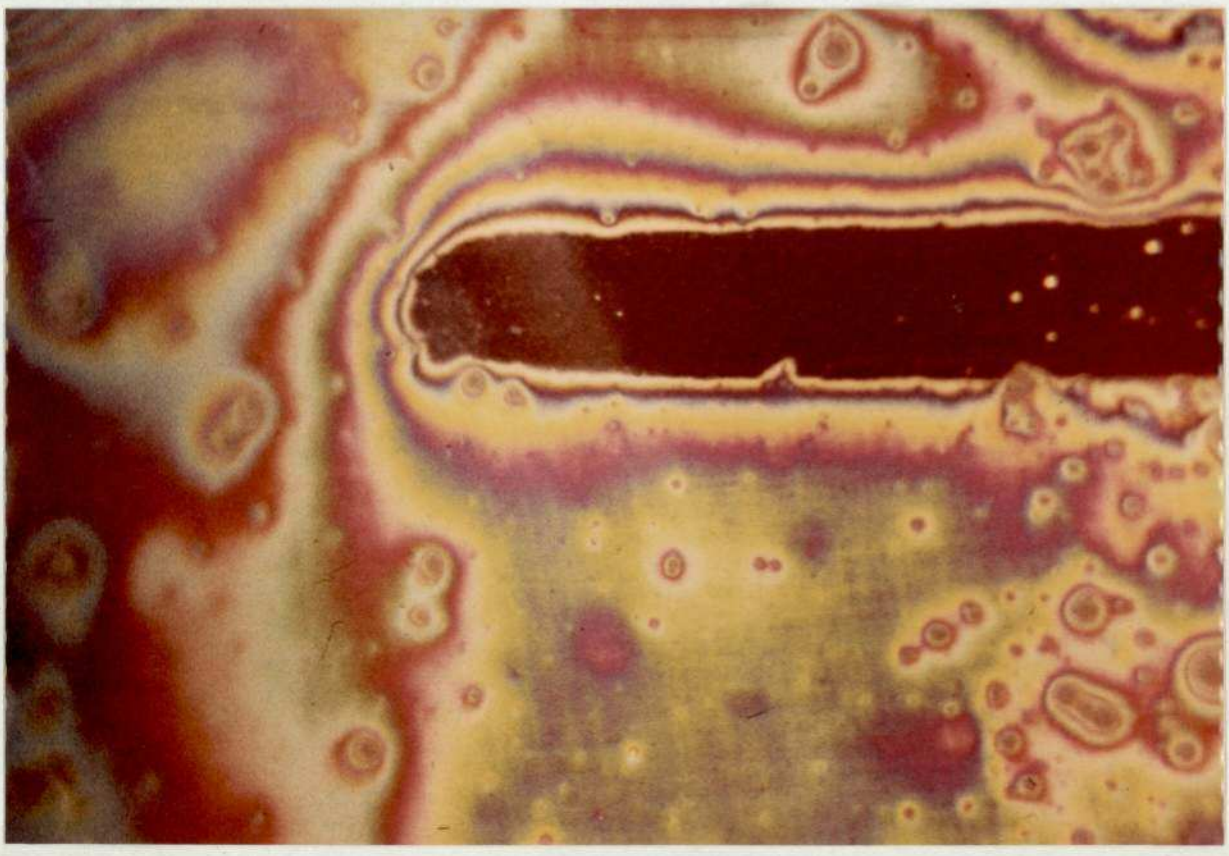


Fig. 3.10 Example of coloured interferogram

considerably more susceptible to 'reciprocity' failure than black and white film because the film is composed of three different layers of emulsion, each having its own 'reciprocity failure' characteristics and in this particular instance it was thought that the blue layer of the film was the one at fault leading to blue overcast films when long exposure times were used. The use of shorter exposure times brought them within the exposure range of the film and gave better colour definition.

3.2. RESULTS

3.2.1. General observations

The initial development of the interference techniques discussed above used a soft transparent silicone rubber in combination with a widely used hydraulic mineral oil, Shell Tellus 27. The specimens had sharp, square leading and trailing edges, but under light loading, an oil film formed between the rubber and the glass, in which interference fringes could be seen. Variation in load or speed caused change in the film thickness which could be seen as changes in the colour in the film at each point, which in turn could be seen to move through the contact whilst the glass was sliding. Because fringes were formed throughout the contact, a visual estimate could be rapidly made of the film thickness throughout the contact.

In general the interference colour patterns under such conditions indicated that the fluid film was uniform across the contact and lacked the 'nip' at the trailing edge of the specimen usually associated with elastohydrodynamic lubrication. However the preliminary tests did confirm that a fluid film formed between the rubber specimen and the glass surface and that disturbances in the film such as would be caused by changes in speed or pressure moved through the film at a speed between zero and the speed of the glass slider, a phenomena studied in greater detail in a later stage.

In addition to the film, it was noted that stopping the glass after a period of movement trapped a certain amount of oil in the contact and, in time, the edges of the specimen contacted the glass surface leaving a 'bubble' of oil trapped between the glass and the rubber. The 'bubble'

disappeared over a period of time, and later experiments showed the reasons for this phenomena.

During the formation of the 'bubbles', the edges of the silicone rubber approached the glass surface until the colour of the contact was white. When the bubble had finally disappeared the complete area of the contact appeared white, indicating that a film of oil approximately 3.5 microinches thick still existed in the contact.

The remaining white film observed was unexpected because at a plain surface comprised of two transparent materials, reflected light undergoes a phase change of 180° if the light initially passes through the less dense material and the contact in this case should appear black, as was found in some later experiments.

The above are some of the phenomena observed during preliminary testing and development of the system which are discussed more fully in the following sections.

3.2.2. Observation of 'static' bubbles in the contact area

When sliding motion between the rubber and the glass was stopped, the fluid in the film formed a 'bubble' in the central part of the contact as the film thickness at the edges of the specimen rapidly thinned to a white film. In many cases the shape of the bubble was circular but this was not necessarily so and possibly depended to a great extent on the contact stress distribution in the rubber specimen itself.

A similar, but much deeper bubble could be formed if the rubber was made to normally approach a stationary glass plate. In this case the depth of the bubble could be 50 light bands, (356 microinches) or more and cover up to 75% of the contact area.

A similar phenomenon has been reported by Dowson (13) in the study of hard elastohydrodynamic lubrication of steel spheres under normal approach conditions. Optical interferometry combined with high speed photography was used to enable the bubble configuration to be evaluated and once formed, the bubbles remained indefinitely.

Observation of several bubbles formed between silicone rubber and a glass surface showed that the bubble in this case was not permanent the size decreasing with time. It seemed possible that the oil gradually

leaked away through the very thin film at the edges of the specimen, but a simple theoretical analysis, Appendix A, revealed that to achieve this at the observed rates would require a considerably higher pressure in the fluid than could possibly be present.

This evidence suggested that the fluid was absorbed into the rubber. In view of the very small volumes of oil involved (approximately $5 \times 10^{-6} in^3$) and the swelling phenomena associated with rubber/oil systems, such behaviour is entirely feasible.

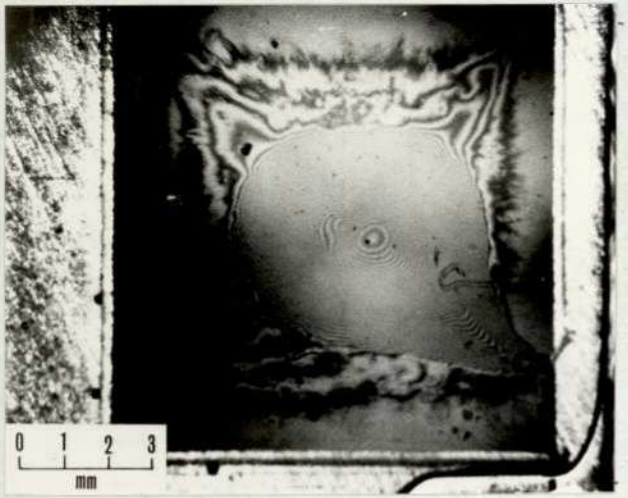
If this was indeed the case, the rate of disappearance of the oil in the bubble would be expected to depend on a number of factors such as the nature of the rubber, the fluid used and the history of the rubber as regards its exposure to the fluid, a new piece absorbing fluid at a higher rate than a previously saturated one.

In order to test this hypothesis, two specimens were tested, a new piece of rubber, and a specimen soaked in the test fluid at atmospheric temperature and pressure for 550 hrs. It was known from previous swell tests that the rubber reached its saturation point in this fluid after approximately 300 hours. The results of these tests confirmed the expectations, the bubble formed in the new piece of rubber disappearing in only 30 minutes whilst 1200 minutes were required by the saturated specimen. In each case a white residual film was formed.

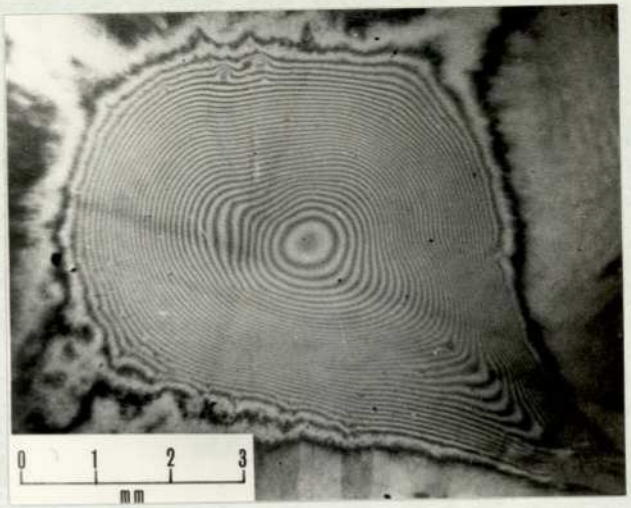
During the period in which the bubbles were disappearing photographs of the fringe patterns were taken at fixed time intervals, figure 3.11. With the aid of a planimeter, the volume of the bubble at each period of time was calculated. A typical result for volume and leakage rate against time is shown in figure 3.12. However since the oil absorption process was expected to follow the usual diffusion equation, the bubble volume was plotted against the parameter (bubble area)$\cdot$x (time)$^{0.5}$ derived in Appendix B. The result, figure 3.13, shows a straight line relationship confirming that the bubble was indeed absorbed into the rubber.

3.2.3. The propagation of disturbances in the film

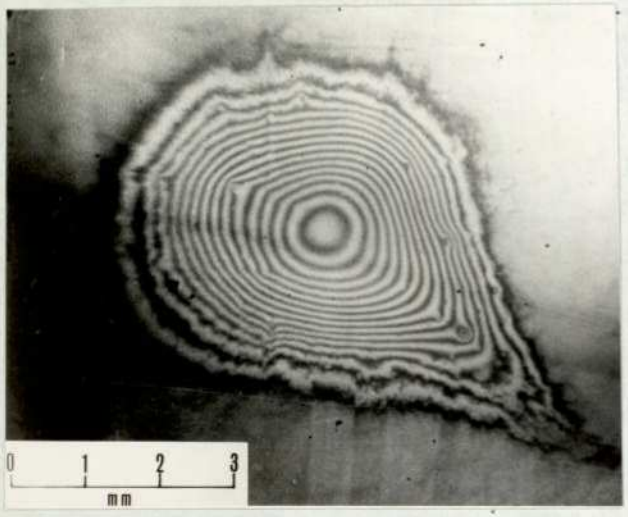
During tests in which the glass was moving, it was noticed that changes in the speed or pressure caused changes in the film thickness and these 'disturbances' propagated through the contact at a speed below that



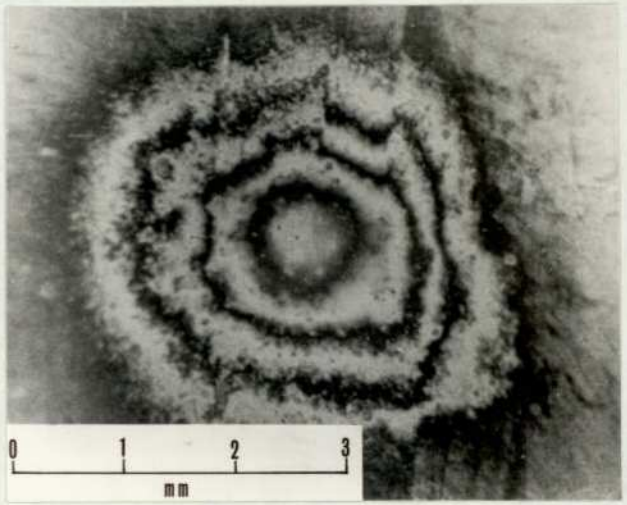
(a) Bubble 2 min. after contact.



(b) 5 min. after contact.

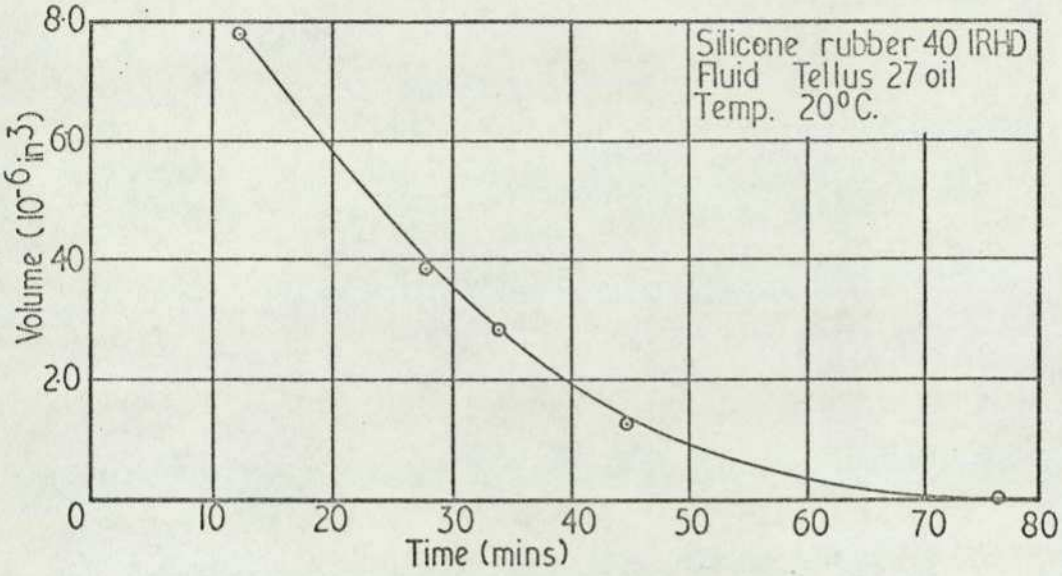


(c) 22 min. after contact.



(d) 42 min. after contact.

Fig. 3.11 Optical fringes in a 'bubble' at four times during the gradual disappearance of the 'bubble'.



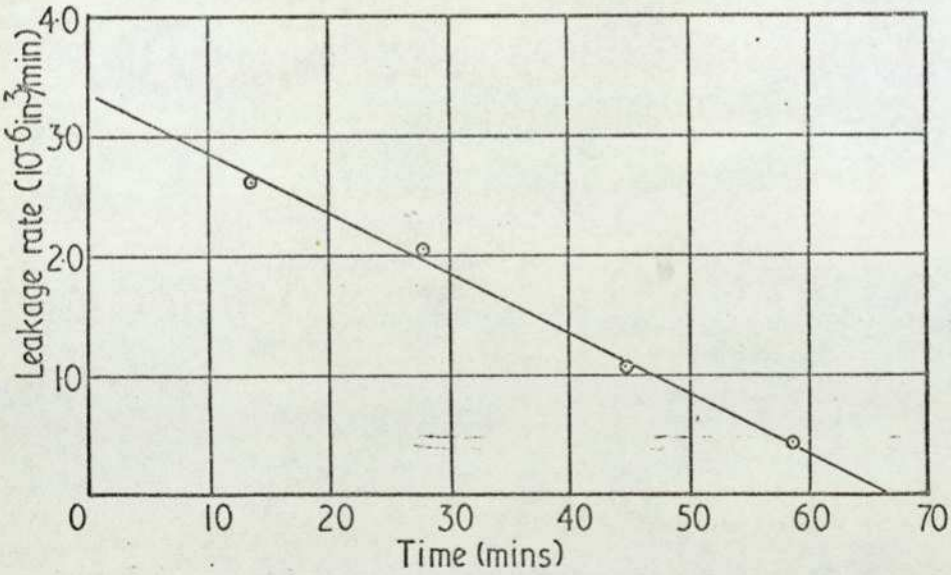


Fig. 3.12 The volume and leakage rate of a 'bubble' through the life of the 'bubble'

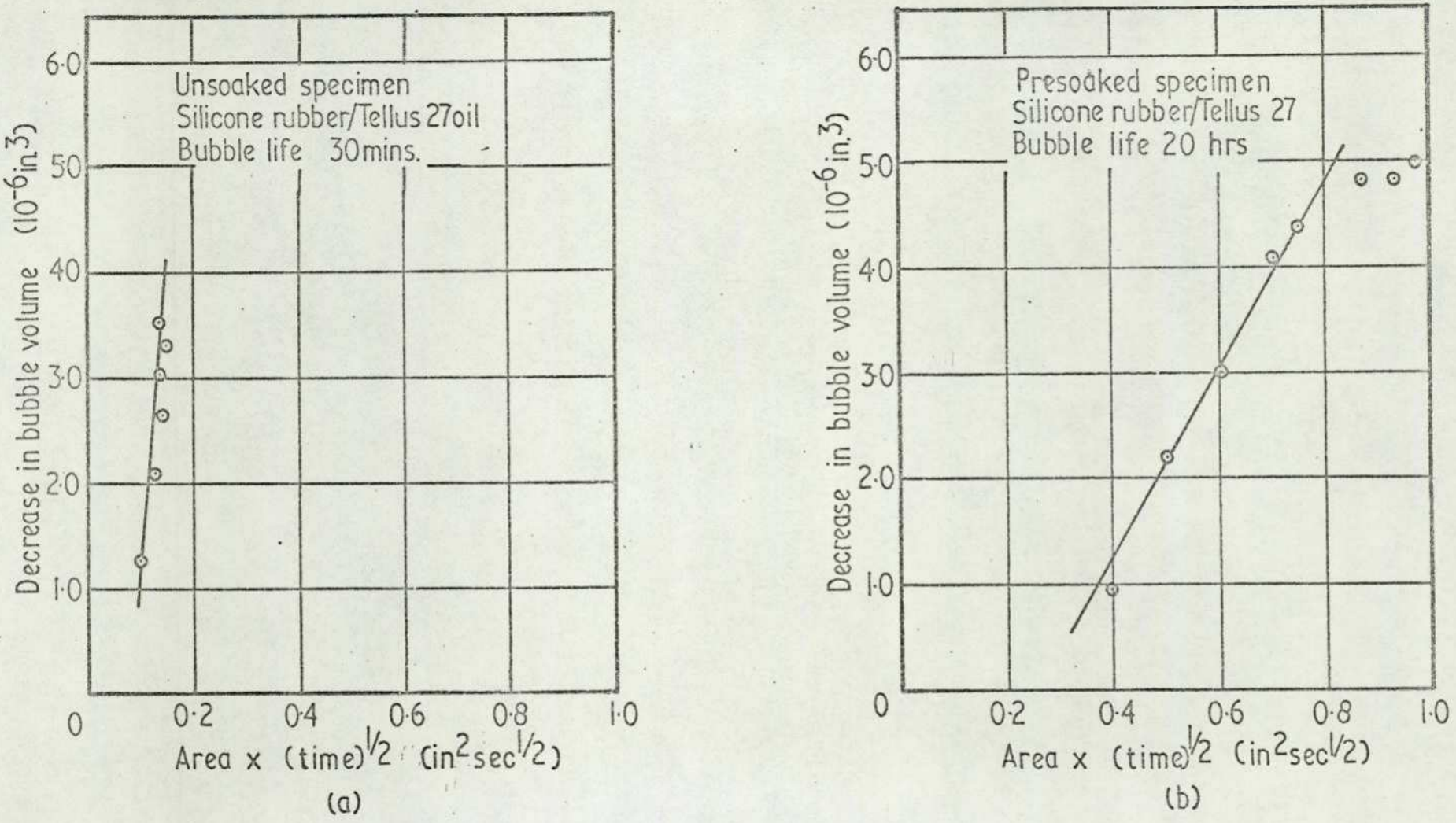


Fig. 3.13 The decrease of 'bubble' volume against the parameter (area) x $(\text{time})^{\frac{1}{2}}$

of the glass. A momentary change of speed or pressure produced a change in the film thickness which was localised to a moving waveform, the film in front of and behind the disturbance remaining the same. The disturbance retained its shape throughout the movement until it was removed from the trailing edge of the contact. Such waveforms are illustrated in figures 3.14 and 3.15. Because there is no slip of the liquid at the glass surface, the fluid in such a waveform is circulated around in the wave. In fairly deep waves in which the liquid contained dust particles, this circulation could clearly be seen.

A similar phenomenon occurs in foil bearings (18). Here changes in speed or load also cause the film thickness to change and the speed of propagation through the contact was shown, theoretically and experimentally to be half the speed of the foil. It seems that a soft rubber surface may behave in a similar way to the foil and the speed of propagation of a disturbance was therefore measured.

This was achieved by marking the front surface of the glass at specified intervals. During reciprocation of the glass, the time between a disturbance passing two consecutive marks was recorded, allowing the speed to be calculated. The speed of propagation was found to be half the speed of the glass as expected.

A simple theoretical analysis of the disturbance propagation, given in Appendix C, shows that if the pressure flow through the contact is zero, and the film is parallel but of different thickness before and after the passage of the disturbance then:

$$U_d = \frac{U_g}{2} \qquad (3.5)$$

The glass surface has therefore to move two contact widths of the specimen before a disturbance can propagate completely through the contact. Similarly a seal will not be fully lubricated until it has travelled at least two seal contact widths. This has particular significance in seal applications requiring short strokes, for example, actuators for powered flying controls on aircraft. In particular, a method sometimes used to overcome breakout friction in hydraulic jacks is to incorporate 'dither', a short stroke cycling of the jack, into the system, with the intention of

keeping the seal lubricated. The reason for the failure of this type of operation is discussed later in section 3.2.9.

3.2.4. Transverse 'black' lines

A phenomenon, observed only with silicone rubber specimens and hydraulic mineral oil was quite different from those already described. This was the appearance of transverse, thin, undulating black lines moving at about half the speed of reciprocation through the contact. The width of the lines was quite small being only about 1% of the contact width but increasing with speed; the length was variable between 10% and 80% of the seal contact. A diagrammatic view of these lines is shown in figure 3.16.

It was noticed that the black lines only seemed to occur in seals with damaged edges and it was thought the lines were in fact rubber debris from the damaged edges, 'rolling' through the contact, but after removal of a specimen exhibiting such lines and inspection under a microscope at a magnification of x 80 with reflected and transmitted light, no debris could be detected.

Further observation of the lines revealed that under short stroke operation, they conglomerated together and immediately on stopping the motion the width of the lines increased and interference fringes could be seen in them. After some time at rest, the lines gradually disappeared as the fluid in them was absorbed into the rubber. This indicated that the lines were in fact 'creases' in the rubber filled with fluid. As the 'creases' were only noticed with seals having damaged edges it was thought that they might be caused by the leading edge of the specimen being unstable, but closer inspection revealed that the lines originated some way behind the leading edge and appeared to be caused by the surface of the rubber buckling under the compressive stresses induced in it by the friction force at the surface.

Bearing in mind that the lines described above are creases in the rubber surface, they can be compared to a similar effect observed by Schallamach (49) which he termed "waves of detachment" obtained with dry contact using both a soft sphere on a hard surface and a hard sphere on a soft surface, but only with soft rubbers (approximately 40 IRHD).

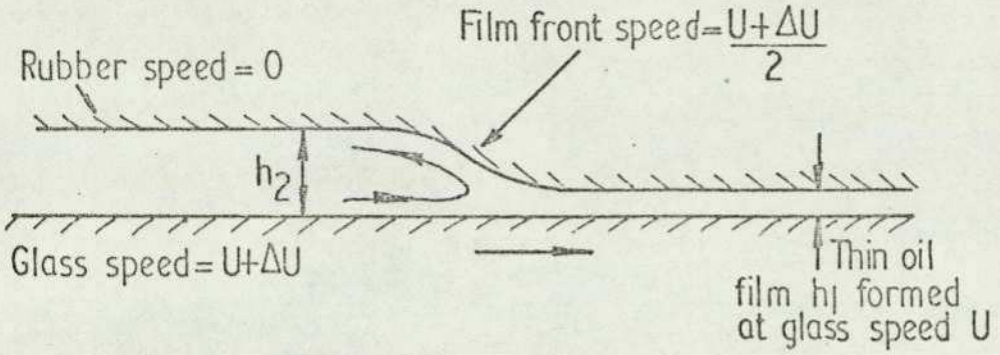


Fig. 3.14 The propagation of a film thickness change caused by a step change in speed or pressure

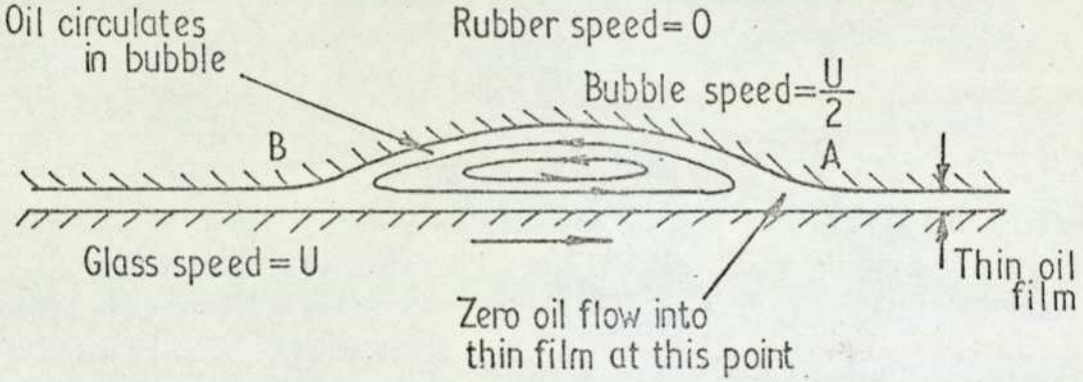


Fig. 3.15 The propagation of a 'bubble' in the oil film

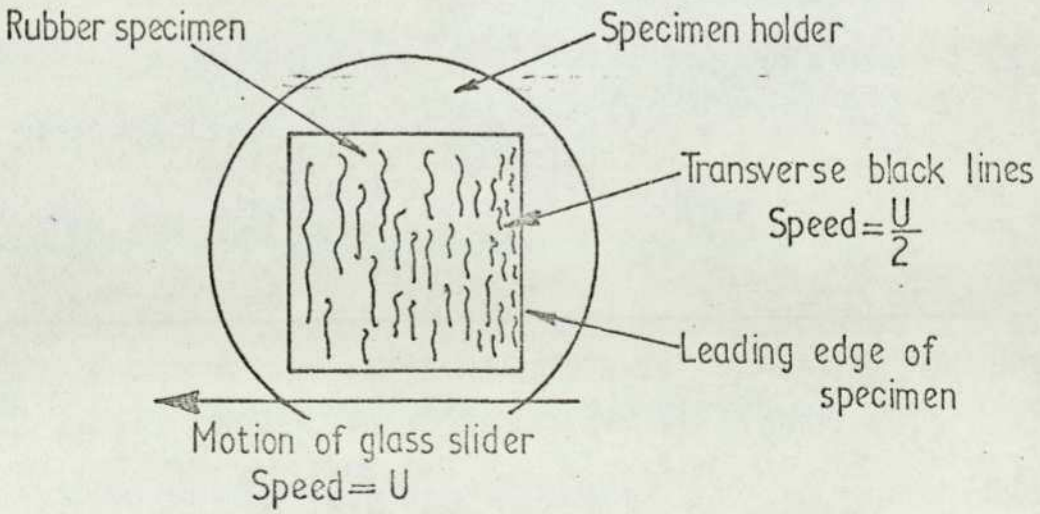


Fig. 3.16 Diagrammatic view of transverse 'black' lines

Whilst the lines and "waves of detachment" appear to be similar phenomenon, their relative speeds across the contact vary tremendously, the lines travelling at approximately half the speed of sliding, the waves of detachment travelling at much higher speeds although one test using a perspex track and a butyl rubber sphere showed creases in the surface which did not propagate across the contact.

A theoretical treatment of the problem by Schallamach indicated that the rubber surface at the leading edge of the specimen would be in compression during sliding and buckling of the surface to relieve the compression would be likely. However at the trailing edge of the specimen the surface should be in tension and therefore the 'waves of detachment' should disappear. This did not occur either with the present black lines or the waves of detachment, and the problem requires further experimental and theoretical evaluation before an adequate explanation can be found.

3.2.5. The effect of specimen edge

The specimens used in the first part of this program had nominally square edges formed by the type of mould used and it was found that under light loads a fairly thick film of oil was formed. However as the load was increased the film thinned until at the loads generally used throughout the program, the film in the contact zone consisted of longitudinal streamers. These were, on closer inspection, found to be channels of fluid up to 60 microinches (1.5 microns) deep: the spacing, depth and width of them being rather random. The spacing between these channels appeared as a white contact if the specimens were of silicone rubber and black if polyurethane rubber specimens were used. Indicating a film of liquid about 3 microinches thick for the former and direct rubber/glass contact for the latter. A typical interferogram of this phenomena is shown in figure 3.17 for a polyurethane rubber specimen.

It was also noticeable that the friction varied a great deal across the contact. Where the contact area was black, the leading edge of the specimen was considerably deformed. At the leading edge of one of the oil channels no such deformation was evident. This effect was most marked with the polyurethane specimens as this material has a coefficient of friction

much higher than that of silicone rubber.

The spacing of the streamers as mentioned before was random, but was changed if the rubber was removed from the glass and then replaced. The leading edge of the specimen appeared to lift or clamp down on the glass, and this determined whether a streamer formed or not. In addition, although the seal edge appeared perfectly square when viewed by eye, under the microscope slight variations in the edge were apparent which would have caused further random behaviour.

The chamfered edge specimens were then tested and similar effects were found. Although the chamfer appeared to blend smoothly with the contact surface, in actual fact a microscopically small ridge was formed which in effect acted in the same way as a square edge, and produced a contact having streamers of liquid separated by areas of rubber/glass contact.

When specimens having a smoothly rounded edge in which the radius blended smoothly with the contact surface were tested completely different behaviour was noticed. Here, the lubricant film was uniform across the complete contact, indicated by a contact of equal colour throughout. Figure 3.18 shows a transverse section of the two types of interface film, taken near the leading edge of the specimen. The section was however typical of over 95% of the length of the contact.

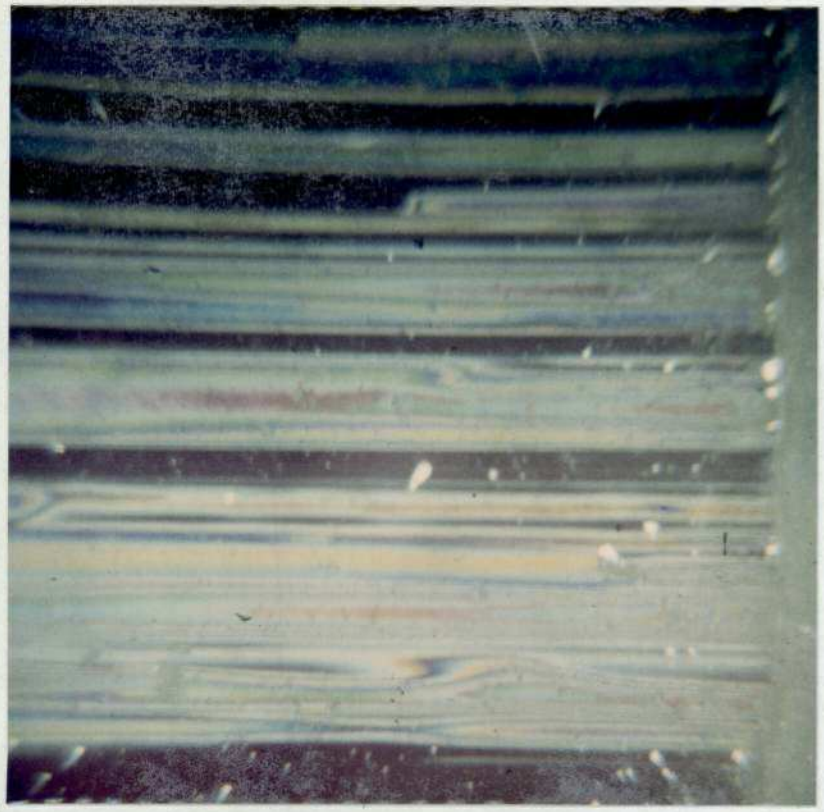


Fig. 3.17 Interferogram of the oil film under dynamic conditions using a square edged specimen

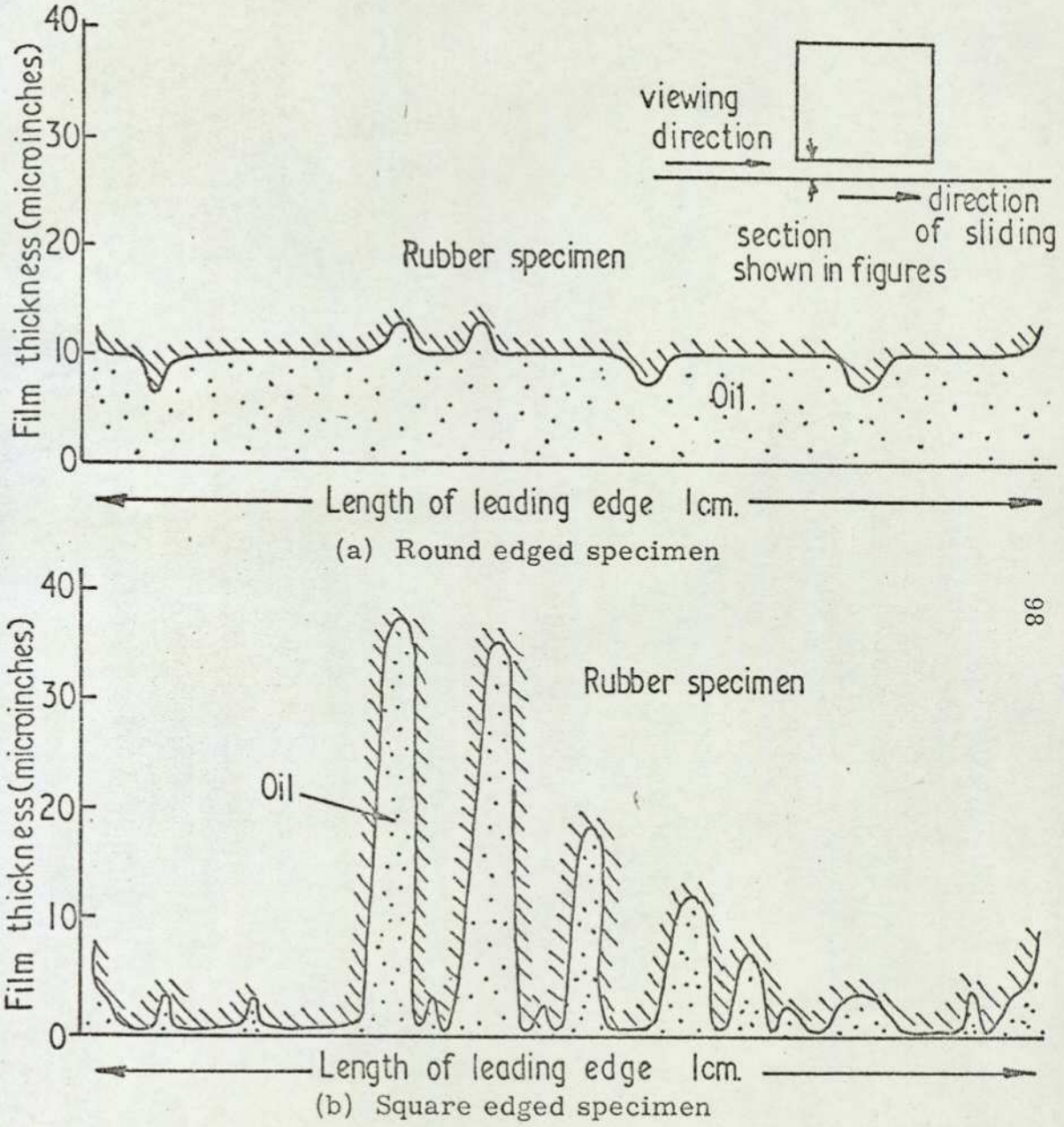


Fig. 3.18 Diagrams showing the transverse film shape near the leading edge of the specimens.

3.2.6. A study of the residual film

When using silicone rubber and Tellus 27 mineral oil, the colour of the contact after the absorption of a bubble was white, and this appeared to be the thinnest film obtainable in any test, representing a film approximately 3.5 micro inches thick. If the rubber contacted the glass, the area should have appeared black, which was the case when polyurethane rubber and silicone fluid were used.

It was originally thought that the residual film was caused by the particular properties of the fluid in very thin films. Increases in apparent viscosity of the fluid in very thin films have been reported, but generally the films in these cases have been very much less than is the present case and this explanation seems unlikely.

Tests were, therefore, carried out to determine whether this residual film was in fact a film of oil or due to some anomolous surface effect of the rubber. For instance, if the rubber surface absorbed significant quantities of fluid causing the surface to swell, the actual oil/rubber interface could be less well defined, the light being reflected some way below the true surface of the rubber, which would be in intimate contact with the glass. This would mean that the actual film thickness would be 3.5 micro inches less than that indicated.

The first test was carried out with a new piece of rubber on a complete dry piece of glass. The result was, as expected, intimate contact between the rubber and glass and a black field of view.

Distilled water was then used as a fluid which would not be significantly absorbed by the rubber. This also gave a black field of view.

It was noticeable that the behaviour of the water in the contact was markedly different to that of oil. When the rubber was brought up normally to the glass with water between, the fluid thinned rapidly to a film approximately 10 micro inches thick before breaking up into randomly distributed 'bubbles' of fluid separated by areas of intimate rubber/glass contact. If a small channel existed to the edge of the contact the water rapidly leaked away. During reciprocation the 'bubbles' remained stationary until conditions were created such that they formed a very thin film of fluid which was rapidly expelled from the contact. The behaviour indicated

that the fluid did not 'wet' either the rubber or the glass and could not therefore act as a lubricant, it being a basic assumption in the theory of lubrication that the fluid 'wets' the two bearing surfaces; that is there is no 'slip' between the fluid and the bearing surface at the interface. This explains the unstable nature of the water bubbles.

The third test used a medicinal grade paraffin which is similar to mineral oils but does not contain the usual additives. The result was the usual white residual film.

The final tests involved fluids such as benzene and trichloroethylene which would significantly swell the rubber. It was thought that the colour of the residual film may be determined by the degree of swell and with high swell fluids the film may become yellow or even blue. A bubble could be formed, with both of the fluids, which rapidly disappeared, leaving a yellowish appearance to the film, which is indicative of a thicker residual film and is consistent with the hypothesis of surface penetration of the light.

However in a rubber which is considerably swollen the light may be reflected from the oil/rubber interface as a diffused beam thereby reducing the property of optical interference. The tests with the high swell fluids are not therefore entirely conclusive.

The above tests have shown that the apparent residual film is a property of the fluid/rubber combination not the fluid alone and that the absorption characteristics and surface activity of the materials used are important factors affecting the behaviour of the specimen.

3.2.7. The effect of viscosity and speed on the film thickness and friction.

Using the MK I specimen holder tests were carried out to determine the effect of speed and viscosity on the film thickness. In order to easily obtain changes in viscosity, silicone fluids in a range of viscosities were used, which entailed using a polyurethane rubber specimen. Because the square edge specimens rarely formed a fluid film, the specimen used had round edges. With the lowest viscosity used (26×10^{-7} reyns) the film thickness was only measurable at the highest speed of 5 ft/min. as the general colour of the contact varied from black to white over the whole speed range indicating a film always less than 3 - 4 micro inches. In tests

in which the film was thin, it was also very uniform in thickness, indicated by a single colour throughout the contact, but for thicker films several colours were visible through the film making the determination of a mean value difficult.

The results obtained for a contact stress of 50lb$_f$/in^2 in a speed range of 0.5 to 5ft/min. and a viscosity range of 26 - 650 x 10^{-7} reyns (20 - 500 cSt) are plotted in figures 3.19 and 3.20. The data here can be made to fall on a single line by plotting the film thickness against the parameter (speed) x(viscosity), on logarithmic scales, figure 3.21 which indicates that

$$h = 2.8 \times 10^{-4} \cdot (\zeta U)^{0.5} \text{ inches} \qquad (3.6)$$

Measurements of film thickness and friction

With the MK II specimen holder, several experiments were conducted with polyurethane rubber/silicone fluid combinations using specimens having square and round edges, with the aim of correlating the visual estimate of film thickness with the measured value of friction. The fluid viscosities used were 26 - 650 x 10^{-7} reyns (20 - 500 cSt.), and a specimen contact stress of 50 lb f/in^2 was again used.

Square edge specimens

With the square edged specimens the behaviour of the fluid film in the contact was very variable. It has been shown previously that the microgeometry of the specimen determines whether a fluid film will form and this appeared to be altered as the various viscosity fluids were tested. Thus with fluids of 20 and 50 cSt, the contact area remained black throughout the stroke length but on changing to the thicker fluids of 200 and 500 cSt, streamers were formed in the contact separated by regions of intimate rubber/glass contact. It is not certain whether this was an effect caused by the fluid viscosity or by the fact that the specimen had to be removed from the holder and cleaned before testing with the next higher viscosity, but the result was that it was not possible to determine precisely the effect of viscosity on the friction. If a bubble was formed in the contact by bringing the rubber specimen up normally to the glass, it was wiped out of the contact as soon as movement of the

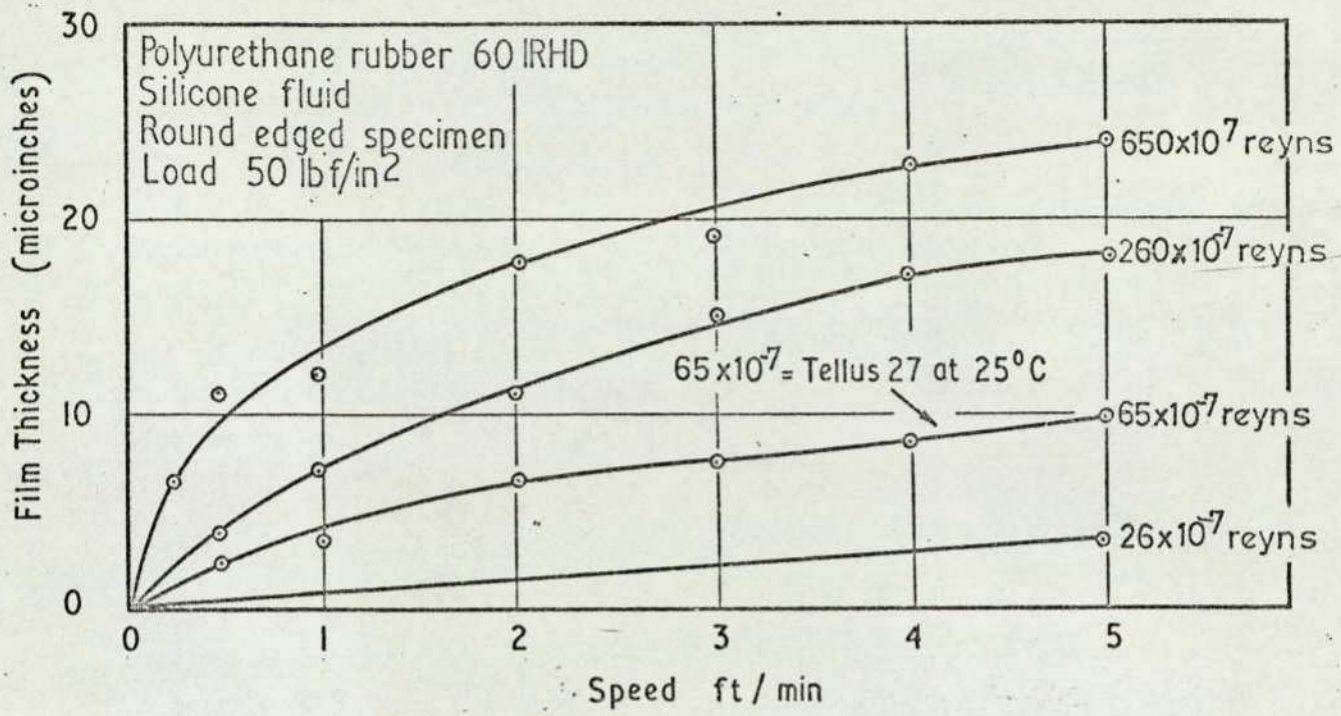


Fig. 3.19 Film thickness against speed for a range of viscosities

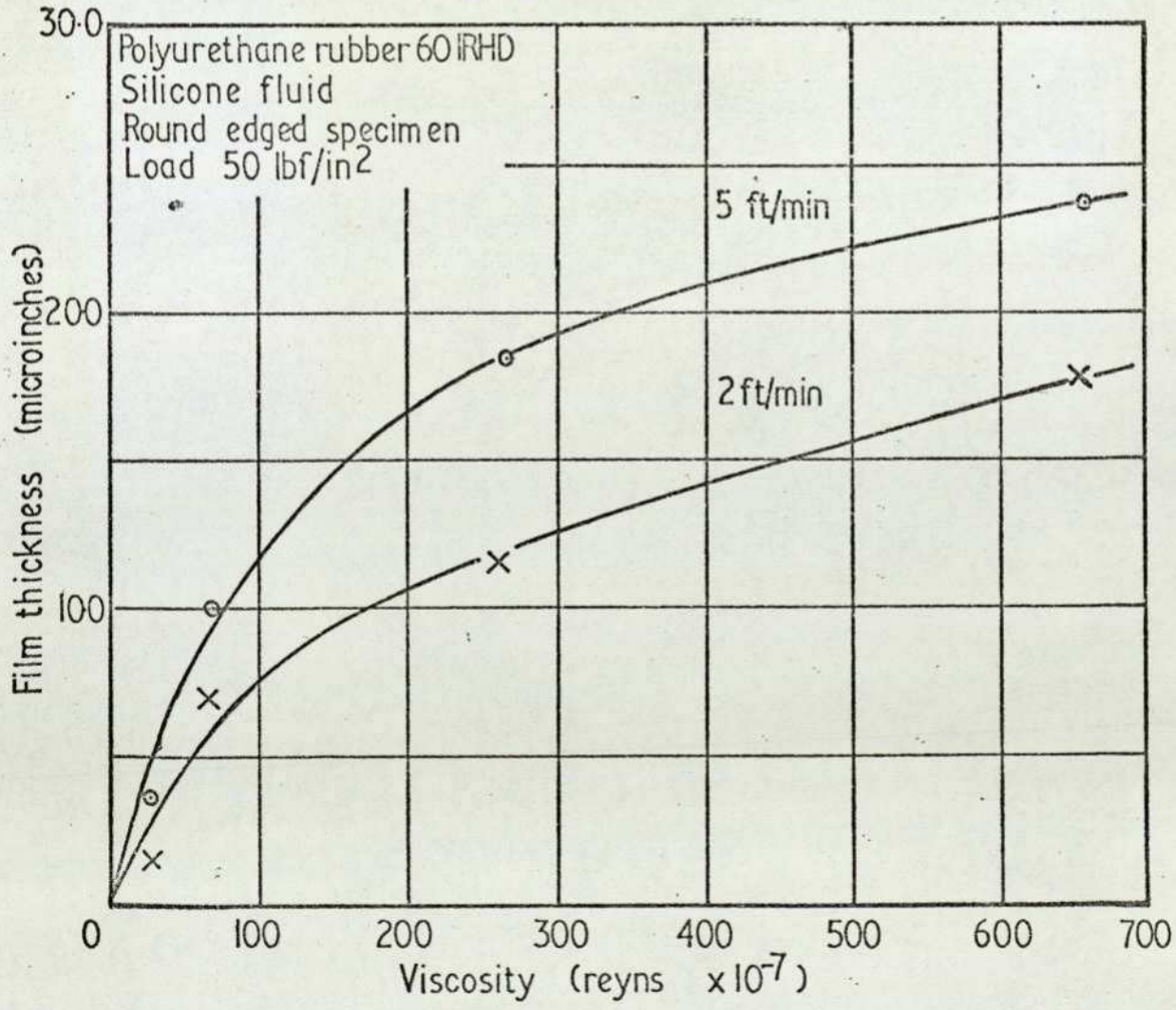


Fig. 3.20 Film thickness against viscosity for two speeds

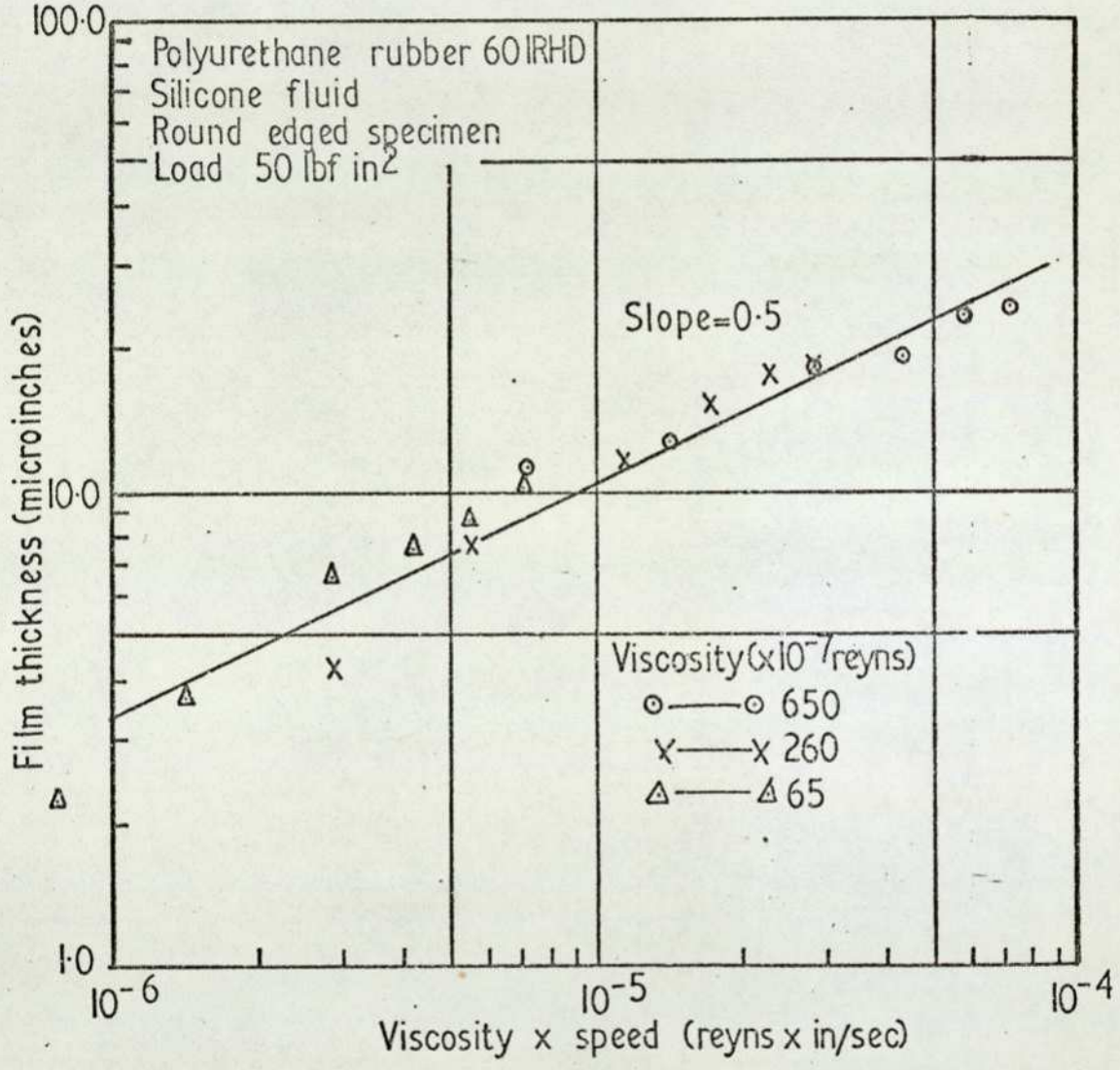


Fig. 3.21 Logarithmic plot of the data of figures 3.19 and 3.20 against the parameter (viscosity) x (speed)

glass began. Thereafter a fluid film formed only occasionally at the changeover point of the stroke, as the trailing edge of one stroke became the leading edge of the next stroke. The small wave of fluid entering the contact at this point traversed the contact at half the speed of the glass, but left behind a very thin film of fluid approximately 3 micro inches thick, which reduced the friction to about 80 lb_f/in^2 from a value of 100 lb_f/in^2 normally associated with these tests. However the friction soon returned to its original value after the glass had moved a few contact lengths.

The friction values recorded were always very high and even when the streamers were formed values of 50 to 70 lb_f/in^2 were recorded. In the absence of the streamers values between 80 and 100 lb_f/in^2 were in evidence.

There was considerable variation in the friction throughout the stroke with all the viscosities tested, even after some time operating at a steady speed, and this was thought to be due to the glass not being parallel with the slideway motion causing the load on the specimen to vary through the stroke. The parallelism was however checked and found to be within 0.0001inches per inch of travel.

A thick fluid film did not form at any of the speeds tested and the friction through the speed range did not change significantly, although the effect of speed could have been masked by the wide variations in friction through the stroke.

As a comparison with the above 'lubricated' contact, tests were conducted using a new, unused specimen of polyurethane rubber and a clean piece of glass, over the speed range 0.5 - 1.0 ft/min. During these tests the range of the friction display meter had to be extended to record the initial friction of 192 lb_f/in^2. Over a number of cycles this gradually reduced to 140 lb_f/in^2, but was still in excess of any values recorded with a lubricant present. This suggests that with a lubricant present, a very thin film of fluid forms, which significantly reduces the friction or the fluid affects the surface properties of the rubber.

Round edged specimens

When round edged specimens were used, a thick fluid film formed and the friction was drastically reduced, in some cases by an order of

magnitude or more.

The film thickness data obtained during these tests , confirmed the results of the similar tests of the previous section. The data when plotted against the parameter (viscosity) x (speed) indicated a relationship of the form.

$$h = 2.8 \times 10^{-4} \cdot (\eta U)^{0.5} \qquad (3.7)$$

In addition to this however the friction data is available corresponding to the measured film thickness and is presented in figure 3.22 a, b and c for the three values of viscosity tested. The values are plotted as bands because of the variation in friction through the stroke. The data for the fluid of viscosity 650×10^{-7} reyns was limited to a maximum speed of 1 ft/min. because the film was very thick and variable throughout the contact making an estimate of the mean film thickness impossible.

The measured values of friction in all cases can be seen to decrease with increasing speed, in the same way as found for the friction of reciprocating elastomer seals, (Chapter 4). Also plotted in figure 3.22 are the theoretical values of friction calculated from the formula:

$$\text{specific friction} = \frac{\eta U}{h} \qquad (3.8)$$

using the measured values of film thickness. The discrepancy between theory and experiment can clearly be seen. In general the theoretical friction increases with speed and, except for the viscosity of 260×10^{-7} reyns at the highest speed, is considerably lower than the measured value. This, in spite of the fact that in these experiments, unlike the capacitance transducer measurements of the film thickness, (Chapter 4), the whole contact area can be seen to be hydrodynamically lubricated.

In view of the nature of the curves obtained the results were replotted on logarithmic scales, figure 3.23, and indicate a relationship of the form:

$$\text{specific friction} \propto (U)^{-0.5}. \qquad (3.9)$$

which is the same as found for the reciprocating seals used in the instrumented rig study. With respect to the friction then, reciprocating seals and the specimens used here behave similarly.

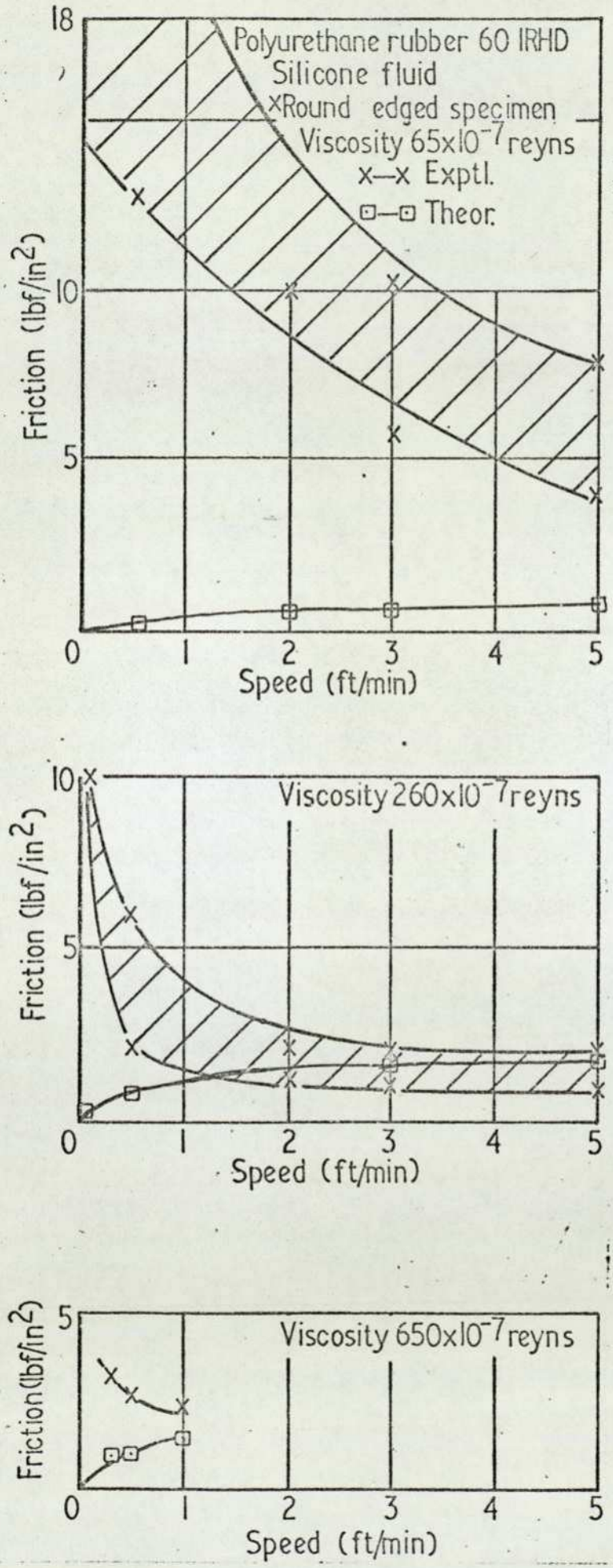


Fig. 3.22 The variation of specific friction with speed for three values of viscosity

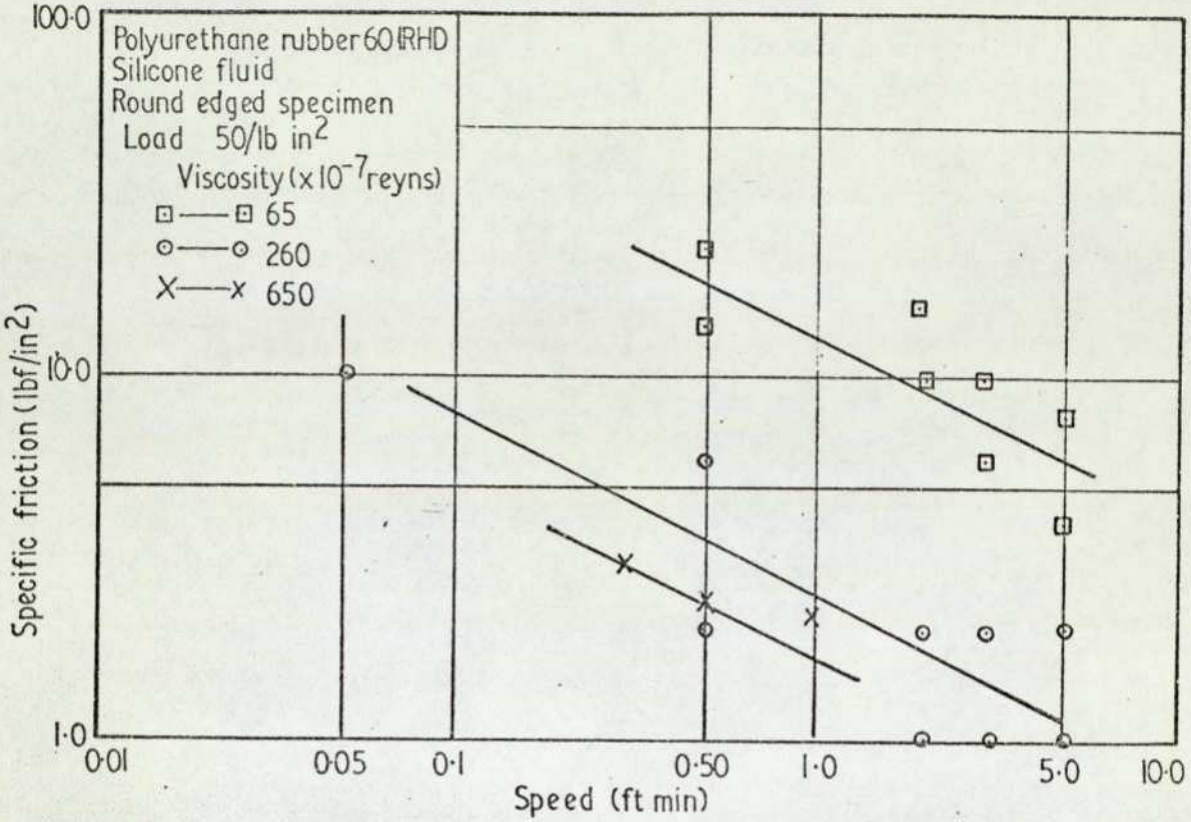


Fig. 3.23 A logarithmic plot of the data of figure 3.22

If the relationship obtained between film thickness and the parameter (viscosity) x (speed) is substituted in the Newtonian friction formula the following relationship is obtained:

$$\text{specific friction} = \frac{(\zeta U)^{0.5}}{2.8 \times 10^{-4}} \qquad (3.10)$$

indicating that the friction should be proportioned to the square root of viscosity and speed. This is obviously not the case in practice as the measured values of friction show:

$$\text{specific friction} \propto (\zeta U)^{-0.5} \qquad (3.11)$$

Two possible explanations of the discrepancy between measured and theoretical values of friction are proposed.

If the theoretical Newtonian equation applies and the friction results are correct, agreement could be reached if the viscosity was inversely proportional to the square of the film thickness, thus:

$$\zeta \propto (h)^{-2} \qquad (3.12)$$

Substitution of this and the experimentally determined relationship for film thickness:

$$h \propto (\zeta U)^{0.5} \qquad (3.13)$$

into the Newtonian friction formula reveals that:

$$\text{specific friction} \propto (\zeta^3 U)^{-0.5} \qquad (3.14)$$

Figure 3.24 gives the present data plotted against the parameter $(\text{viscosity})^3$ x (speed) and shows good agreement with the above expression. However this is only true if the initial assumption is valid, and whilst increases in viscosity of fluids in very thin films have been reported, the films measured here are very much thicker and this explanation does not appear to be very likely.

A second explanation of the discrepancy and one which appears to be more credible in view of the nature of the friction curve, involves the microasperities in the rubber surface. Because the film is thin, it could be penetrated by microasperities giving very small areas of rubber/glass contact. In total these could appreciably affect the friction, but individually would not be visible with the low magnification used to

study the interference fringes.

Both explanations obviously require further investigation.

3.2.8. Stick-slip behaviour

During the study of the effect of viscosity on the film thickness it was noticed that the phenomenon of stick-slip was evident during tests with the lowest viscosity fluid of 26×10^{-7} reyns. Whilst the effect could easily be viewed by eye it was difficult to assess the amplitude and frequency of the motion. However by taking a short film-sequence of the phenomenon and reviewing it using an analytical projector, it was possible to determine the displacement of a point on the rubber surface with respect to time. This is shown in figure 3.25.

The stick periods were rarely of the same duration whilst the slip periods, although shown to be of .04 seconds duration may have been variable and much shorter than this without being detectable by the method used. The upper limit of time is based on the fact that the film was taken at 24 frames/sec giving a time period between frames of 0.04 seconds.

An inconsistency in the graph is the varying slopeof the stick period, which should have been constant had the rubber been moving at the same speed as the glass. However possible explanations are:

(i) the rubber could have been slowly sliding along the glass even during the stick period.

(ii) the glass velocity may not have been as constant as previously assumed.

It was noticeable that the slip periods did not always consist of a single 'slip' back to the original position but could take the form of several smaller 'slips'.

3.2.9. The effect of short stroke lengths

Previous results have shown that disturbances in the fluid film caused by changes in velocity, load or direction of motion are propagated through the film at half the speed of the glass and therefore in order for them to traverse the contact completely requires the glass to travel two contact widths. Displacements of less than this are referred to as short strokes and in this situation a fully developed fluid film is never formed.

Stroke lengths of this order are found frequently in practical

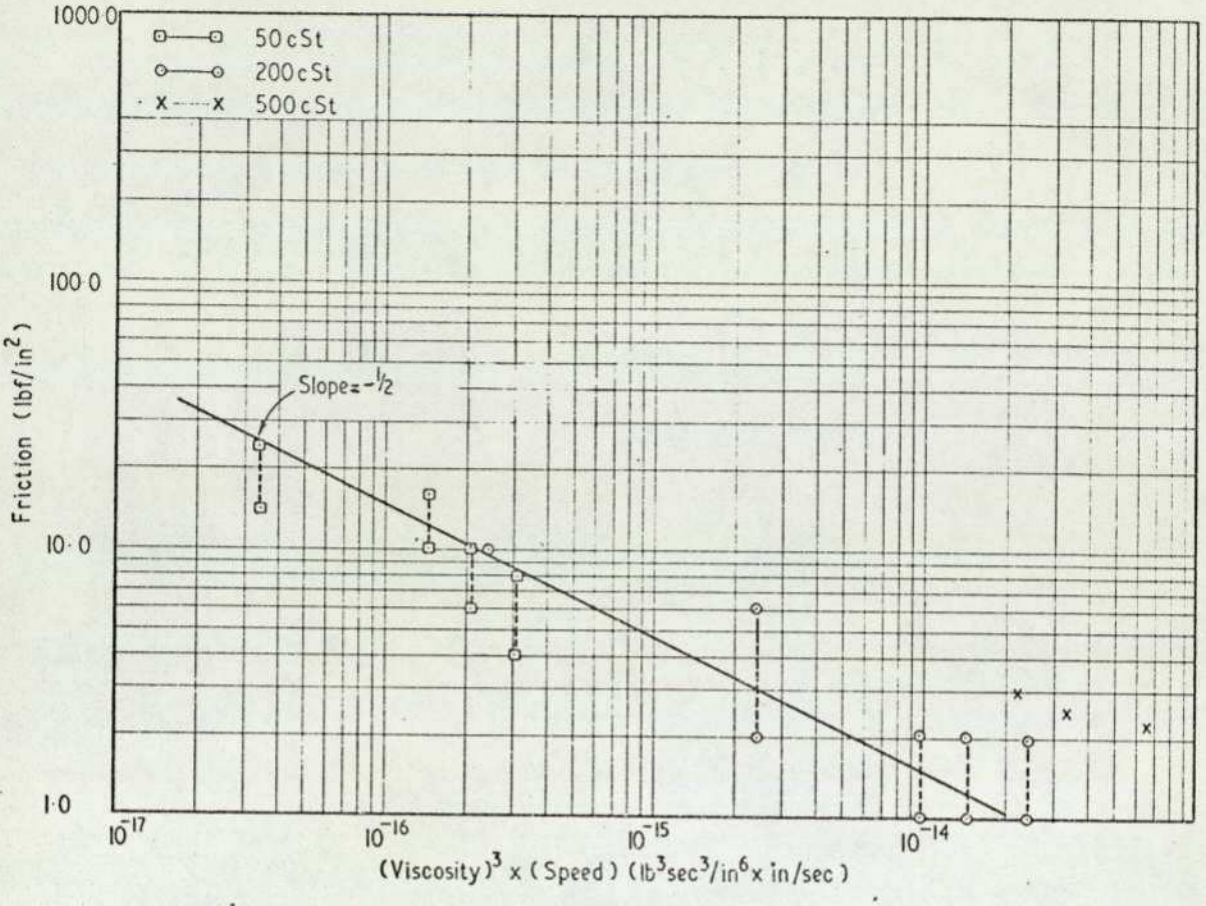


Fig. 3.24 The specific friction against the parameter (viscosity)^3 x (speed)

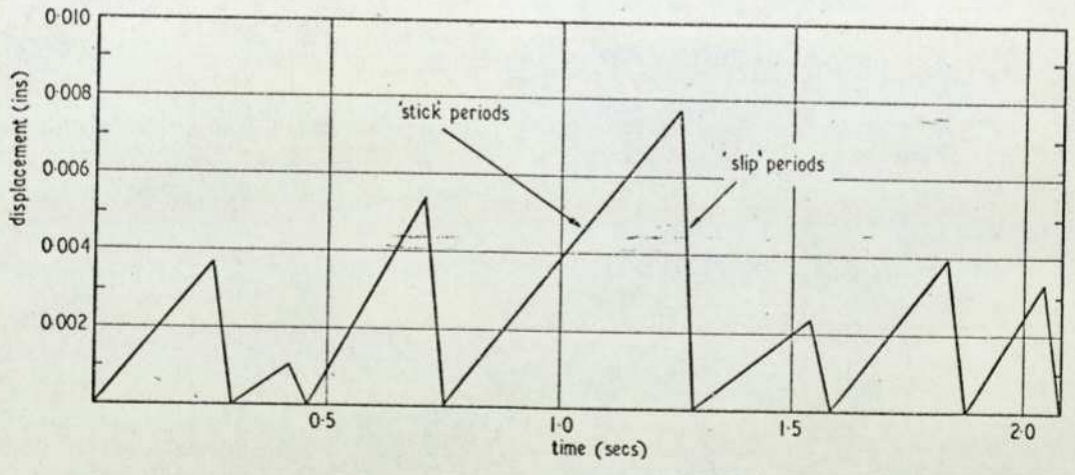


Fig. 3.25 The displacement of a point on the rubber surface during a stick-slip phase

situations, and it is therefore of interest to investigate the fluid film behaviour under such conditions.

In the tests conducted a steady state film was set up by long stroking a round edged seal, then an extra limit switch was switched into the circuit causing the stroke length to be reduced immediately to a previously set value.

Sequence of events during short stroke cycling

The sequence of events during short stroke operation can be explained with reference to figure 3.26. At (a) the film is that formed during long stroke cycling and in general appears to be stable and permanent. On switching to short stroke operation (b) a lubricant film front is drawn in from the left hand edge of the specimen and travels at half the speed of the glass and therefore half the distance in the same time. This front moves half way across the contact whilst the glass moves one contact width (d). The motion is now reversed (e) and a film front enters the right hand edge of the specimen whilst the initial film front retracts. The area of contact can then be divided into 3 regions, the lubricated parts of the contact regions A and C, and a region, B, which does not receive any fresh supply of lubricant during the stroking operation and is continuously moving across the contact, (f) - (j). The width of region B obviously depends on the stroke length and in this example is 50% of the contact width for a stroke length of one contact width. Decreasing the stroke length, increases the width of region B and increasing the length, decreases region B until for a stroke length of two contact widths the seal is fully lubricated at all times

Short stroke length operation with poly urethane rubber and silicone fluid

The behaviour of the fluid in region B can be divided into two forms:

(i) if the stable film formed during long stroking was thick, as would be the case with a high viscosity oil, it remained in region B almost indefinitely. It also remained even if the load was considerably increased and the film behind the film fronts reduced. In this situation short stroke cycling would not affect the performance of the seal.

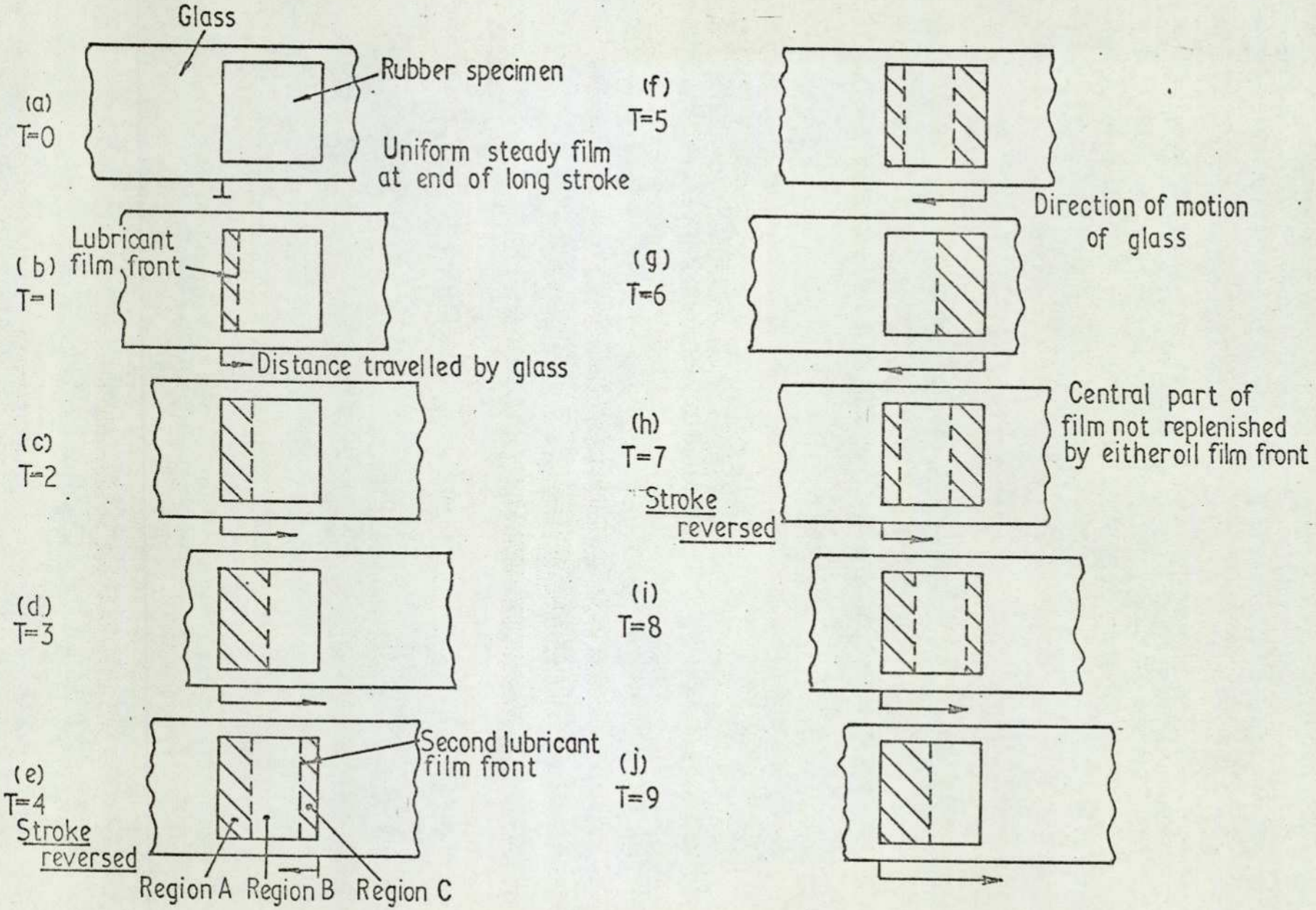


Fig. 3.26 Formation of the lubricant film during short stroke operation

(ii) if the stable film formed during long stroking is thin, of the order of 10 micro inches, the film in region B thins during the short stroke operations as the oil disappears in two ways, firstly by being trapped in the advancing and retreating film fronts, and secondly by absorption into the rubber. The film thins to such an extent that intimate rubber/glass contact occurs at points in the region, this contact area increasing as cycling continues. During this period the friction rapidly increases from low values of 5 - 10 lb_f/in^2 to that expected with zero film thickness of 80 - 100 lb_f/in^2 . The rapid increase in friction when the film began to break down is shown in figure 3.27 for a number of speeds. It can be seen that at the low speeds the breakdown began after only a few short stroke cycles, but for the highest speed this did not occur until 80 cycles. Because of the inertia of the reversing motor and the slide system, the actual length of the short stroke cycle depended on the speed of reciprocation and increased with speed. The large number of cycles before breakdown at a speed of 4 ft/min. may have been due to an increased stroke length, and not entirely due to the speed. However once initiated the breakdown was rapid and the friction increased at a rate of approximately 4lb_f/in^2 per cycle. The intimate rubber/glass contact points gradually enlarged with continued cycling and the area between them filled with the oil expelled from the contact areas. The film thickness at edges of the contact areas could be seen to increase and decrease on the alternate strokes. As this oil film built up it was mechanically expelled from the contact.

Under these conditions, the specimen underwent severe deformation, the rubber surface in the contact adhering to the glass and moving with it until slipping occurred which, in many cases, entailed a shear strain in the rubber of 25% or more of the seal contact. The consequences of this severe strain could be very important in practice, as the rubber on either side of the intimate contact regions experienced high alternating tensile and compressive stresses which could rapidly lead to fatigue failure of the rubber. This did in fact occur during these tests, the result being the formation of transverse splits in the rubber surface and the eventual breaking away of pieces of rubber around the splits.

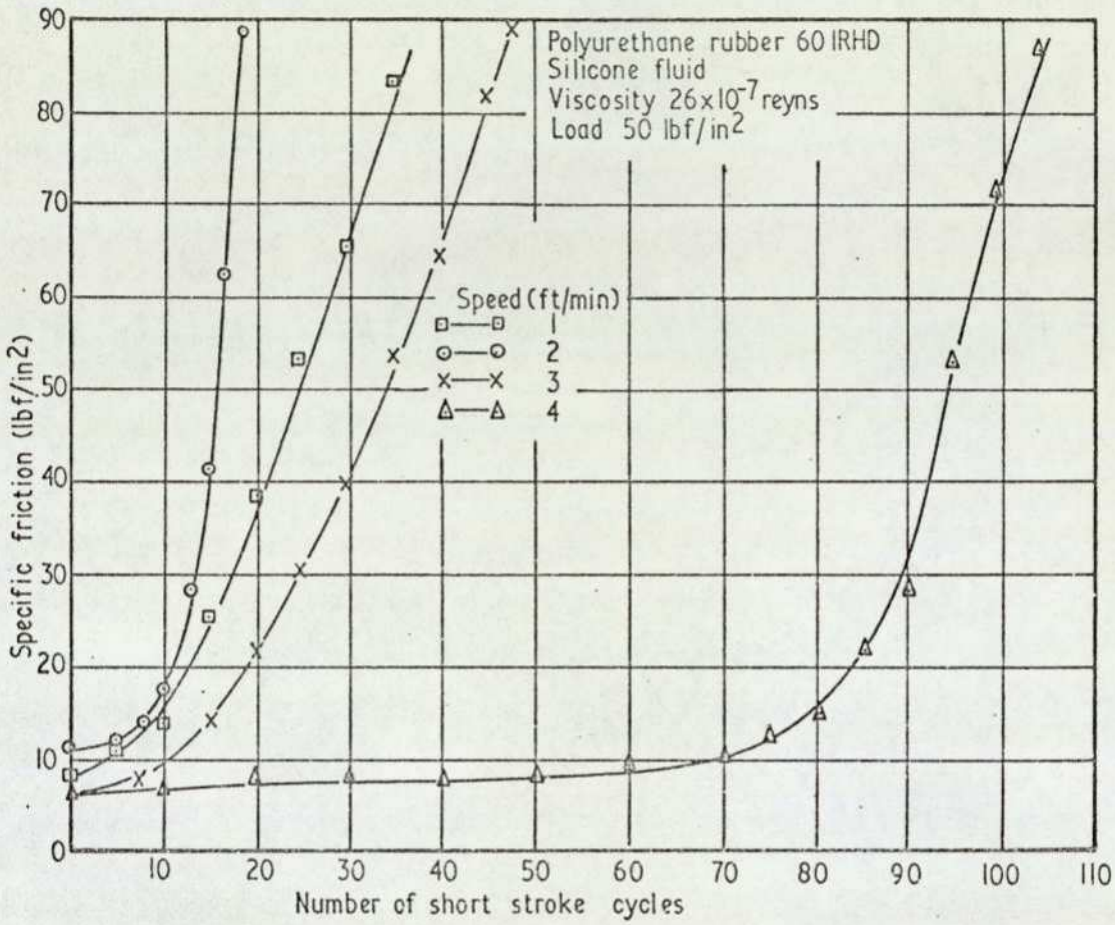


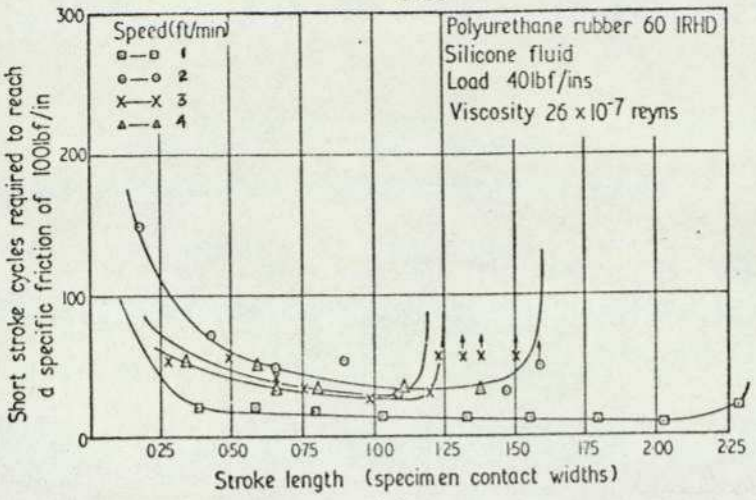
Fig. 3.27 The specific friction of a specimen against the number of short stroke cycles

The number of cycles before film failure occurs was measured by arbitrarily defining failure as the point when the friction reached a value of 100 lb_f /in^2. Using this criteria tests were conducted over the speed range of 1 - 4 ft/min., a viscosity range of 26 x 10^{-7} to 260 x 10^{-7} reyns and short stroke lengths from 0.02 to 2.0 specimen contact widths. The data is show in figures 3.28 (a), (b) and (c).

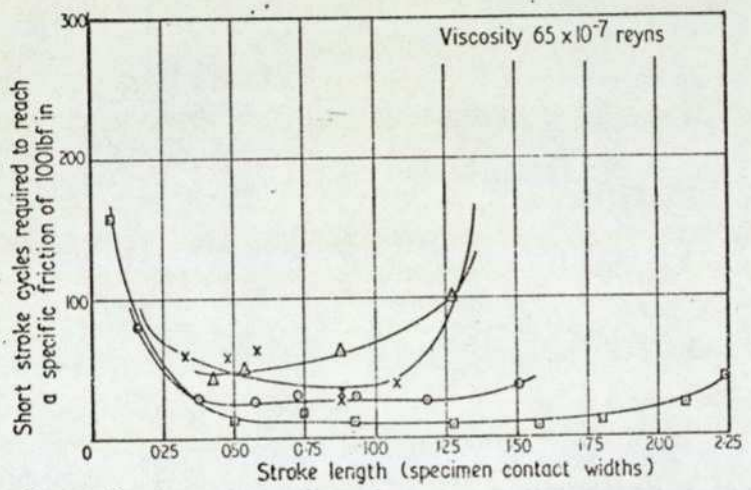
All three graphs show similar behaviour in that the number of cycles to film breakdown for stroke lengths of less than 0.5 contact widths was high and increased as the stroke length decreased. However as the stroke length increased to between 0.5 and 1.0 contact widths the film failed fairly rapidly. This range depended to some extent on the viscosity and the speed, and for the low speeds and viscosities extended to stroke lengths of over two contact widths. Above stroke lengths of one contact width the number of cycles to failure generally increased. As the stroke exceeded two contact widths the lubrication became complete and failure did not occur.

In general it appears that the most critical range of stroke lengths are between 0.5 and 1.5 contact widths. Above the upper end of the range region B is becoming very narrow and the fluid film is becoming more fully developed, the life therefore increasing. At the lower end a different phenomena occurs. With the rubber in intimate contact with the glass it moves with the glass and in doing so deforms. If the deformation stress does not exceed the friction stress for the maximum movement of the glass, then the rubber does not slip. The recorded friction is in this case not that due to sliding but that due to the rubber deformation, and the friction never reaches a maximum value of 100 lb_f /in^2. The critical stroke length for rubber deformation only is approximately 0.30 contact widths figure 3.28. (c)

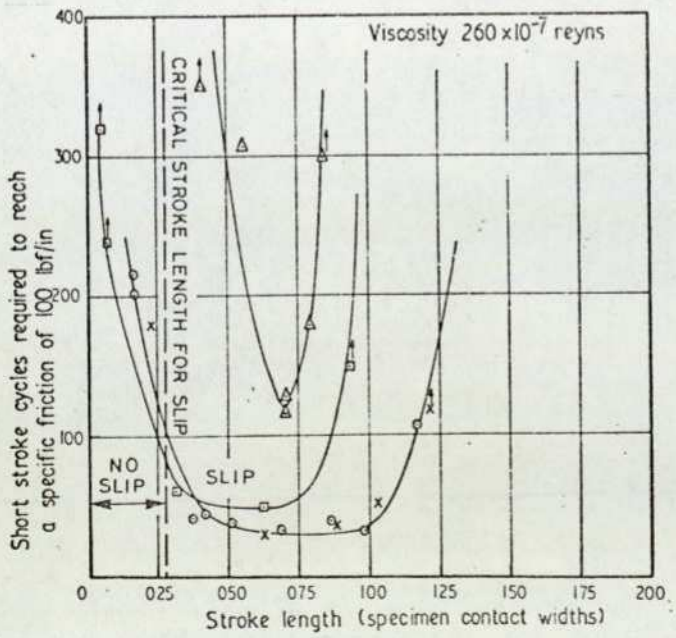
Both speed and viscosity affected the results as generally the film breakdown took longer at the higher speeds and viscosities, these creating a thicker film initially during the long stroke operation. In fact for the higher speeds and viscosities than those tested film breakdown may not occur at all, the situation mentioned previously with thick initial films.



(a)



(b)



(c)

Fig. 3.28 The number of short stroke cycles required to reach a specific friction of 100 lbf/in^2 against the short stroke length

Short stroke length operation with silicone rubber and mineral oil

When silicone rubber and an hydraulic mineral oil were used the breakdown of the fluid film during short stroke operation was completely different to that described in the previous section.

The specimens used were of silicone rubber of hardness (40 IRHD) with rounded edges.

During long stroking a stable film was formed approximately 10 micro inches thick in both directions of motion. When switched to short stroke operation the oil film in the central region of the contact separated over three or four cycles into transverse channels of fluid, the area between the channels attaining the white residual film; with continued short strokes, the channels of fluid conglomerated together to form longer channels which were eventually expelled mechanically from the contact, the central region B then retaining completely the white residual film observed in the stationary bubble studies. This sequence of events occurred over the whole speed range.

3.2.10. Application of a pressure differential

An attempt to create a pressure differential across the specimen was made possible in the MK II specimen holder. Reference to figure 3.9 will show that in addition to friction measurements it was possible to insert a hypodermic tube through the adjusting screw and into the rubber specimen. With a hole of the same size as this tube in the specimen it was hoped that pressure could be applied via the hypodermic tube to the recess formed by the hole in the specimen, forming a pressure differential from the centre to the edge of the specimen.

The soft silicone rubber was used for these tests because only low pressures could be used on the glass surface, the maximum being limited to 50 lb_f/in^2.

When reciprocated, even without pressure applied, the sharp edge at the centre hole did not allow any film formation and the lubrication was therefore generally poor. Applying the maximum pressure to the centre of the specimen, when it was stationary, or moving, did not cause

any visible change in the film profile. Unfortunately higher pressures were not possible without considerable modification to the rig, which was thought not to be worthwhile at that time.

3.2.11. Ciné film

Most of the results pertaining to the optical rig are qualitative and observations are difficult to present adequately in report form. However advantage was taken throughout the program to film the various phenomena as they occurred. In order to present these as clearly as possible a silent film lasting approximately ten minutes was produced from the film taken. This is available for reference at:

BHRA Fluid Engineering
Cranfield, Bedford.

3.3. Discussion.

The interferometric method of studying lubricated rubber/glass contacts was very successful and has been very informative about the behaviour of the oil film in such contacts. A number of important phenomena have been observed which can be related to reciprocating seal performance.

Possibly the most important observation is the absorption of the oil bubbles into the rubber. This is of considerable practical significance in understanding the phenomena termed 'stiction' or 'breakout friction' associated with seals at rest. The 'breakout' friction generally increases with time and was previously considered to be due to the gradual squeezing out of the fluid in the contact. The present work has shown that this is not so.

A further observation has revealed the importance of the micro-geometry of the specimen edge in determining the behaviour of the film, and this could be used to control seal performance through the initial design. Further analysis of the cross sections of figure 3.18 show that although a square edged specimen forms channels of fluid and part of the contact is dry, the area through which fluid can pass is approximately the same as that for the round edge specimen, and leakage past the two specimens is likely to be of the same order. The friction of the square edge specimen

will however be conside rably higher.

Disturbances in the fluid film have been shown to propagate at half the speed of reciprocation and this entails that the seal must travel at least two contact widths before complete lubrication occurs. In systems having stroke lengths less than this, the fluid film breaks down and in many cases this could lead to fatigue failure of the seal material.

The friction measurements have provided confirmation of results obtained in the instrumented seal rig (Chapter 4) in which the values of friction have been an order of magnitude or more higher than would be expected from viscous shearof a fluid film having the measured values. In the optical rig the complete area of contact was observed to be lubricated and although possible causes of the excessive friction have been put forward none appears to explain the facts adequately. It is obvious that further investigation is required.

CHAPTER 4

INSTRUMENTED SEAL STUDY

4.1. DESIGN AND DEVELOPMENT OF TEST RIG

4.1.1. Introduction

A test rig used by Nau(37) had a capacitance transducer mounted in the reciprocating shaft, which measured the film thickness of reciprocating seals operating as rod seals. The transducer which was circular and 0.08 inches in diameter did not give sufficiently localised measurements, the seal length being only 0.375 inches and in addition was difficult to instal.

For the present work, an improved capacitance transducer was required in addition to a pressure transducer and the design above was rearranged so that the seals reciprocated with the shaft, allowing the transducers to be mounted into the wall of the pressure vessel. This situation simulates the piston in bore configuration, the seals sealing on their outside diameter. It was assumed that both rod and piston seal configurations would yield similar results.

4.1.2. General layout

The rig design was based on a standard BHRA reciprocating seal test rig with suitable modification to the pressure vessel. The general layout is shown in figure 4.1.

The cast iron yoke A was fixed rigidly to a metal framework, freestanding on the floor. The top and bottom of the yoke were provided with linear ball bushings B, through which a 2 inch diameter shaft could be reciprocated whilst positively located radially. The shaft was a tube of hardened steel having a thick layer of hard chrome on the outside diameter, the centre being used to circulate cooling water if necessary.

A pressure vessel D was fitted to the centre of the yoke and usually contained the test seals, the shaft being reciprocated through the centre of the seals thus simulating a rod seal. The reverse situation, as used here, was simply achieved by mounting the seals on to a carrier, rigidly attached to the shaft, and reciprocating the shaft, seal carrier and seals in the smooth bore of the pressure vessel.

The pressure vessel was not mounted rigidly in the yoke but was free to move vertically in the linear bearings E, it was thus fixed radially but had free movement axially. A cross member, bolted rigidly at its

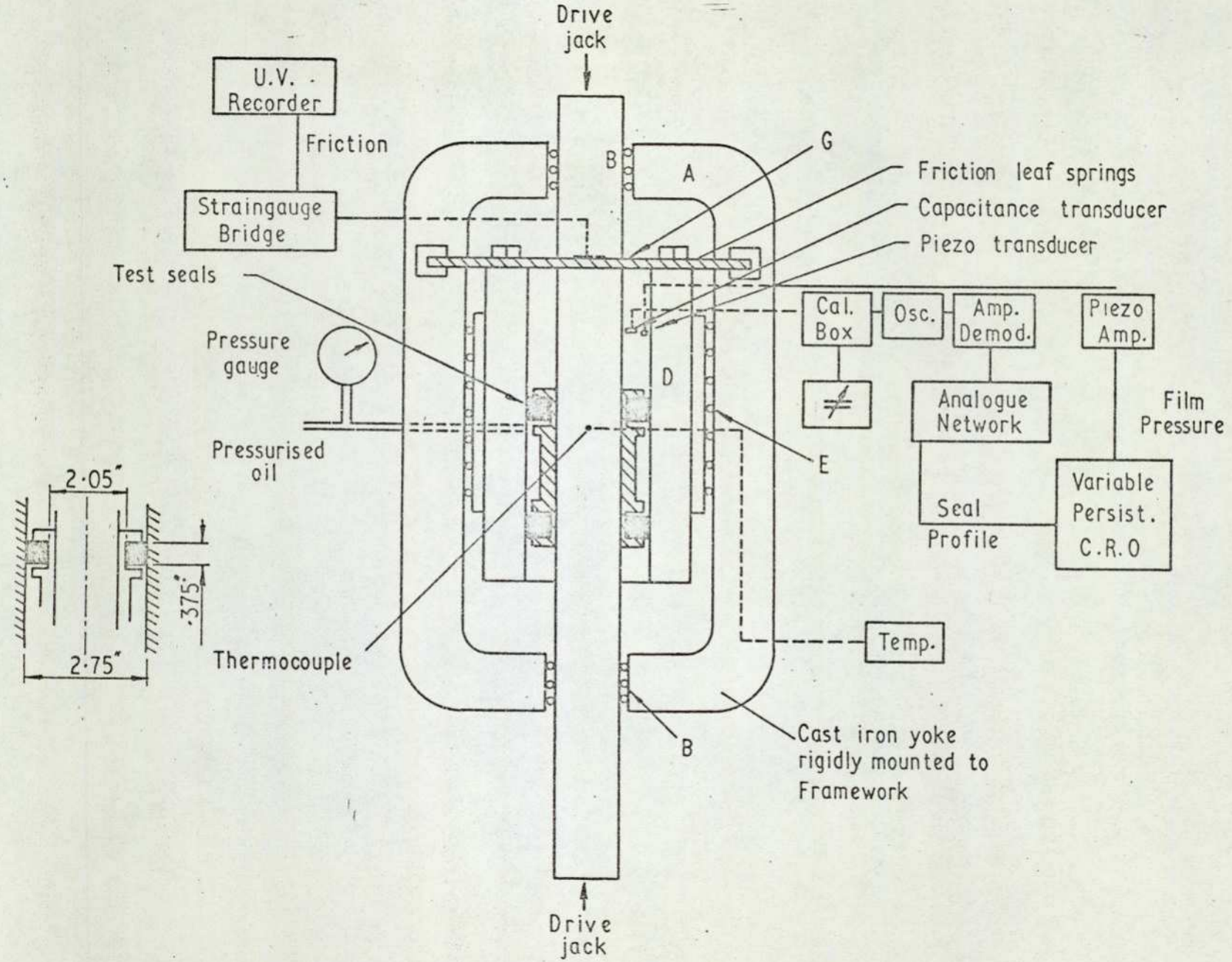


Fig. 4.1. General layout of instrumented reciprocating seal test rig.

centre to the top of the pressure vessel, had its ends rigidly fixed to the plate leaf springs G, in turn fixed rigidly to the main framework of the rig. The vessel could therefore only move against the force of the springs and strain gauges attached to the springs allowed the friction of the seals to be accurately measured.

Pressurised fluid from a vane pump was fed, via a change over valve and flow control valve, to the driving jacks at each end of the shaft and allowed the shaft to be reciprocated at speeds up to 50 ft/min..

The change over valve was operated electrically by an electronic switch receiving signals from microswitches actuated by the shaft at either end of the stroke. The length of the stroke could therefore be determined by the position of the microswitches, the speed being determined by the flow control valve.

4.1.3. Pressure vessel design and transducer mountings

The pressure vessel consisted of a stainless steel cylinder of approximately 2.75 inches internal diameter with a 1.25 inch wall thickness. The outside being machined for mounting in the linear roller bearings and incorporated taper wedges at each side allowing alignment of the bore with the shaft. Alignment was carried out using an alignment telescope, and shaft/cylinder concentricity was better than 0.0005 inches.

The sealed pressure was supplied through a hole at the mid-section of the vessel which limited the stroke of the seals to slightly less than half the length of the vessel which was 6.25 inches long.

The film thickness and pressure transducers were mounted as close together as physically possible in the wall of the vessel at the mid-point of the stroke, on the same circumferential line. The method of mounting is shown in figure 4.2. The pressure transducer was screwed into the pressure vessel and had a shoulder on the end to prevent gaps between the probe and the vessel due to the thread. The film thickness transducer had a tapered body and was pressed and held in by means of the bolt.

After assembly, the faces of the transducers were ground at the same time as the bore of the vessel to ensure conformity of the faces

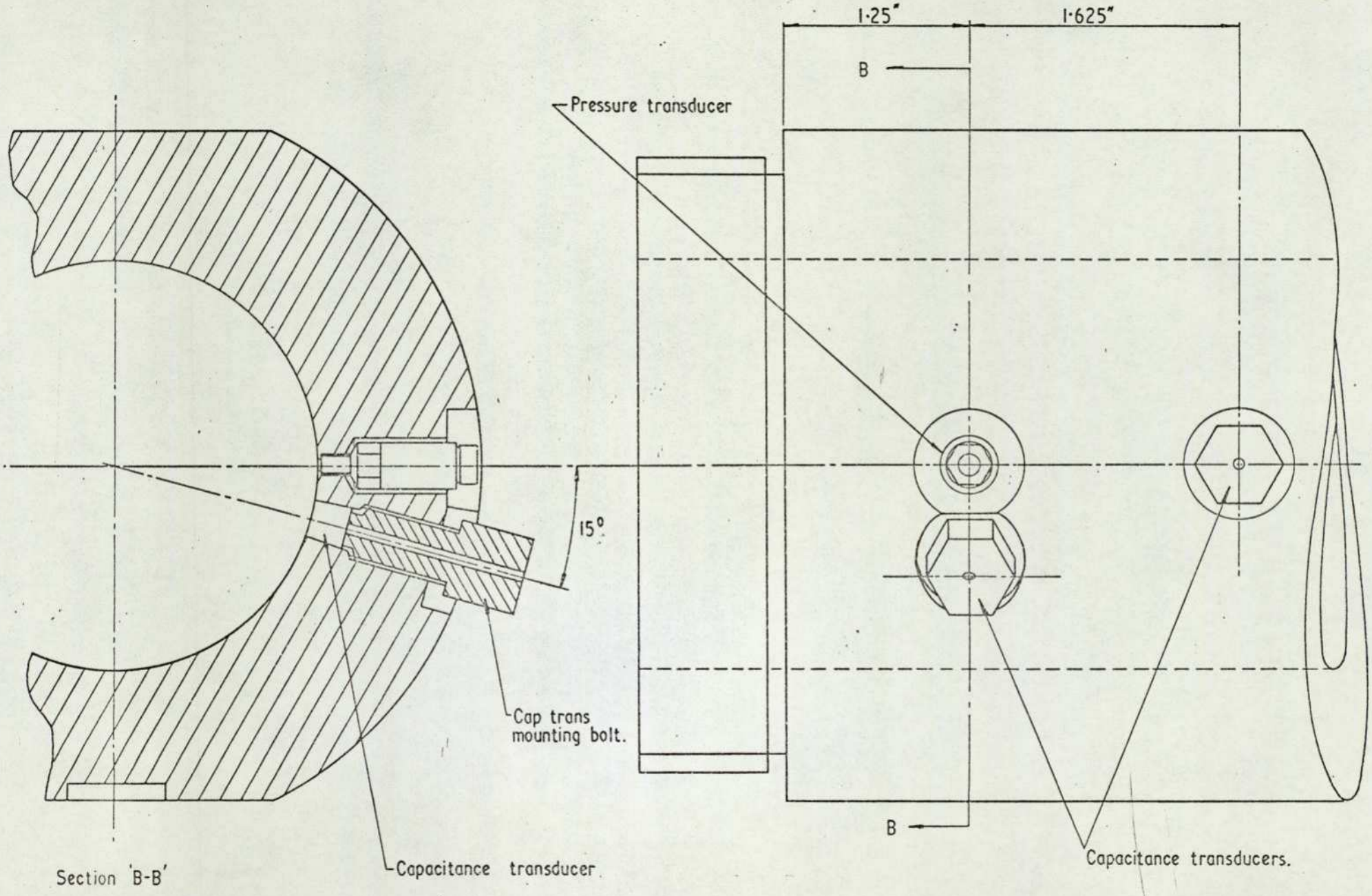


Fig. 4.2. Method of mounting the transducers in the pressure vessel.

with the bore. Initially the surface finish of the bore over which the seals moved was approximately 10 micro inches CLA, but subsequent wear by the seals and light honing reduced this value to 5 micro inches CLA.

4.1.4. Seal Carrier and Shaft

The seals were mounted on detachable end pieces screwed into the centre body of the seal carrier, figure 4.3. The back-up clearance for the seals was determined by the outside diameter of the end pieces on the atmospheric pressure side of the seals and the bore of the vessel. Each end piece also had an 'O' ring seal on the inside to prevent leakage of oil between the seal carrier and shaft. With the seal carrier correctly assembled and positioned on the shaft a separate ring was butted to each end of the carrier and fixed in place by means of grub screws, thus preventing the carrier moving on the shaft.

4.1.5. Seals

The seals used were of a conducting nitrile rubber, the conductivity being achieved by loading the rubber with a high percentage of carbon black. The majority of the results were obtained using a hard rubber (90 IRHD), a softer rubber of 74 IRHD became available towards the end of the test programme. Details of the physical properties of the rubbers are given in Appendix D.

The hard seals were obtained as moulded 3/8 inch square section rings from the Precision Rubbers Division of the Dunlop Company Ltd. and ground on the internal diameter to the required radial section of approximately 0.250 inches with the seal edges left in the "as moulded" condition. In the light of results obtained in the optical rig study, it was realised that the microgeometry of the seal edge was of considerable importance and the moulded sides of each seal were then ground so that the edges between the side faces and the running surface were square.

To obtain round edged seals, the edges of a number of seals were rounded by hand on a lathe, using emery paper. Care was taken to ensure that the radius blended smoothly with the running surface of the seal. The radius of the edge was of the order of 0.010 to 0.020 inches.

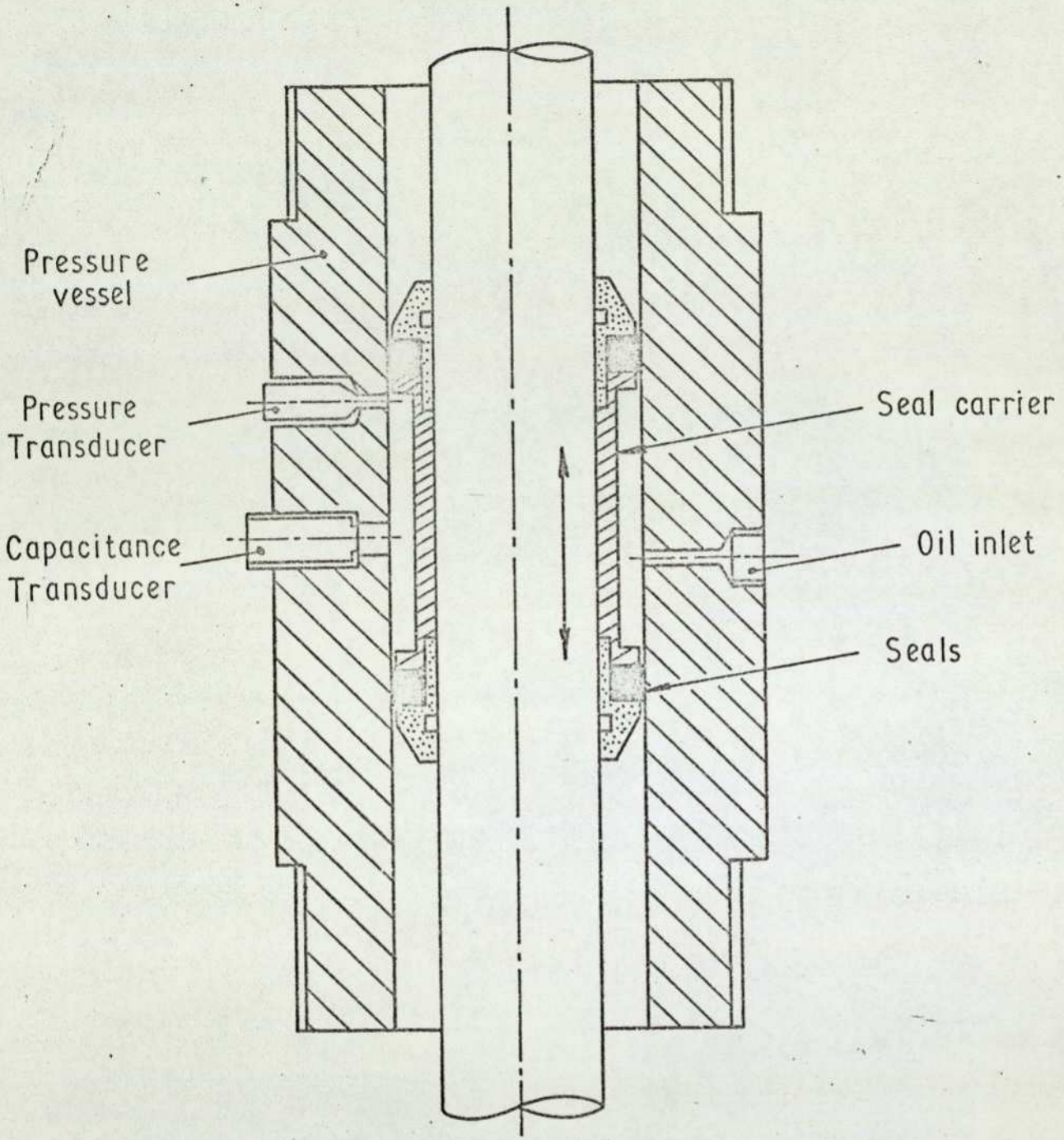


Fig. 4. 3. Reciprocating shaft with seal carrier.

The soft rubber was in the form of a block 3 inches square and 3/8 inch thick and the seal was cut and ground to size from this. This meant that the running surface of these seals was ground rather than moulded.

4.1.6. Fluid

The fluid used throughout the test program was Shell Tellus 27, a hydraulic mineral oil having a viscosity of 7.5×10^{-6} reyns (52 cP) at 25°C and 3.75×10^{-6} reyns (26 cP) at 40°C

4.1.7. Controlled Variables

Speed

The speed of the shaft was controlled by a flow-control-valve in the pressurised oil supply line. The speed was constant throughout the stroke, varying only at the change over point. The speed could be set to a maximum of 100 ft/min. but was only varied up to 50 ft/min. for the present work, this covering the speed range of the majority of jacks.

The shaft position was measured by a displacement transducer which provided a make and break connection every 0.1 of an inch. This switched a resistance/capacitance circuit to provide a voltage pulse which could be recorded on an ultra-violet recorder, together with a mains frequency time-base. This allowed the speed to be calculated, any variations in the speed to be readily checked, and the stroke length to be measured.

The stroke length was controlled by two microswitches which could each be moved independently to give a maximum length of 3.2 inches, which was used for the majority of the tests. At the end of a stroke the pressurised oil was switched to the opposite jack, changing the direction of motion of the shaft, this change-over was very rapid giving an almost instantaneous reversal of the shaft.

Sealed pressure

The pressure between the seals was initially provided by an air-hydropump and could be varied from 0 to 1000 lb_f/in^2.

Later this was modified when the lower seal was replaced by a

floating bush, the leakage of which exceeded the capacity of the air-hydropump. An axial piston pump which could supply an increased flow rate over the same pressure range was then fitted. The pressure was displayed on a Bourdon tube pressure gauge.

Temperature

The usual method of temperature control on this type of rig is by circulation of cooling water through the shaft, a 3Kw heater and a flow control valve in the water supply providing a degree of manual control of temperature. For testing seals mounted in the pressure vessel this is found to be adequate. With the present test arrangement of a seal carrier on the shaft, the degree of control was not adequate because of the high thermal resistance between the shaft and seal carrier and an automatic temperature control unit was built to improve the control. The temperature was measured using a thermocouple mounted in the oil in the pressure vessel.

For the tests using the floating bush and hence a high flow rate of oil through the pressure vessel, the temperature was controlled via the circulating oil, in turn temperature controlled via a 3Kw heater and an oil cooler. It was found that this system enabled the temperature in the pressure vessel to be controlled to within $\pm$ 2^{o}C during a test run.

All the tests were made within the temperature range 20^{o}C to 50^{o}C., the lower temperature being limited by the atmospheric temperature, the upper limit being imposed by the epoxy resin adhesive used in the construction of the transducers.

Surface finish of the bore of the pressure vessel

Initially the bore of the cylinder over which the seals moved was measured and found to be approximately 10 micro inches CLA. However subsequent wear due to reciprocation of the seals and light honing brought the finish down to approximately 5 micro inches CLA.

Back-up clearance (BUC)

This is the radial clearance between the cylinder bore and the seal carrier into which the seal can extrude under the action of the pressure differential across it. Ideally the clearance should be as small as possible, but due to machining tolerances values from 0.001 to 0.005 inches or more may occur in practice.

The extrusion clearance throughout most of this test programme was 0.003 inches, but in later tests values of 0.005 inches and 0.010 inches were also used.

Seal interference

The interference of a seal is the difference between the radial thickness of the seal and the clearance between the base of the seal groove and the cylinder bore. For 'O' rings this can be of the order of 20% of the cross section but for square section rings is usually nearer to 10%. During the major part of the programme the initial interference was kept constant at 0.005 ins., or 2%, due to the high hardness of the seal material, but this might increase or decrease during the life of the seal because of elastomer swelling, shrinkage or wear. By inserting various thicknesses of metal shim under the seal, the interference force could be increased and later tests used this method to vary the interference from 0.005 to 0.010 inches.

Seal hardness

The requirement for a conducting rubber initially limited the hardness of the rubber to a high value, 90 IRHD, but later one seal was obtained with a hardness of approximately 70 IRHD.

Fluid Viscosity

As the same fluid was used throughout the program, the viscosity could only be changed by operating the rig at different temperatures. In practice this entailed reducing the cooling water flow and allowing the temperature of the oil to rise slowly throughout the period of test. The viscosity could in this way be varied over the range 37.5×10^{-7} to 85.0×10^{-7} reyns.

This method may not give the same result as operating with fluids of different viscosity but constant temperature, as properties of the rubber such as hardness, resilience and swell will all be affected by the temperature and will themselves cause variations in the film profile and friction.

4.1.8. Dependent Variables

Seal friction force

The friction force of the seals during reciprocation was transmitted via the vessel and a U channel to strain gauged springs at the front and rear

of the steel framework, the pressure vessel being free to move axially in the yoke by means of the linear roller bearings.

The strain gauges were arranged in a full bridge network, the output of which was recorded on an ultra-violet recorder. The galvanometer used had a frequency response of 35 c/s and with a suitable damping resistance was capable of continually recording the movement of the springs and hence the friction of the seals.

Calibration of the friction measuring device was carried out by means of dead weight applied either directly to the U section channel or by means of a lever arrangement to allow calibration in an upward direction. The calibration was linear over the range used. The friction force was recorded continuously throughout the stroke, but a marker was incorporated to indicate the point in the stroke where the film profile was measured. The plotted friction values are therefore precisely related to the measured film thickness.

The test rig design as normally used, entails the use of two seals in the pressure vessel and the measured friction is therefore that of the two seals. On any stroke of the rod one seal is operating on an outstroke whilst the other is on an instroke and the measured friction is therefore the mean of the two strokes. Müller (34) however had shown that the friction of the two strokes could be widely different and this appeared to be confirmed by the film thickness measurements of Series 2. Several methods of measuring the friction of a single seal were then considered and the one adopted consisted of replacing the lower seal on the seal carrier with a bush having a close fit in the bore of the pressure vessel. Measurements of the friction of such a bush indicated that it was negligible compared to that of a seal and it was therefore used for all subsequent test series.

Seal leakage

Two methods of measuring leakage were used during the test programme:

(a) Direct collection of leakage. For individual seals, this method was possibly the most accurate, but for very low leakages, the time required to obtain a measurable sample was excessive.

(b) The second method consisted of measuring the total amount of fluid supplied to the pressure vessel. This was fairly simple to do by monitoring the movement of the piston of the air hydro-pump supplying the pressurised fluid.

When using the floating bush, only the first method could be used, and because of the time involved to obtain sufficiently reliable readings, the leakage was only measured in a few tests.

Film thickness

The measurement of the film thickness under a reciprocating seal poses problems due to the very stringent requirements. These are:

(a) the film to be measured is in the range of zero to a few hundreds of micro inches.

(b) the pressure varies rapidly as the seal passes the probe and the probe must not deflect significantly.

(c) the probe dimensions must be as small as possible, particularly in the axial direction

Design of capacitance transducer

Using conducting rubber seals and a circular section capacitance transducer mounted in a 2 inch diameter rod, Nau (37) had shown that measurement of the film thickness under a reciprocating rubber seal was feasible. Theequipment used for that work was available and was taken advantage of for the present tests.

The circular capacitance probe of Nau (37) was 0.080 ins. in diameter and in order to improve the resolution the new probe was in the form of a rectangle of axial length 0.020 inches. It was necessary however to increase the circumferential length to retain the same probe area as previously, and it was thought that this would be acceptable as the film thickness in a circumferential direction seemed unlikely to change significantly along the circumferential length of the probe, 0.2 inches.

The probe design can be seen in figure 4.4. The centre portion was of copper shim 0.020 inches thick and the main body formed from a standard taper pin. During assembly the centre portion was insulated from the body by 0.004 inches thick glass sheet at the sides and at the base, the whole being bonded together with epoxy resin. The connecting

lead was arranged to leave the probe along the centre line in order that a bolt with a central hole could be used to force the probe into the tapered hole in the main pressure vessel, where it was bonded with epoxy resin. Care was taken to ensure that the probe was precisely normal to a central line through the pressure vessel.

After assembly of the probe into the main vessel the final grinding of the bore of the vessel ensured that the probe face conformed to and was flush with the bore.

Calibration of capacitance transducers for fairly thick films can be achieved using mechanical devices to steadily vary the distance between the transducer and a second conducting surface. However, this assumes that the distance can be reliably and accurately measured by other means. In the case of seal films, the thickness was expected to be in the range up to 300 micro inches which would have been difficult to measure in the confines of a bore only 2.75 inches in diameter.

The problem of calibration was overcome through a knowledge of the area of the probe, measured using a travelling microscope after assembly in the vessel, the dielectric constant of the fluid, and the complete capacitance circuit of the transducer which allowed the film thickness to be calculated. A complete description of the capacitance method is given in Appendix E, and an error analysis of the film thickness measurement in Appendix F.

Dynamic pressure measurement

Severe limitations of space and frequency response limited the choice of transducers for the purpose of measuring the dynamic pressure under the seal during reciprocation. To obtain localised values of pressure, the transducer should measure the pressure over as small an area as possible, ideally at a point. A good frequency response was required because the pressure rises rapidly from zero to the system pressure as the seal passes the probe. For a 0.375 inch seal travelling at 30 ft/min, the traverse time is only 37 millisecs. Finally the compliance of the transducer must be extremely low otherwise its deflection will disturb the film pressures being measured.

Design of pressure probe

A piezo crystal pressure transducer was the only type meeting the compliance requirement although the sensing area of the smallest transducer available was 4 mm diameter compared to the required 1 mm diameter maximum.

Several methods used to reduce the probe area also reduced the effective frequency response and also created another problem. A transition chamber to reduce the area was required and this had a small but finite volume. A simple calculation showed that the compression of the oil in this, due to the change in pressure from zero to system pressure, was equivalent to the volume of a large area of the oil film around the probe. The volume of oil over this area would in effect be 'sucked' into the transition piece starving the area around the seal of oil and leading to erroneous results.

In the final transducer, figure 4.5, the transition was achieved by using a small metal piston bonded at one end to the sensing area of the transducer and sealed at the other end with epoxy resin to prevent oil flowing into the space remaining. This eliminated the problem of the compression of the oil, although it reduced the sensitivity of the transducer. Calculations showed that the epoxy resin seal would not significantly affect the minute deflections required by the piezo crystal to measure the pressures likely to be encountered. Calculations were also carried out to ensure that the transition piece would not buckle under the end load applied to it.

The transducer after fitting to the transition piece was fairly temperature sensitive, possibly due to differential expansion of the transition piece and the metal piston. However it was thought that because of the large mass of steel around the transducer when installed and the short time in which the seal would be actually passing the probe, this would not introduce serious errors.

4.1.9 Recording and processing of results

MKI - Ultraviolet recorder and digital computer processing

For the preliminary tests, the output voltage of the demodulator was recorded using an ultra violet recorder. It was found, however, that

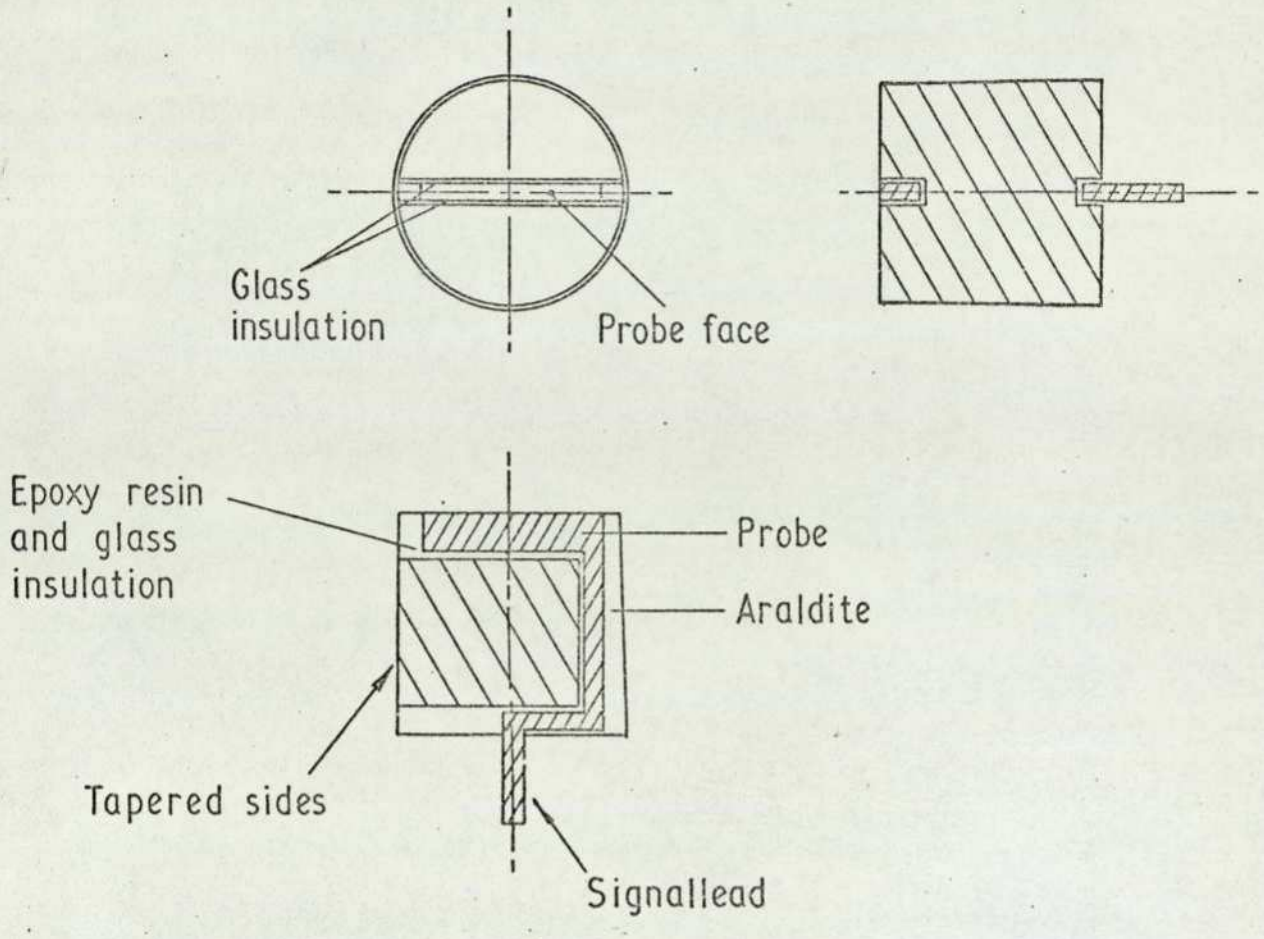


Fig. 4. 4. Capacitance transducer design.

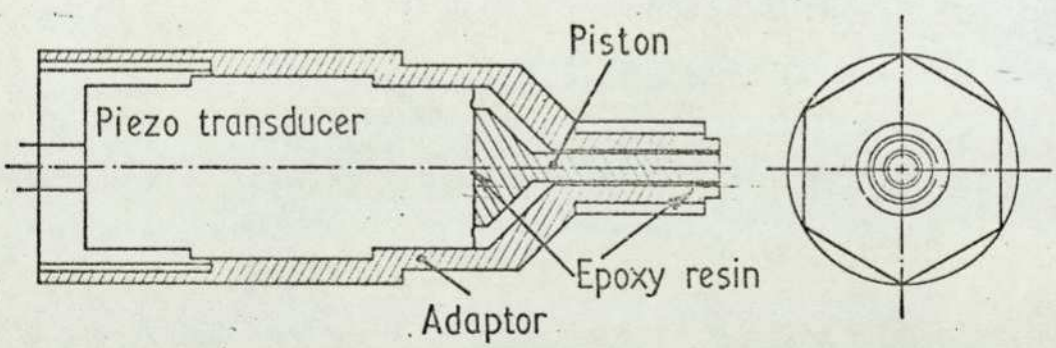


Fig. 4. 5. Pressure transducer design.

the frequency response of the galvanometer was too low for the rapid film variations occurring within the seal film profile.

A further difficulty arose due to the non-linearity of the measuring system, and replotting the UV recorder trace onto a linear scale involved measurement of the recorded trace from the zero film thickness line and calculating the film thickness at a considerable number of points along the seal length. The method was both tedious and extremely time consuming.

A digital computer program was later used to do the calculations and plot the graphs but the total time taken for analysis was still excessive.

A rough check on the number of tests to be completed showed that a better method of analysis was required if the experimental work was not to be limited by the physical task necessary to convert the recorded results to actual seal shapes for easy comparison.

MK II - Analogue computer and dualbeam storage oscilloscope

Several methods of analysis were then reviewed. In particular analogue tape recording of the demodulator signal and subsequent digitisation by an analogue/digital computer system using computer graph plotting techniques was considered, but was ruled out because of the cost of such a system.

The possibility of an on-line analogue computing network was then considered and appeared to be the ideal solution, particularly as a small general purpose analogue unit was available. This was duly set-up and arranged to solve equation (E21) of Appendix E.

Because the UV galvanometer had a poor frequency response and required more power to drive than the analogue computer could supply, an oscilloscope was used as a recording device, thus eliminating both problems. Initially a standard dual beam unit was used but recording of the results was difficult due to the need to use an oscilloscope recording camera and the poor reliability of the internal triggering mechanism of this particular oscilloscope. In view of these problems a dual beam storage oscilloscope was obtained and fitted with an external triggering signal, which improved the procedure immensely. Reliable triggering could be obtained together with easy viewing of the true film shape during

running and simple recording of the result once the film shape was stored on the oscilloscope. The recording camera used was a standard 35 mm SLR camera.

4.1.10. Details of experimental procedure

These are set out in Table4.1and are briefly described below.

Series 1

The seals used for this series were ground to size on the inside diameter of the seal. The sides of the seal were not ground. Two nominally identical seals were used in the rig, the uppermost being the test seal.

The film thickness pressure and friction signals were recorded using an ultra-violet recorder, the film thickness result being processed by digital computer and plotted via an on-line graph plotter.

The test procedure was to set the required test pressure and increase the speed in steps from 10 ft/min to 50ft/min. At each speed the rig was allowed the run for at least 5 minutes to allow the conditions to stabilise before recordings were made. After the maximum speed had been reached, the speed was reduced to the minimum and the next higher pressure selected and the procedure repeated until the maximum pressure was reached.

It was not possible to record the bulk oil temperature during this series.

Series 2

The tests were conducted on a new seal ground to the correct radial section.

The instrumentation was modified by incorporation of an analogue computer to enable the film thickness signal to be linearised before being recorded. Recording of the film thickness and pressure profiles was by dual-beam storage oscilloscope, the trace being photographed with a 35mm camera.

Calibration of the film thickness recording was from a fixed capacitor which provided calibration marks corresponding to calculated values of film thickness.

When removed from the rig the seal was deeply scored in two places. The cause was traced to partial seizure of the seal carrier in the bore. Fortunately this did not occur in the vicinity of the probes, and

would, therefore, not be expected to have affected the results.

The test procedure was the same as for Series 1, but in addition the temperature of the bulk oil could be measured.

Series 3

Because of the seizure of the seal carrier in Series 2 the end piece of the carrier was replaced with one of phosphor bronze and the trouble did not occur subsequently.

Also incorporated into the rig for these tests was the floating bush, allowing friction measurements of a single seal.

The test procedure was the same as for Series 1, the temperature being held at 40°C throughout.

Series 4

In view of the findings relating to the seal edge in the interferometric study (Chapter Three), the sides of the seals for Series 4 were ground to provide a sharp corner at the ends of the sliding contact. (For the previous tests the edges were left as moulded). The atmospheric edge of the seal was reformed by grinding if any extrusion damage occurred. The seals were marked to ensure that they were replaced in the same relative position.

For Series 4 the test procedure was modified the pressure being increased in steps over the range whilst keeping the speed constant. The effect of pressure on the film shape was much more pronounced than the effect of speed and this procedure gave a clearer indication of when the film profile had stabilised after a change in the conditions of test.

Series 5

Considerable trouble had been experienced in previous tests with drifting and failure of the frequency demodulator unit and for Series 5 this was therefore replaced with a transistorised version obtained from the same manufacturer. This unit required modification by the manufacturer to be compatible with the transducer system but operated reliably throughout this series of tests.

The test procedure was the same as for Series 4.

TABLE 4.1

Series		1	2	3	4	5
Seals	Test Seal	Rect. Sect. Ring	Rect. Sect Ring	Rect. Sect. Ring	Rect. Sect. Ring	Rect. Sect. Ring
	2nd Seal	Rect. Sect. Ring	Rect.Sect. Ring	Floating bush	Floating bush	Floating bush
	Edges	Undefined	Undefined	Undefined	Ground square	Ground sq. & round
	Hardness	90 IRHD	90 IRHD	90 IRHD	90 IRHD	90 & 70 IRHD
Recording Method		UVR	Analogue Comp. +DBSO	Analogue Comp. +DBSO	Analogue Comp. +DBSO	Analogue Comp. +DBSO
Analysis Method		Comp. & graph plotting	Direct readout	Direct readout	Direct readout	Direct readout
Controlled Variables and Range	Speed	10-50 ft/min	10-50 ft/min	10-50 ft/min	2-10 ft/min	10-50 ft/min
	Pressure	200, 400, 600, 1000 lbf/in^2	200, 500, 1000 lbf/in^2	200, 400, 600, 800 1000 lbf/in^2	200, 400, 600, 800, 1000 lbf/in^2	0, 200, 400, 600, 800, 1000 lbf/in^2
	Temperature	Not recorded	Recorded 30, 40, 50°C	Recorded 40°C	Varied to change Viscosity 20-40°C	30°C
	Stroke length	-	-	-	Film measured thro'out slide length	-
	Circumference	-	-	-	Film measured around circumference	-
	Viscosity	-	0.59, 0.375, 0.26x10^{-5} reyns	0.375 x 10^{-5} reyns	.375--85 x 10^{-5} Reyns.	0.59 x 10^{-5} reyns
	Interference, in.	0.005	0.005	0.005	0.005	1.001, .003, .005, .008, .010
	Back up clearance, in.	0.003	0.003	0.003	0.003	.003, .005, .010
	Repeatability	-	-	-	Repeatability checked.	-
Measured Variables	Film thickness	*	*	*	*	*
	Spec. Mean	*	*	-	-	-
	Fric. In & Outstroke	-	-	*	*	*
	Leakage	-	-	*	-	-
	Pressure profile	*	-	-	-	-
Modifications			Temp. meas. added Seal carrier material changed to phosp.bronze	Float. bush used as 2nd seal.	-	New demodulator used Mod. seal carrier
Test Procedure		Vary speed over constant pressure	Vary speed over constant pressure	Vary speed over constant pressure	Vary pressure over constant speeds	Vary pressure over constant speeds

SUMMARY OF TEST SERIES

4.2. RESULTS

4.2.1. Preliminary tests: Series 1

Film Profiles

For this series of tests the transducer system gave a non-linear calibration of film thickness versus UV recorder deflection, typical examples of which are shown in figure 4.6., in which both zero and infinite film thickness are recorded. The true film shape is difficult to envisage from this but a number of traces were processed on a digital computer and corrected profiles figure 4.7 were obtained. Part of the excessive curvature of these profiles derives from the computer curve setting procedures.

The different behaviour on the instrokes and the outstrokes show clearly in figure 4.7. At low pressures, figure 4.7 a and b, the film profiles are similar for both strokes, but as the pressure is increased they become increasingly different. The outstroke profiles show an increasing 'nip' as the pressure rise tends to form two 'nips' one at each end of the seal; this is particularly noticeable in figure 4.7 c for a pressure of 400 lbs_f $/in^2$, but at 800 lbs_f $/in^2$, the whole film appears to have increased with pressure, except at the lowest speed.

Speed seems to have had very little effect on the film profile except at the highest pressure on the outstroke. In general, an increase in speed increased the film thickness.

In figure 4.8 the film profiles of figure 4.7 are shown for a range of pressures at each speed and this shows more clearly the effect of pressure on the film. At the lowest speed this is very small but becomes more significant as the speed increases, thus at 50 ft/min the effect of pressure is considerable, the film almost becoming greater than the limit of the transducer. This is noticeable on both strokes.

The minimum film thicknesses are compared in figure 4.9 which again brings out the difference between the instrokes and the outstrokes, and the enhanced speed effects at higher pressures for the outstrokes. Also shown is the surprising fact that whereas the minimum film thickness on an instroke decreases with pressure, the reverse situation occurs for outstrokes.

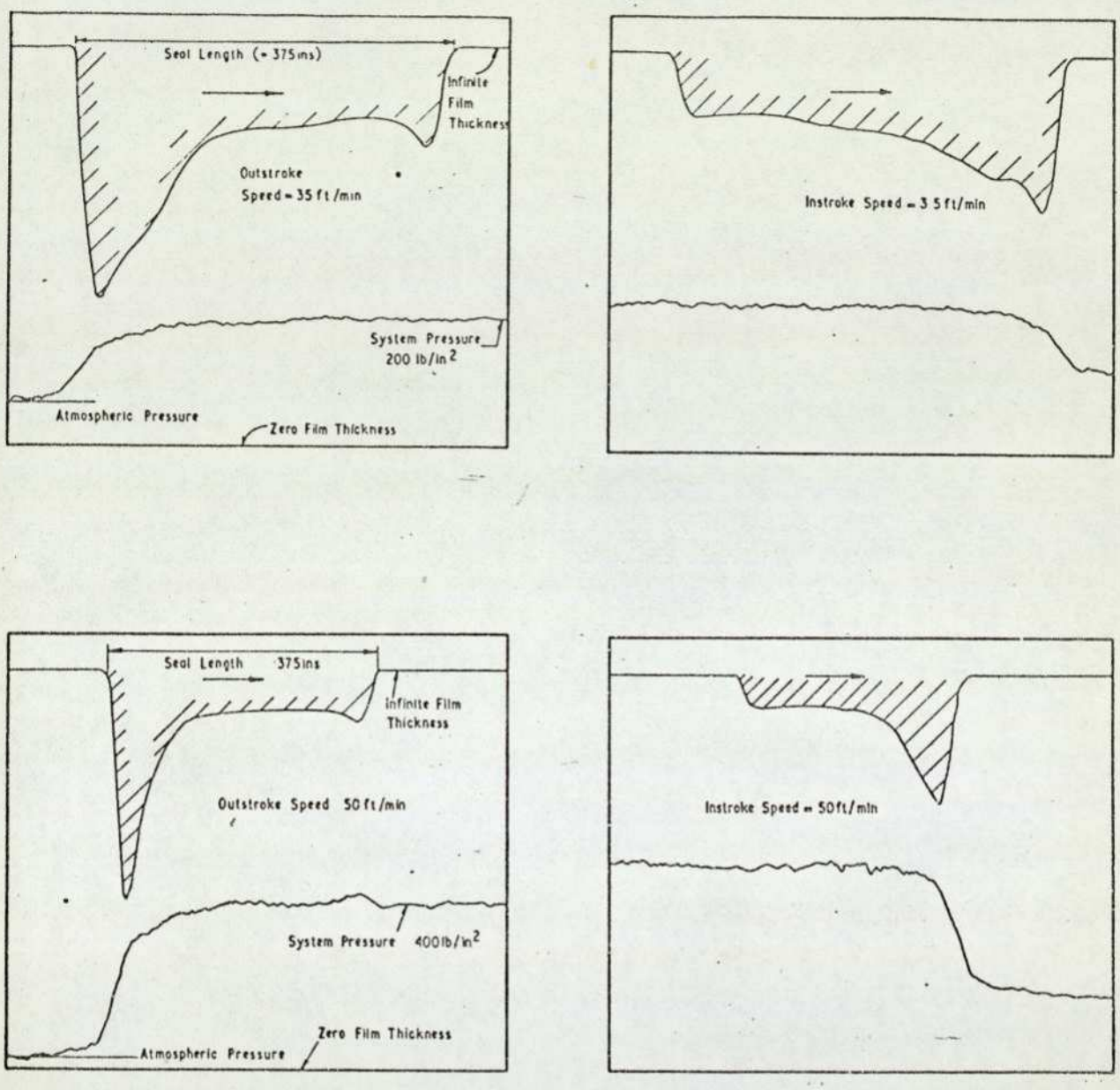


Fig. 4. 6. Examples of UV recorder traces of film thickness and pressure: Series 1.

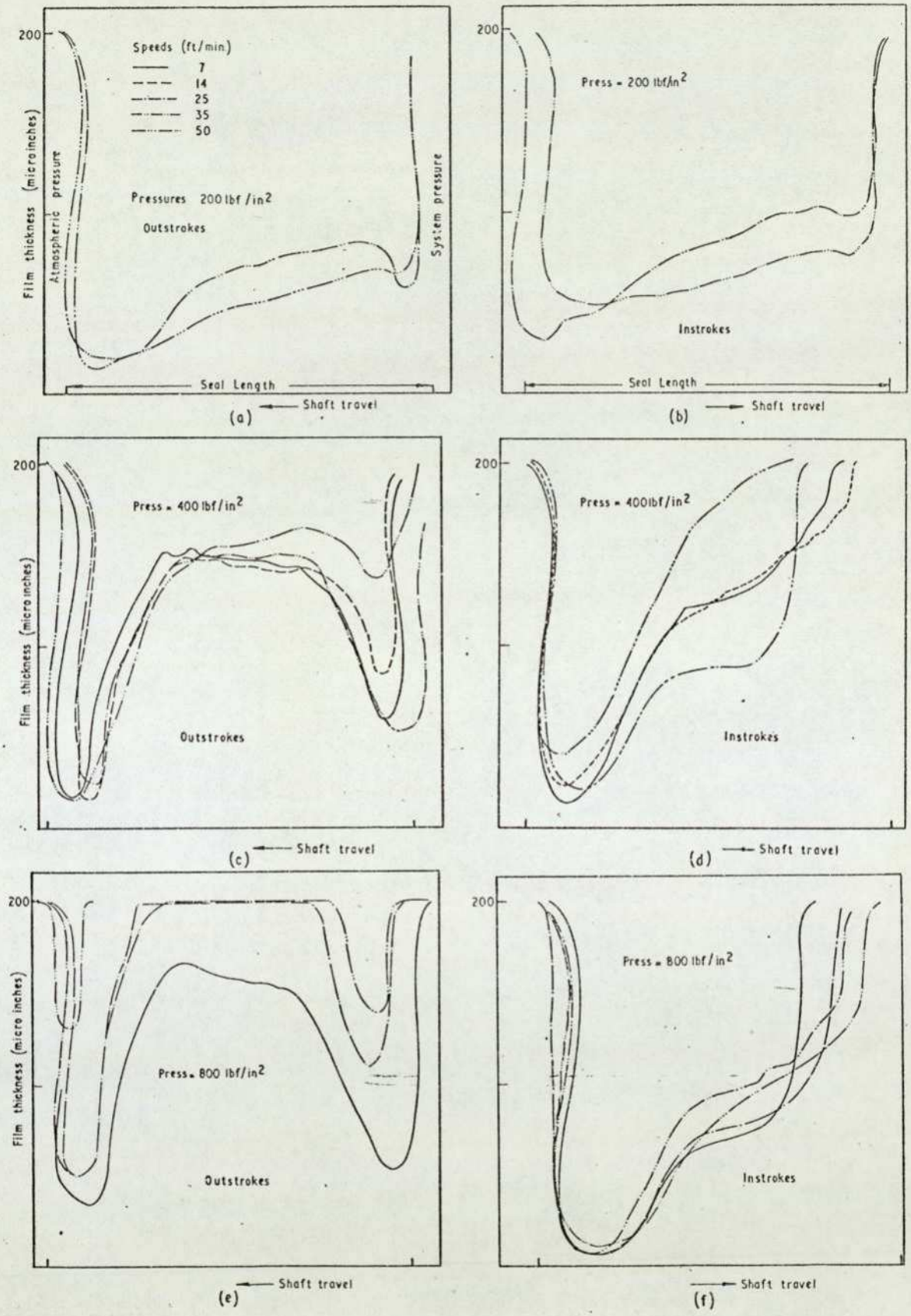


Fig. 4.7 Film profiles plotted by digital computer: Series 1

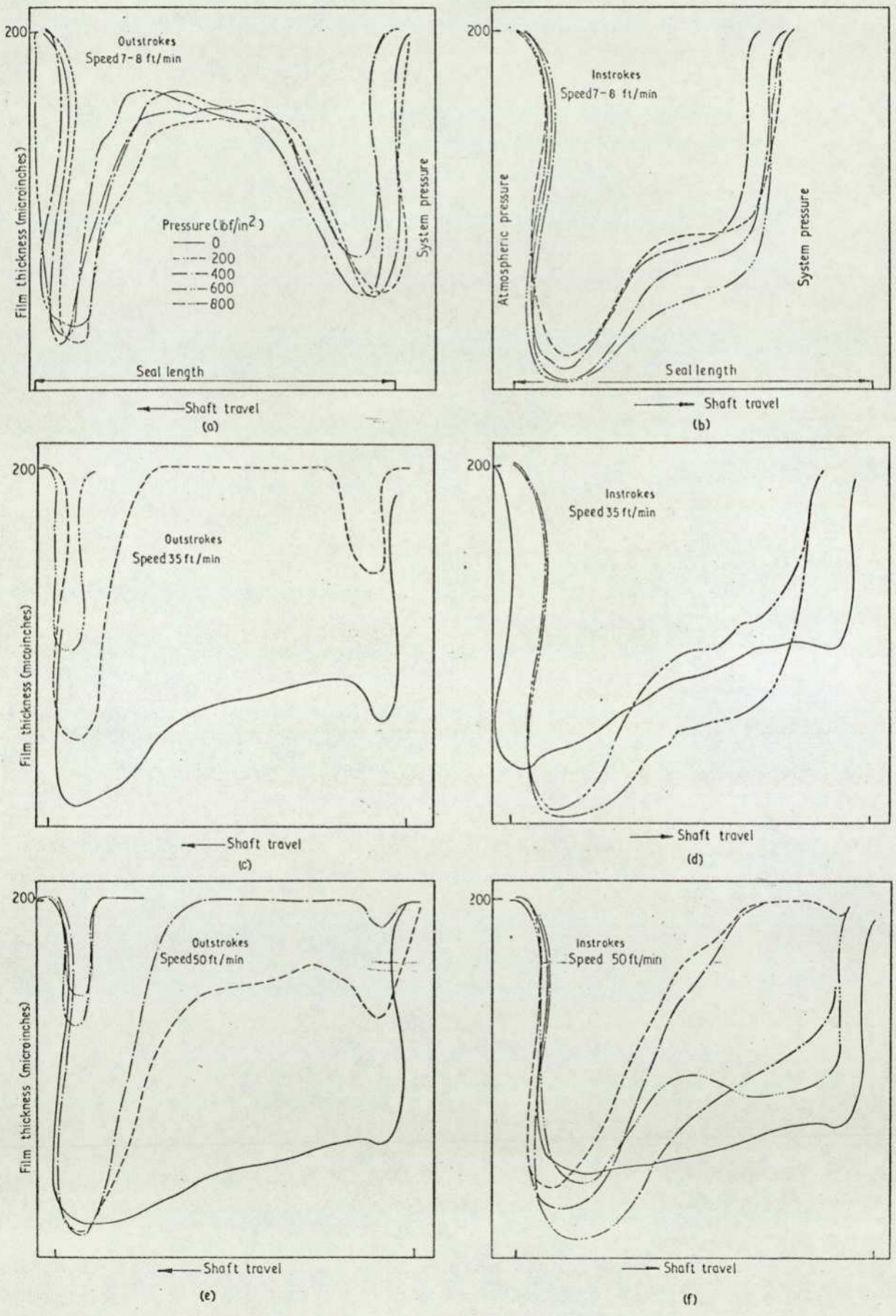


Fig. 4. 8. Film profiles plotted by digital computer: Series 1.

Later results indicated that the film profiles obtained during these tests were characteristic of a low interference seal. The 'inverse' analysis of Reynold's equation indicates that the double 'nip' profile could also be caused by slight changes in the interference stress. This is discussed more fully in a later section.

Film pressures

The recorded film pressures of figure 4.6 present no calibration problems as the values of pressure at each end of the seal are known and the calibration is linear.

Simultaneous pressure and film thickness profiles are shown in figure 4.10 for pressures of 200 and 1000 lb_f/in^2 and a speed of 50 ft/min. Unlike film thickness, pressure varies across the seal in a very similar fashion on both strokes. The pressure maintains a fairly uniform high value over the inner 90% of the seal, falling rapidly near the outer end at the film 'nip'. This situation can be understood when it is appreciated that the film pressures must be closely similar to the contact stress exerted by the seal, which originates from the combined effects of initial interference and the system pressure transmitted by the rubber seal axially and radially.

Specific friction.

Figure 4.11 shows the friction values obtained during Series I and it must be remembered that these are the mean for the two strokes. The magnitudes of the specific friction values are typical of those obtained with many types of elastomer seal. For the speed range tested the friction decreases with increasing speed. The effect of pressure appears to be pronounced at low pressures, but not at the higher pressures of 600 and 1000 lb_f/in^2. This confirms earlier findings (39) where the phenomenonis explained in favour of the progressive flattening of rubber asperities until the real contact area becomes independent of increased load.

4.2.2. Film Profiles

Series 2 - 5.

Outstrokes

The outstroke film profiles of Series 1 showed a 'nip' at both ends of the seal, but in the later series this was not typical and may have

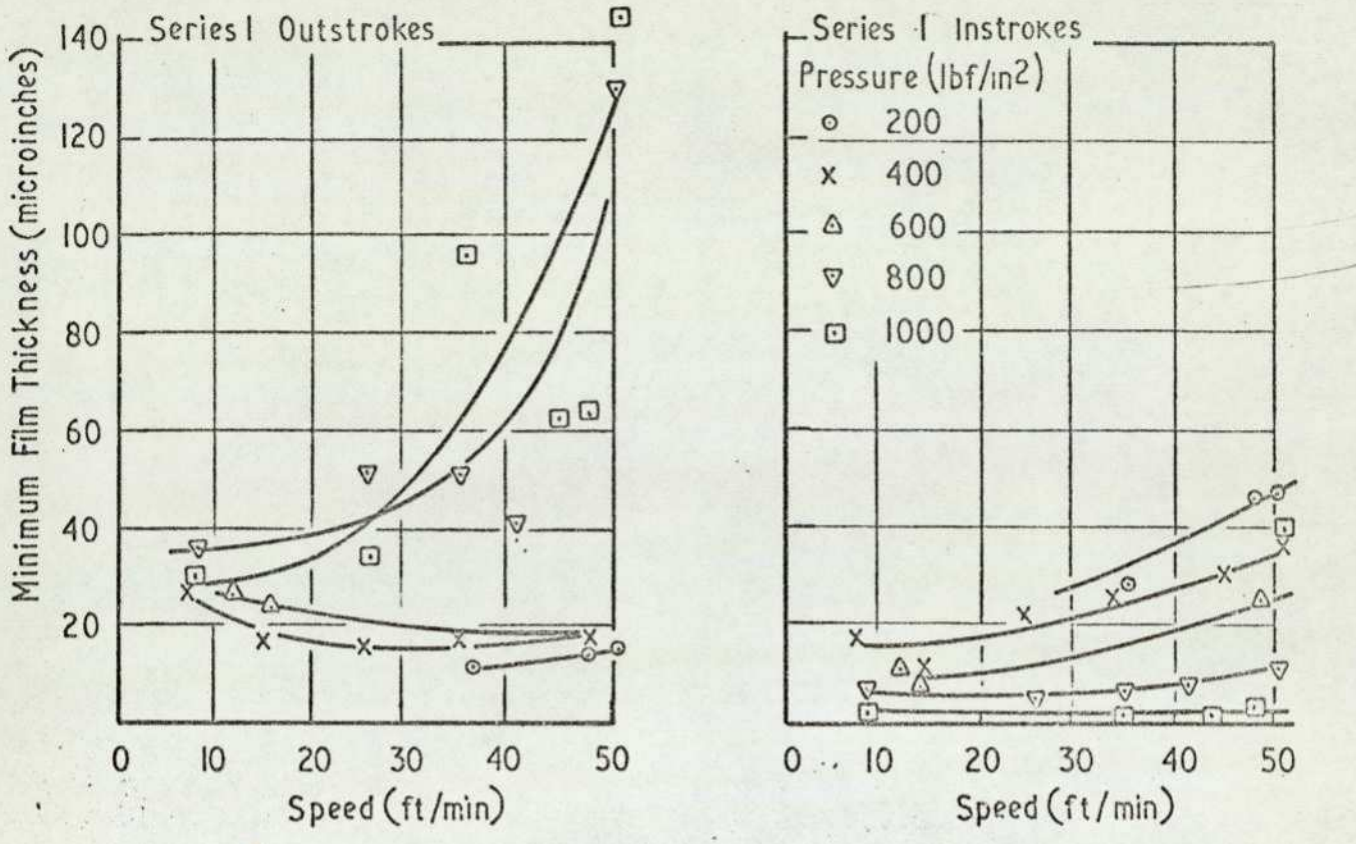


Fig. 4.9. Minimum film thickness against speed: Series 1.

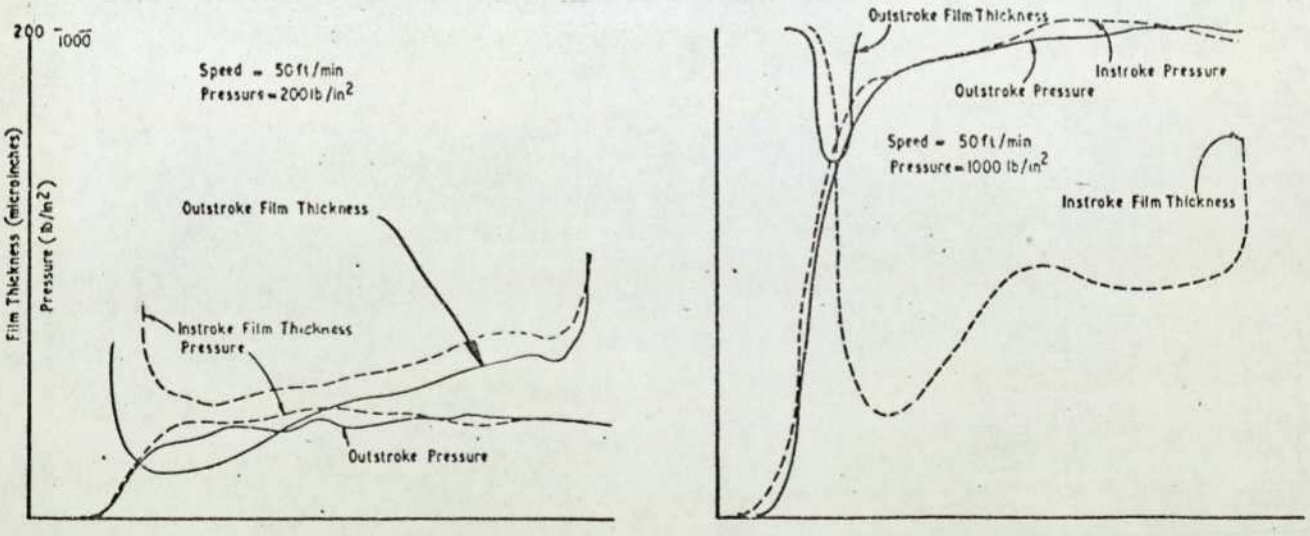


Fig. 4.10. Examples of film thickness and pressure profiles: Series 1.

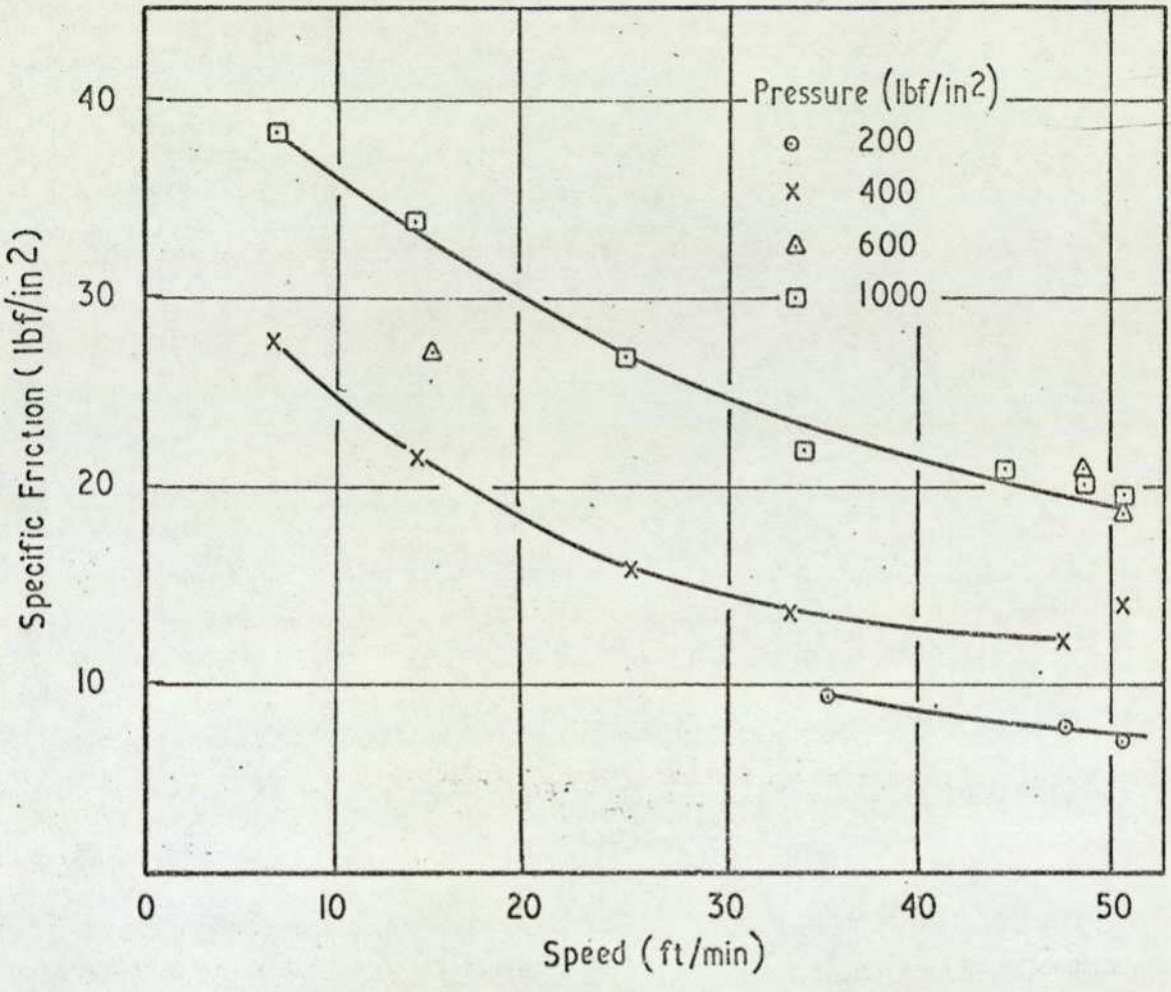


Fig. 4.11. Mean specific friction against speed: Series 1.

been due to the contact stress distribution of this particular seal. Generally the outstroke profiles were of the form expected in elasto-hydrodynamic lubrication, i.e. having a parallel tapered profile over most of the contact with a pronounced 'nip' at the atmospheric side of the seal. There was, however, considerable variation within this basic envelope of film shapes.

Because of the wide variation in the film profiles it is difficult to present the results in terms of a 'characteristic' film thickness; therefore, in many cases the seal profiles themselves are presented to illustrate particular features. Where minimum film thicknesses are plotted it should be remembered that in general the film shape was also changing.

Speed effects

The outstroke speed has considerable effect on both the film profile and the minimum film thickness, the interactions being exceedingly complex.

The film profiles obtained during Series 3 tests figure 4.12 show only slight variations with speed, as do the minimum film thicknesses figure 4.13 which vary only slightly above and below a value of 100 micro inches. However, in other tests, notably those of Series 2 and Series 5, the behaviour of the seal was completely different. For Series 2 the minimum film thickness increased with speed in most tests but decreased for a pressure of 200 lbf /in.^{2} In Series 5 the minimum film thickness, figure 4.14, increased rapidly with speed, and the film profiles figure 4.15 were also considerably affected.

Although the tests of all series were carried out under nominally the same conditions, two major differences are evident, (a) in Series 2 and 3 the seal edges were 'as moulded' but in Series 5 they were carefully ground square in response to the results of the optical study and (b) in Series 2 and 3 the range of speeds was covered for each pressure in turn whereas in Series 5, the pressure range was covered for each speed in turn. At first sight it appears that these differences between tests of Series 3 and 5 have caused significant differences in the seal behaviour, but there is also considerable difference in the behaviour of the seals of Series 2 and 3 which were conducted in the same way. However for

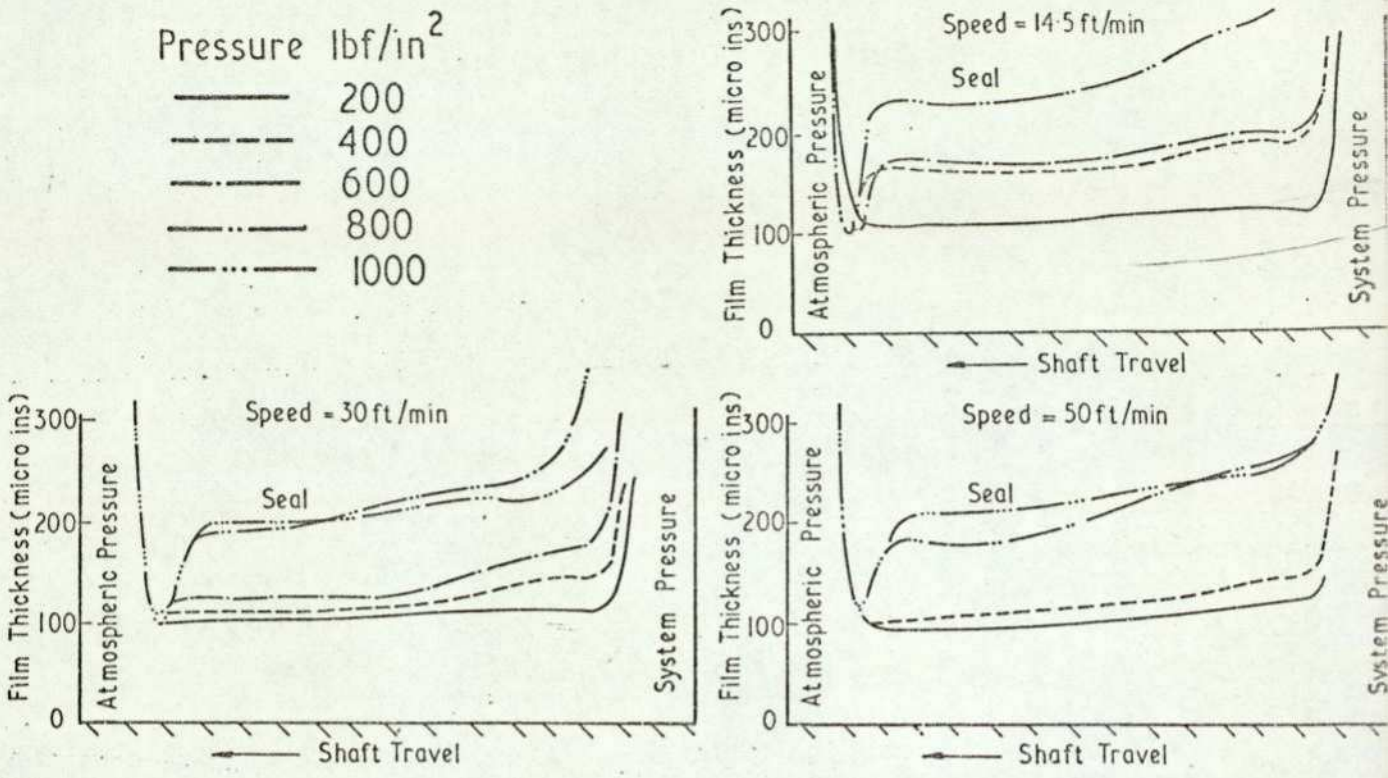


Fig. 4.12. Outstroke film profiles: Series 3.

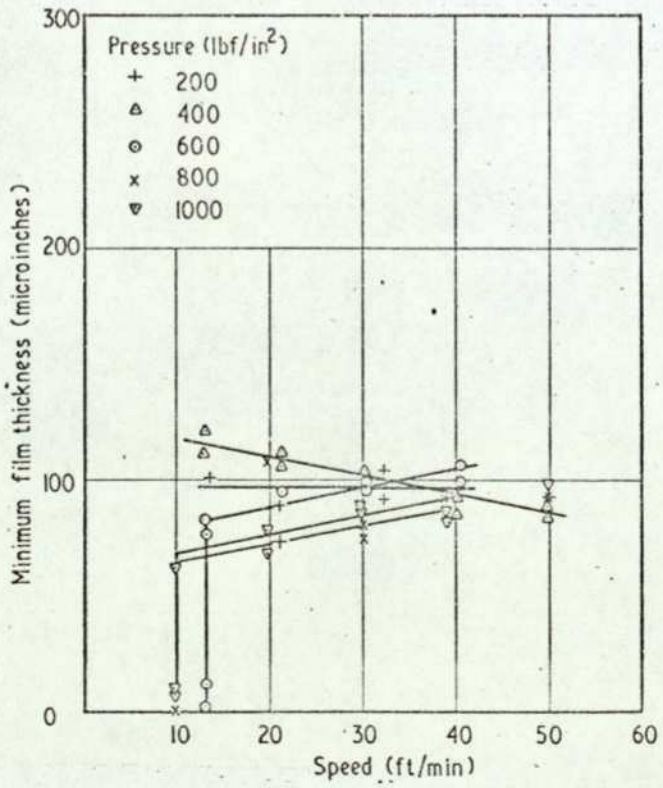


Fig. 4.13. Outstroke minimum film thickness against speed for a range of pressures: Series 3.

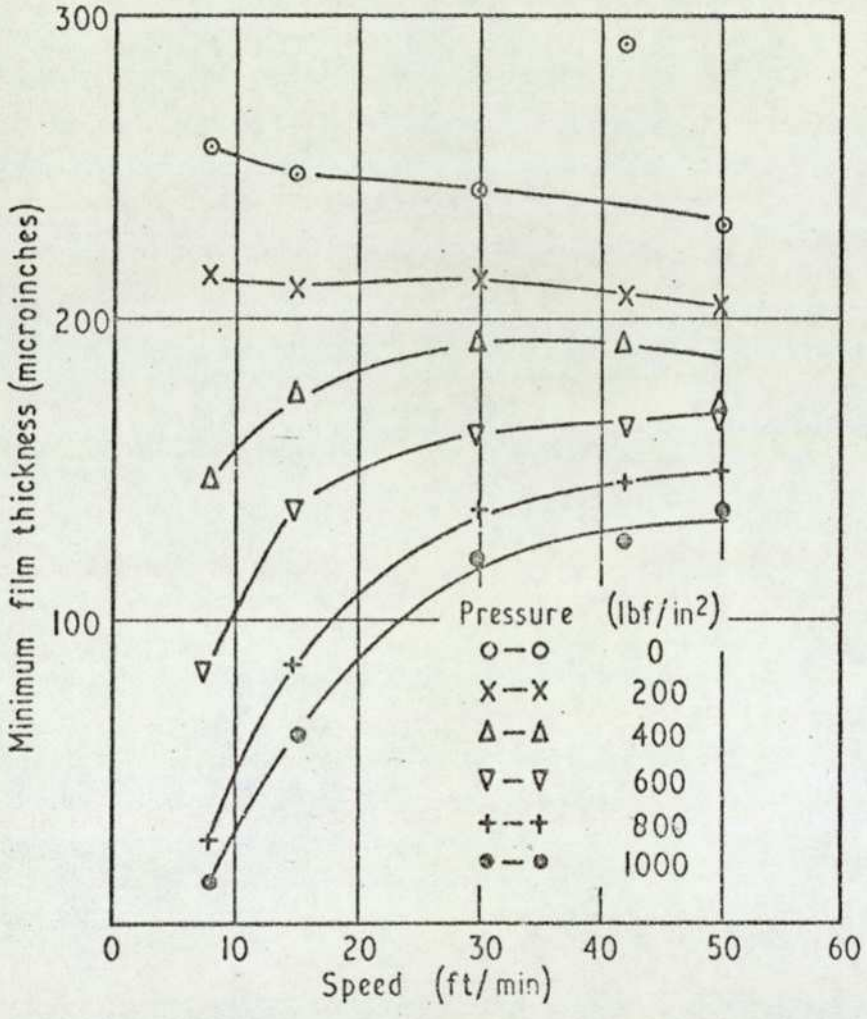


Fig. 4.14. Outstroke minimum film thickness against speed (rubber hardness = 90 IRHD): Series 5.

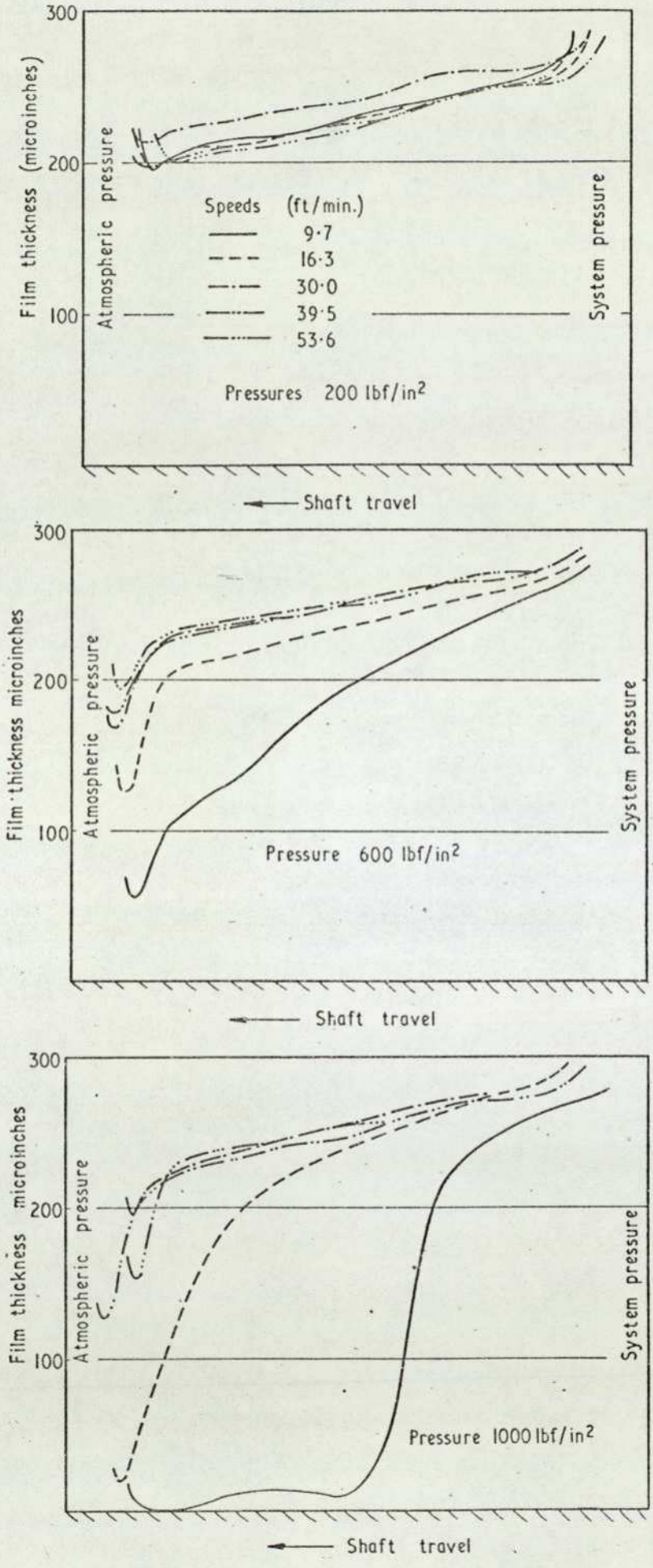


Fig. 4.15. Outstroke film profiles (rubber hardness = 90 IRHD): Series 5.

Series 2 and 3 the seal edge was undefined and changes in the micro-geometry of the seal edge or the contact stress profile could have accounted for the observed differences.

A phenomena only recorded during tests of Series 2 and 3 was an instability of the film profile at a speed between 10 and 15 ft/min. and for all the pressures tested. The unstable profiles randomly changed from an expected shape with an outlet 'nip' and a thick film inboard to a very thin film of about 10 micro inches thickness or less. The most likely cause of this instability seems to be the microgeometry of the seal edge which would be important during the very thin film stage. The effect only occurred at very low speeds and it is possible that the hydrodynamic pressure developed at this speed was not sufficient to sustain the film once it had formed. Typical profiles obtained at constant speed and pressure are shown in figure 4.16. This particular instability is not the same as that recorded in later tests.

In tests of Series 5, the effect of speed became more pronounced as the sealed pressure increased, and the minimum film thickness thinned, this shows clearly in figure 4.15. At first sight the minimum film thickness appears to depend on the sealed pressure, but further consideration of figure 4.15 suggests that the effect of speed may depend not directly on the pressure but on the absolute value of film thickness. The data appears to be divided into two regimes.

(a) Where the film thickness is large, that is greater than 150 micro inches, the affect of speed is small.

(b) For much thinner films the effect of speed is considerably greater.

Thus in a seal in which the contact stress distribution and the seal geometry create conditions in which a thin film forms the minimum film thickness will show considerable variation with speed, the pressure having relatively little effect. If a thick film is formed, pressure will have considerable effect and the speed much less.

These effects can be explained in terms of the hydrostatic and hydrodynamic pressures in the fluid film. The theoretical analysis of the seal lubrication problem (chapter 5) shows that the outstroke film profile can be approximated to a Rayleigh step bearing. It can be shown (Appendix G)

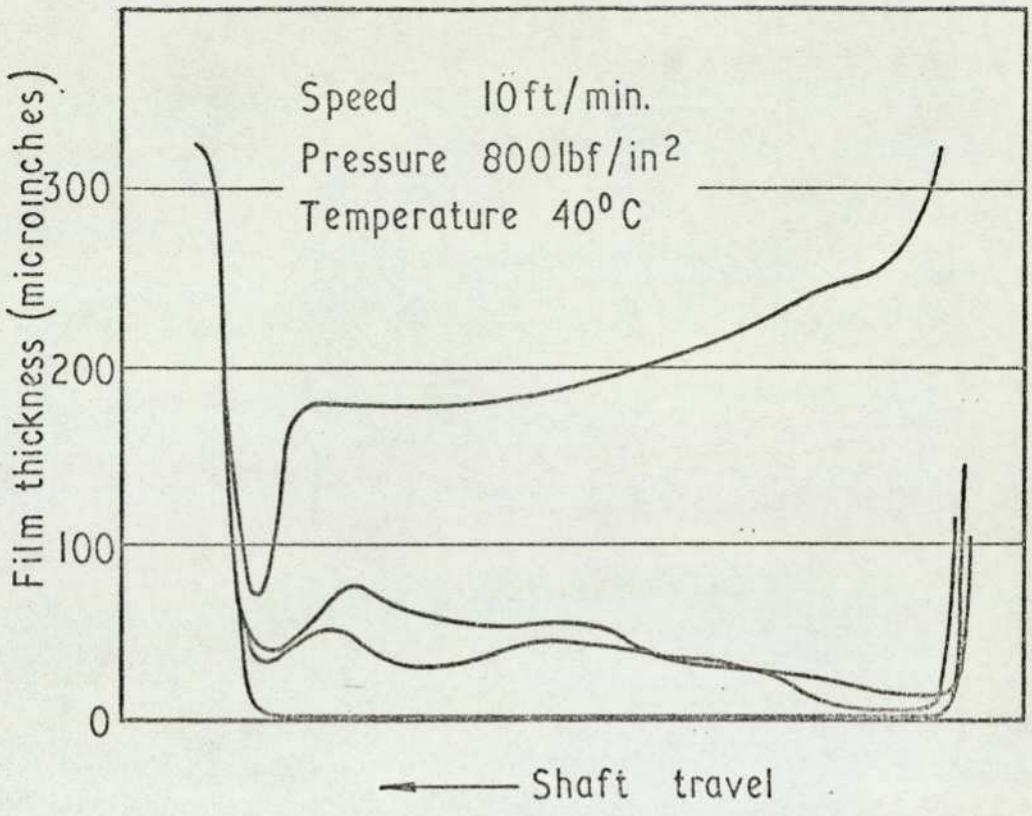


Fig. 4.16. Unstable film profiles near a speed of 10 ft/min: Series 3.

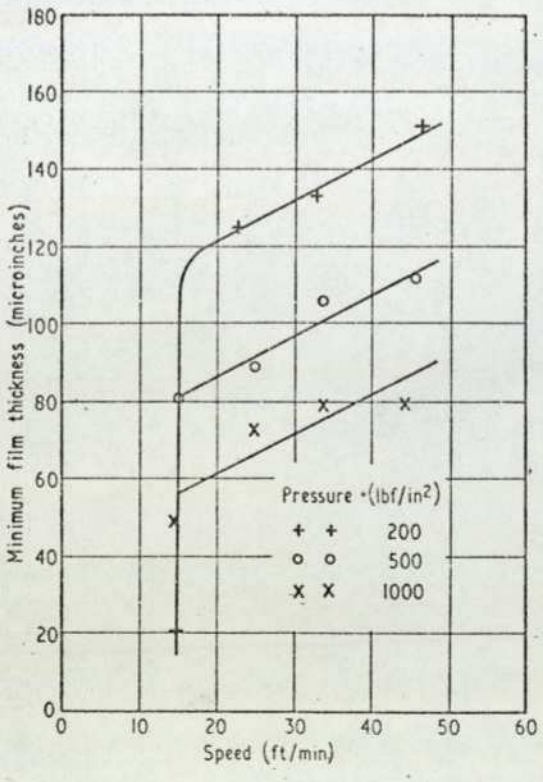


Fig. 4.17. Outstroke minimum film thickness for three values of sealed pressure: Series 2.

that the maximum hydrodynamic pressure developed by such a bearing is proportional to the speed, and inversely proportional to the square of the film thickness. Therefore for a thick fluid film, the hydrodynamic pressure in the fluid film is small and the seal deflection is almost entirely due to the hydrostatic pressure in the film. For thin films however, the hydrodynamic pressure becomes predominant and the seal deflection is almost entirely dependent on this pressure component which is itself dependent on the speed.

Pressure effects

The sealed pressure applied to the seals has also had widely varying effects on the minimum film thickness. Thus for Series 1, figure 4.9a the unexpected result was found that the minimum film thickness increased with the sealed pressure for all the speeds tested. Similar tests during Series 2 showed the opposite effect, figure 4.17, as the minimum film thickness decreased considerably with pressure, a five fold increase in pressure reducing the film by a factor of two. The above two effects are however absent in the results of series 3, figure 4.13, where the minimum film thickness is almost independent of both pressure and speed.

Another seal of nominally the same dimensions also used during Series 3 showed a significant decrease in minimum film thickness as the pressure increased, but the rate of decrease was dependent on the speed. The profiles, figure 4.18, show that most of the film was above the limit of the instrumentation and the only part recorded was the 'nip' at the low pressure end. The minimum film thickness values are plotted, for a range of speeds, against pressure in figure 4.19. At the slowest speed of 2.14 ft/min., the behaviour is similar to that of the films on instrokes and the relationship can be written:

$$h_{min} \propto (Ps)^{-2.0} \qquad (4.1)$$

but as the speed increases the index decreases until at the highest speed it is -0.5, thus

$$h_{min} \propto (Ps)^{-0.5} \qquad (4.2)$$

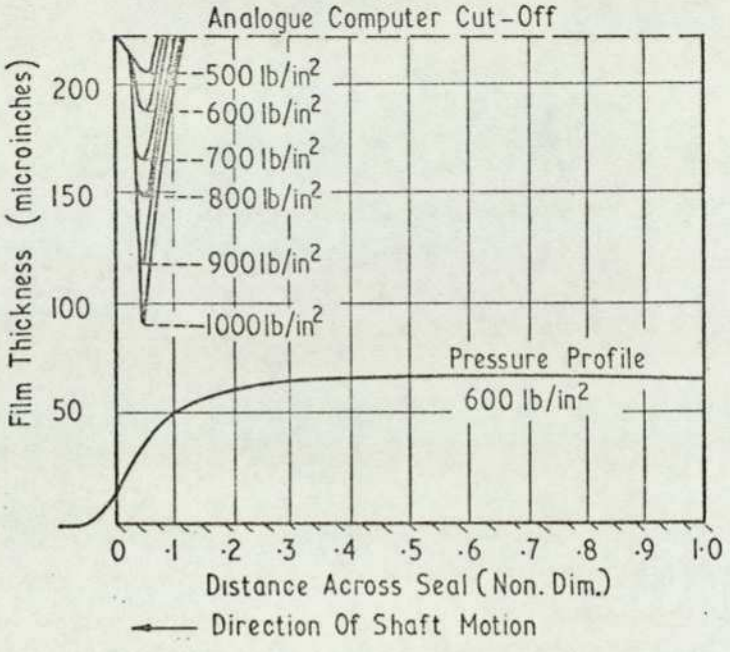


Fig. 4.18. Outstroke film profiles for several values of sealed pressure (T = 30°C): Series 4.

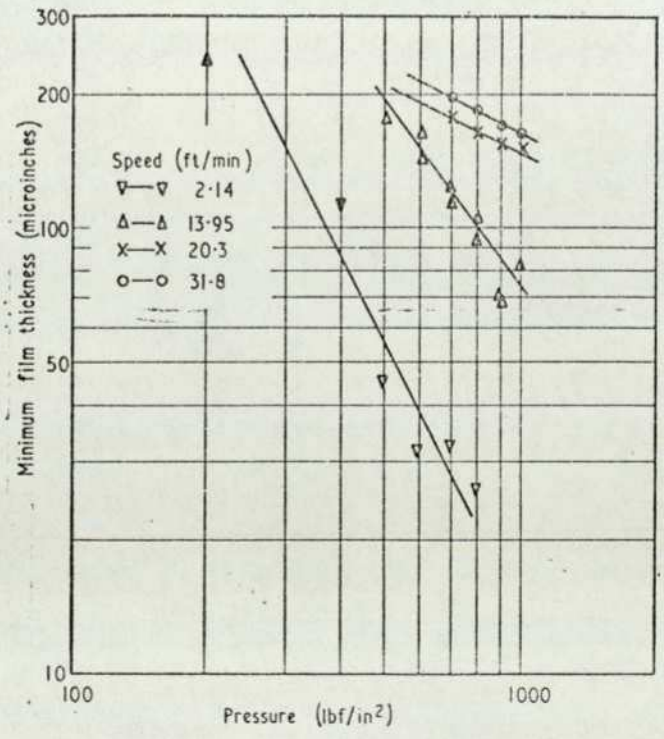


Fig. 4.19. Minimum film thickness against pressure for a range of speeds (T = 30°C): Series 4.

A further phenomena was observed during the tests of Series 5. The minimum film thickness and the film shape were affected by the pressure in two ways. As the pressure increased from zero the film thickness decreased until a minimum value was reached at a pressure of 600 lb_f/in^2. Further increase in the pressure then resulted in an increase in the film thickness. This behaviour was recorded during tests having various interference values and was consistent throughout.

For most of the outstroke films recorded the majority of the film has been much thicker than the limit of the instrumentation, thus the minimum film thickness has been studied in more detail than the rest of the film. For the seal used in Series 3 however, the film throughout the contact was recorded allowing the complete profiles to be studied for the effects of pressure.

Closer inspection of the film profiles of Series 3, figure 4.12, reveals a considerable effect of pressure on the general film shape. It can be seen that for all speeds, the profile changes from a parallel film at zero sealed pressure to an elastohyrdrodynamic form at higher pressures as the film thickness over the majority of the contact increases with pressure whilst the film under the 'nip' remains almost constant.

As far as practical applications are concerned the minimum film thickness is not as important as the film thickness, h^*, where the pressure gradient is zero, and from a knowledge of the pressure profile, h^* must occur at a point well away from the 'nip' where the film is considerably affected by the sealed pressure. As the leakage can be directly calculated from a knowledge of h^*, that is

$$q = Uh^*/2 \qquad (4.3)$$

the outstroke leakage must be increased by the increase in the sealed pressure.

Further unstable film profiles

In attempting to extend the data of Section 4.3.9 a series of tests were conducted with a new seal having rounded edges. The outstroke film profiles at first appeared to be as expected whilst the pressure was slowly increased. However at a pressure of 600 lb_f/in^2. the profile changed from

a thin tapered film to a much thicker one having a parallel section with a nip at the atmospheric edge. The complete change occurred over several cycles of the seal under constant speed and pressure conditions and was stable before and after. The various profiles recorded are shown in figure 4.20. The pressure at which this behaviour occurred varied between 600 and 800 lb_f/in^2 when the pressure was increasing and between 200 and 400 lb_f/in^2 with the pressure decreasing when the change was from a thick to a thin film. The speed during these tests was 30 ft/min. and therefore the behaviour appears to be different from the instability mentioned earlier.

In general the outstroke film behaviour can be summarised as follows:

(i) The minimum film thickness can decrease rapidly with pressure (Series 2), in Series 1 it increased whilst for Series 3 it remained almost independent of speed and pressure. The tests of Series 5 also showed different behaviour in that the minimum film thickness initially decreased with pressure, but at a pressure of approximately 600 lb_f/in^2 it started to increase.

(ii) The major part of the seal contact excluding the 'nip' appears to increase with the sealed pressure. The theoretical study, Chapter 5, shows a similar effect of pressure where increasing the pressure slightly reduces the minimum film thickness but increases the film thickness at the pressurised side of the seal.

Instrokes

On an instroke, the seal experiences a completely different form of operation to an outstroke in that the hydrostatic pressure gradient and the shaft velocity are in opposing directions. In the majority of cases this results in a film profile which is almost parallel throughout the contact. Examples of such profiles are shown in figure 4.21. For this reason, the instroke film profile can be represented adequately by the minimum film thickness.

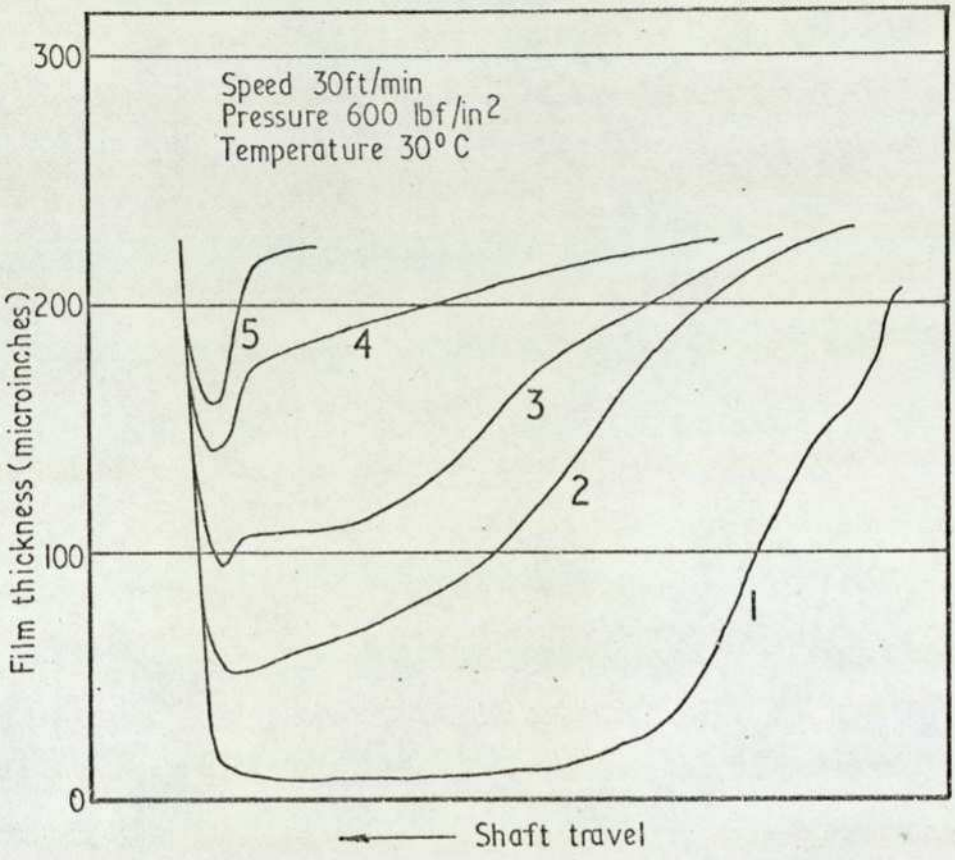


Fig. 4.20. Unstable film profiles recorded at constant speed and pressure (rubber hardness = 90 IRHD, Seal edge: round, Buc = 0.005 in., interference = 0.005 in.): Series 5.

Speed effects

The effect of speed on the minimum film thickness during instrokes is shown in figure 4.22 for a range of pressures. The scatter in points for pressures of 800 and 1000 lb_f/in^2 reflects the errors of measurement mentioned in Appendix F. However for the thicker films the data indicates a relationship of the form:

$$h_{min} \propto (speed)^{0.5} \qquad (4.4)$$

which would be expected if the seal were operating in a hydrodynamic lubrication mode. These results were typical of many tests throughout the program.

Pressure effects

Figure 4.23 shows minimum film thickness data from Series 4 plotted against pressure for a range of speeds. It can be seen that the film thickness decreases rapidly with pressure up to pressures about 500 lb_f/in^2. The data when plotted logarithmically shows a relationship of the form

$$h_{min} \propto (Ps)^{-2.0} \qquad (4.5)$$

combining this with the relationship for speed found previously, it is found that:

$$h_{min} \propto U^{0.5} \cdot Ps^{-2.0} \qquad (4.6)$$

The film thicknesses recorded for pressures above 500 lb_f/in^2 are of the order of the surface roughness of the bore of the vessel and although a lubricant film is indicated it is unlikely that the seal operates in a fully hydrodynamic mode and some boundary lubrication would be expected.

4.2.3. Specific friction

In the literature survey it is noticeable that most friction data has been presented as a friction force per seal or as a coefficient of friction. Neither of these is ideal, the former because it depends on the contact area of the seal, the latter because the coefficient of friction of elastomer materials, unlike that of more rigid materials, depends on

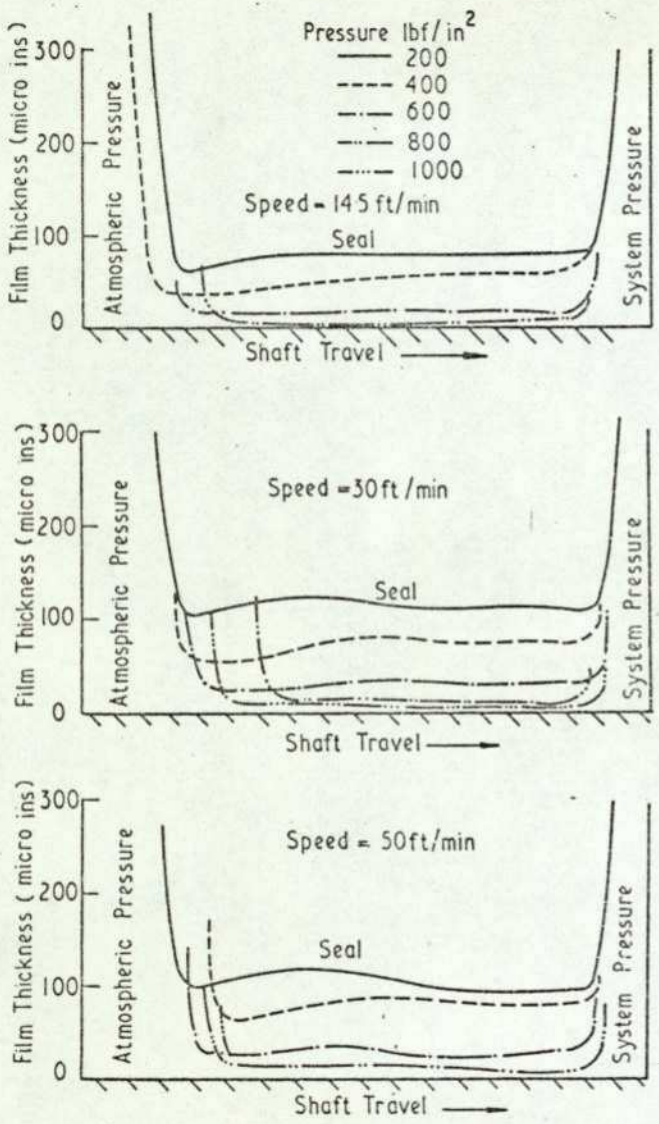


Fig. 4.21. Instroke film profiles: Series 3.

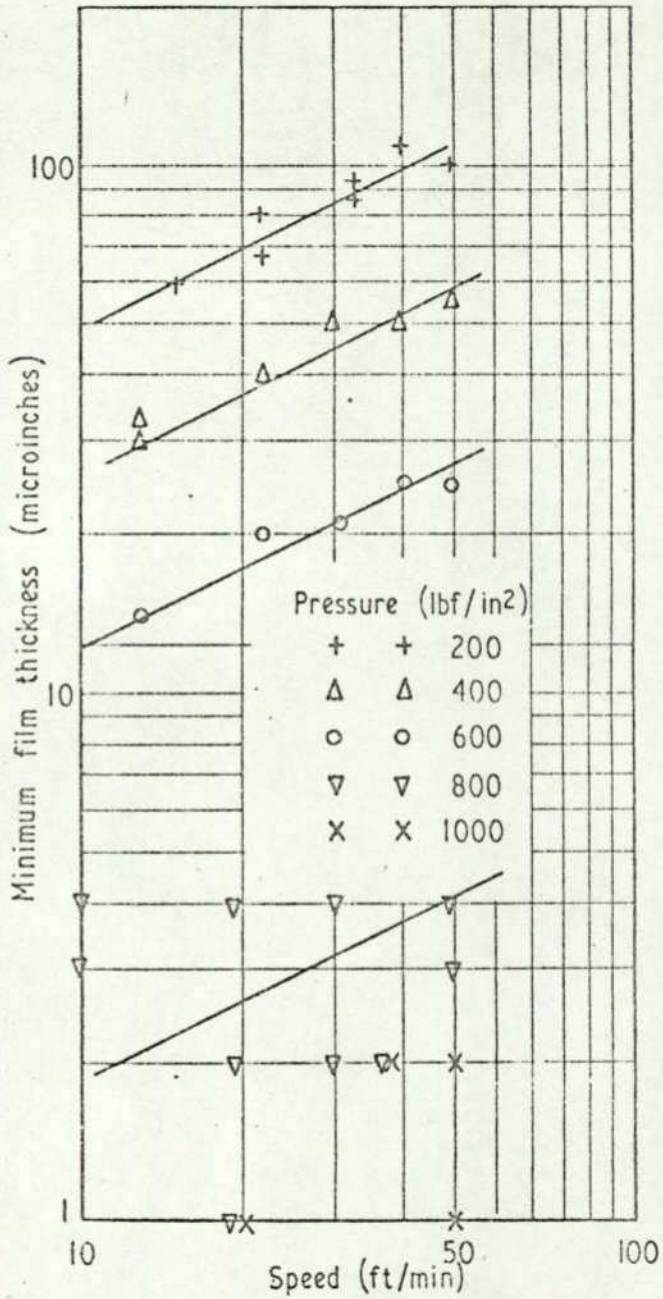


Fig. 4.22. Instroke minimum film thickness against speed for a range of pressures: Series 3.

the contact pressure. It is preferable therefore to present friction data as the specific friction defined as:

$$\text{specific friction} = \frac{\text{seal friction force}}{\text{seal contact area}} \qquad (4.7)$$

Mean specific friction of two strokes

The series 2 tests used two nominally identical seals and the recorded friction is therefore a mean of an instroke and an outstroke. As the tests proceeded it became evident from the measurements of the film thickness that the two strokes behaved very differently and therefore the friction would also differ. Further it was realised that the friction of different seals even of nominally the same dimensions could behave quite differently from each other. Measuring only the mean value for the two strokes therefore would not allow correlation with the film thickness measurements and this provided added incentive to develop a technique to allow the measurement of the friction of a single seal.

The present data however had one advantage in that it could be readily compared with that of other workers. With this in mind the data obtained is shown in figure 4.24, in which the specification is plotted against the parameter (viscosity) x (speed). This parameter has been used previously by Nau (39)to correlate seal friction coefficients obtained for different fluid viscosities. The data of figure 4.24 follows the same relationship as found by Nau (39) that is:

$$\text{mean specific friction} \propto (\zeta U)^{-0.5} \qquad (4.8)$$

The absolute values of friction and the fact that the mean friction values decrease with speed appears to indicate that the seals operate in a partially boundary lubricated mode. However, the film thickness measurements in Series 2 indicate that a thick fluid film formed on the outstrokes and a thin film on the instroke. From this it was concluded that the friction should be low for the outstroke operating under full hydrodynamic conditions and high for the instroke operating under boundary lubrication conditions.

From the data of figure 4.24 it can also be shown that the sealed pressure affects the friction in the following way:

$$\text{mean specific friction} \propto (Ps)^{-0.5} \qquad (4.9)$$

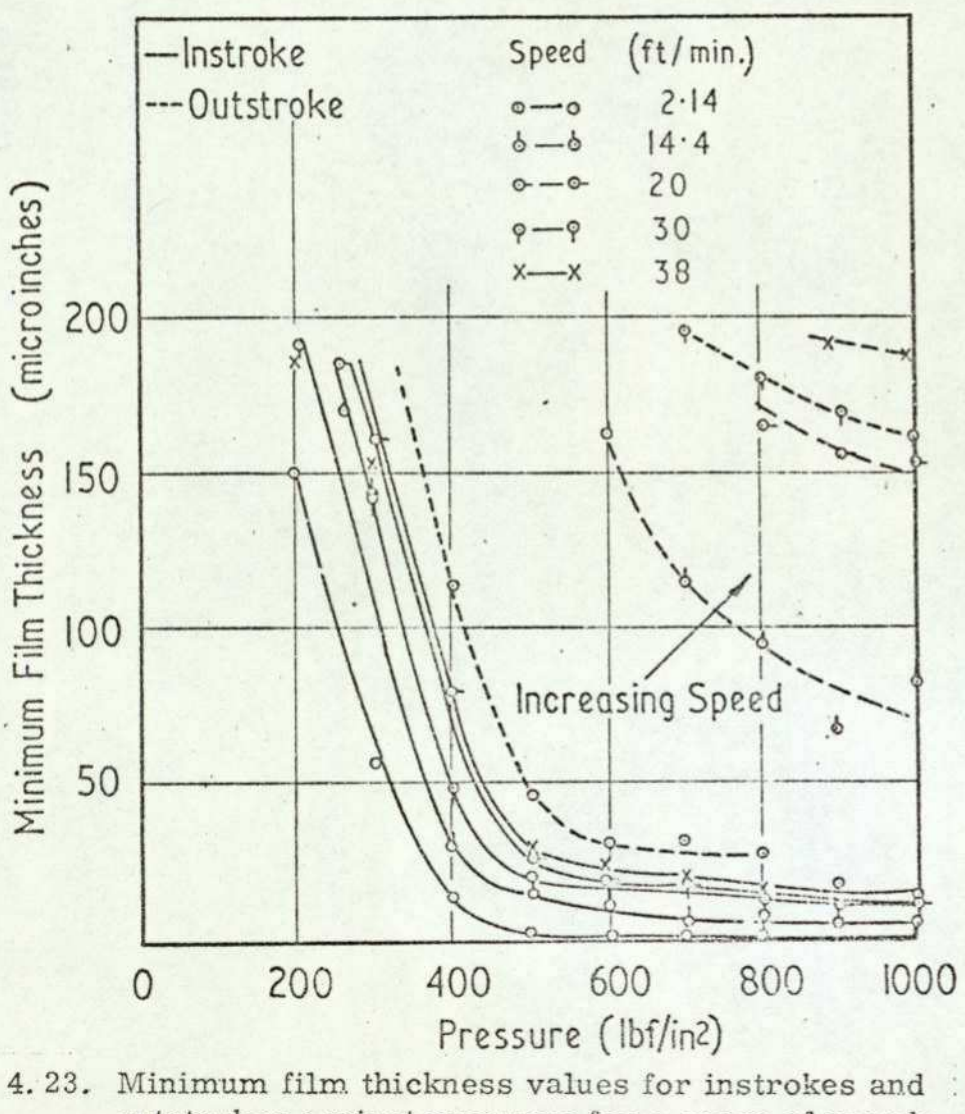


Fig. 4.23. Minimum film thickness values for instrokes and outstrokes against pressure for a range of speeds. (T = 30°C): Series 3.

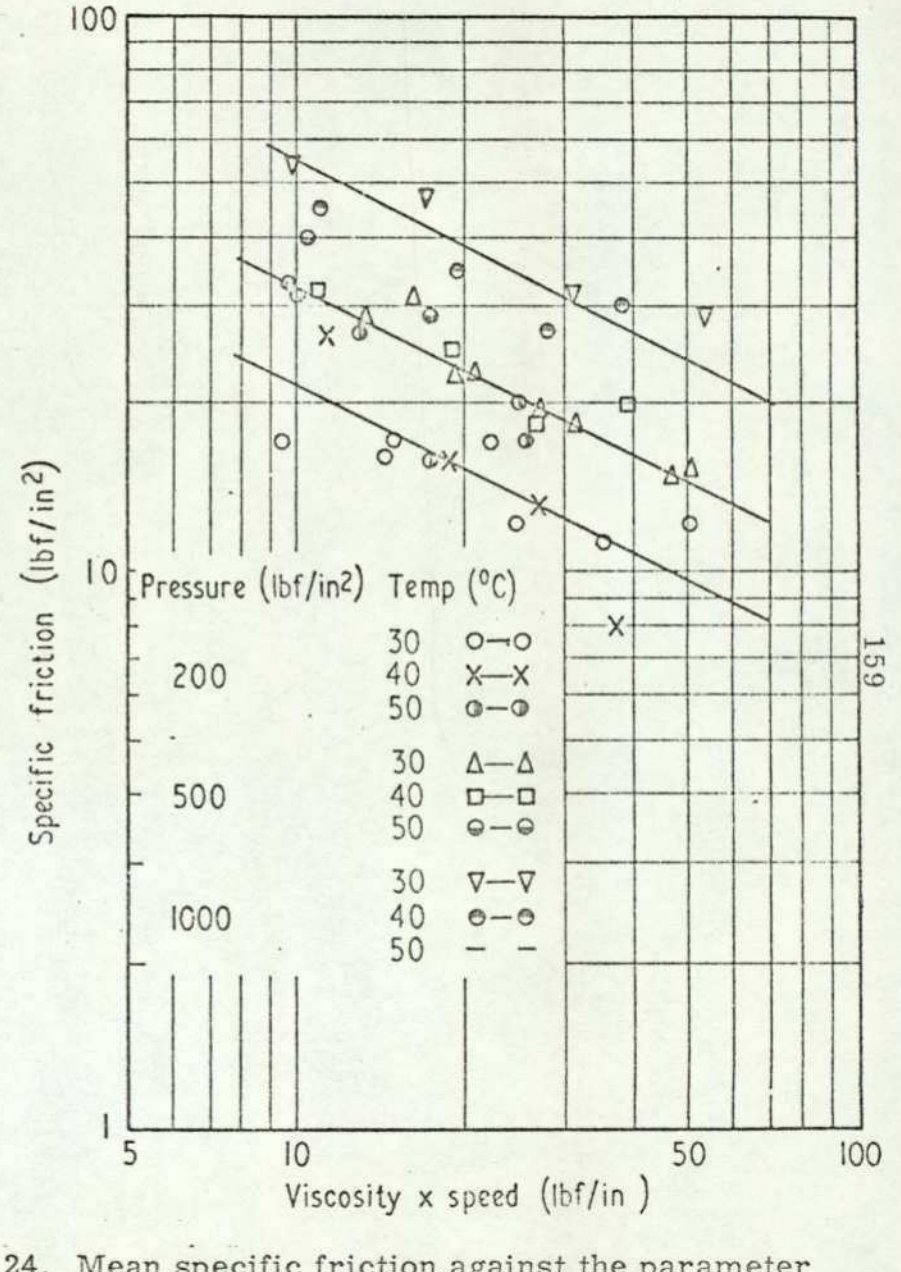


Fig. 4.24. Mean specific friction against the parameter (viscosity) x (speed) showing the effect of temperatur (or viscosity) and pressure: Series 2.

Nau (39) found that:

$$\mu \propto (Ps/E)^{-1} \qquad (4.10)$$

for values of $(Ps/_E)$ greater than 0.1. However the present values of the parameter $(Ps/_E)$ range from 0.08 to 0.4 and the data from Nau(39) for this range is more nearly represented by the relationship:

$$\mu \propto (Ps/E)^{-0.5} \qquad (4.11)$$

Transposing this relationship to a value of specific friction results in:

$$\text{mean specific friction} \propto (Ps \cdot E)^{0.5} \qquad (4.12)$$

agreeing with the results of the present tests.

Combining the present results for effect of viscosity, speed and pressure on the mean specific friction forms the relationship:

$$\text{mean specific friction} \propto (P_s/\tfrac{1}{2} U)^{0.5}. \qquad (4.13)$$

The units of the right handside of this expression are $(TL)^{-0.5}$ rather than FL^{-2}, and obviously the specific friction is affected by variables which are as yet not included in the expression.

Specific friction of instrokes and outstrokes: Series 3 - 5

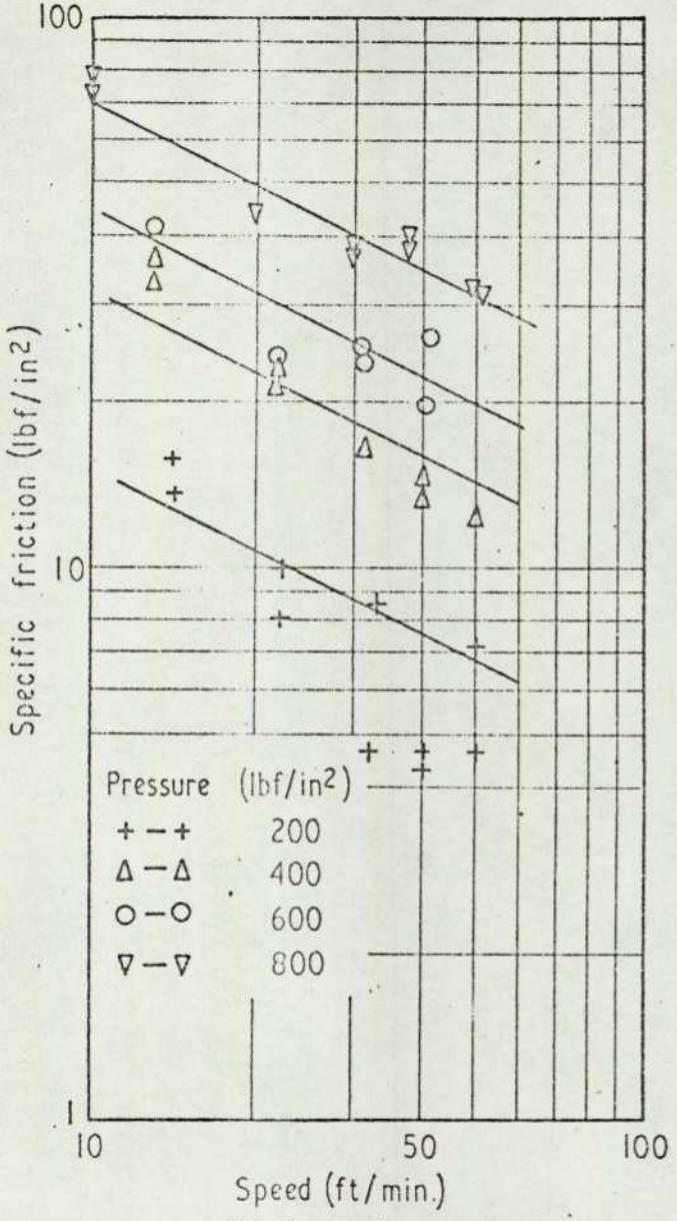
Series 3 was the first to utilise the floating bush to allow measurement of the friction of a single seal, but the bush contacted the bore of the vessel during tests at 1000 lb_f/in^2, and this result was therefore not used in the analysis.

The remaining data is shown in figure 4.25. The difference in friction between the two strokes is immediately obvious. For pressures in excess of 200 lb_f/in^2, the instroke frictions are almost an order of magnitude greater than the outstrokes. The effect of speed on the friction is however the same as previously found for the mean:

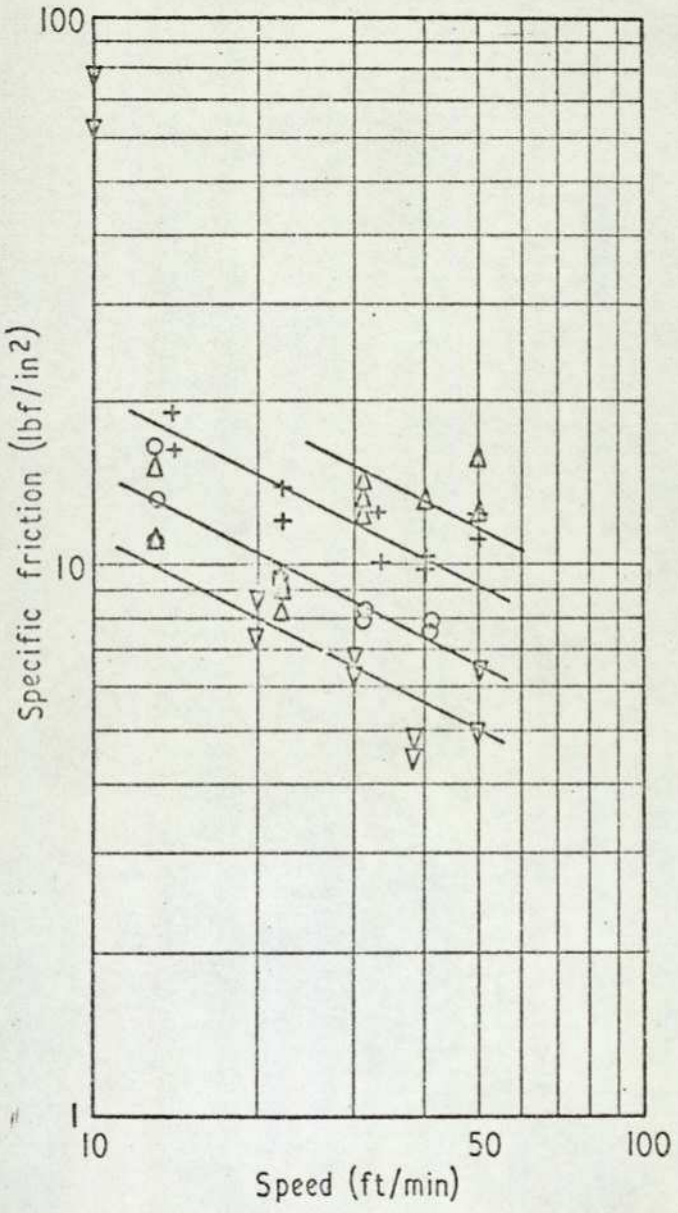
$$\text{specific friction (outstroke)} \propto (U)^{-0.5} \qquad (4.14)$$

$$\text{specific friction (instroke)} \propto (U)^{-0.5} \qquad (4.15)$$

The relationship for the outstroke friction was unexpected, as measurements of the film thickness had shown a hydrodynamic film about



(a) Instroke



(b) Outstroke.

Fig. 4.25. Specific friction against speed for a range of pressures: Series 3.

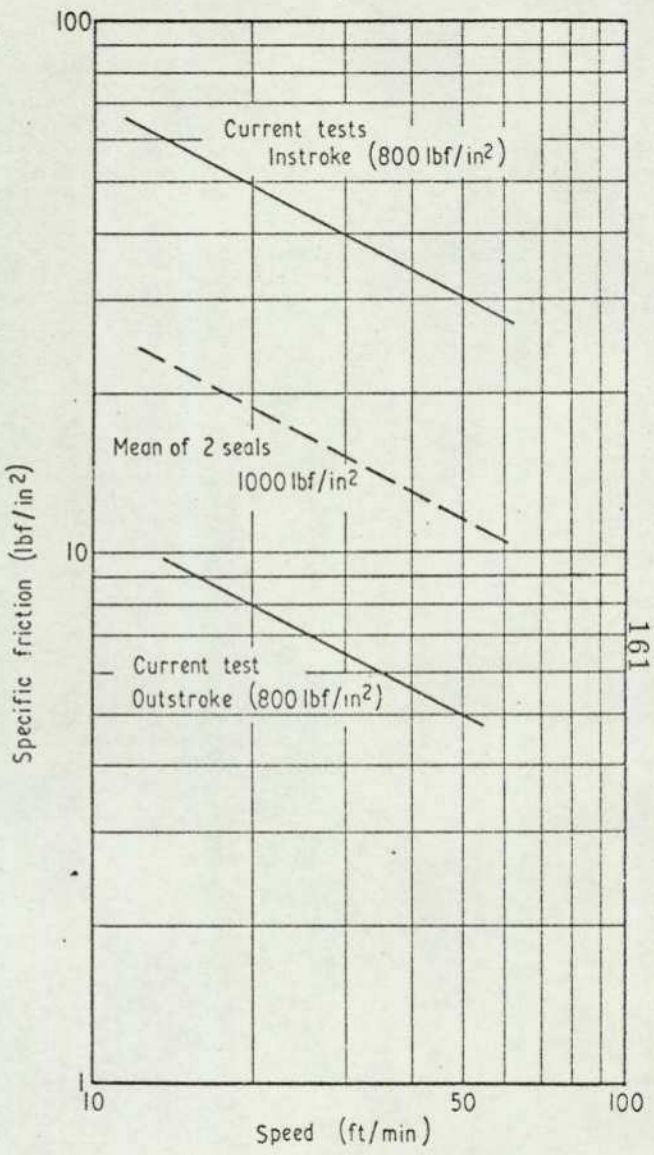


Fig. 4.26. Comparison of the separate instroke and outstroke values of friction with the mean values of Nau (39)

100 - 200 micro inches thick and for this situation the friction should theoretically have increased with speed. Also measurements of the instroke film thicknesses, indicate a hydrodynamic mode of lubrication and the friction of this stroke should increase with speed.

A comparison between this data and that obtained by Nau (39) for the mean of instroke and outstroke is shown in figure 4.26 and there is good agreement.

The main difference between the individual stroke frictions and the mean is that the specific friction increases with pressure for instrokes, but decreases for the outstrokes. This again was an unexpected result, but it is consistent with the effect of pressure on the film thickness, that is an increase in pressure causes the film to increase and the friction to decrease for the outstroke, and the reverse for the instroke. Quantitatively the agreement between friction and film thickness is poor. Appendix H shows that the specific friction of a parallel annular clearance, having a pressure differential along it and relative motion of the two surfaces can, without appreciable error, be calculated from:

$$\text{specific friction} = \frac{2U}{h} \qquad (4.16)$$

For the typical values of viscosity, film thickness and speed of the present tests, the theoretical friction is of the order of 1 lb_f/in^2, but the measured values are an order of magnitude or more greater than this. A similar discrepancy was found in the optical study of the problem.

The behaviour described above was typical of the majority of the test program although the outstroke friction values did not always decrease with pressure and some results were obtained in which the friction was either increased only slightly or was not affected by the pressure, figure 4.27 Furthermore, results of Series 5 sometimes showed an opposite effect, the outstroke frictions being higher than the instroke, but the film profiles were also somewhat different to those described above. The significance of these apparently anomalous results will be discussed later.

4.2.4 Leakage

The net leakage of reciprocating seals is the difference between the oil taken out on the shaft during the outstroke and that returned to the system on the instroke. It can be shown (19, 20, 21) that the Poiseuille component of flow can be considered negligible compared to the Couette flow

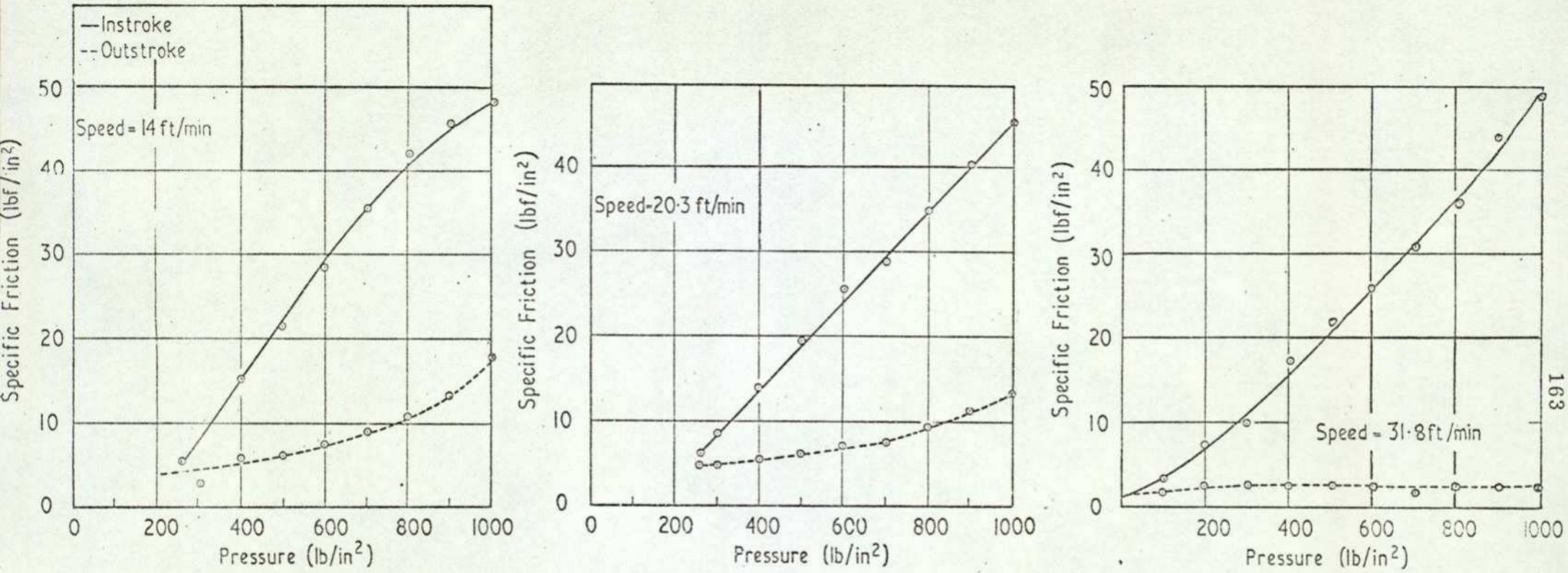


Fig. 4.27. Specific friction against pressure showing the difference between instroke and outstrokes for three speeds (T = 30°C): Series 4.

for the thin film conditions under which seals operate.

Bearing this in mind, the leakage data of Series 2 tests can be compared to the measured film profiles. For the majority of the tests the instroke film profiles are very thin and the amount of oil returned to the system on this stroke is very small; the outstroke film profile is therefore critical in determining the net leakage of the seals. The tests at a sealed pressure of 1000 lb_f/in^2, figure 4.28 show little leakage at speeds of up to 12 ft/min. but at speeds above 20 ft/min. the leakage was much higher and this is qualitatively in agreement with the film profiles of these tests where the outstroke film profiles increase significantly between 12 and 20 ft/min., but remain fairly constant above this. It is difficult to calculate the leakage from the film profile as the value of h* is not known, but Δh^*, the difference between h_i^* and h_o^* can be calculated from the net leakage. For a pressure and speed of 1000 lb_f/in^2 and 39 ft/min. respectively, Δh^* is 270 micro inches, and this agrees fairly well with the film thickness near the pressurised end of the seal, fig 4.29 which is where the pressure gradient would be expected to be zero.

The measured leakages at pressures of 200 and 300 lb_f/in^2 also reflect the measured film profiles as for all these tests the films were thin for both the outstroke and the instroke. A discrepancy is evident for a pressure of 200 lb_f/in^2 as here the leakage decreases with increasing pressure. The film profiles for these tests suggest that the instroke film profile was thicker than the outstroke and theoretically the net leakage would be negative in this case. However as mentioned in a later section, the measurement of film thickness is only achieved at one point on the circumference and other parts of the seal may have been operating in a different way.

For the higher pressures of 500 and 1000 lb_f/in^2 the net leakage is related to speed in the following way:

$$q \propto (U)^{0.75} \qquad (4.17)$$

The film profiles of Series 3 tests were more consistent than those of Series 2 and this is reflected in the measured leakage rates shown in figure 4.30. The effect of speed over the whole speed range is the same and of the form:

$$q \propto (U)^{0.76} \qquad (4.18)$$

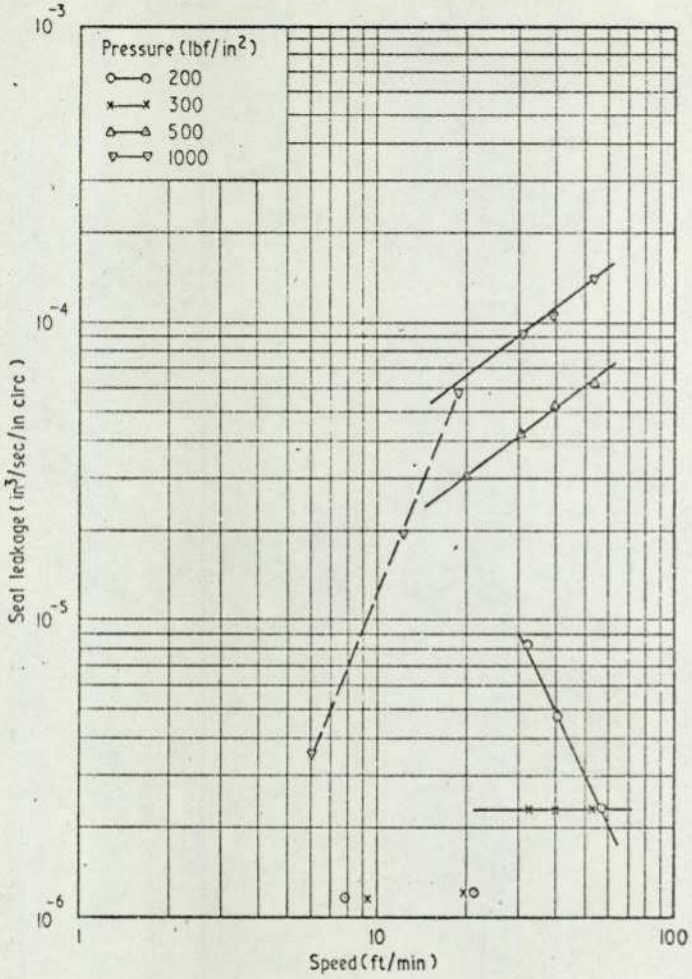


Fig. 4. 28 Mean seal leakage against speed: Series 2

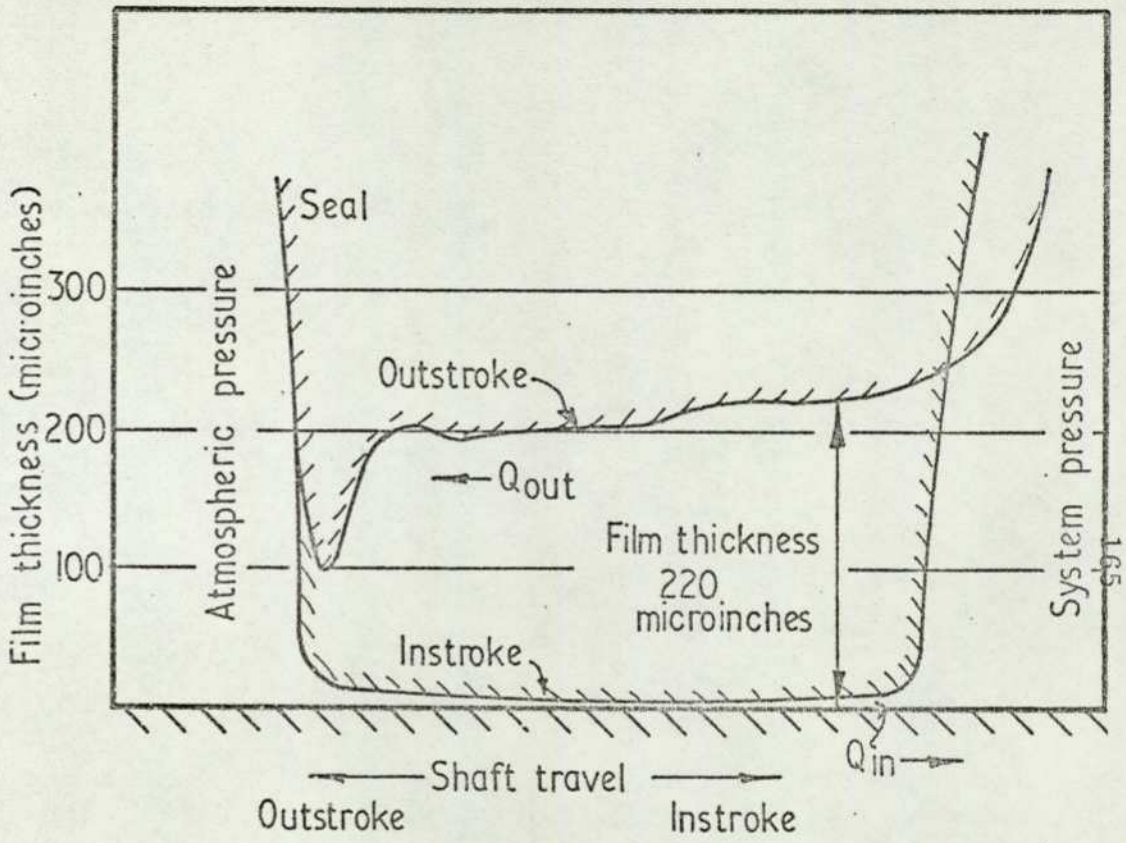


Fig. 4. 29 Film profile illustrating the cause of seal leakage: Series 2

the indices between the two series of tests being almost the same. It is evident however that pressure has increased the leakage steadily and a graph of leakage against pressure for a speed of 30 ft/min. is shown in figure 4.31; the relationship is of the form:

$$q \propto (P_s)^{1.76} \qquad (4.19)$$

However the leakage values recorded at 800 and 1000 lb_f/in^2 appear to be reaching a limit and the leakage would be expected to level off to a constant value for pressures much above 1000lb_f/in^2.

Although the leakage increases with pressure this is not because of an increase in the level of Poiseuille flow but due to the increase in the film thickness on the outstroke and the decrease on the instroke, an effect caused by the increase in pressure.

4.2.5. Circumferential film thickness variations

In Section 4.2.3 it was noted that the specific friction values obtained were about an order magnitude higher than expected from the measured values of film thickness, also the friction decreased with speed instead of increasing as would be expected if the seal were lubricated hydrodynamically. This suggests that the seal operates in the mixed boundary/hydrodynamic regime. However, all measurements of outstroke film thickness have shown a lubricant film considerably thicker than would be expected under these conditions

The capacitance transducer measures the film thickness at only one point on the circumference of the seal and a possible explanation of the above dilemma might be that the seal was not hydrodynamically lubricated all the way round its circumference. It is well known that the coefficient of friction of rubber on steel surfaces is high and can reach values exceeding unity. If this is so, only a small percentage of the seal area needs to be operating in the boundary regime to result in the values of friction recorded.

To test this hypothesis measurements were made of the film thickness around the circumference of the seal. Because of the configuration of the rig it was impossible to move the probe around the seal, therefore the seal was rotated in its groove, the film profile being measured at eight

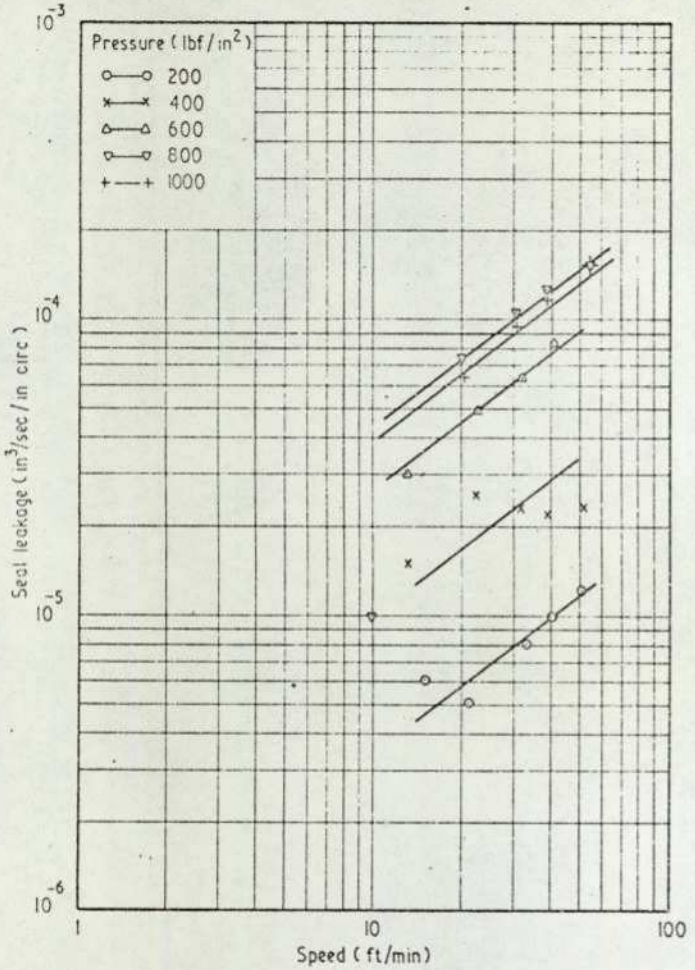


Fig. 4. 30 Mean seal leakage against speed: Series 3

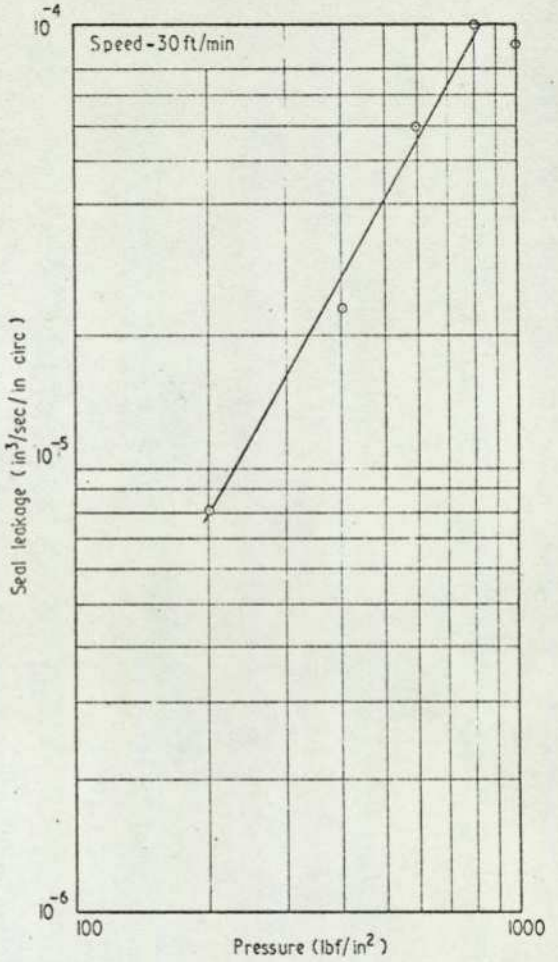


Fig. 4. 31 The effect of pressure on the mean seal leakage: Series

circumferential positions.

The results for the instrokes, figure 4.32, show a roughly sinusoidal double peaked variation in minimum film thickness around the seal at all pressures. The values of film thickness for a sealed pressure of 400 lb_f/in^2 shows the greatest variation. It is not possible to show the corresponding behaviour for the outstroke since the film was mostly above the range of the instrumentation. The method of changing the position of measurement by rotating the seal in the groove may itself have given rise to some variation in the measured film thickness around the circumference. The seal interference could have changed at the film thickness measuring point due to minor variations in the radial thickness of the seal around the circumference. However, in spite of these possible sources of error, a lubricant film was certainly present at all circumferential positions on both instroke and outstroke and there is no confirmation that sections of the seal operate with a thin film.

4.2.6. Variations in film thickness and friction through the stroke. Film profiles

The film thickness profiles wereusually measured at the mid-point of the stroke where the film was assumed to have reached a stable condition, but it is important to know how the film behaves throughout its stroke.

Measurement of the film thickness through the stroke was achieved by reducing the stroke length steadily, so that the transducer was progressively offset relative to the mid-point of the stroke.

It is convenient to discuss the results in conjunction with figure 4.33 in terms of a rod seal operation. As the rod starts on the instroke, the film thickness rapidly decreases as the stroke proceeds until at a point 40% of the way through the stroke, the film thickness reaches a minimum value and thereafter remains constant until the end of the stroke. During this stroke oil is being dragged into the system by the shear forces in the fluid film. It is clear that the total amount of oil returned to the system on this stroke depends on the rate at which the film reduces in the first part of the stroke. The slower the film collapse, the more fluid will be returned.

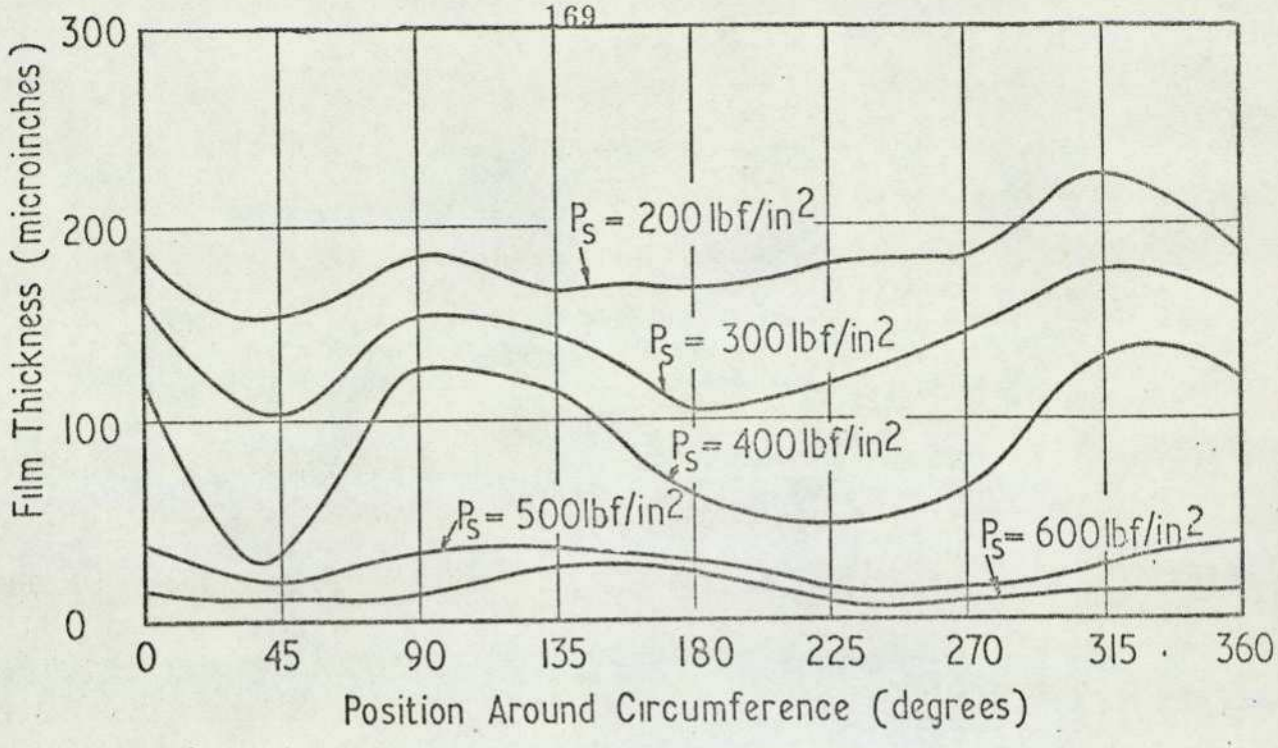


Fig. 4.32. Variation of instroke minimum film thickness around the circumference of the seal. (T = 30°C), Series 4.

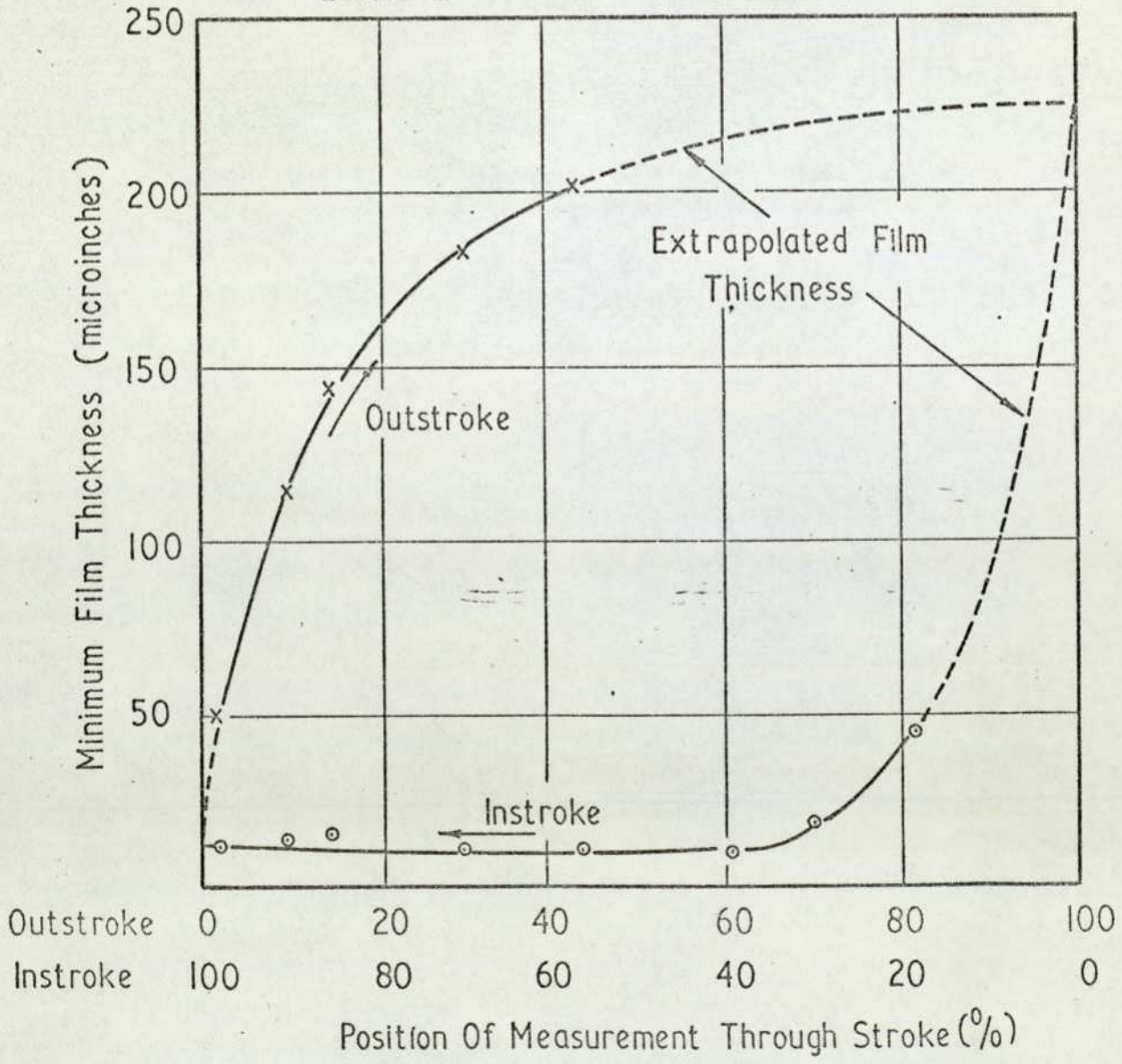


Fig. 4.33. Variation of minimum film thickness through the stroke (T = 30°C): Series 4.

As the change over point from instroke to outstroke is reached, the fluid film is very thin, but as the outstroke begins the film rapidly increases until again at40%of the stroke length the film has virtually reached a stable thick film condition which is maintained for the rest of the stroke.

A further important point emerges from figure 4.33. The distance the seal moves before a steady film profile is reached is 40% of the total stroke length and in this particular case the seal length was 20% of the stroke length. Thus the seal travels two contact widths before a stable film is attained. This confirms results of the optical study in which it was shown that 'disturbances' in the fluid film propogate at half the speed of reciprocation.

The above results show that there are three regimes of significance. If the seal has moved less than one seal length, oil entering the film at one side will not have reached the other side and in this case the seal would run partly dry. Up to the completion of two-seal lengths of travel the oil film will be in a transition state, not having reached the steady state which exists for strokes of more than two seal lengths.

Specific friction

The variation of specific friction through the stroke is shown in figure 4.34. As expected from the film profiles, the friction increases at the beginning of the instroke rising to a steady value at the 40% point and conversely for the outstroke.

These results are confirmed by the friction traces for full length strokes, figure 4.35. These are the recorded friction traces for a speed of 39.5 ft/min over the pressure range 0 to 1000 lb_f/in^2. At the end of the instroke, the friction is high and, as thestroke direction changes, this high friction creates an initially high friction on the outstroke, point A, but as the outstroke proceeds a thick fluid film forms and the friction rapidly decreases to asteady valueat point B. At the beginning of the instroke point C the friction is low, but increases rapidly as the fluid film decreases at point D. The distance travelled by the seal during the rapid decrease in friction on the outstroke and the increase on the instroke is shown to be two seal contact widths.

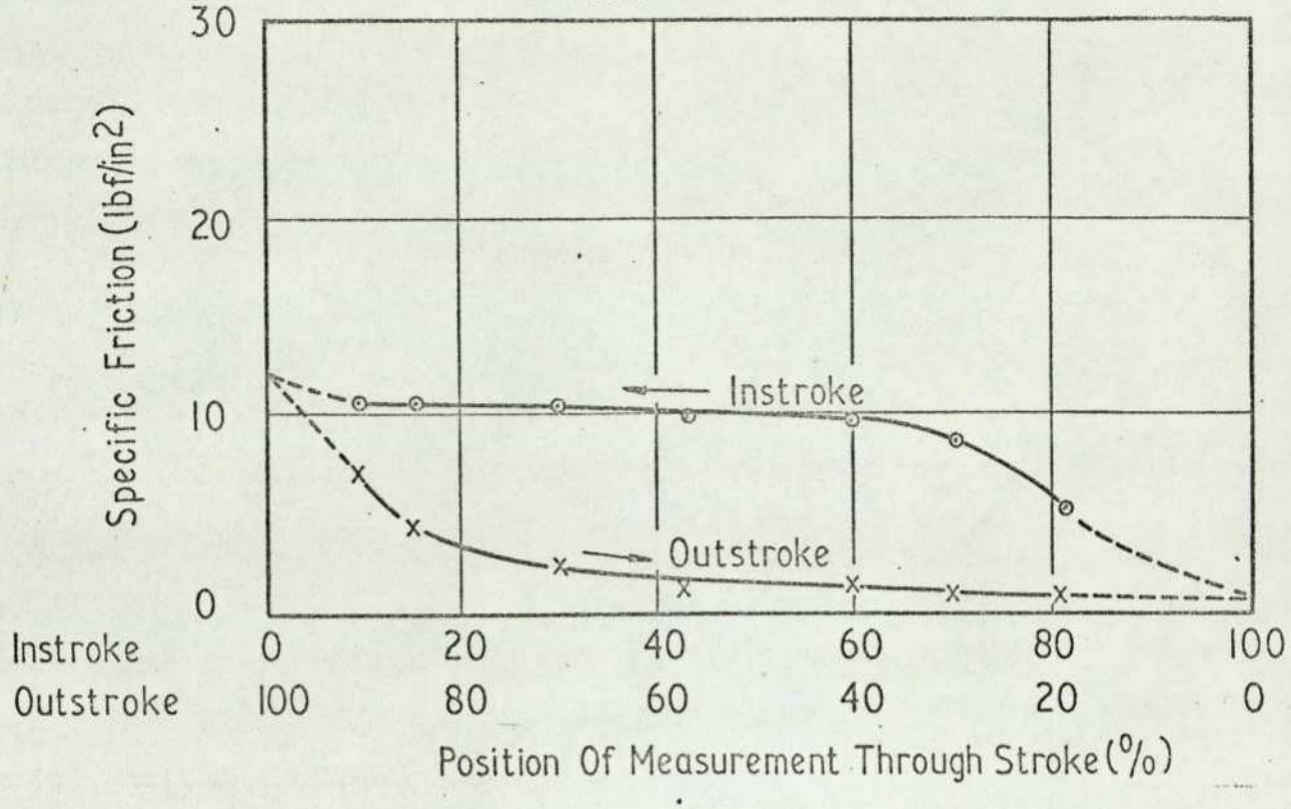


Fig. 4. 34 Variation of specific friction through the stroke (T = 30°C): Series 4.

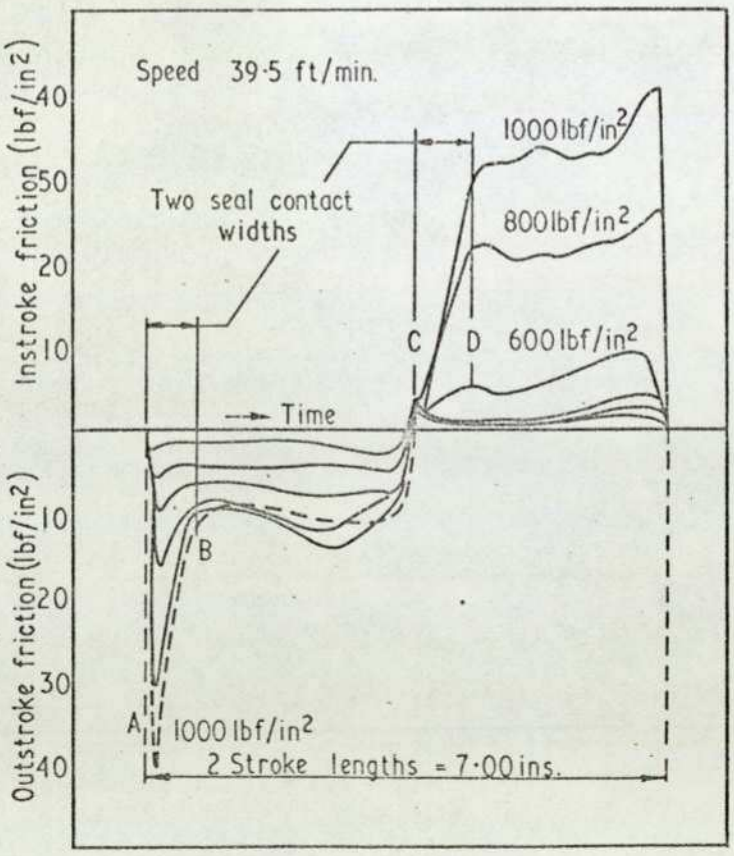


Fig. 4. 35. UV. recorder traces of specific friction through the stroke (T = 30°C): Series 4.

Short stroke length behaviour

The measurements of the film profile throughout the stroke length have shown that the seal must travel more than two seal contact widths before a stable fluid film is formed. But for many applications such as powered flying controls and hydraulic jacks in which dither is induced to prevent the build-up of static friction under stationary conditions, stroke lengths shorter than two contact widths may be necessary. The optical rig has shown that under these conditions the fluid film breaks down and could cause rapid failure of the seal. It would therefore be advisable to study the lubricant film under these conditions

However measurements of film thickness made by a single transducer in a film, the thickness of which varies with both time and position are not very meaningful. This can be understood from figure 4.36 which shows a hypothetical series of seal film profiles at times T_1 - T_5. A single tranducer traversing the seal during this time would record a trace as drawn by the dotted line and this clearly has no physical significance on its own.

Such dynamic changes in the film shape could be measured using several capacitance tranducers spaced axially along the bore. The particular design of transducer used here wouldlend itself well to this type of application. Optical interferometry could also be used to record the complete film shape at any instant of time, but a feasibility study revealed considerable technical difficulties in applying this method to the present rig and the method was not pursued.

4.2.7 The effect of fluid viscosity

To assess the effect of viscosity on the film thickness and the specific friction of the seal, tests were conducted at various temperatures. The temperature range was approximately 20 - 40°C giving a range of viscosity from 0.375×10^{-5} to 0.9×10^{-5} reyns.

Outstrokes. With the seal tested, (Series 4) the film profiles were all very thick and for all the tests the majority of the film was thicker than the cut-off limit of the analogue computer.

For a pressure of 300 lb_f/in^2, the whole of the outstroke film was greater than the cut off limit of the instrumentation. Minimum film thickness values at the other pressures tested are shown in figure 4.37 plotted

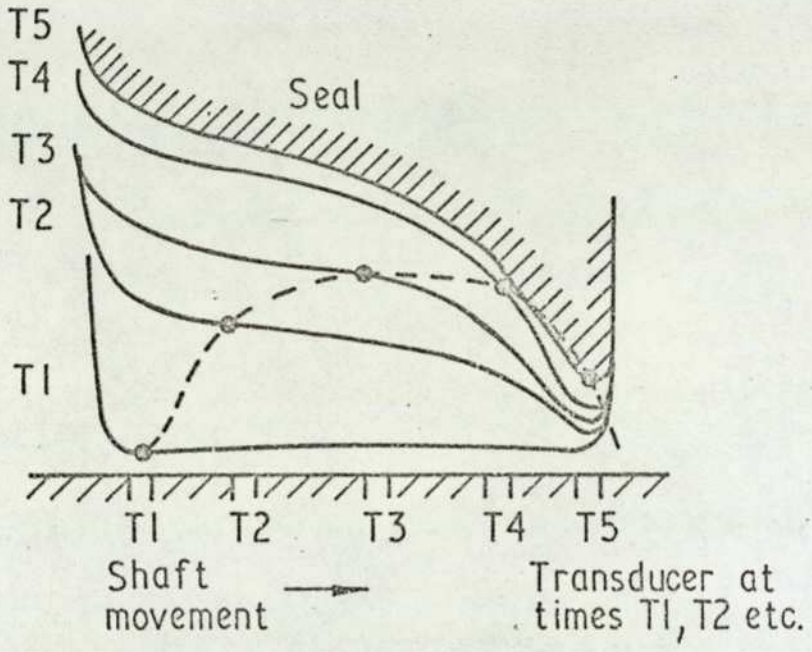


Fig. 4.36. Measurement of dynamic film thickness profiles at five points in time.

against the bulk fluid viscosity. The results indicate a relationship of the form:

$$h_{min} \propto (\zeta)^{0.5} \qquad (4.20)$$

For a constant film thickness, the specific friction of a seal should, from the Newtonian friction formula, increase with increase in viscosity the relationship being:

$$\text{Specific friction} = \frac{\zeta U}{h} \qquad (4.21)$$

However the measured values of minimum film thickness show an effect of viscosity of the form:

$$h_{min} \propto (\zeta)^{0.5} \qquad (4.22)$$

and combining this with equation 4.3 we get:

$$\text{specific friction} \propto (\zeta)^{0.5} \cdot U \qquad (4.23)$$

The expected increase in specific friction with viscosity was measured during these tests, figure 4.38, but the index was less than expected, being 0.22. However this calculation is based on measurements of the minimum film thickness and previous sections have shown that the mean film thickness can vary in a different way to this, particularly for the outstroke. The unknown relationship between mean film thickness and viscosity may have given better qualitative agreement.

Instrokes

The instroke film profiles are much thinner than those of the outstrokes and the film decreases with the viscosity of the fluid. The values of the minimum film thickness when plotted against the bulk viscosity of the oil, figure 4.39, shows two regimes. At low pressure, 300 lb_f/in^2, the film thickness is greater than 100 micro inches and the relationship between minimum film thickness and fluid viscosity is:

$$h_{min} \propto (\zeta)^{0.5} \qquad (4.24)$$

which indicates that the seal was hydrodynamically lubricated.

For higher pressures, however, the film was much thinner and the following relationship was found:

$$h_{min} \propto (\zeta)^{2.4} \qquad (4.25)$$

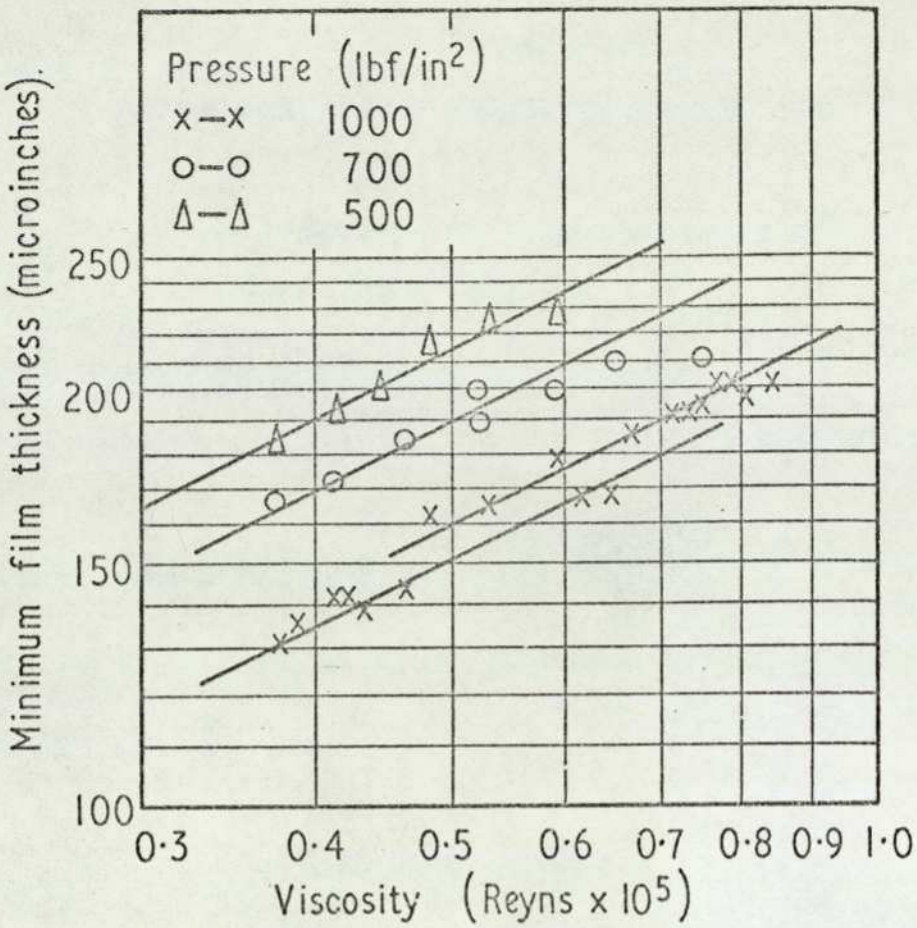


Fig. 4. 37. Outstroke minimum film thickness against viscosity: Series 4.

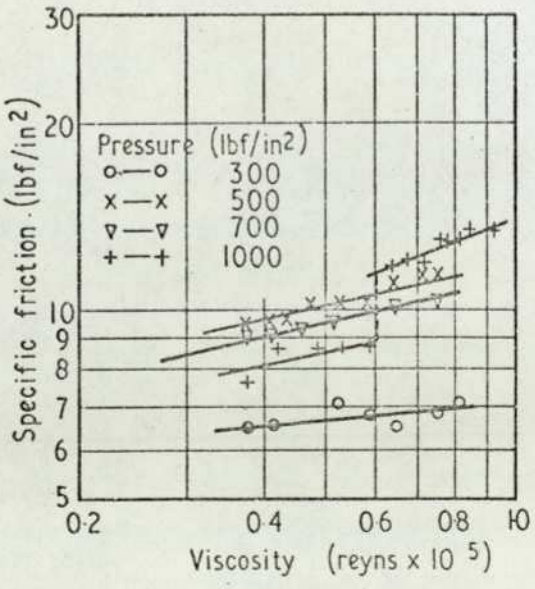


Fig. 4. 38. Outstroke specific friction against viscosity: Series 4.

This latter relationship is in marked contrast to that found for thin films from the optical rig results in which the former relationship was found to fit the experimental data. However in the present case the sliding speed and hence the frictional heating were much higher which could have caused a large reduction in the viscosity of the fluid passing through the contact.

The specific friction values for the instrokes, figure 4.40, follow a relationship of the form:

$$\text{specific friction} \propto (\zeta)^{-1.5} \qquad (4.26)$$

for pressures of 300, 500 and 600 lb_f/in^2, which is unexpected when compared to the results for the outstrokes and the optical rig study.

However the relationship between minimum film thickness and viscosity when substituted in the Newtonian friction formula gives:

$$\text{specific friction} \propto (U)\cdot(\zeta)^{-1.4} \qquad (4.27)$$

which shows good agreement with the measured values of friction.

For higher pressures, 700 and 1000 lb_f/in^2 the data is more scattered and for a pressure of 1000 lb_f/in^2 there appears to be two regimes with a step change between them, the friction being almost constant for the viscosities tested in each region, in spite of the film thickness being considerably affected by the viscosity.

For these tests therefore there appears to be no agreement between film thickness and viscosity either qualitatively or quantitatively.

4.2.8. The effect of seal hardness

The theoretical analysis, Chapter 5, shows that the film thickness decreases with increasing elastomer hardness, although the general film profile remains almost the same. The experimental results also show similar changes in film thickness but the film profiles are widely different.

Film profiles

Figures 4.12 and 4.21 show typical film profiles for the seals of hardness 90 IRHD and the instroke and outstroke film profiles are shown to differ widely. However profiles for the softer seal show completely different behaviour in that both strokes have a similar profile which has in some cases two 'nips', one at each end of the seal. This double 'nip' profile

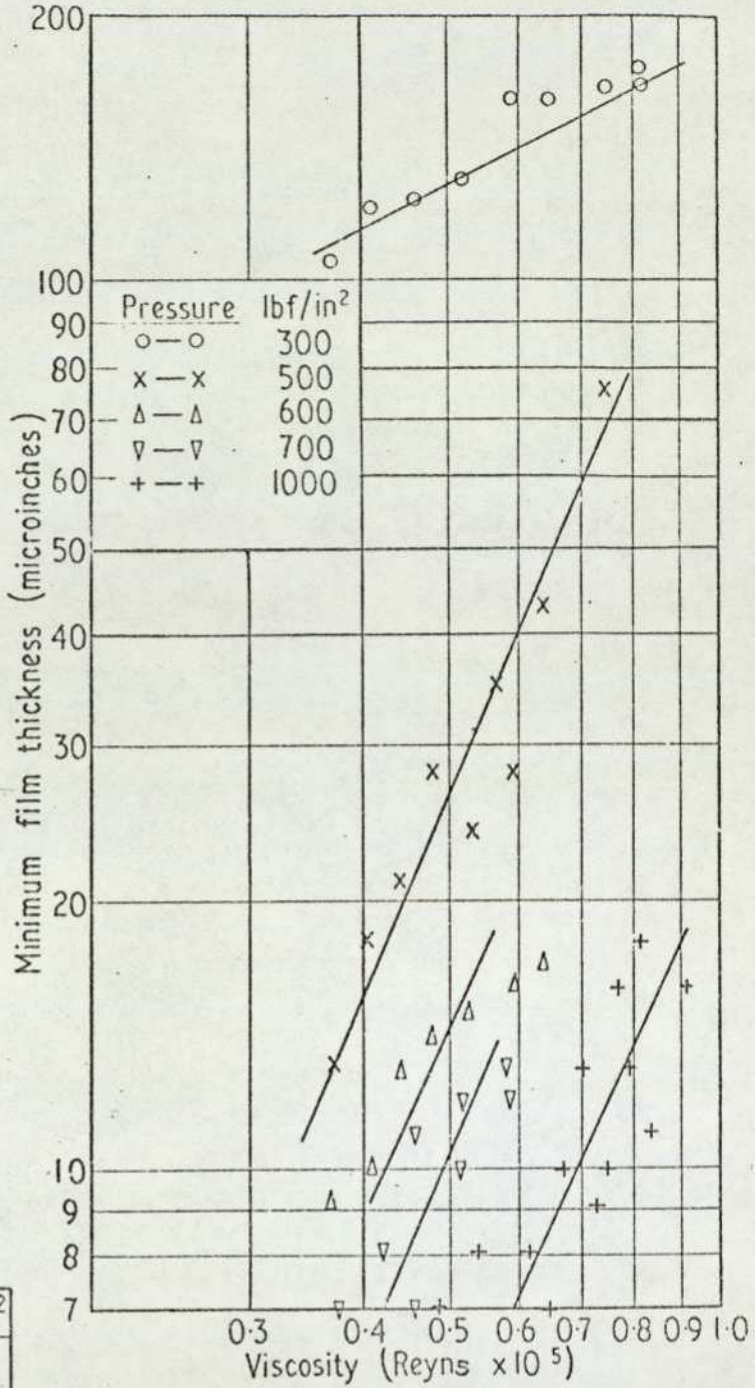


Fig. 4.39. Instroke minimum film thickness against viscosity: Series 4.

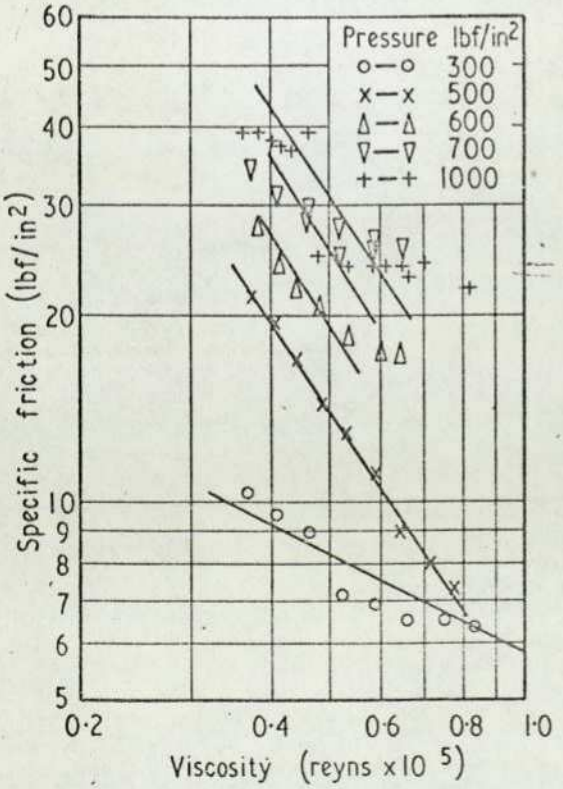


Fig. 4.40. Instroke specific friction against viscosity: Series 4.

is very similar to those recorded for the harder seal in Series 1 and also by Nau (37) which were obtained using a seal of hardness 90 IRHD but of 0.375 inches radial section and used as a rod seal. The instroke profiles of the soft seal, figure 4.42, show that as the pressure increases, the film thickness under the 'nip' at the pressurised side of the seal also increases. A different effect occurs at the atmospheric side of the seal where the minimum film thickness at first decreases with pressure but, for pressures above 400 lb_f/in^2, starts to increase. The 'nip' also extends along the contact. The outstroke film profiles generally behave similarly, but are in most cases considerably thicker. The effects described above were unexpected in the light of previous experience using seals of hardness 90 IRHD, but with the same radial interference for both hardnesses of seal the interference stress would be different and the results of a later section indicated that this variable is of considerable importance in determining the film thickness. Variation in interference stress along the contact could also affect the film profile. The different behaviour of the two hardnesses of seal could therefore be accounted for by changes in the interference stress.

Apart from the hardness change, the method of manufacture of the two seals could also have affected the interference stress profile. Thus the seal of hardness 90 IRHD had an 'as moulded' sliding surface whereas the 70 IRHD seal was cut from a blank of rubber and ground to size on both inner and outer diameters

Specific friction

In spite of the fact that the film profiles were much thicker for the softer seal the values of specific friction obtained were approximately the same for both hardnesses and generally in the range 10 - 50 lb_f/in^2. Figures 4.27 and 4.41 indicate the values obtained for both seal hardnesses. against pressure. The behaviour of both can be seen to be similar at some speeds in that the outstroke friction values are low, and the instroke values higher. However at other speeds, the specific friction values for the softer seal were less consistent and in some cases the outstroke friction values were higher than the instroke values.

Again, the values of friction were much higher than expected from hydrodynamic shear of the fluid film and this is particularly so for

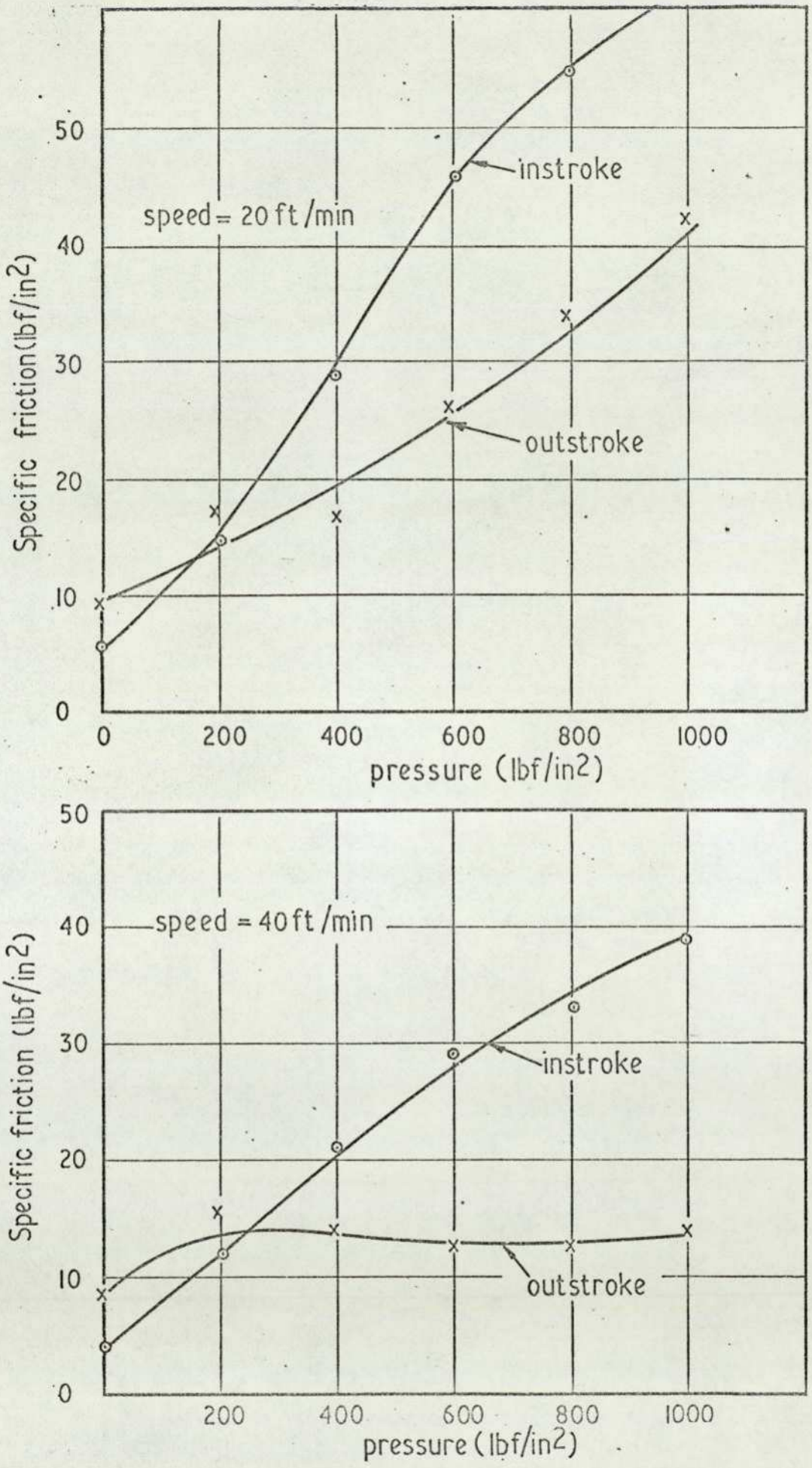


Fig. 4.41. Specific friction against pressure for instrokes and outstrokes (rubber hardness = 70 IRHD, Buc = 0.005 in., interference = 0.005 in.): Series 5.

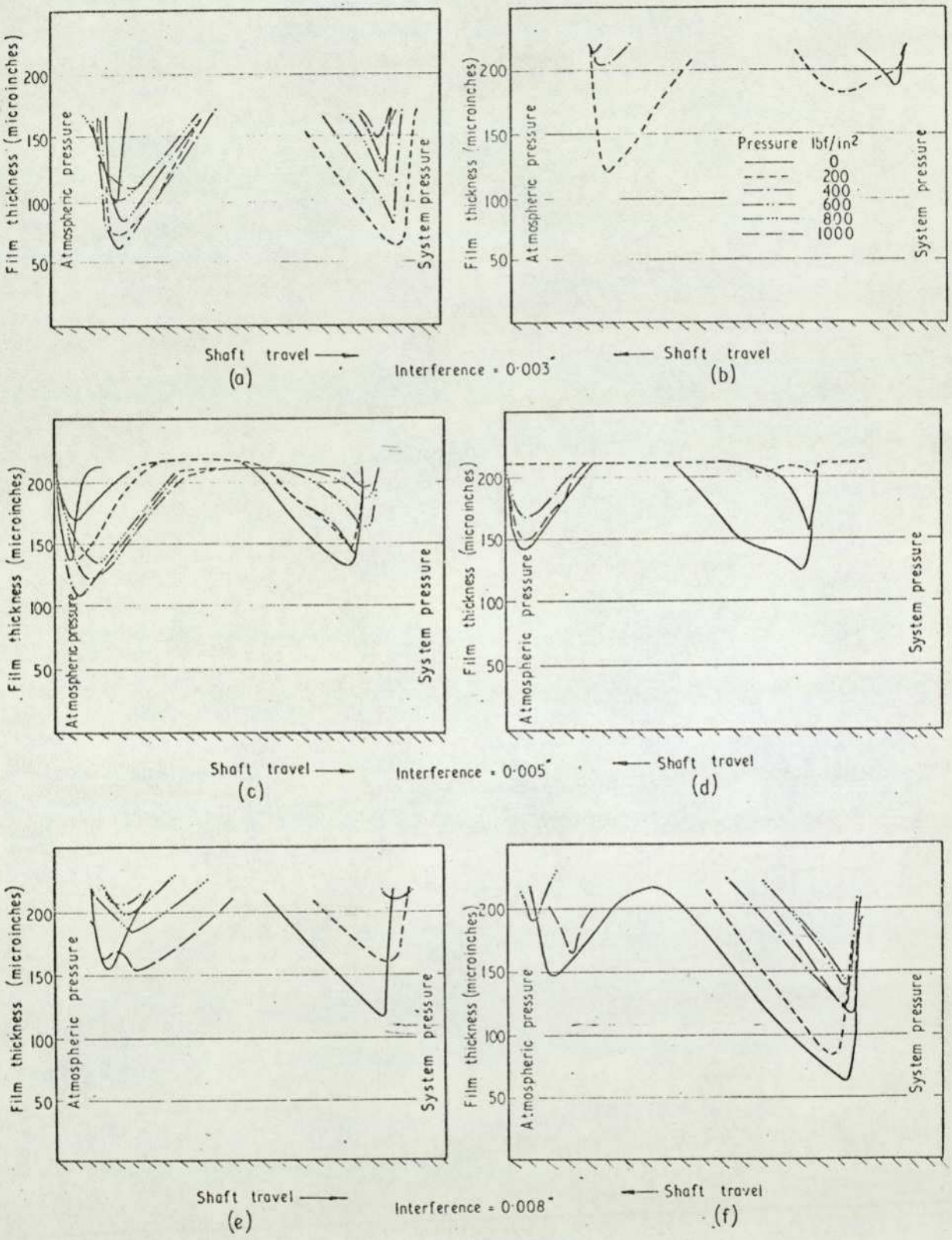


Fig. 4.42. Film profiles for different values of seal interference (rubber hardness = 70 IRHD), Buc = 0.005 in.): Series 5.

the softer rubber where the film was much thicker than for the hard seal.

4.2.9. The effect of seal interference

The interference stress of a particular seal is generally calculated from a knowledge of the linear radial dimension of the seal, the seal groove depth and the Young's Modulus of the material. The interference stress is usually fairly low and for the seal used with 0.005 inches interference, was about 50 lb_f/in^2.

The seal material, the elastomer, has a Poisson ratio of almost 0.5 and transmits the sealed pressure as would a fluid. The pressure therefore also acts radially at the contact surface of the seal.

With the seal stationary the total contact stress is therefore the sum of the hydrostatic and interference stresses. In systems where the sealed pressure is high, the interference stress, in comparison, is small, and as such would not be expected to influence, to any great extent, the behaviour of the seal. However, if during reciprocation of the seal a fluid film is formed between the seal and the mating surface, the pressure in the lubricant film will balance to a considerable extent, the stress in the seal material. In this situation, the interference stress assumes more importance, and will therefore influence the behaviour of the film profile.

The theoretical analysis demonstrates that the seal outstroke film profile is analagous to the Rayleigh Step Bearing and in Appendix G, this analogy is used to evaluate the possible effect of the interference stress on the film thickness.

Seals of hardness 70 IRHD - Film profiles

As described previously the soft seals generated film profiles unlike those found for the harder seals. However qualitative assessments of the effect of seal interference can be made in a study of figure 4.42. This shows both instroke and outstroke film profiles for the three values of interference tested.

In general it can be seen that the outstroke films decrease with interference as expected, but the instroke film thickness unexpectedly increases with interference. The reason for this is at present unclear, although the step bearing analogy, Appendix G, does indicate the possibility of a negative film stiffness under certain conditions and this could be

related to the behaviour of the seal.

Specific friction

The specific friction for both seal strokes and the various values of interference for a nominal speed of 40 ft/min. are shown in figure 4.43. Whilst the points show considerable scatter it can be seen that the interference, particularly for the instroke has a considerable effect, an increase of interference from 0.003 inches to 0.008 inches increasing the friction from 13 lb_f/in^2 to 60 lb_f/in^2 at 800 lb_f/in^2 pressure. In view of the effect of interference on the film profile, this effect is the complete opposite of that expected. However it has already been demonstrated that the measured friction values are always in excess of the theoretical values and therefore there is no specific reason why the friction should qualitatively agree with the film thickness. There are obviously other unknown and uncontrolled factors influencing the friction of the seals.

The outstroke friction values are almost the same for the values of interference of 0.003 and 0.005 inches but are almost doubled by the increase of interference to 0.008 inches. These values do at least correspond qualitatively.

Because of the considerable scatter in the results only a qualitative conclusion can be reached which is that the interference has affected the friction values of the seal more than the film thickness and increasing the interference increases the friction. The effect is however less pronounced for the outstrokes than for the instrokes.

Seals of hardness 90 IRHD (round edges)

Film Profiles

Typical film profiles are shown in figure 4.44 for the two interferenc values of 0.001 and 0.006 inches.

The outstroke film profiles for an interference of 0.001 inches show a film gene rally greater than 150 micro inches throughout most of the contact with a pronounced 'nip' at the atmospheric side of the seal, as expected from previous experience and the effect of increasing the interferenc has been to reduce the mean film thickness and extend the 'nip' across the contact. The effect of pressure on the minimum film thickness has also been reduced by the increased interference

In figure 4.45 the minimum film thickness values are shown and

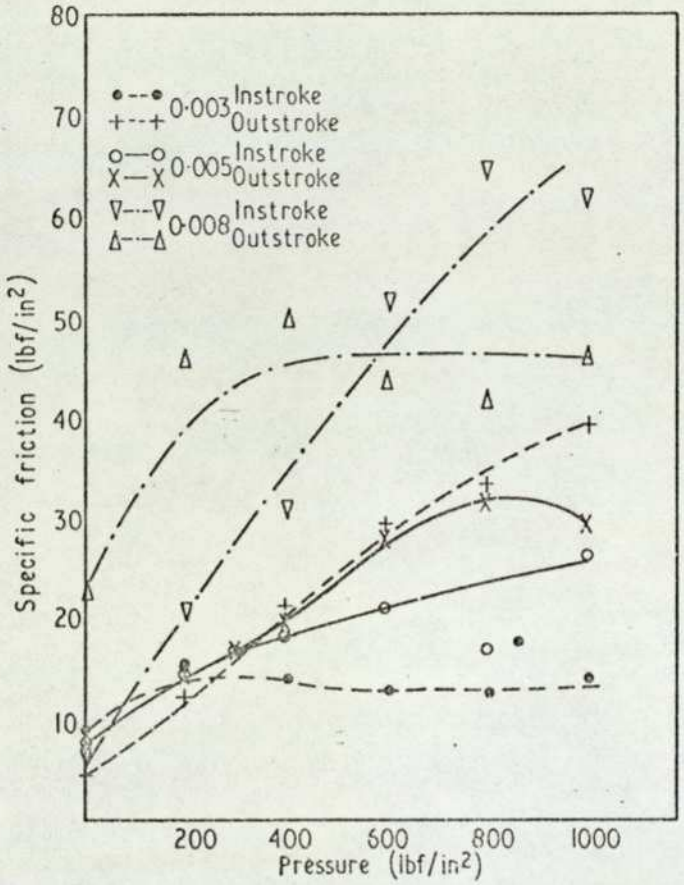


Fig. 4.43. The effect of seal interference on the specific friction (rubber hardness = 70 IRHD, Buc = 0.005 in.): Series 5.

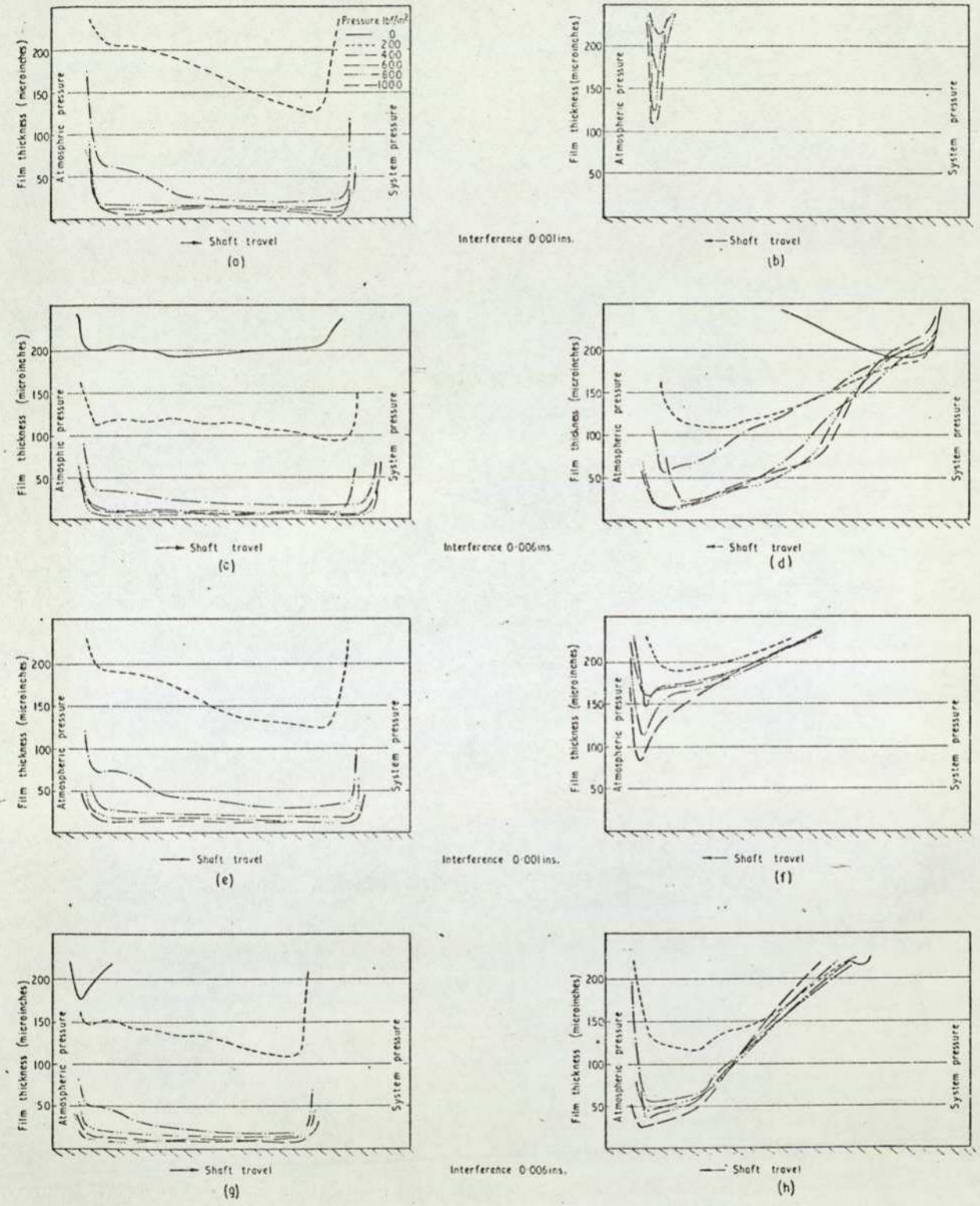
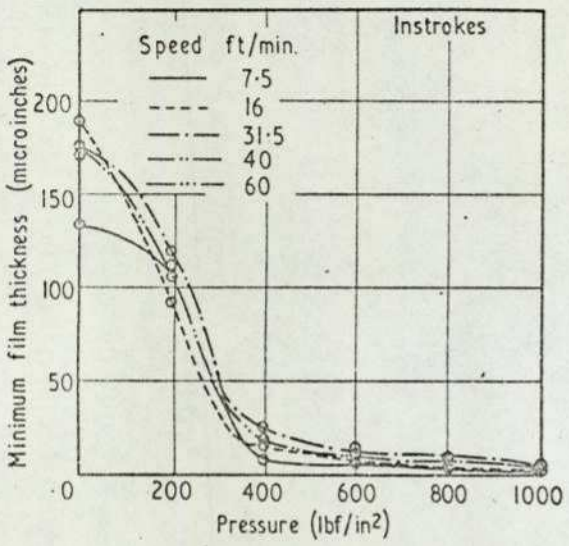
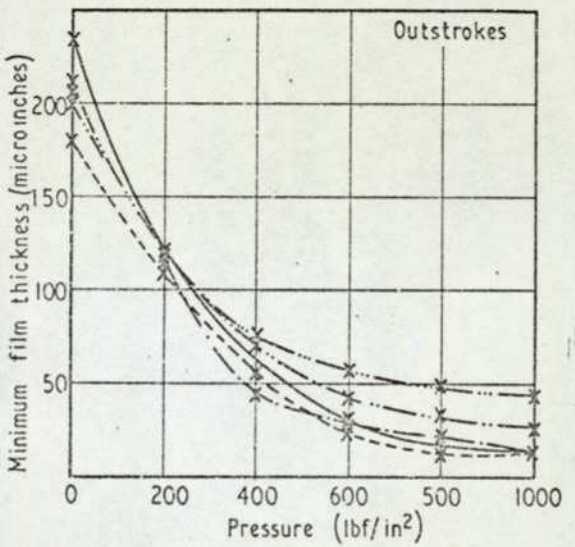
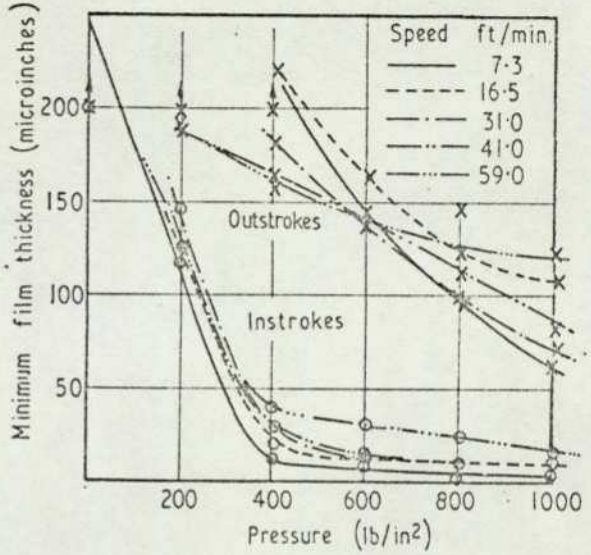


Fig. 4.44 The film profiles of a round edged seal for two values of seal interference (rubber hardness = 90 IRHD, BUC = 0.005 ins: Series 5
Speed: (a), (b), (c), (d) 16 ft/min. Instroke: (a), (c), (e), (g).
(e), (f), (g), (h) 40 ft/min. Outstroke: (b), (d), (f), (h).





(a)
Interference 0·006 in.



(b)
Interference 0·001 in.

Fig. 4. 45 Minimum film thickness values for the film profiles of figure 4. 44

the effect of interference can clearly be seen, particularly for the outstrokes.

For the instrokes, the effect of interference is slight for pressures greater than 400 lb_f/in^2, where the value of film thickness is small, but is more significant at the lower pressures where for the high interference a maximum value of film thickness was 175 micro inches. For the low interference seal, the maximum was 250 micro inches.

The most significant difference between the two values of interference was on the outstroke, where the minimum film thickness for the high interference seal behaves in a similar manner to that expected for instrokes. The minimum film thickness values for the low interference seal are considerably higher and show a greater dependence on the speed of reciprocation.

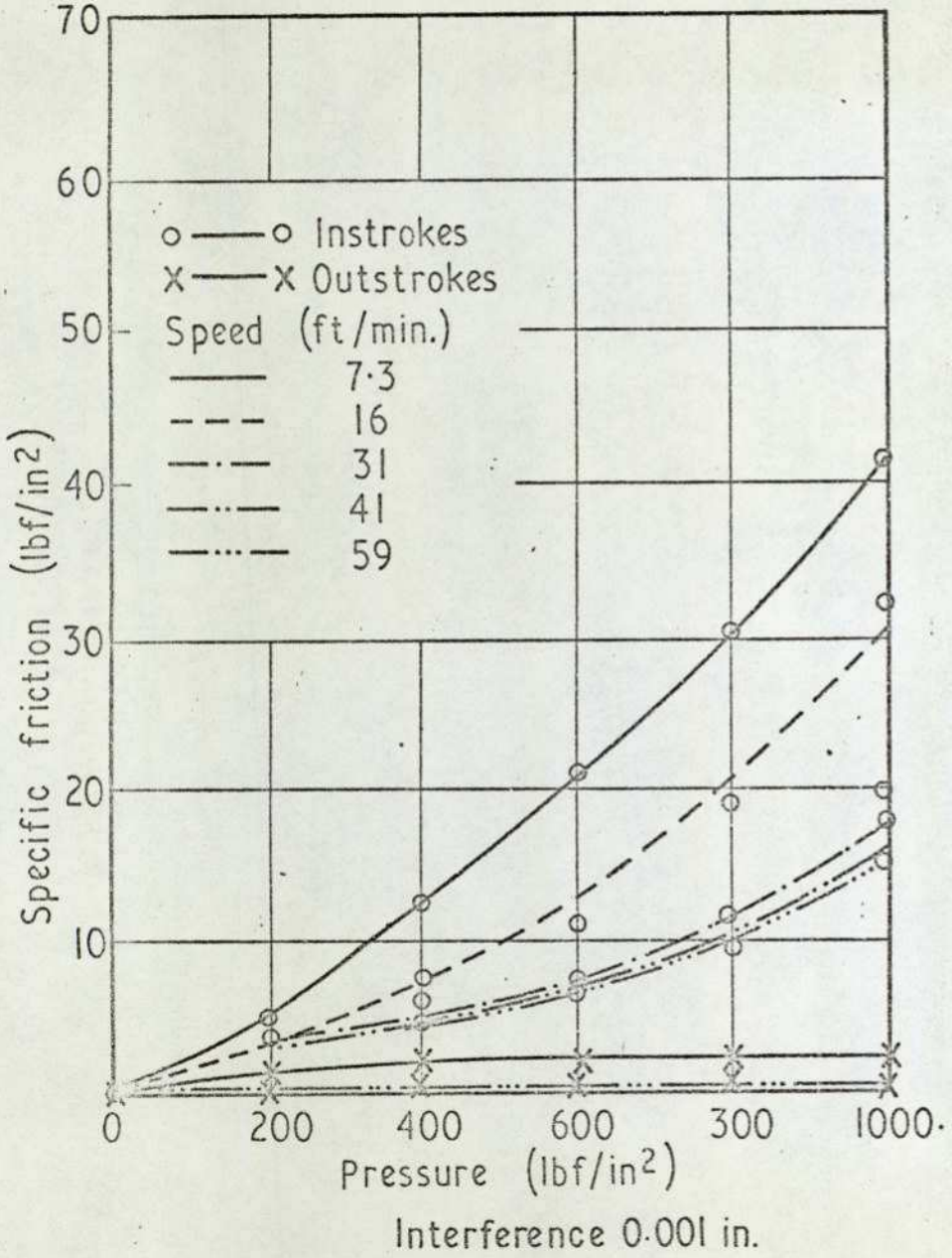
Specific friction

The specific friction as a function of pressure figure 4.46 also reflects the change of interference stress, but in this case the most significant change is found to occur for the instrokes. The outstroke frictions being small show little change with interference although in general they appear to be lowest for the lowest interference seal and this is shown clearly at the lowest speed.

The interference has a large effect on the instroke friction particularly at low speed and high pressure. At zero pressure the difference in friction between instroke and outstroke agrees qualitatively with the measurements of film thickness.

Seals of hardness 90 IRHD (Square edges)

It is noticeable that the specific friction data obtained during tests with this particular seal were the reverse of those normally expected, that is the outstroke values were higher than those of the instroke. The ultra violet recorder traces were rechecked to determine whether the reversal was due to wrong analysis but no such error could be found and it was assumed that the effect was due to the seal/groove geometry. In view of this, the data obtained from this seal has been treated in isolation and it must be assumed that the results reveal the effect of the test variables, although they cannot be used as a direct comparison with results obtained previously using different seals.



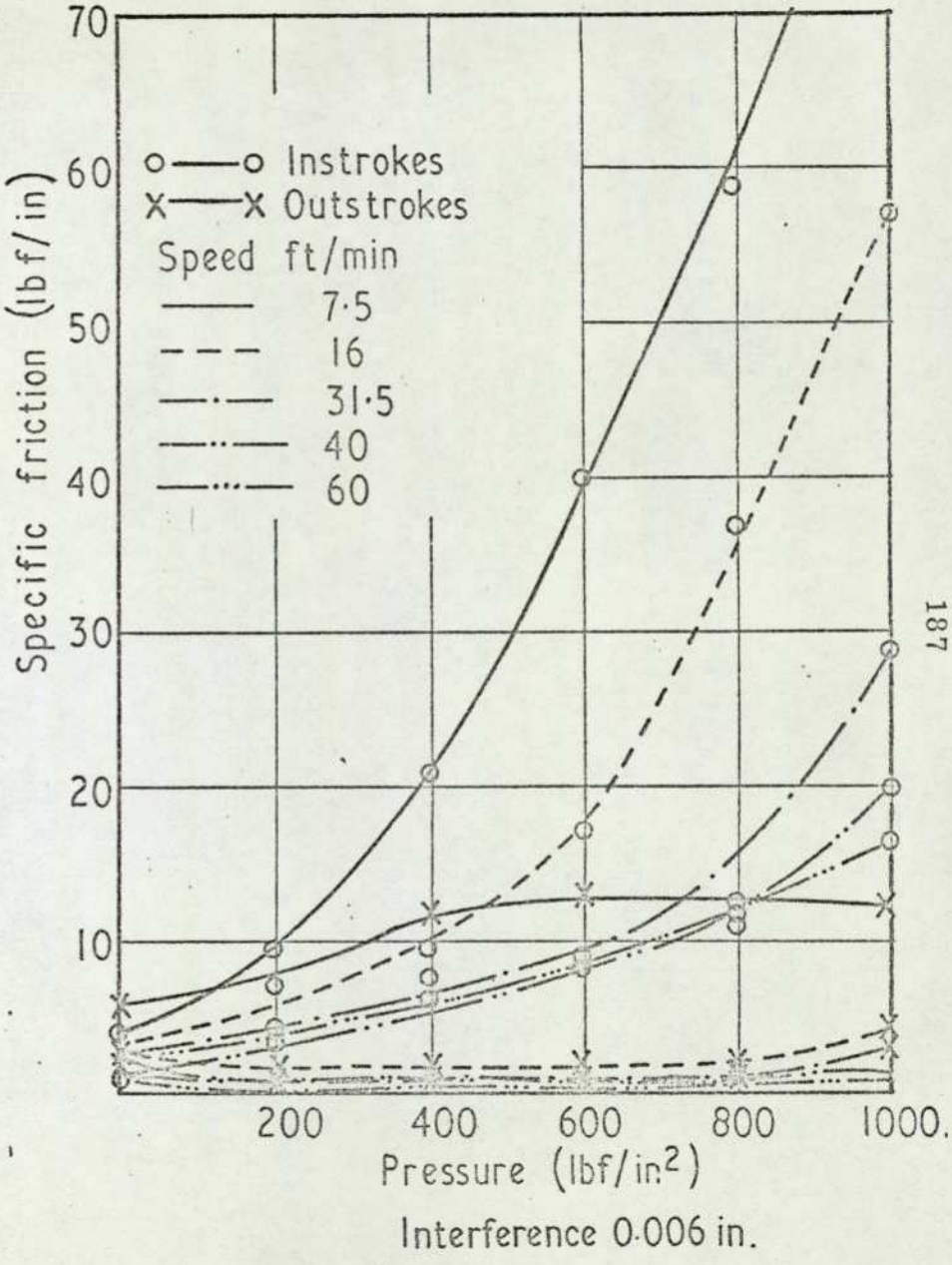


Fig. 4. 46 Specific friction values for the film profiles of figure 4. 44

Film profiles

The film profiles obtained for the three values of interference, and a speed of 30 ft/min. are shown in figure 4.47. It can be seen that the effect of interference is considerable and even an increase of 0.003 inches reduces the outstroke film thickness drastically. At the highest value of interference 0.010 inches the outstroke film profile is reduced to that normally expected only of an instroke.

Figure 4.48 shows the minimum film thicknesses which can be seen to be considerably affected by the interference. The values of film thickness nearer to the pressure side of seal, where h* would be expected to occur also follow a similar pattern, which indicates that the seal leakage would at first decrease with pressure but then start to increase. However, it could be reduced considerably by an increase in the interference. Thus for a sealed pressure of 1000 lb_f/in^2 the leakage would be reduced by a factor of four if the interference were doubled.

Figure 4.47 also shows typical instroke film profiles and it can be seen that the interference has again had considerable effect on the film thickness. In particular there is a large 'nip' at the atmospheric edge of the seal which decreases in width as the interference increases. It is obvious that the minimum film thickness at zero pressure is not typical and the film thickness of the pressure edge of the film is used as representative of the film thickness in this case.

The effect of the seal interference can be seen from figure 4.49 in which the instroke minimum film thickness is plotted against the radial seal interference. This is for a speed of 30 ft/min., but similar behaviour occurred at other speeds. At pressures less than 400 lb_f/in^2 a thick film was formed which was very dependent on the interference but at higher pressures and thinner films the dependence in absolute terms is much less. As a percentage the increase of interference from 0.005 to 0.010 inches reduced the film thickness by approximately 50%.

Specific friction

The specific friction for both instroke and outstroke is considerably affected by the seal interference, reflecting the large effect of interference on the film profiles. Thus the outstroke film thickness was very thin for an interference of 0.010 inches and the friction at the lowest speed reached

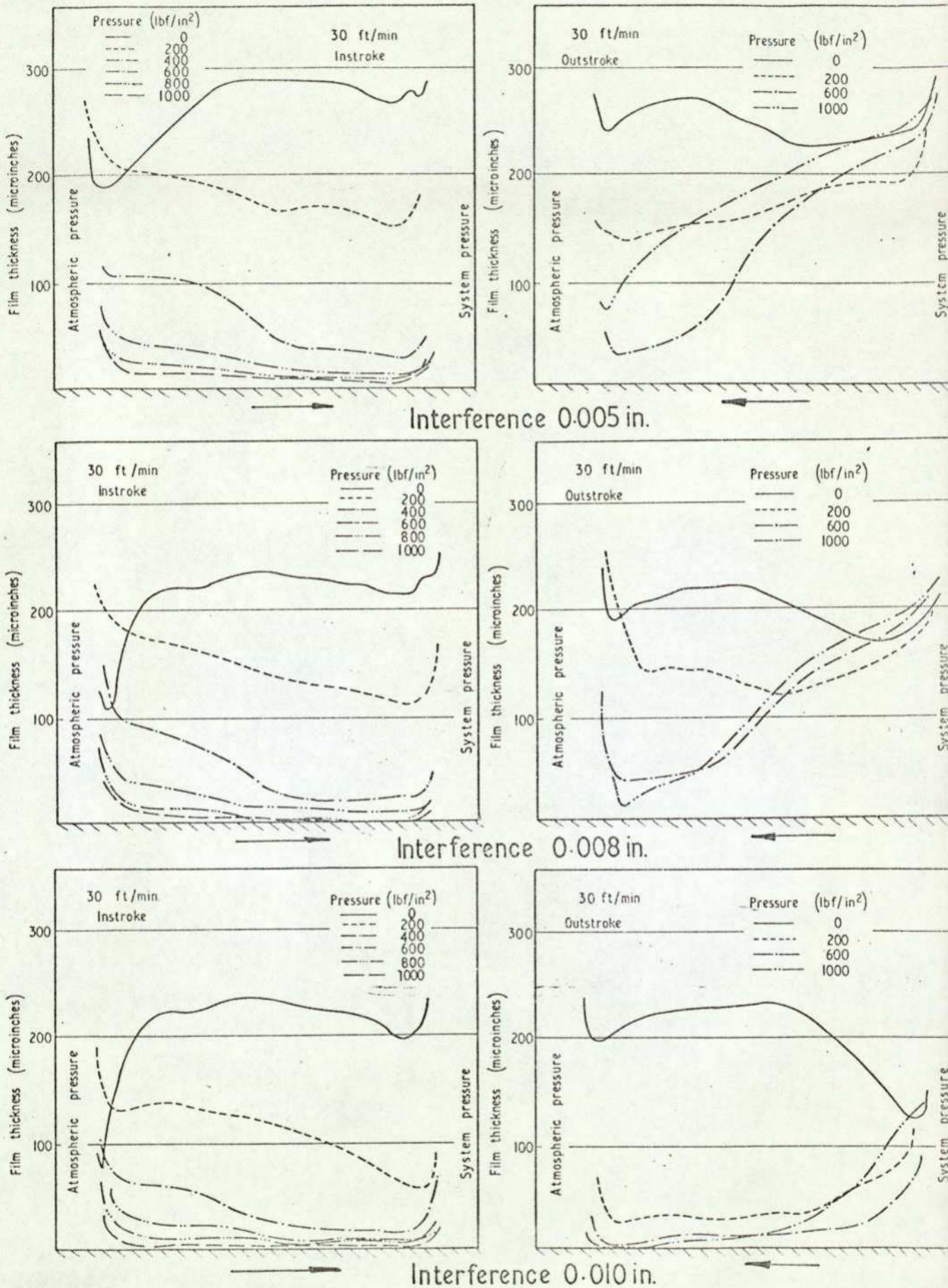


Fig. 4.47. Film profiles for different values of seal interference. (rubber hardness = 90 IRHD, Buc = 0.005in.): Series 5.

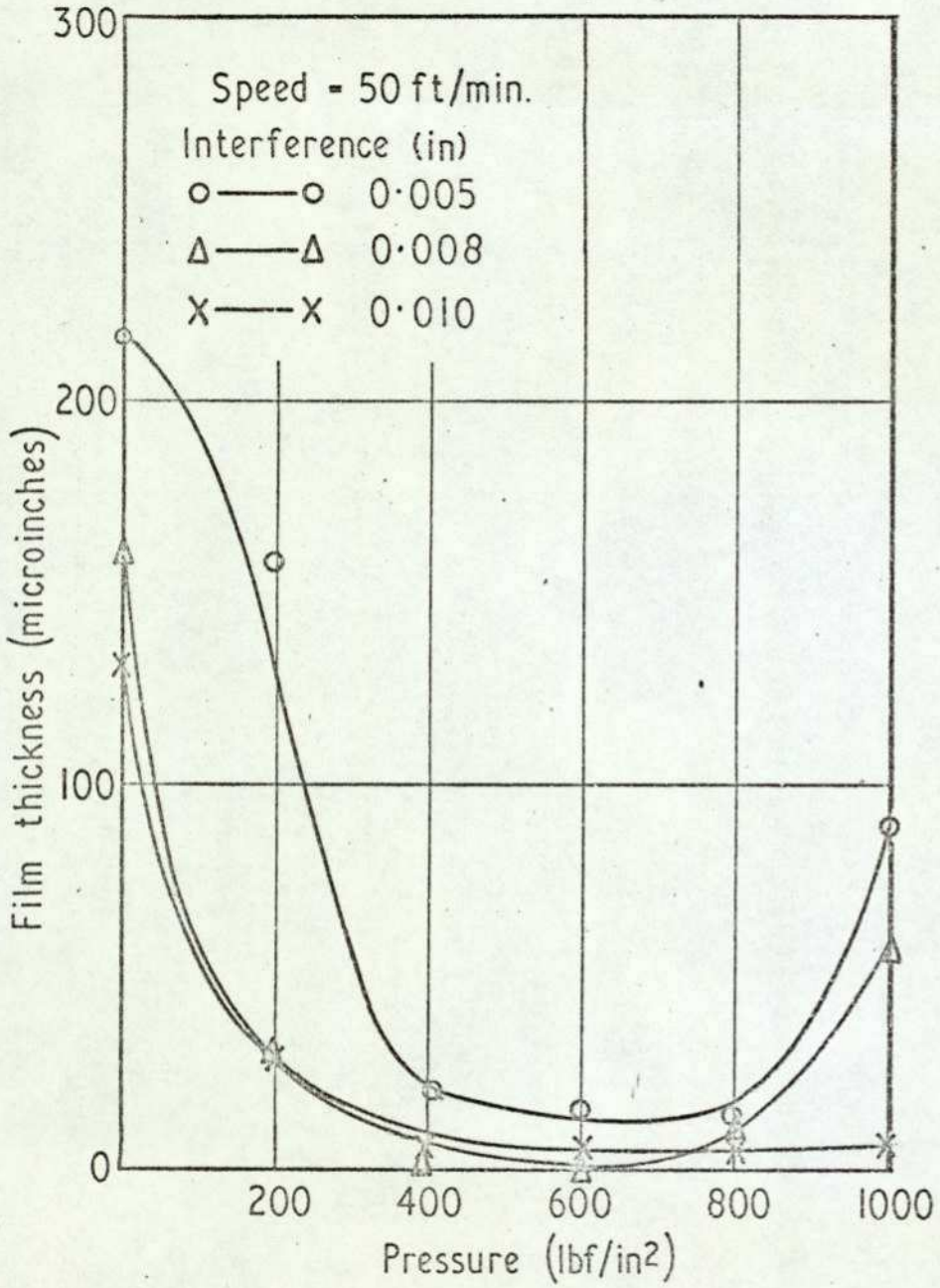


Fig. 4.48 Minimum film thickness against pressure

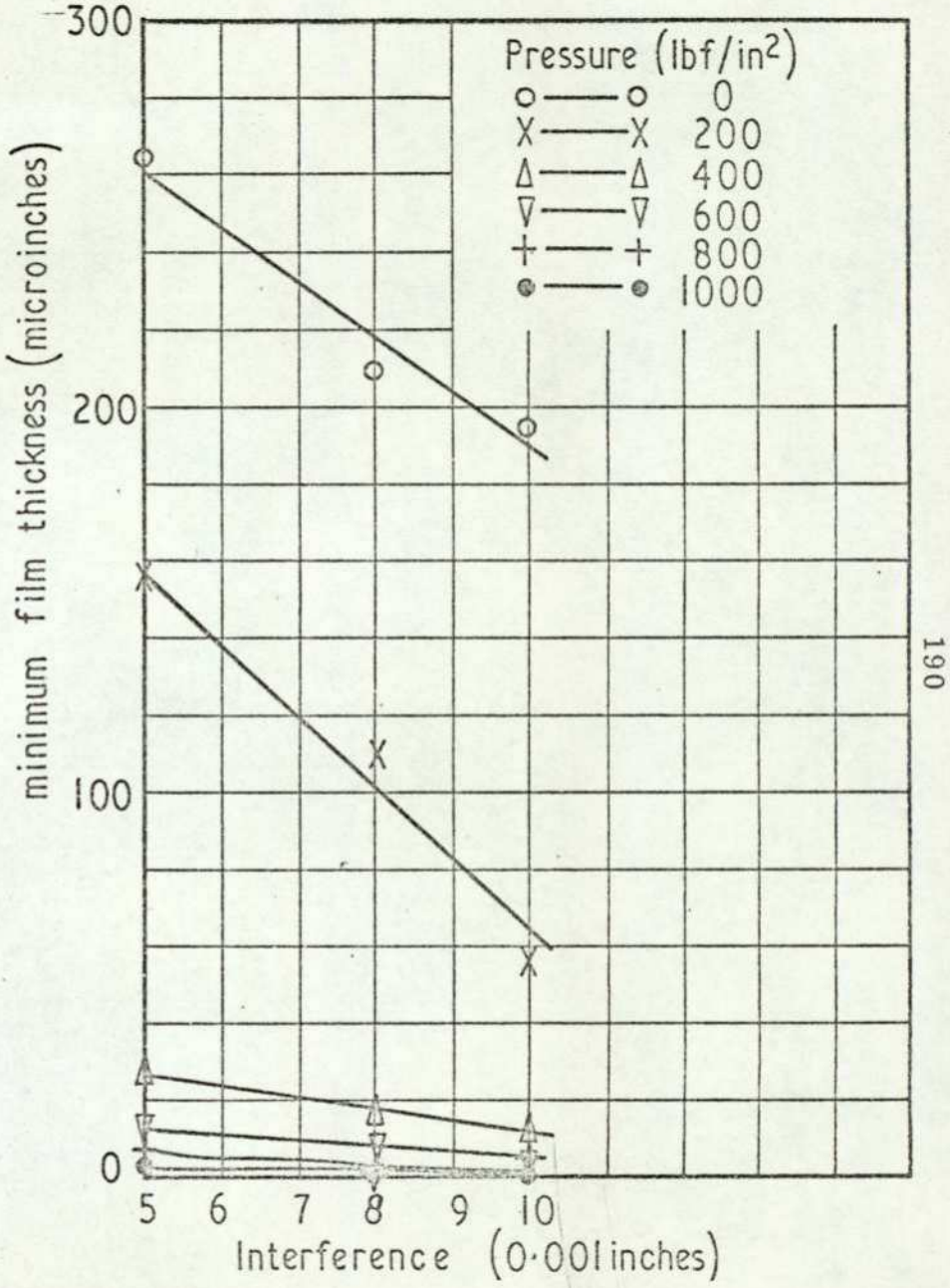


Fig. 4.49. The effect of seal interference on the instroke minimum film thickness (rubber hardness = 90 IRHD

100 lb_f/in^2, a value higher than that usually expected of instrokes. The outstroke values of specific frictions for the three values of interference are shown in figure 4.50(a) for a speed of 30 ft/min.

The effect of interference on the instroke value of specific friction can be assessed from figure 4.50(b). The fact that the slope of the lines is constant indicates that the mode of lubrication for all values of interference is the same in spite of the wide variation in the film thickness. The relationship between the specific friction and the seal radial interference can be shown to be of the form:

$$\text{specific friction} \propto (\text{radial interference})^{1.55} \qquad (4.28)$$

4.2.10 Back-up clearance effects

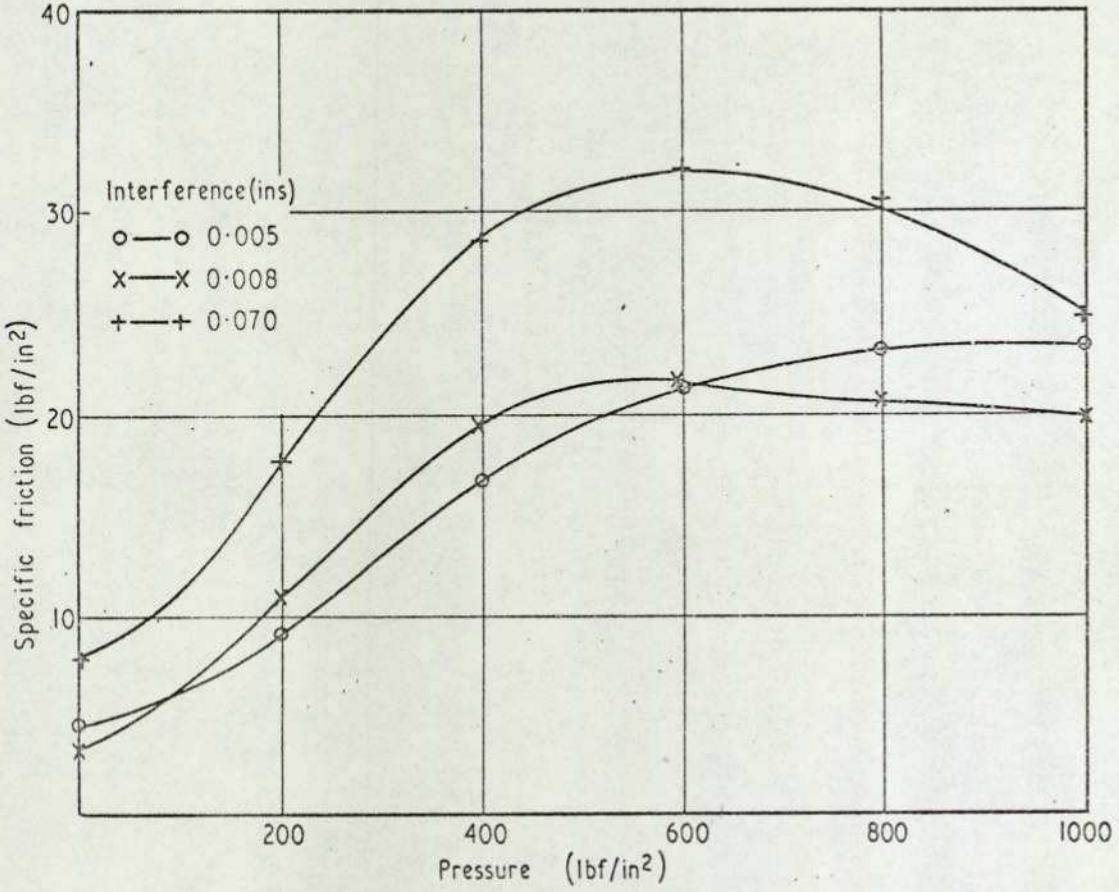
The seal used for these tests was that used for the previous section, the effect of seal interference and the anomolous results reported there were also found to occur here. It must therefore be assumed that any difference between the two sets of data was in the main caused by the differences in the back-up clearance, and would be similar for seals operating with more typical behaviour.

The back-up clearance has been shown in other work(19, 20, 21) to be important to the lubrication of the seal, particularly during the instroke where the extruded part of the seal edge can create a smoothly convergent entry condition for the fluid.

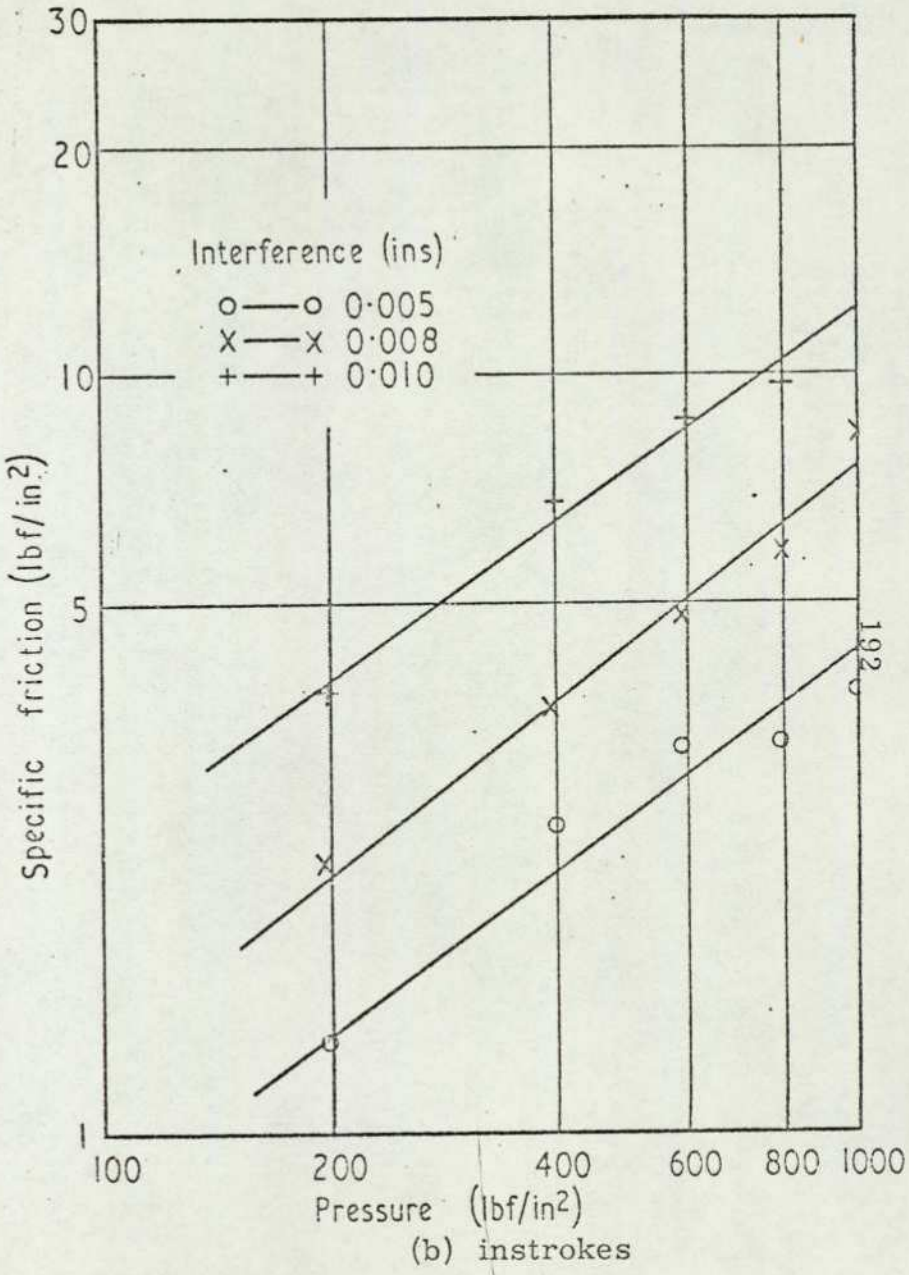
Film profiles

The outstroke film profiles are shown in figure 4.51 for the speed and pressure range tested and the two values of back-up clearance. Comparing the results for the two values reveals a significant difference in the film profiles and thickness. The effect of increasing the back-up clearance being to increase the film thickness.

This effect was surprising as the extrusion profile was expected only to affect the instroke film. For the outstroke the leading edge and therefore the important edge as far as the lubricant film is concerned, is the high pressure edge of the seal which is unaffected by the degree of back-up clearance on the atmospheric side of the seal. The same seal was used with both back-up clearances and therefore for any given sealed pressure the extrusion depended only on the back-up clearance. This obviously affects the radial contact stress at the atmospheric edge of



(a) outstrokes



(b) instrokes

Fig. 4.50 The effect of seal interference on the specific friction (rubber hardness = 90 IRHD, BUC = 0.005 in): Series 5

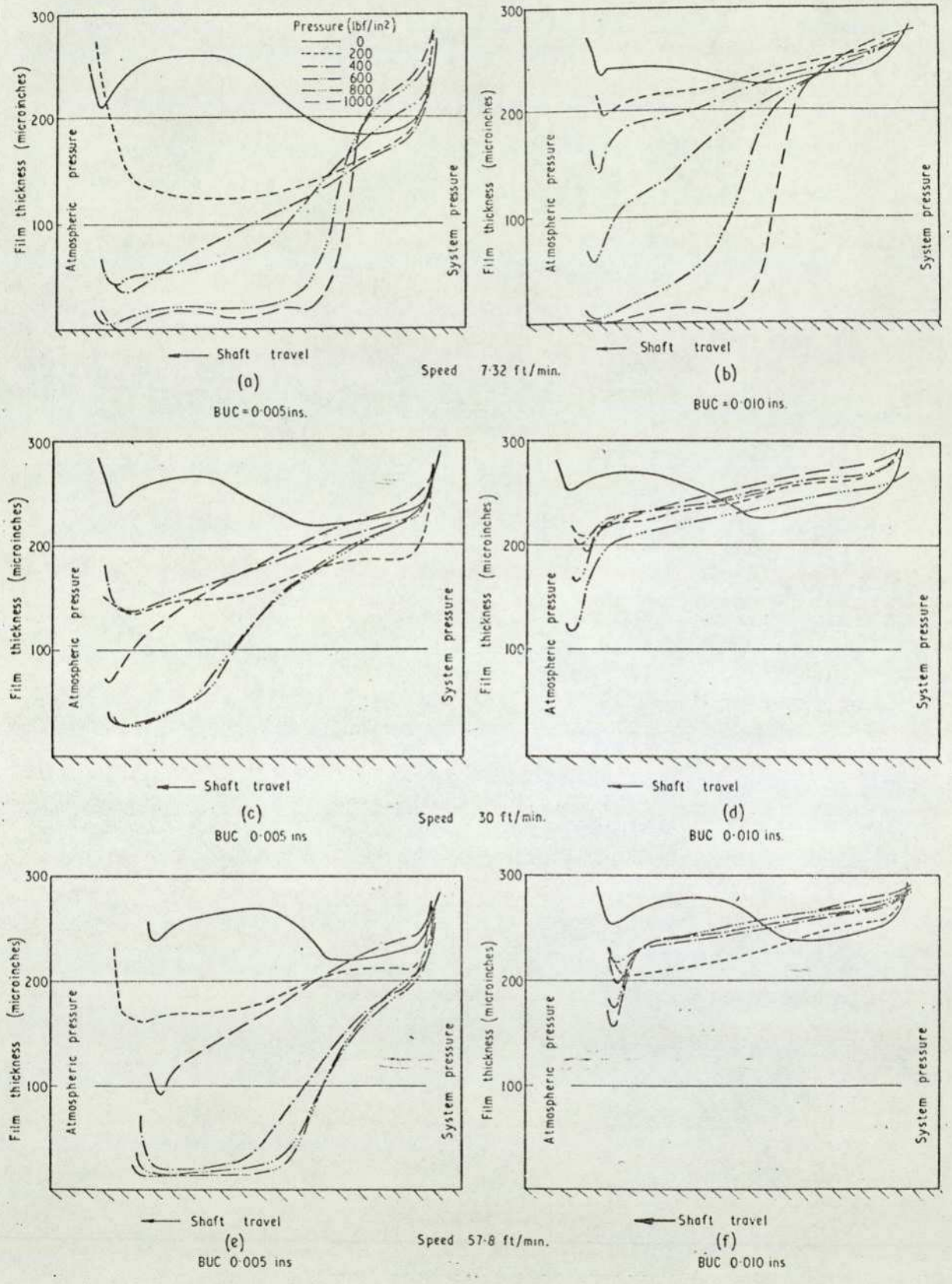


Fig. 4.51. Outstroke film profiles showing the effect of back-up clearance (rubber hardness = 90 IRHD, interference = 0.005 ins.): Series 5.

the seal which, from the results, appears to affect the stress throughout the seal although the extent to which this occurs is not known at present.

Qualitatively, the results show that increasing the back-up clearance, increases the film and therefore the leakage of this stroke.

The minimum film thickness values for the instroke for the two back-up clearances are shown in figure 4.52 and whilst there is considerable scatter in the results, particularly at high and low values of film thickness, relationships of the form:

$$h_{min} \propto (U)^{0.83} \quad \text{for a back-up clearance of 0.005 inches} \quad (4.29)$$

and $h_{min} \propto (U)^{0.7}$ for a back-up clearance of 0.010 inches (4.30)

can be formed. The previously determined index of 0.5 for a back-up clearance of 0.003 does not seem to apply for these tests although conditions, apart from the back up clearance were nominally the same.

In figure 4.53 the minimum film thickness plotted against pressure for a speed of 20 ft/min. clearly shows the effect of both pressure and back-up clearance.

The effect of pressure can be written:

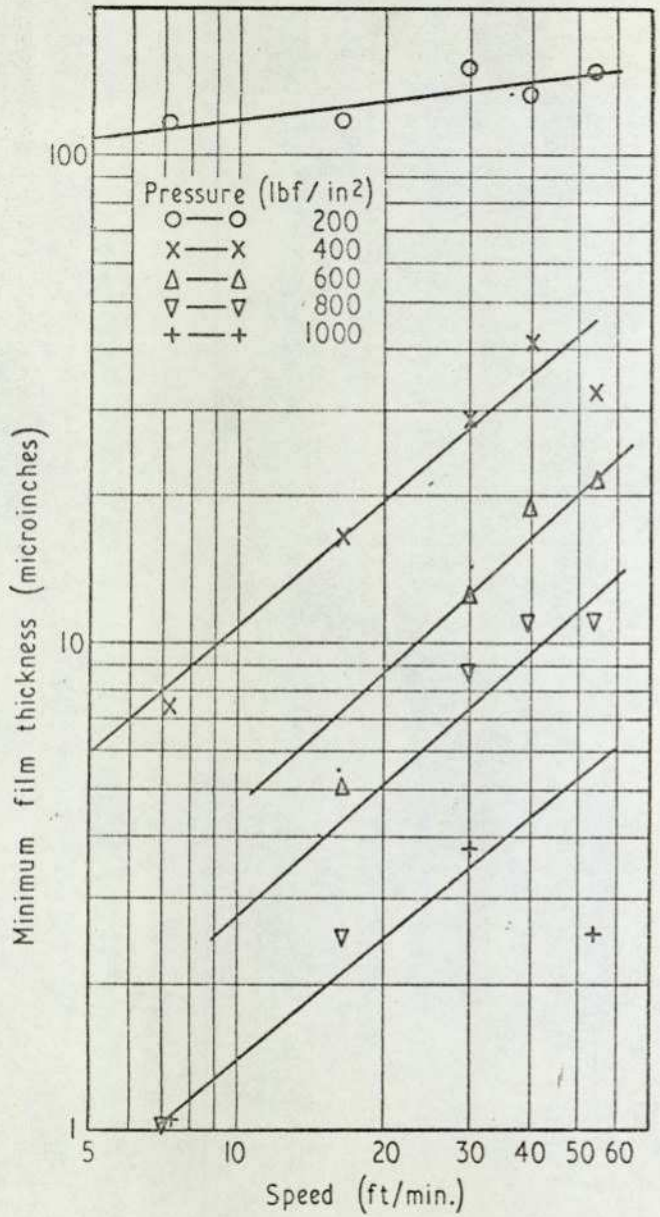
$$h_{min} \propto (P_s)^{-2.27} \quad \text{for a back-up clearance of 0.005 inches} \quad (4.31)$$

and $h_{min} \propto (P_s)^{-1.86}$ for a back-up clearance of 0.010 inches (4.32)

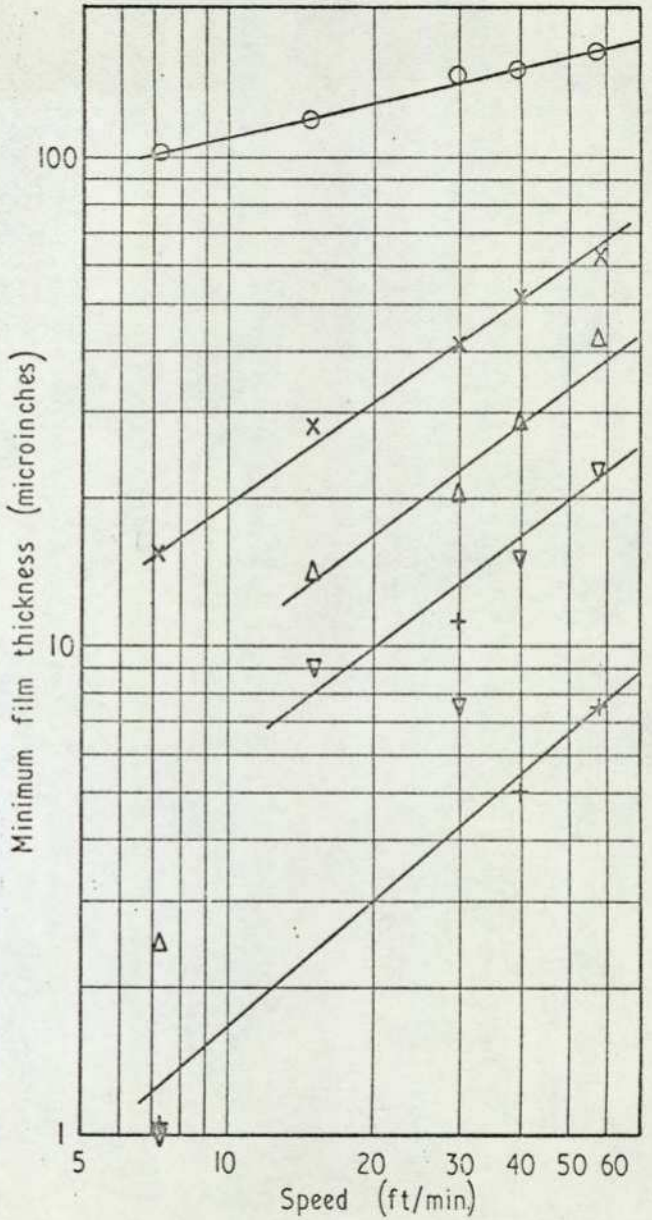
The above results show that the effects of speed and of pressure on the minimum film thickness appear to be themselves affected by the back-up clearance, and there may therefore be an optimum value of back-up clearance for particular applications. However in Section 4.3.2 these effects are found to be as follows:

$$h_{min} \propto (U)^{0.5} \cdot (P_s)^{-2.0} \quad (4.33)$$

and in the present tests the differences in the indices could be due to experimental error. If this is accepted, the effect of increasing back-up clearance is simply to increase the film thickness.



(a) Buc = 0.005 inches.



(b) Buc = 0.010 inches.

Fig. 4.52. The effect of back-up clearance on the minimum film thickness (rubber hardness = 90 IRHD, interference = 0.005 ins.): Series 5.

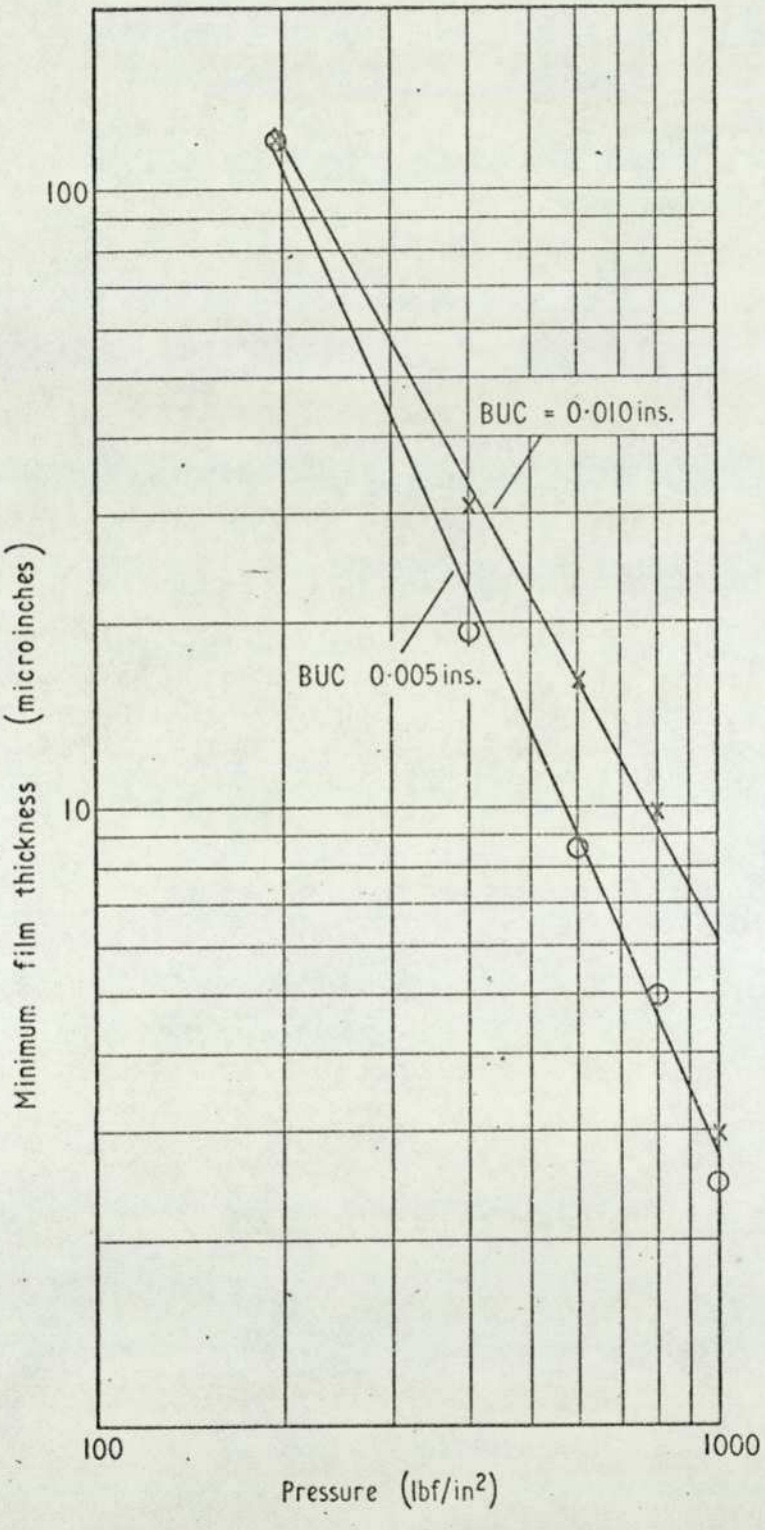


Fig. 4.53. The effect of back-up clearance on the instroke minimum film thickness for a speed of 20 ft/min. (rubber hardness = 90 IRHD, interference = 0.005 in.): Series 5.

Specific friction

Whilst the friction values are the reverse of the expected behaviour, they do show the effect of the change in back-up clearance. The film profiles of both strokes were shown to increase with increased clearance and the friction values for a speed of 30 ft/min. are shown, in figure 4.54, to decrease with back-up clearance, as expected. The effect was the same for all the speeds tested.

4.2.11. The effect of seal edge profile

Results obtained from the interferometric study (Chapter 3) indicated that the lubrication of square edge seals would probably be very variable around the circumference of the seal due to slight variations in the micro-geometry of the edge, and that round edged specimens would make the development of a continuous lubricant film more probable.

The present tests were conducted to determine whether the seal edge had any significant effect on the lubrication of a seal. Four series of tests were conducted as follows:

(i) Both seal edges square

(ii) The atmospheric seal edge rounded to approximately 0.020 inches.

(iii) Seal used for (ii) reversed; that is the round edge towards the system pressure.

(iv) Both seal edges rounded to approximately 0.020 inches.

The same seal, of 90 IRHD, was used for all tests.

Film Profiles

For the outstroke the important edge is that on the high pressure side of the seal, the inboard edge. However section 4.3.10 has shown that the degree of extrusion can affect the film profile throughout the contact and although the back-up clearance for these tests was kept constant, the change in seal edge form itself would affect the extrusion profile and therefore the film throughout the contact. The film profile could therefore depend not only on the seal inlet edge form, but also on the trailing edge form. This would be particularly true for the outstroke.

Figure 4.55 shows the outstroke film profiles for a speed and pressure of 600 lb_f/in^2 and 30 ft/min. respectively, for the four geometrics, but similar results were obtained for other speeds and pressures.

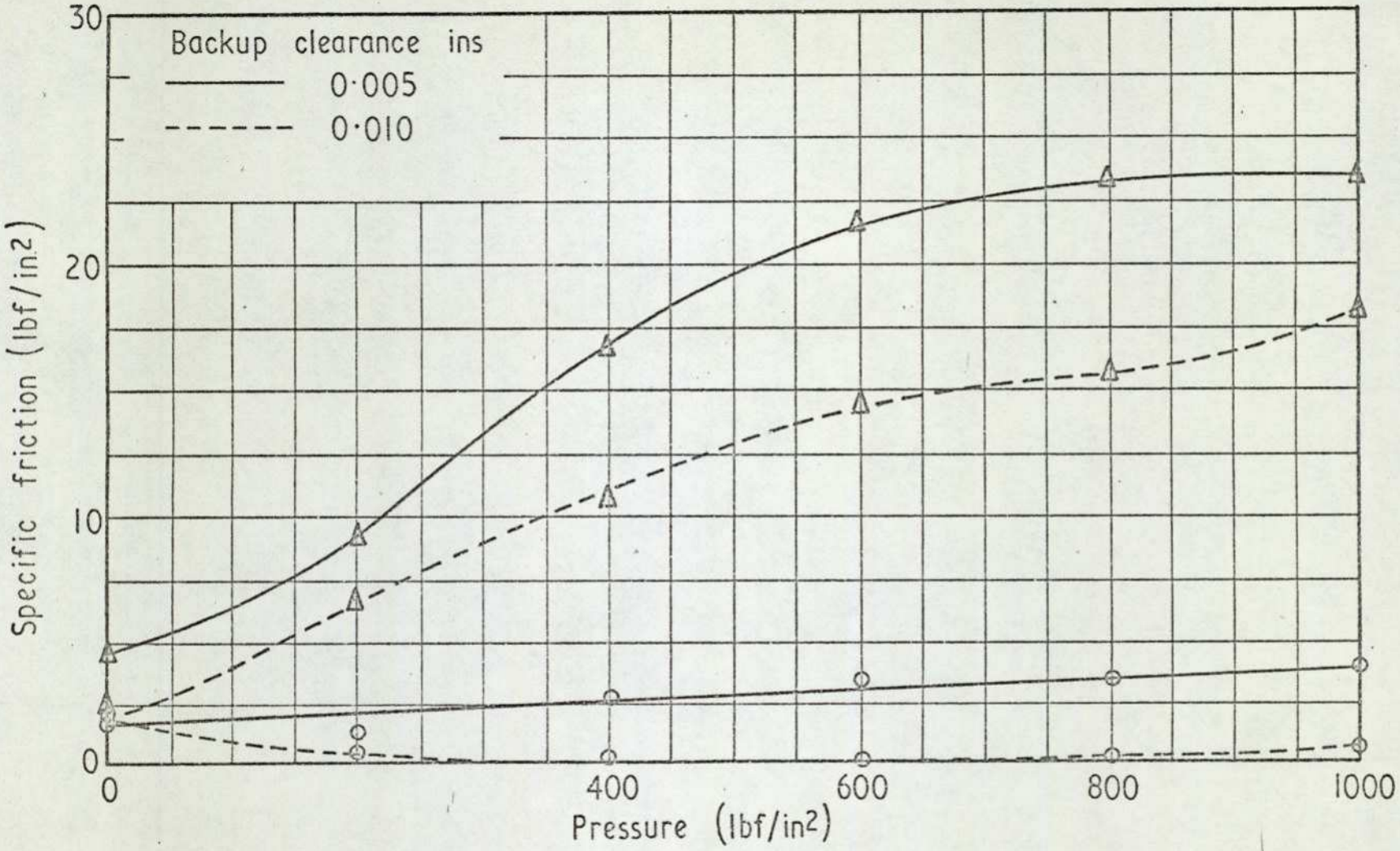


Fig. 4.54. The effect of back-up clearance on the instroke and outstroke values of specific friction. (rubber hardness = 90 IRHD, interference = 0.005 inches): Series 5.

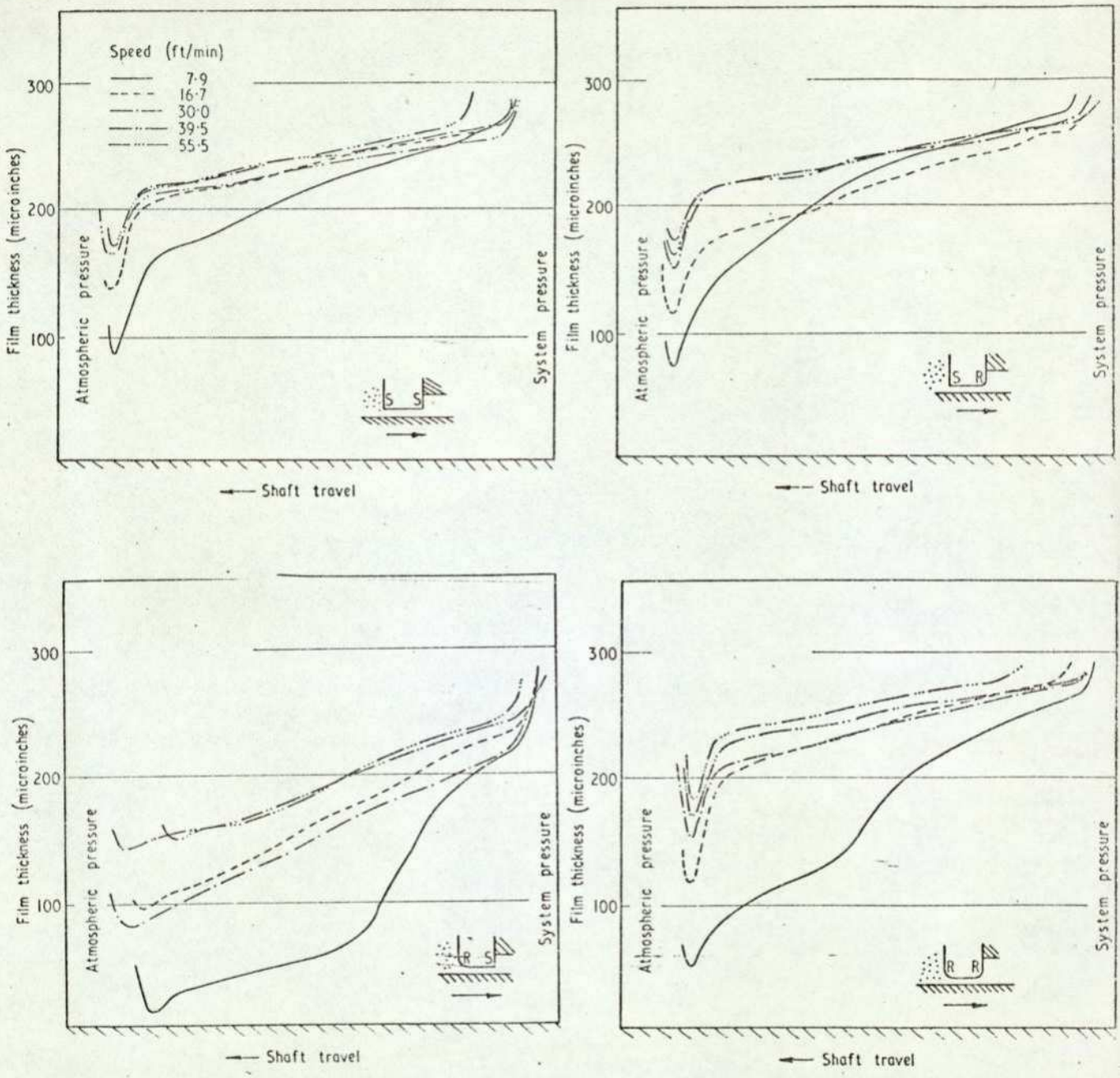


Fig. 4.55. Outstroke film profiles for four seal-edge geometries (rubber hardness = 90 IRHD, interference = 0.005 in., Buc = 0.005 in.): Series 5.

The results were surprising, in view of the effect of specimen edge found in the interferometric study (Chapter 3) as the seals with the round edges inboard gave the thinnest films; with square edges inboard the film was thicker and of a more typical EHL form. However the two applications were operating under somewhat different conditions. For instance, the specimens with a square edge used in the interferometric study did not form a fluid film at all, but square edged seals have always been found to form a film. This may be due to differences in the microgeometry of the edges of the specimen and the seal. The seal leading edge appears to be only of importance in that it enables a film to form initially, and once formed plays no further part in the lubrication process. The speeds were also different, and the seal operated with a pressure differential whilst the specimen did not.

It has been mentioned that the trailing edge of the seal should affect the film profile throughout the contact, and a further study of figures 4.55 reveals this to be so for both round and square leading edges. Thus with a square leading edge the film thickness is less with a round trailing edge than with a square trailing edge, but with a round leading edge the opposite effect is found, that is the thinnest film is obtained with the square trailing edge.

To obtain the thinnest film and hence the lowest leakage for this stroke therefore the leading edge of the seal needs to be rounded whilst the trailing edge is left square.

For instrokes the extruded part of the seal assumes considerable importance as this is, in this situation, the leading edge and should have a considerable effect on the film profile. This was in fact the case and in figure 4.56 film profiles are presented for a speed and pressure of 40 ft/min. and 400 lb_f/in^2, which shows this effect clearly. The film profiles for other speeds and pressures gave similar results. The reason for the increased film formed by a square edged seal is thought to be the shape of the extruded part of the seal, which provides a favourable inlet profile to the seal. The round edge seal extrusion, although not simulated, would be expected to take a form which provides a poor inlet condition

For the instroke the trailing edge of the seal is the high pressure edge and as such the edge form would not be expected to affect the film

profile. Such an effect was however found; with a square leading edge, the round trailing edge increased the film thickness, the opposite effect to that occurring with the seal having a round leading edge.

However in general, for pressures greater than 400 lb_f/in^2 the effect of the leading edge can be ignored for the instroke as the film thickness is very small and changes in the seal edge geometry are unlikely to significantly affect the film thickness in absolute terms.

Specific friction

The values of specific friction recorded for the outstrokes were all small, approximately 2 - 6 lb/in^2 and as such are not sufficiently accurate to warrant a detailed study. However even these very low measured values of friction are still an order of magnitude or so greater than that expected from a theoretical value calculated from the measured values of film thickness using the usual friction formula.

The effect of the seal geometry on the film thickness is reflected in the specific friction data figure 4.57. Here specific friction is plotted against sealed pressure for the four geometrics and a speed of 20 ft/min. It can be seen that over the whole pressure range, the seals having a square leading edge, that is on the atmospheric pressure side of the seal, have a lower friction than seals having a round edge and the divergence between the two geometries increases as the pressure increases. This effect is qualitatively in agreement with the film thickness data.

At sealed pressures above 400 lb_f/in^2, the film thickness values are small and, as regards the leakage of the seals, the inlet profile of the seal will not be of great importance. However, the specific friction is considerably affected by the form of the seal inlet profile and at 1000 lb_f/in^2 the specific friction could be reduced by a factor of two by using a square edge in place of a round edge. The difference between the two friction values is obviously not due to measurable changes in film thickness, but the interferometric study (Chapter 3) indicated that only a very thin film of oil is required between an elastomer and a hard surface to reduce the friction significantly from that of a dry contact. Although the seals used for the present tests were unlikely to be operating under dry conditions, the contact stress pattern of the seal on the shaft, being different for round and square edges, could cause small immeasurable changes in

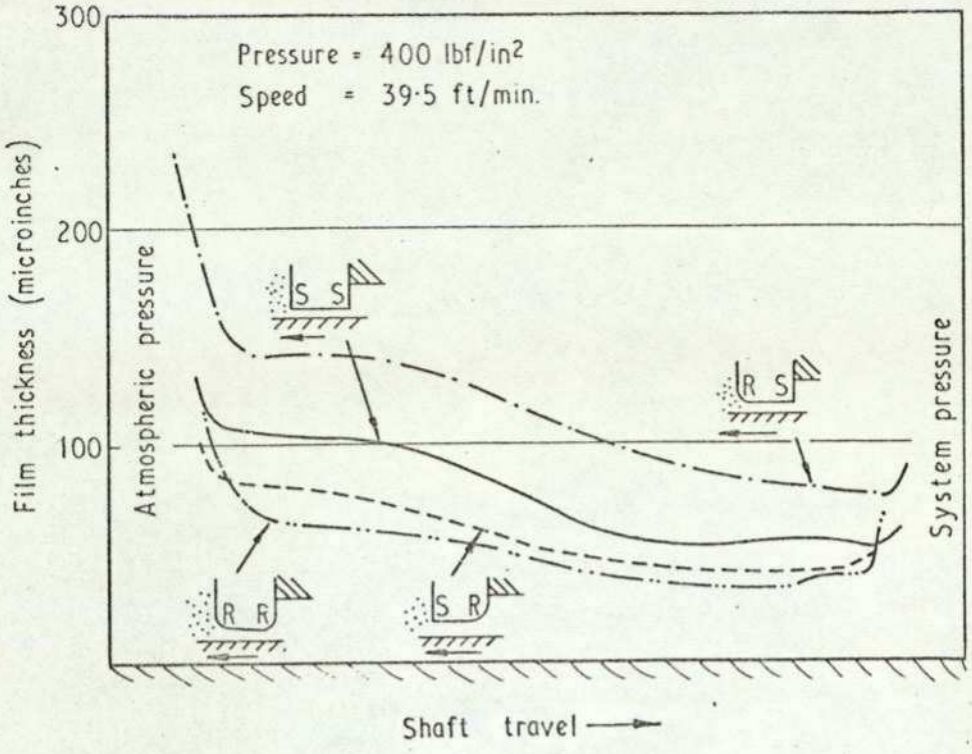


Fig. 4.56. Instroke film profiles for four seal edge geometries (rubber hardness = 90 IRHD, interference = 0.005 in. Buc = 0.005 in.): Series 5.

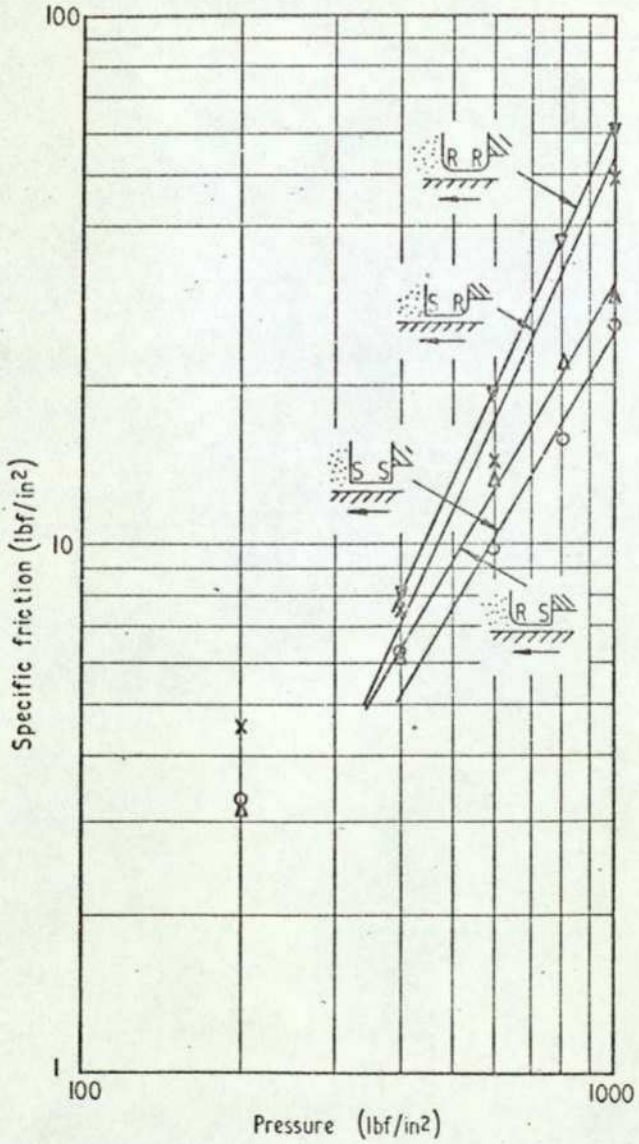


Fig. 4.57. Instroke specific friction against pressure for four seal-edge geometries (rubber hardness = 90 IRHD, interference = 0.005 in., Buc = 0.005 in.): Series 5.

the lubrication of the seal which could lead to significant variations in the specific friction.

4.2.12. Alternating sealed pressures

On a practical hydraulic jack, the pressure differential across the seal will not be constant, as was the case during the present tests. The pressure differential across the rod seal of a double acting jack would be equal to the system pressure during an instroke and zero on the outstroke.

The present work has shown that, in general, for a constant pressure differential across the seal the outstroke film is thick, whilst the instroke film, for pressures abo ve400 lb_f/in^2, is very much thinner. With alternating pressures on the seal, the film thickness may not respond quickly enough to the step changes in pressure to form films of the same order, and application of the present results to a practical system would not have been strictly correct. A number of tests were therefore conducted with alternating pressure applied to the test seal of between zero and the system pressure, which was varied between 0 and 1000 lb_f/in^2.

The pressure cycling was achieved by incorporating in the oil supply line a solenoid valve which was switched at the end of each stroke. The film thickness was measured at the centre of each stroke.

The results show that over the whole pressure range of the present work, the seal responded immediately to a change in pressure. For example with zero pressure on the outstroke the film thickness was above the 200 micro inch cut-off limit of the analogue computer and for the return stroke at 1000 lb_f/in^2 the film was less than 10 micro inches thick.

For a practical jack situation, it appears that the leakage caused by an alternating system pressure may well be worse than that expected for seals having a constant pressure differential.

4.2.13. Repeatability

The data presented in this report has shown considerable variation in the values of film thickness and friction for different seals of nominally the same geometrical size under the same conditions of speed and pressure. It has been assumed that much of this variation was due to slight differences in unknown variables from seal to seal. It was also noticed however that tests under the same conditions could rarely be repeated from day to day even using the same seal, and the data presented is therefore of necessity only applicable to the test seal and the conditions of the particular day on which the tests were conducted. The variations in test results are a feature of all elastomer seal research and are by no means confined to reciprocating seals.

Some attempts were made during this program to bring to light variables which were causing variations in film thickness and friction from time to time. These were simply to check the repeatability, not from seal to seal, but with a single seal over a period of time.

The first attempt was to run the rig for a period of five hours under the same conditions of speed, pressure and temperature, and measure the film thickness and friction at various intervals of time through the test period. The results showed that, within the accuracy of the instrumentation, neither the film thickness or the friction changed significantly.

A second attempt increased the pressure in steps to the maximum at a constant speed, as would be done during a standard test procedure, the pressure then being progressively reduced in the same way. Five minutes were allowed for the film to reach a steady state after the change. These results did show some variation between increasing and decreasing the pressure figure 4.58, which could indicate that the seal has changed in some way as a result of working at the higher pressures, but a great deal of the apparent variation could be due to the increase in the temperature of the bulk oil as the pressure increased.

From the above it can be seen that the repeatability for tests done in the space of a few hours was reasonably acceptable.

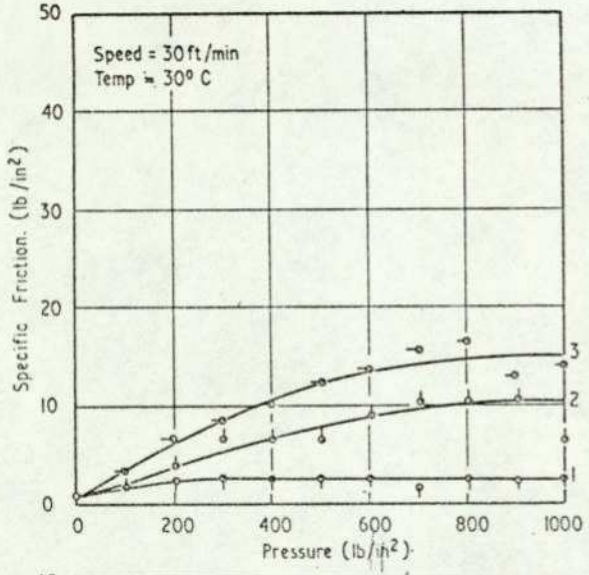
The third type of test comprised the repitition of a standard procedure on three occasions spaced at intervals of 12 and 18 days, the rig being left stationary between each repeat, with the seals remaining in the cylinder bore in contact with the oil but unpressurised. The behaviour of the specific friction was as expected for each program but increased with time. This is indicated by the number against each curve in figure 4.59 which shows the order in which the programs were carried out. The minimum film thickness values, figure 4.60, also show considerable variation between each program but there is no obvious order to the result.

It is well known that seal leakage and friction measurements are rarely repeatable and it appears that the film thickness shows a similar lack of repeatability. This is an area which requires a considerable amount of further work before reliable and repeatable results can be obtained

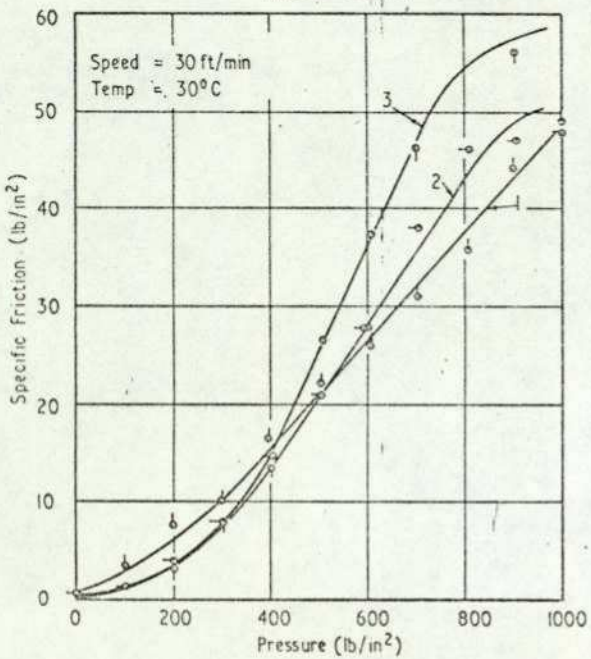
4.3. DISCUSSION

The film thickness profiles that were measured during this part of the test program differed considerably from those envisaged by early workers in this field and are notable for the wide variation in the profile, particularly for the outstroke. There is also considerable difference between the profiles for the two strokes, the instroke film profile being generally of a thin parallel nature apparently operating under boundary lubrication conditions, whilst the outsroke film profiles show considerable variation from an almost parallel film to a profile having a thick film over most of the contact with a pronounced 'nip' near the atmospheric side of the seal. This is a profile typical of elastohydrodynamic lubrication.

The effect of sliding speed and pressure on the film profile is complex, particularly for the outsrokes. The instroke film profiles behaved more consistently and in general decreased rapidly with increase in the sealed pressure. For pressures greater than 500 lb_f/in^2 the film was less than 10 micro inches thick and the seal could be considered to be operating in the boundary lubrication regime. An increase in speed, as expected, resulted in an increase in the instroke film thickness. This behaviour suggested that the seal was operating under hydrodynamic lubrication



(a) Outstroke.



(b) Instroke.

Fig. 4.59. Specific friction against pressure for a test program repeated at intervals of 12 and 18 days. The order of test is as shown by the numbers 1, 2 and 3. ($T = 30^{\circ}C$). Series 4.

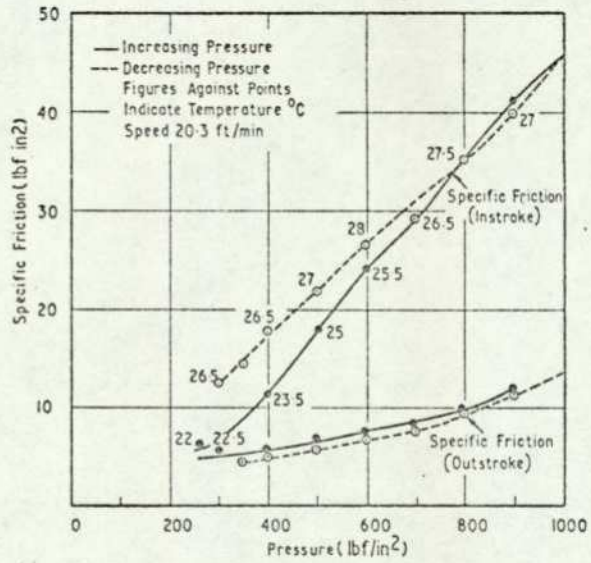


Fig. 4.58. The effect of increasing and decreasing the sealed pressure on the specific friction: Series 4.

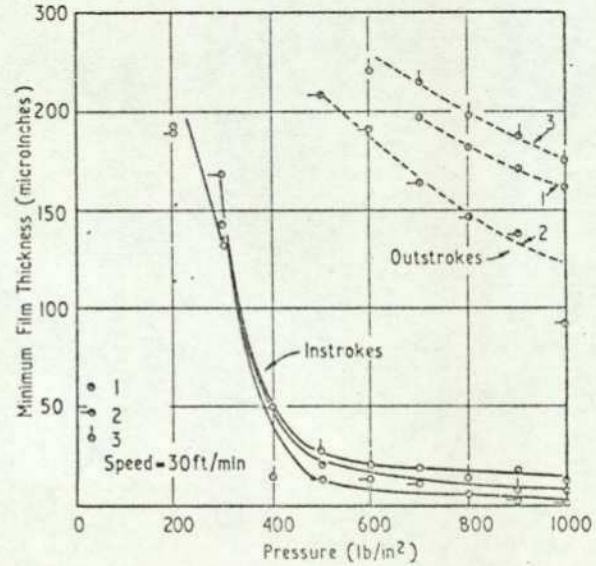


Fig. 4.60. Minimum film thickness against pressure for a test program repeated at intervals of 12 and 18 days. The order of test is as shown by the numbers 1, 2 and 3. ($T = 30^{\circ}C$). Series 4.

conditions. The outstroke behaviour was generally variable from seal to seal although in general an increase in speed tended to increase the film. The behaviour with respect to press ure was unexpected in that many tests indicated that the film over the majority of the contact increased with pressure whilst the minimum film thickness remained the same. The film thickness h* would, from the form of the pressure profile, be expected to be in the region of the contact in which the film increased with sealed pressure and therefore the leakage of the seal on the outstroke would increase with pressure.

At first the behaviour of the outstroke film profile appears to be very confusing, but in view of the interferometric and theoretical studies three possible lubrication regimes appear to exist.

(i) a boundary regime where the film is very thin, that is less than 10 micro inches, and parallel.

(ii) a hydrodynamic regime in which the film takes a tapered form, decreasing towards the atmospheric edge of the seal. In this form the hydrodynamic component of the film pressure is dominant.

(iii) A hydrostatic regime in which the seal forms a film having a thick parallel section with a pronounced 'nip' at the atmospheric edge of the seal. In this regime the hydrostatic component of the film pressure is dominant.

Between each regime is a transition region in which the lubrication modes on either side can exist. This region is not fixed in width, but the general concept is of a gradual change between each mode of lubrication. Figure 4.61 indicates the three regions proposed, with the shape of the film profile expected in each. The transition bands are drawn as broad bands at present as the factors affecting the limits of the bands are not yet fully understood.

Film profiles measured on one particular seal in Series 2 can be used to illustrate the seal behaviour proposed in figure 4.61 . The film profiles of figure 4.62(a) are for a range of speeds at a constant sealed pressure of 500 lb_f/in^2 and all are of the tapered profile form, expected in the hydrodynamic region of figure 4.61. The seal therefore moves along a horizontal line below the band B D in figure 4.61. Increasing the pressure

1000 lb_f/in^2, figure 4.62(b) results in moving this horizontal line up to a point above BD. Here the seal profile begins in the boundary region and moves directly into the hydrostatic region and there appears to be no purely hydrodynamic film profile. In figure 4.62(c) the seal profiles for a range of pressure at a constant speed of 40 ft/min. are shown. These again begin in the boundary region, but move vertically, passing through the first transition band into the hydrodynamic region, through the second transition band and finally into the hydrostatic region.

In practice the width of the transition regions may be variable and could reduce to zero in which case an unstable film could occur. This was in fact observed and recorded on two occasions. In Series 5 the film was seen to change from a hydrodynamic to a hydrostatic form at a constant pressure and speed. The film profiles are shown in figure 4.20. In the second case the film appeared to oscillate between the boundary and hydrostatic regions at a low constant speed of approximately 10 ft/min. and these are illustrated in figure 4.16.

It seems likely, in the light of the present results, that the boundaries of the transition bands are determined by the seal/groove geometry and the seal contact stress distribution and under certain conditions the width of the band reduces to zero, In general however the recorded behaviour of the seals appears to suggest that the transition will be more gradual, the limits being defined by as yet uncontrolled variables

Throughout the tests the friction of the seals has been of the same order as previously measured by other workers, but the present results have an increased values as the friction has been recorded separately for each stroke and can be correlated to the measured film thickness. The results have shown a wide difference between the two strokes, the instroke friction being much higher than that of the outstroke. In view of this, many results published previously as a mean friction of the two strokes should be used with caution where the seal friction is of vital importance.

In comparing the measured values of friction with a theoretical value based on the measured film thickness, a large discrepancy was found, the measured value being an order of magnitude or more greater than

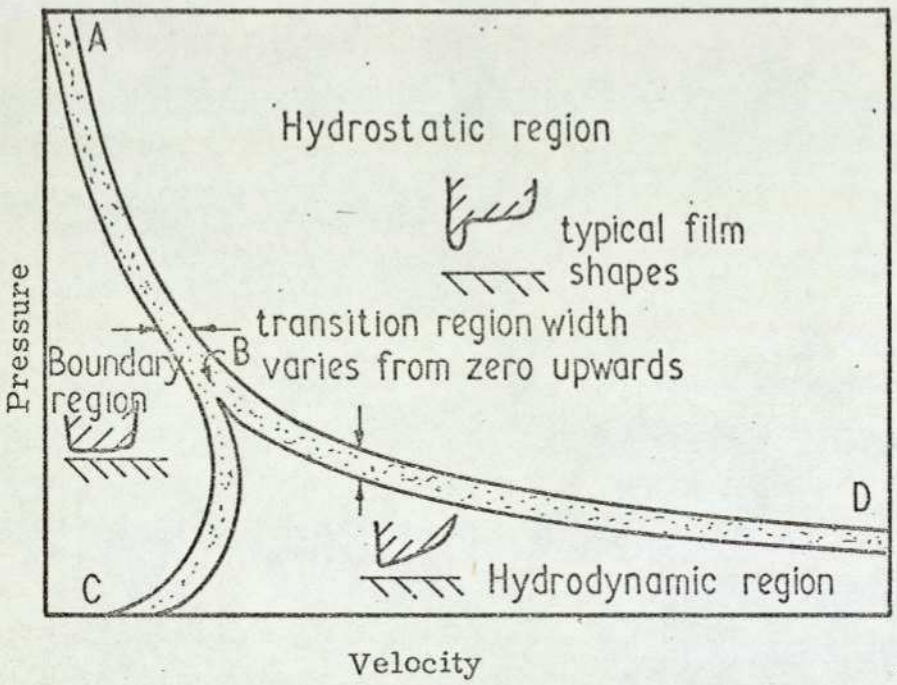
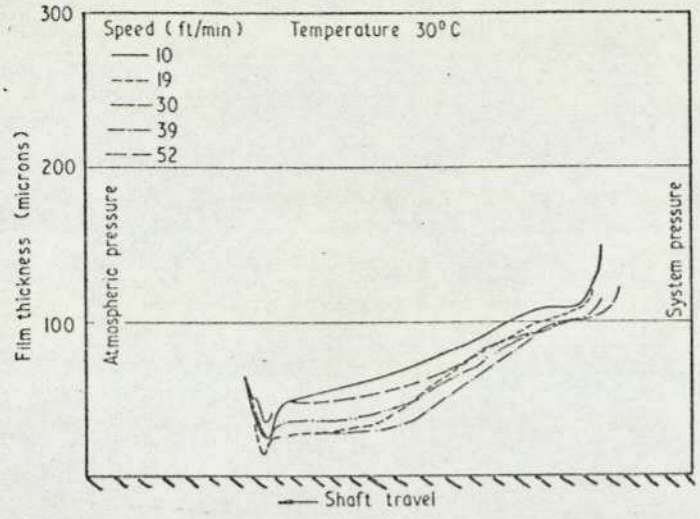
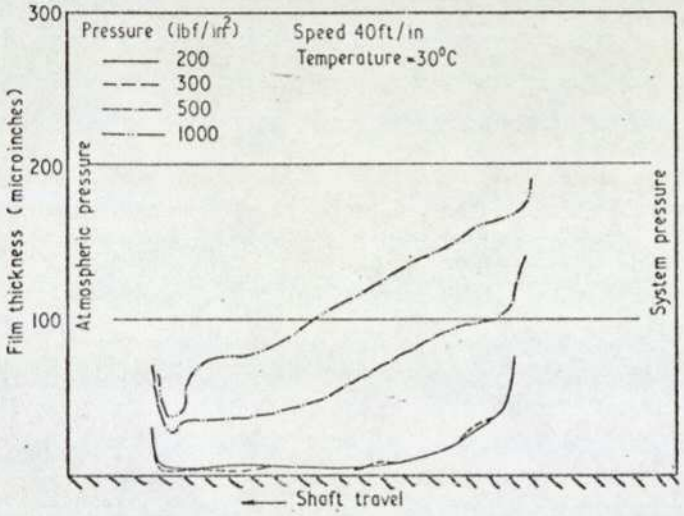


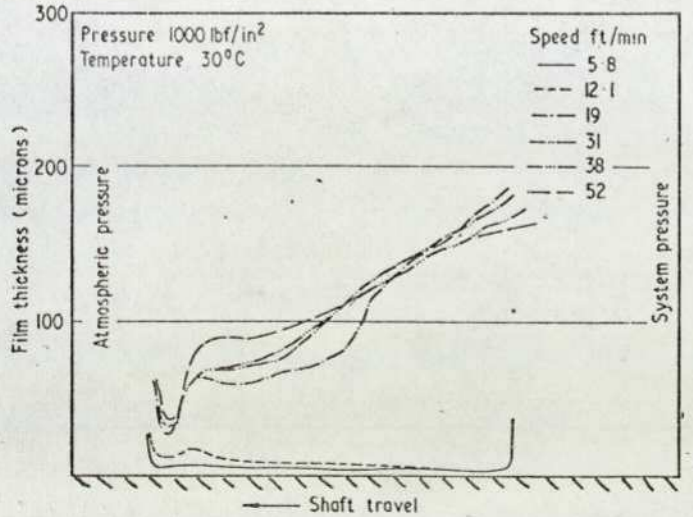
Fig. 4.61 P.V. diagram showing the three lubrication regimes occurring for seal outstrokes.



(a)



(b)



(c)

Fig. 4.62. Examples of film profiles exhibiting behaviour explainable by the P. V. diagram of figure 4.61.

expected theoretically. Qualitatively however the friction values were related to measured film thickness in that a thin or thick film resulted in a high or low friction respectively.

The leakage of the test seal was only measured in a few instances because of the considerable time involved in collecting a measurable amount of fluid, particularly where the leakage rate was very low. It was also felt that seal friction data for each stroke would be of more value than the net leakage for the present study. In view of the poor repeatability of the film thickness measurements from day to day it is perhaps fortunate that friction measurements were considered more important. It is obviously of considerable importance to measure leakage but at present there is no practical method whereby the leakage can be quickly measured for each separate stroke which is essential if the results are to be related to measurements of film thickness. The leakage rates obtained are therefore of necessity the net leakage measured over many complete cycles and as such can be related to the measurements of other workers.

In the present tests a relationship between leakage rate and speed of:

$$q \propto U^{0.75} \qquad (4.34)$$

was obtained which is at variance with all other relationships shown in Section 2.9 of the literature survey. However the leakage of a particular seal will depend on many factors, some of which will not be directly related to the seal. For instance whether the jack operates vertically upwards, downwards or horizontally or whether the rod is extended for a long period of time will all affect the leakage. In addition, the geometrical configuration of the seal and housing will considerably affect the performance of the seal. This is clearly shown in the work on interseal pressure by Field and Nau (19, 20, 21) in which it is shown that a seal can pump oil from atmospheric pressure up to at least 6500 lb_f/in^2, under continuous cycling conditions. Therefore although the usually accepted relationship between leakage rate and speed is:

$$q \propto U^2 \qquad (4.35)$$

it may not apply for seals tested in different conditions, and in general the leakage of a particular seal will not be predictable.

The measurements of film thickness and friction through the stroke length have shown that film thickness variation caused by the change in direction at the end of each stroke are propogated through the film at half the speed of the seal or the shaft. Operation of the seal with stroke lengths of less than two seal contact widths will not allow an hydrodynamic filmto form right across the contact and rapid seal failure may result. Failure of the seal could occur very quickly where a seal, previously unexposed to a fluid of high swell properties, was used almost immediately under such conditions.

Of the five common seal variables tested all have affected the film thickness and profile although the most significant was the seal interference stress which is discussed in detail in Chapter 6. The other variables had less effect.

An increase in viscosity resulted in an increase in the film thickness which was more pronounced on the instrokes where Couette flow opposes the Poiseuille flow.

In general a softer rubber would be expected to result in a thicker film although under conditions of equal contact stress with all hardnesses of material the film thickness would not be affected to the extent found in the present tests.

The back-up clearance affected the film thickness and an increase in this variable increased the film thickness. This was probably due to the degree of seal extrusion, which would increase with back-up clearance, modifying the pressure distribution throughout the contact.

The seal edge form appears to affect the film only slightly, but in general the results were the opposite of that found in the interferometric study, that is the square edged seals resulted in a thicker film than those having the round edges. An explanation possibly lies in the relative values of film thickness. During the interferometric study the speeds and hence the films were much thinner than in the seal study. Also the square edge specimens never formed a film at all and in these conditions the seal edge is of considerable importance. However the reciprocating seals all operated with much thicker films particularly on the outstrokes and the seal edge in this case would be of less importance. This would be particularly so once the film had formed. Further, the low pressure

edge of the seal is considerably modified in practice by the extrusion into the back-up clearance and this in fact creates a good inlet condition for the instroke if the seal has a square edge. In this situation the observed result would be expected. It was unexpectedly found that both seal edges affect the film profile to some extent, possibly through the form of the pressure profile. As the net leakage is the result of outstroke leakage less instroke leakage it is important to minimise the outstroke film thickness but obtain the maximum instroke film thickness. In the present tests these film thickness conditions were obtained for a seal having a round edge on the high pressure side of the seal and a square edge on the atmospheric side.

The repeatability of the results is discussed in Chapter 6.

CHAPTER FIVE

A THEORETICAL APPROACH

5.1. INTRODUCTION

The object of conducting a theoretical analysis of a reciprocating rubber seal is to be able to predict the seal's behaviour, in particular leakage rates and friction and also to obtain an insight into the operating condition likely to lead to early failure of the seal by reason of inadequate lubrication. Once a proven theoretical evaluation is available it is relatively easy to examine a wide range of operating variables over the range of practical interest. It is also less costly than experimental evaluation. Also, of course, a true understanding of the operation of a seal could possibly lead to improved seal designs and operating conditions.

A basic assumption necessary for such a theoretical evaluation is that the seal operates hydrodynamically. The experimental results have indicated that although the measured film thickness values suggest hydrodynamic lubrication for outstrokes, the instrokes operate in most cases with a very thin film and the lubrication mode is possibly boundary. In addition the measurements of friction suggest boundary lubrication for both strokes, the measured frictions being considerably higher than expected theoretically from the measured film profiles, and reducing with increased speed, whereas an increase would be expected theoretically.

It is also necessary, if not essential, in order that improved design procedures can be suggested, that the results of both experiment and theory agree within the limits of an acceptable error. The experimental program has brought to light many phenomena which as yet are not fully understood, and the conclusion reached must be that variables which are unknown at present affect the performance of the seal. These obviously cannot be included in any theoretical program, and therefore any theory proposed at the present state of the art cannot be fully embracing, but can however provide a basic understanding of the problem. Once this is achieved, further variables can, as they become known, be incorporated into the theoretical solution.

5.1.1. The 'inverse' form of Reynold's equation

For rigid bearing surfaces, such as those forming thrust or journal bearings, the geometry of the film profile is fixed, and, in the

simplest case the pressure distribution and load bearing capabilities of the bearing can be calculated using the following one dimensional form of Reynold' s lubrication equation:

$$\frac{dp}{dx} = 6\zeta U \left\{\frac{h - h^*}{h}\right\} \qquad (5.1)$$

Susbstituting for h in terms of x, the distance across the seal, allows direct integration of the equation for p., providing the relationship between h and x is simple. However, even for relatively simple geometries, an analytical integration of the equation becomes extremely cumbersome and for elastohydrodynamic lubrication contacts the film profile is exceedingly complex making an analytical solution impossible

For elastohydrodynamic contacts, such as occur in gear teeth, or ballbearings the film thickness under operating conditions is extremely thin, of the order of a few micro in ches and the pressure in the fluid film under dynamic conditions can be taken to be almost identical to that under static conditions. Further, the shape of the majority of such contacts can be reduced to that of a cylinder in contact with a flat plane for which the contact stress distribution can be calculated from the well known Hertz formula.

Thus a situation is formed which is the reverse of the 'classical' problem, that is the pressure profile is known and we require to calculate the film thickness. This is the' inverse' solution to Reynold's equation and requires the solution of the cubic equation.

$$GH^3 - H + 1 = 0 \qquad (5.2)$$

which is derived in Appendix I.

In general a unique solution is not possible as h*, the film thickness where the pressure gradient is zero, is unknown. However it is possible to obtain the shape of the film profile if the pressure profile is known. This has been evaluated for several assumed seal pressure profiles in the following section and indicates film profiles very similar in shape to thoseactually measured in Chapter 4.

5.1.2. Solution of the EHL problem

For contacts in which the deflection of the bearing or lubricated surfaces is significant, the solution of Reynold's equation alone is not sufficient to obtain a unique solution. There also has to be a simultaneous solution of the elasticity equation governing the deflections of the lubricated surfaces.

Several alternative methods of successive approximation could be used for this, but some are generally unsuitable. Figure 5.1(a) shows a scheme which has been used successfully for 'hard' EHL contacts such as those formed by gear teeth or ball bearings. In this method an initial pressure profile is assumed and the film shape determined using the 'inverse' solution of Reynold's equation. The seal deflections are then calculated using the elasticity equation. If the film shape and the seal deflections are not in agreement the pressure profile must be revised and the procedure repeated. The main disadvantage of the method lies in the need to revise the pressure profile each time and makes the method difficult to automate.

An identical scheme is shown in fig. 5·1(b) except that the film profile is used as initial data, but the method is generally unsatisfactory because small errors in the film thickness appear as magnified errors in the pressure profile and successive iteration rapidly diverge from the require solution.

In the final scheme of figure 5·1(c), the film profile or the pressure profile can be used as initial data but generally the pressure profile is preferred. The main advantage of this method of solution is that automatic iteration of the equations is achieved without the need to revise the pressure of the film profile at each iteration. This method was used successfully in the present study to calculate the film profile under a reciprocating seal and is described in more detail in Section 5.3.

5.1.3. The stress balance in the seal

In operation the experimental work has indicated that a stable fluid film would be expected to form between the seal and the sliding surface, providing the speed was constant. In this condition the stresses in the seal must be balanced by the pressure in the fluid film.

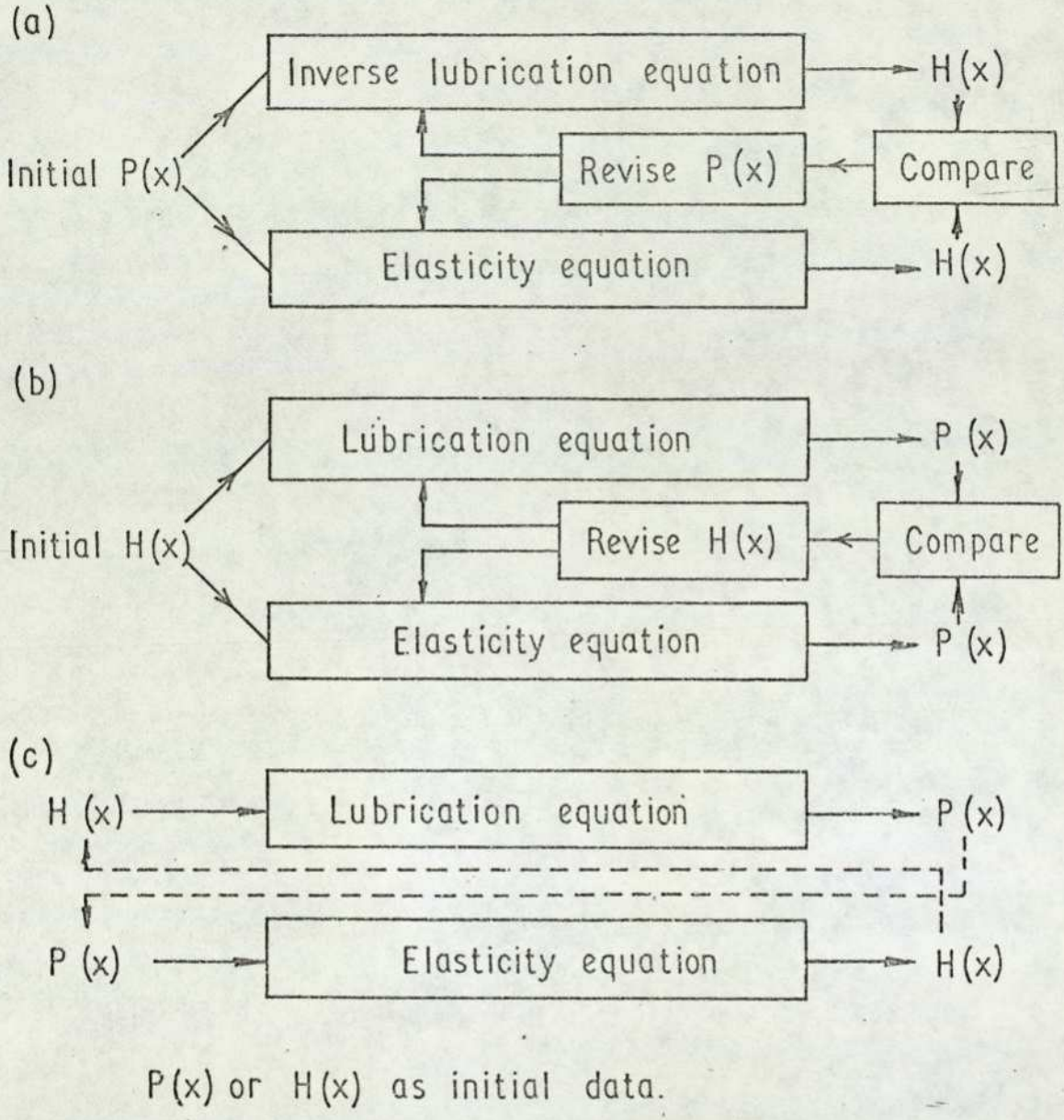


Fig. 5.1. Schemes for the simultaneous solution of Reynold's equation and the elasticity equation.

The contact stresses in the surface of the seal are formed in three ways:

(i) The seal is initially an interference fit on the shaft, that is the radial thickness of the seal is greater than the radial depth of the groove into which it is fitted. This creates an interference stress, Q_i.

(ii) The seal material has a Poisson ratio of almost 0.5 and therefore transmits the sealed pressure as if the rubber were a fluid. The sealed pressure therefore also acts to some extent in a radial direction. This is obviously not true at the low pressure edge of the seal because here the contact stress must be zero. There is therefore an unknown stress distribution in the seal due to the sealed pressure, Q_s.

(iii) In addition, during operation the seal is deflected slightly to allow a fluid film between the seal surface and the sliding surface. This creates an additional stress in the seal, S.

The pressure in the fluid film is created in two ways:

(i) the hydrodynamic pressure developed due to the relative motion of the seal and its mating surface, P_d

(ii) the hydrostatic pressure created by the pressure differential across the seal, P_{st}

For a stable fluid film all the above stresses must be balanced by the pressures, thus:

$$Q_i + Q_s + S = P_d + P_{st} \qquad (5.3)$$

In the theoretical analysis the seal stresses, Q_i and Q_s are combined in the stress Q, the stress S is referred to as S and the pressures P_d and P_{st} are calculated as a combined pressure P unless specifically referred to as hydrodynamic or hydrostatic components.

5.1.4. Seal types

Two types of seal occur in hydraulic jacks, the piston seal in which the outside diameter of the seal is the sliding contact and rod seals sealing the pressurised fluid from atmosphere, here the sealing surface is the inside diameter of the seal. In similar situations both are expected to lead to similar results and in general the theoretical analysis is related to rod seals.

5.2. Derivation of Seal profiles using the 'Inverse' form of Reynold's equation.

The 'inverse' approach to the derivation of seal profiles is based on the fact that the form of the pressure profile in the seal is known generally from the experimental program. Slight changes to this, in combination with the 'inverse' solution to Reynold's equation can reveal, qualitatively at least, the seal film profile and the range of profiles possible.

The graphical solution to the inverse equation is shown in figure 5·2 for both positive and negative values of $H, (= h/h^*)$ the negative portion being required for the monotonic pressure profiles which may occur with seals.

The analysis is divided into two parts, covering the outstrokes and the instrokes.

The outstrokes

The notation and axes are as shown in figure 5·12 The leakage of such a seal can be written as:

$$q = \frac{-h^3}{12\zeta}\frac{dp}{dx} + \frac{Uh}{2} \qquad (5.4)$$

indicating that both Poiseuille and Couette leakage must be positive, that is from the high pressure to the low pressure.

Also the film thickness, h, must for physical reasons always be positive, and as the leakage can be calculated from:

$$q = \tfrac{1}{2} U h^* \qquad (5.5.)$$

in which both q and U are positive, h^* must also be positive, and the film profile under these conditions must be determined from the positive H part of the graph of figure 5·2. There must therefore be a pressure maximum in the pressure profile and the film thickness h^* exists in the length of the seal contact.

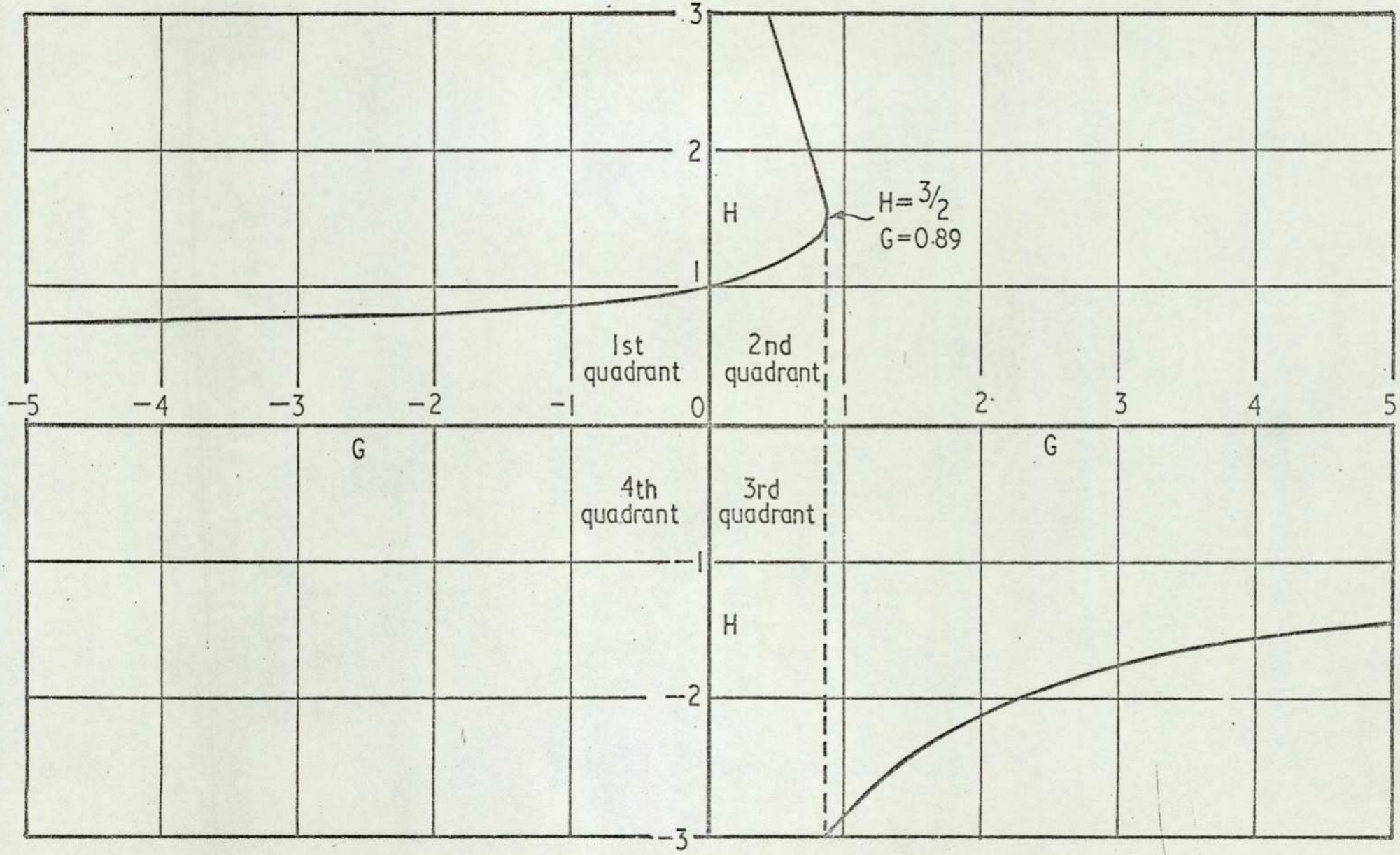


Fig. 5.2. Graphical solution to the 'inverse' form of Reynold's equation.

The instrokes

The leakage of a seal for an instroke can be written:

$$q = \frac{-h^3}{12\zeta}\frac{dp}{dx} - \frac{Uh}{2} \qquad (5.6)$$

and the Poiseuille and Couette flow terms have opposite signs. This results in two possible types of leakage.

(i) Negative leakage: In this case the Couette flow is greater than the Poiseuille flow and the net leakage from low to high pressure. This phenomena is known to occur occasionally in seal applications (19, 20, 21), and arises where the value h is very small. For typical seal properties this is around 100 micro inches.

(ii) Positive leakage: here Poiseuille flow predominates and leakage is from high to low pressure as expected.

Analysis of these two conditions is given below:

(i) Negative leakage (from low to high pressure)

In this case both q and U are negative, and substitution in equation 5.5 shows that h* must be positive, again resulting in a positive value of H and the instroke seal profile for a seal having negative leakage must also be determined from the top half of the graph of figure 5.2.

A negative leakage such as this infers that the negative shear flow caused by the negative velocity must exceed the positive pressure flow. A limit will however be reached when shear flow equals pressure flow; that is from equation 5.6: $h_{max} = (6\zeta U/dp/dx)^{0.5}$ (5.7)

At values of film thickness greater than this the net flow becomes positive.

(ii) Positive leakage (from high to low pressure)

The shear flow equation 5.5 for this case indicates that h* must be negative:

$+q = \frac{1}{2}(-U)(-h^*)$

Because h* is the film thickness where the pressure gradient is zero, there can be no pressure maximum in the pressure profile of the seal and hence h* does not occur in the seal contact. The pressure profile

is therefore monotonic.

H is therefore negative and the film profile is determined from the lower part of the graph of figure 5.2.

The above results can be summarised in the form of a table.

TABLE 5.1

Term	Outstroke	Instroke	
		Case 1	Case 2
q	positive +q	negative -q	positive +q
U	positive +U	negative -U	negative -U
h^*	positive $q=\frac{1}{2}(U)(h^*)$	positive $-q=\frac{1}{2}(-U)(h^*)$	negative $q=\frac{1}{2}(-U)(-h^*)$
H	positive $H=h/h^*$	positive $H=h/h^*$	negative $-H=h/-h^*$
$dp/dx=0$	maximum in pressure profile	maximum in pressure profile	monotonic pressure profile

5.2.1. Derivation of the outstroke film profile

Central film profile

From the above table it can be seen that for all types of seal the outstroke film profile must be determined by the upper half of the graph of figure 5.2 and must of necessity include a pressure maximum in the pressure profile. If a pressure profile of this type is taken the central film shape can be determined as follows:

1. At the point where $dp/_{dx} = 0$; G = O and from figure 5.2

$$H = 1$$

$$\therefore \quad h = h^*$$

2. On the atmospheric side of this point $dp/_{dx}$ is negative and so, therefore, is G, and the film thickness is determined from the first quadrant of the figure 5.2. At the maximum value of $dp/_{dx}$, and hence the minimum value of G, the film thickness must also be a minimum.

3. On the pressurised side of the point $dp/_{dx}$ is positive and hence the film thickness is determined from the second quadrant of figure 5.2. At the point of inflexion where G has its maximum positive value of 0.89;

$$H = {}^{3}/_{2} \cdot H_{G=0}$$

$$\therefore \quad h = {}^{3}/_{2} \cdot h^{*} \qquad (5.8)$$

There are thus three values of film thickness the position of which can be determined if the pressure profile is known, to form the film profile at the centre of the seal contact, figure 5.3.

Inlet film profile

At the seal inlet edge, the pressure gradient, $dp/_{dx}$ must be zero, but between this point and the point where G has its maximum value of 8/9 a number of pressure profiles are possible, which can significantly effect the form of the film profile. Four of these are given in the following section.

(i) The film thickness decreases again to h* and $dp/_{dx}$ is zero at the edge of the seal. This would appear to be unlikely, figure 5.4(a).

(ii) The film thickness increases rapidly as the value of G becomes very small. At the seal edge therefore the film thickness is very large and $dp/_{dx}$ almost zero. This is shown in figure 5.4(a)

(iii) The pressure profile could undulate and form a 'nip' at the high pressure end of the seal. This is illustrated in 5.4(b) showing the double 'nip' film profile occasionally obtained experimentally in Chapter 4.

Points A and B are points of inflexion in the pressure profile and the value of G at these points could be between 0 and 0.89, and the film thickness must be between h* and 3/2·h*

Whilst at point C the value of G must be a maximum, it is possible that G is also a maximum at points A and B, resulting in a film shape of figure 5.4(c)

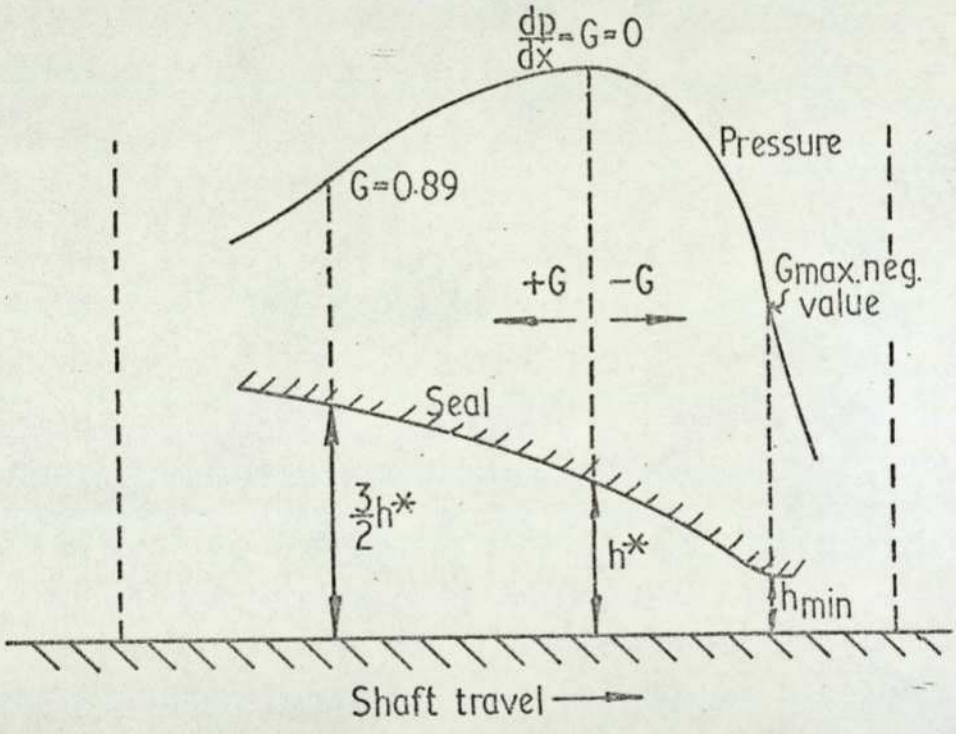
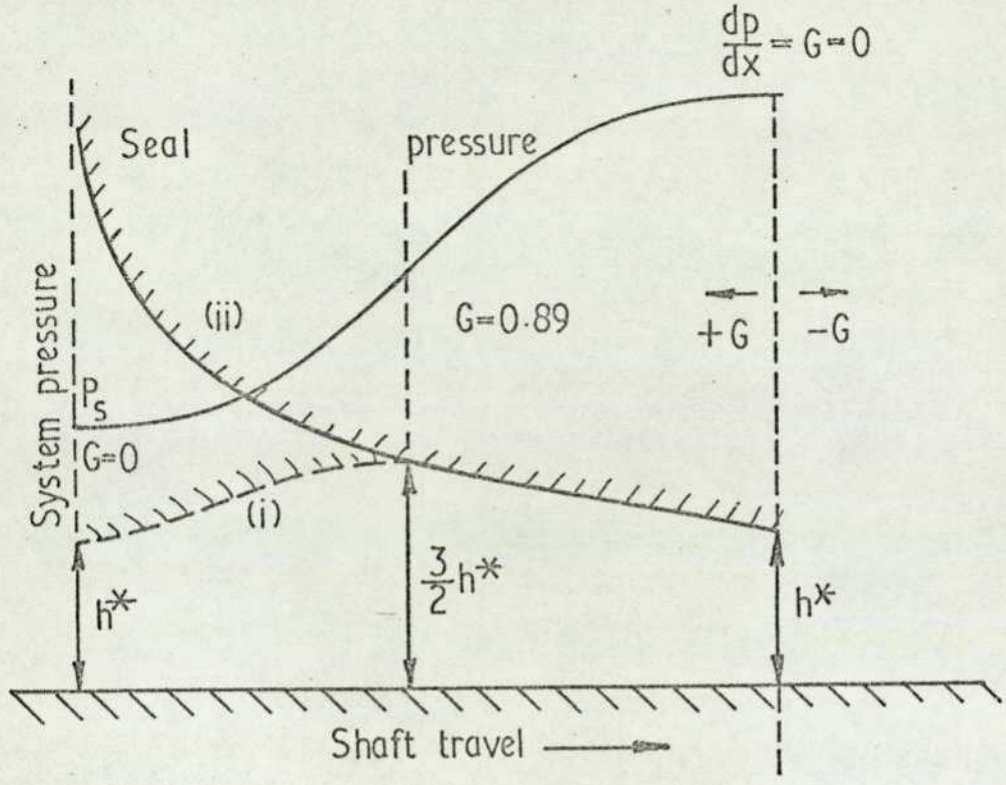
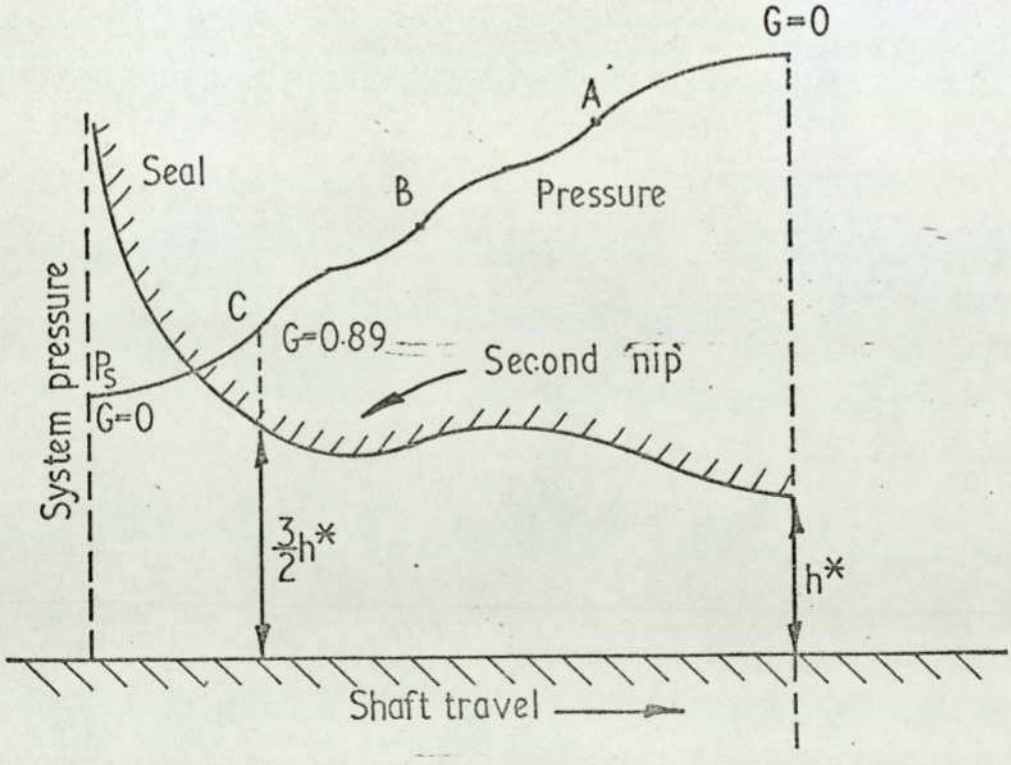


Fig. 5. 3. Derivation of the central film profile for an outstroke.

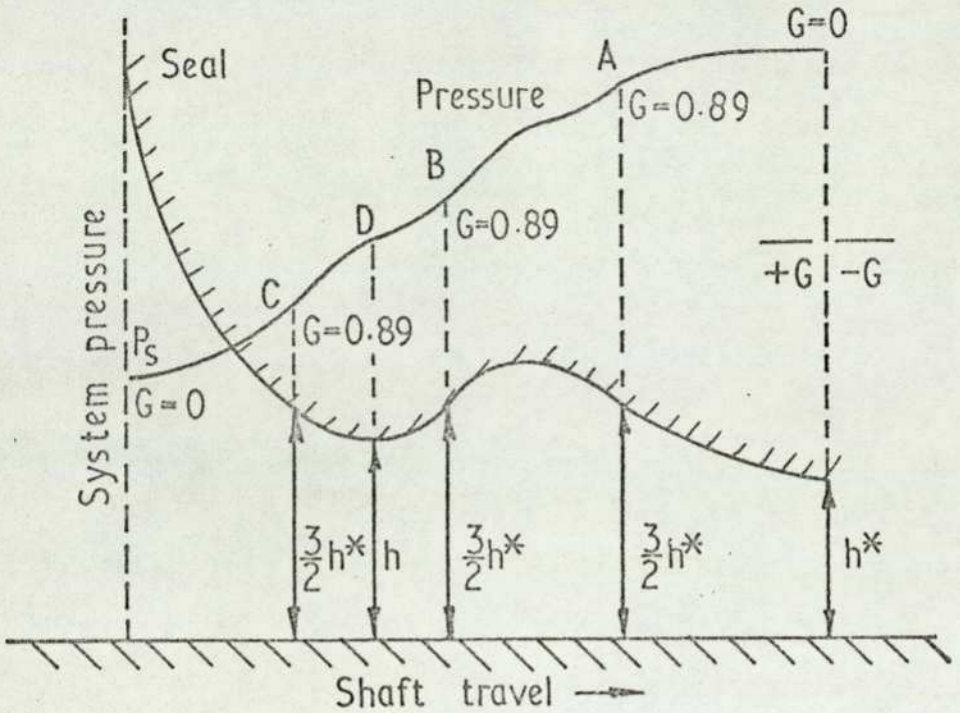


(a)

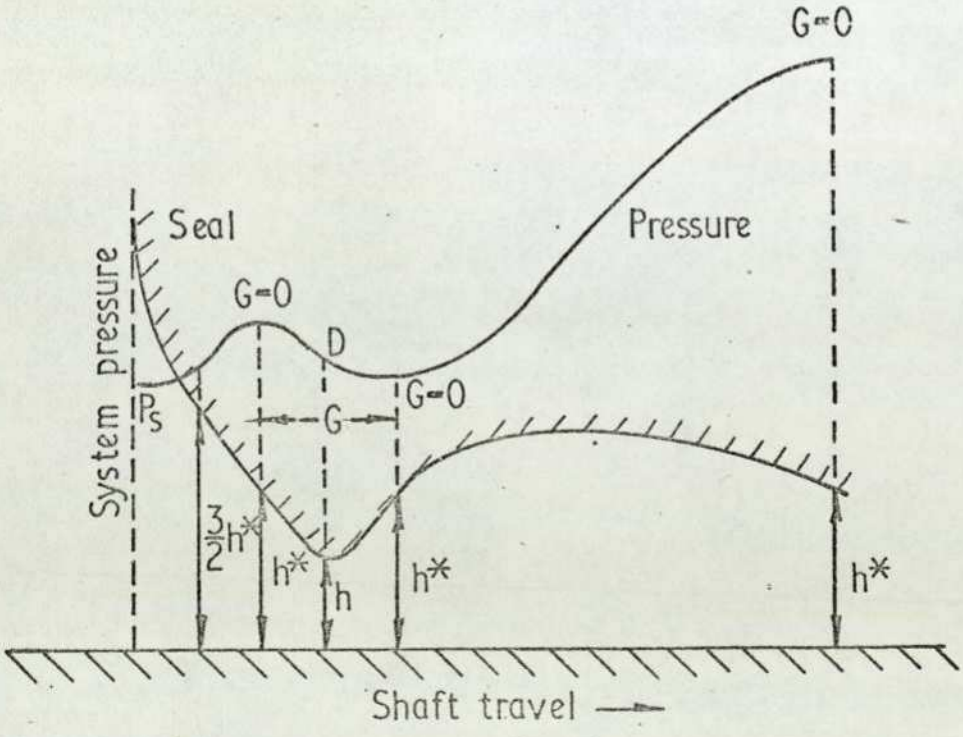


(b)

Fig. 5.4. Derivation of the inlet film profile for an outstroke.



(c)



(d)

Fig. 5.4. Derivation of the inlet film profile for an outstroke.

(iv) A similar film shape to (iii) would occur for a pressure profile of figure 5.4(d)

The film profiles of (iii) and (iv) whilst appearing very similar in shape would result in different values of h at point D. Thus h at point D, for the pressure profile of (iii) must be between h = h* (dp/dx = 0) and h = 3/2 h*: for the pressure profile of (iv) h could take values between h = h* and h = 0 (G is negative). A determination of hat the second 'nip' could therefore indicate the form of the pressure profile.

Outlet film profile

The minimum film thickness of the seal occurs at the maximum negative slope of the pressure profile, figure 5.5.

The pressure profile at the atmospheric edge of the seal could take three possible forms:

(i) a reduction in the negative slope of $dp/_{dx}$ to a zero value at the edge of the seal. The film thickness at the seal outlet would then be h*

(ii) Because G at the point of minimum film thickness is negative the value of G must become positive at some point in order for the film thickness to exceed h* at this exit. The pressure profile must therefore pass through a minimum where G = O.

(iii) In order that the film thickness can increase to infinity at the seal exit, G must attain a maximum positive value at a point after the minimum, the gradient then decreasing to almost zero at the exit. This pressure profile would occur in practice and infers that there may be a cavitation region at the exit of the seal.

General film profiles

From the foregoing three sections two generalised film shapes seem probable:

1. A film shape having a single 'nip' with a minimum film thickness at the point where the pressure gradient has its largest negative value.

2. A film shape having two or more undulations, one of which has a minimum film thickness value.

These two forms and the pressure profiles are shown in figures 5.6 and 5.7.

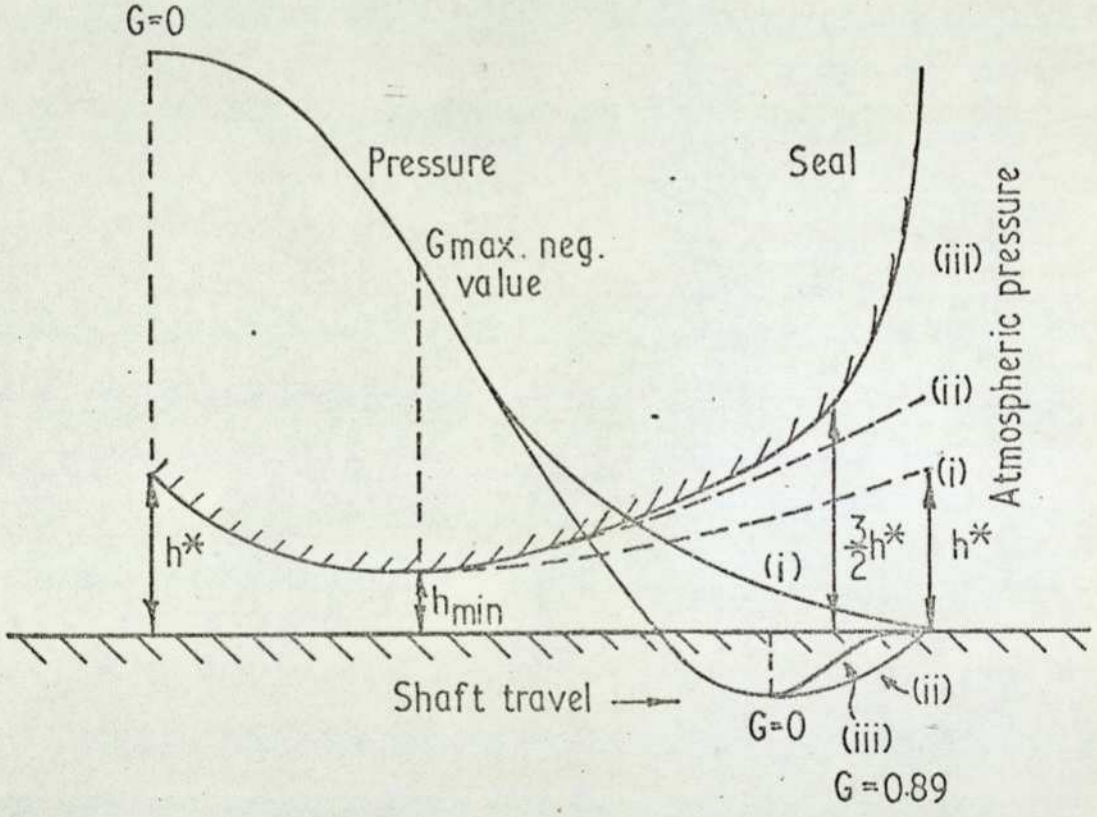


Fig. 5.5. Derivation of the outlet film profile for an outstroke.

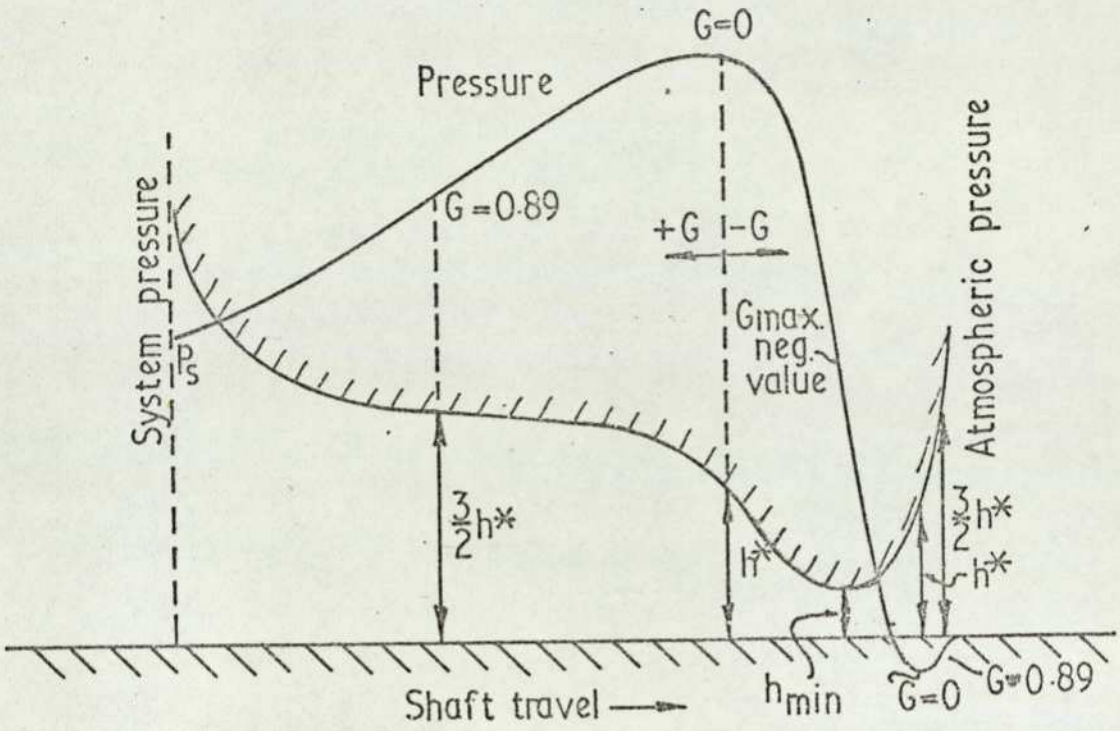


Fig. 5.6. General film profile - single 'nip' - outstroke.

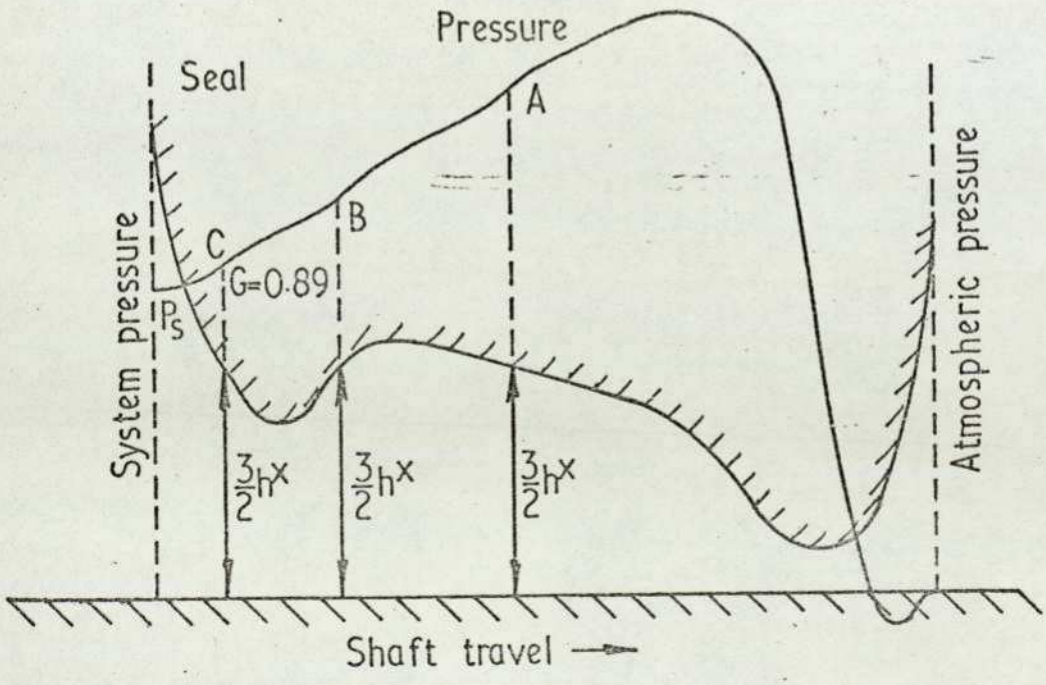


Fig. 5.7. General film profile - double 'nip' - outstroke.

The film profile further depends considerably on the positions of the various predetermined values of G in the pressure profile.

Examples of the effect of the positions of these factors on the film profile are shown in figure 5.8.

5.2.2. Determination of the instroke film profile

From Table 5.1. it can be seen that the instroke film profile can be determined for positive leakage or negative leakage, depending on whether pressure flow is greater than shear flow or not.

Negative leakage - central film profile

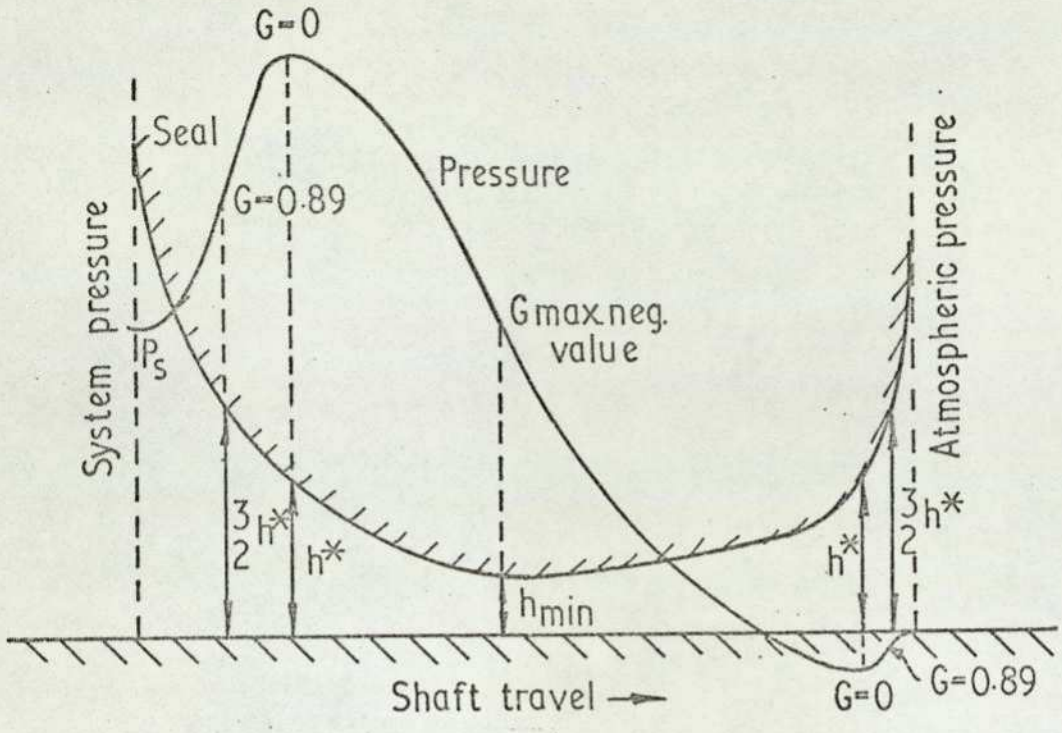
The case of negative seal leakage entails that there is a pressure maximum somewhere in the pressure profile of the seal, the position of which is generally unknown. However because the velocity of the shaft is now negative G assumes the opposite sign to that obtained on the outstroke. This is illustrated in figure 5.9

As for the instroke the positions of film thickness h*, 3/2h* and hmin. can be determined from the pressure profile as shown in figure 5.9.

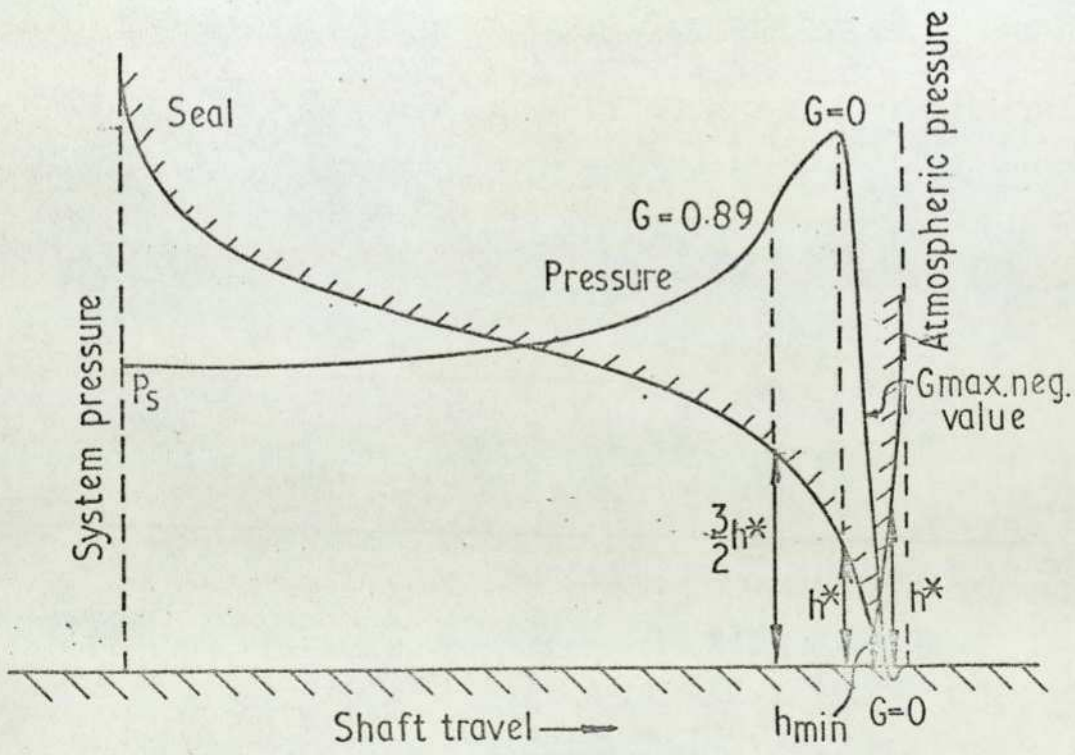
Inlet film profile

For the instroke the inlet profile is the atmospheric edge of the seal and cavitation at this point for the instroke is unlikely. The pressure gradient can therefore decrease towards zero as the film thickness increases in the second quadrant of figure 5.2. The film profile is shown in figure 5.9

In a similar way to the outstroke a 'nip' could be formed at the inlet to the seal figure 5.4.



(a)



(b)

Fig. 5.8. General film profiles showing the effect of the positions of the predetermined values of G.

Outlet film profile

For a pressure gradient decreasing to a value of zero at the pressurised end of the seal, the resulting film profile would be that of (i), figure 5.10. A more likely form however would be similar to the outlet profile of the outstrokeof figure 5.5., in which a pressure less than the system pressure is generated hydrodynamically at the outlet region. Because of the high system pressure cavitation would be unlikely and the film profile would be that of (ii), figure 5.10.

General film profile

From the foregoing sections a general film profile can be formed figure 5.11a. It can be seen that as for outstrokes a multiplicity of seal profiles can be derived from the pressure profiles, by positioning the particular values of G at different places, but the general shape for instrokes will remain the same, that is, a film which is for the most part almost parallel, with the minimum film thickness probably occurring near the middle of the seal but certainly away from the atmospheric edge of the seal. In practice it is probable that the hydrodynamic pressure generation at the inlet to the seal is extremely rapid, tending to give the more 'square' appearance to the seal profile of figure 5.11b.

Positive leakage

For this case the pressure profile is monotonic and therefore determined by the third quadrant of figure 5.2. The film profile is generally indeterminate, although measured pressure profiles for the instrokes and the outstrokes appear to be very similar.

In general, the minimum film thickness will occur at the maximum value of G, near the inlet edge of the seal, but the value of it and the rest of the film will be indeterminate.

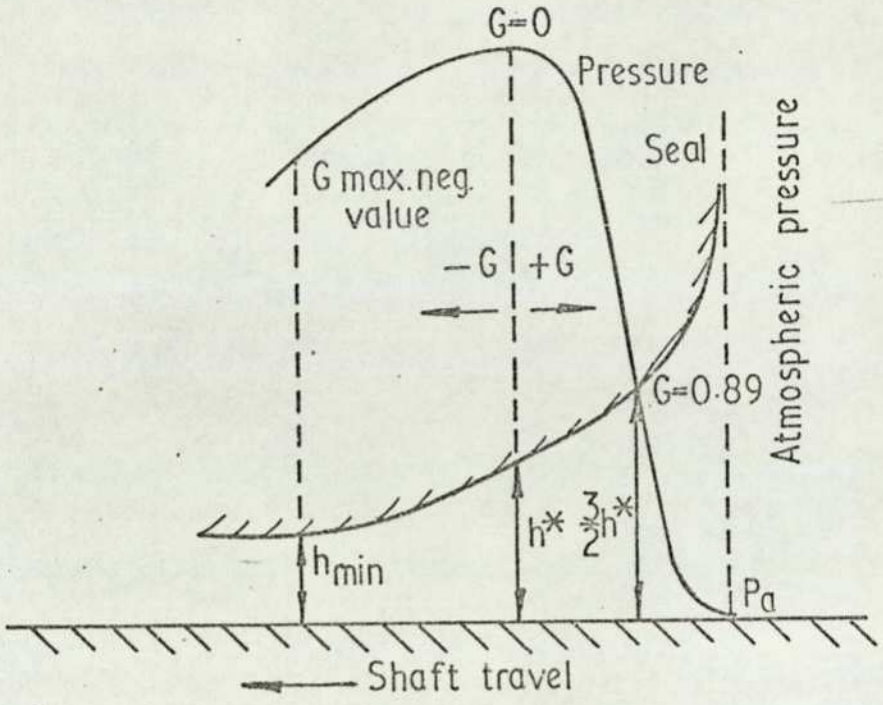


Fig. 5.9. Derivation of the central film profile for an instroke.

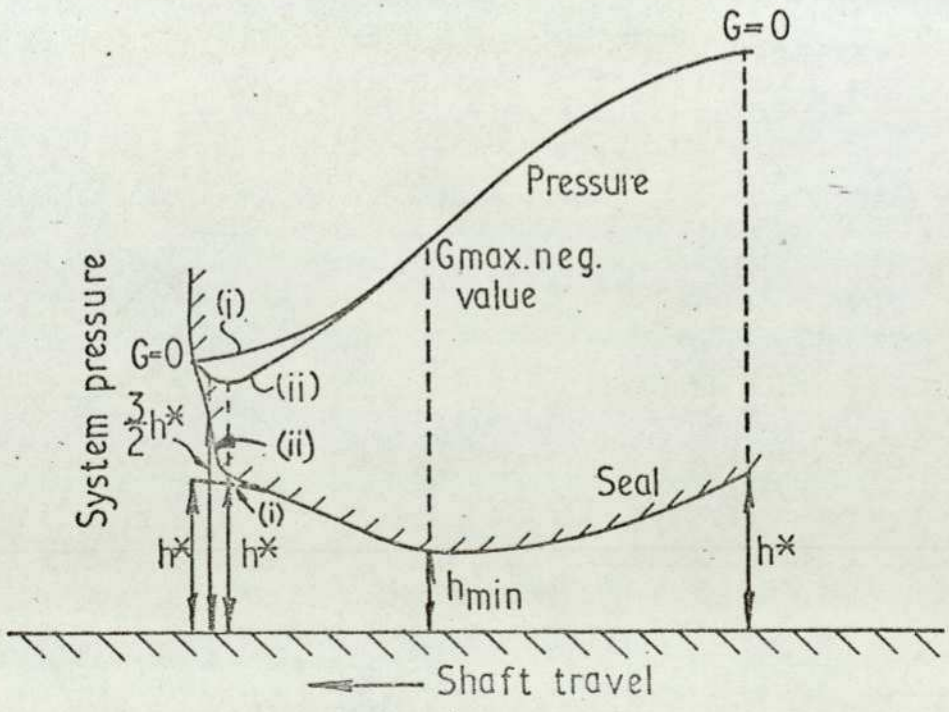
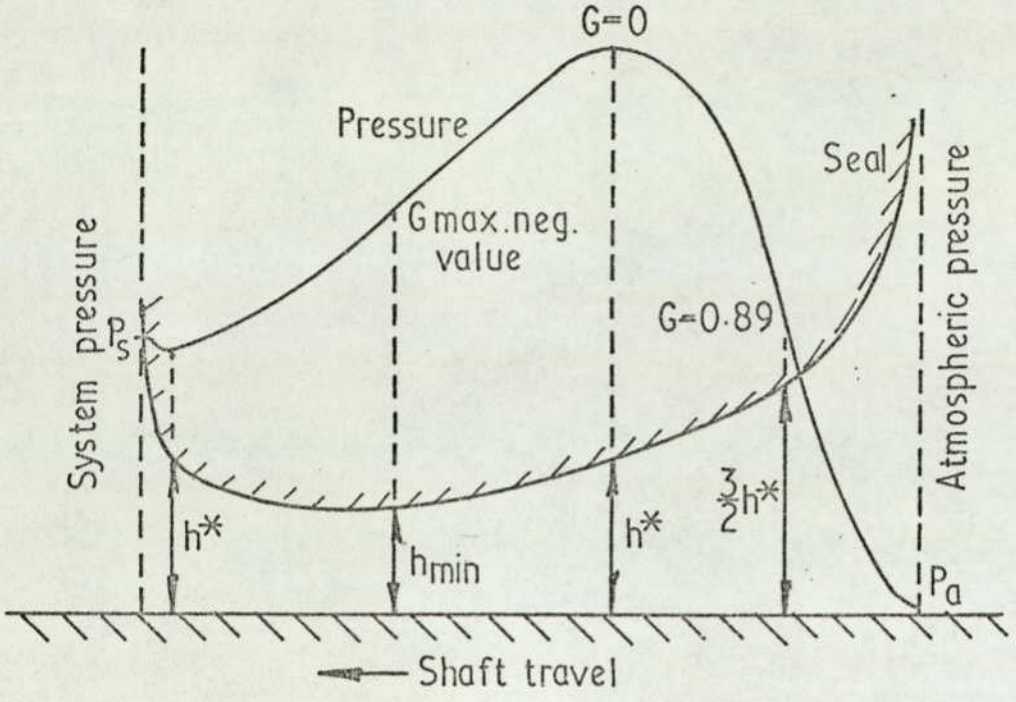
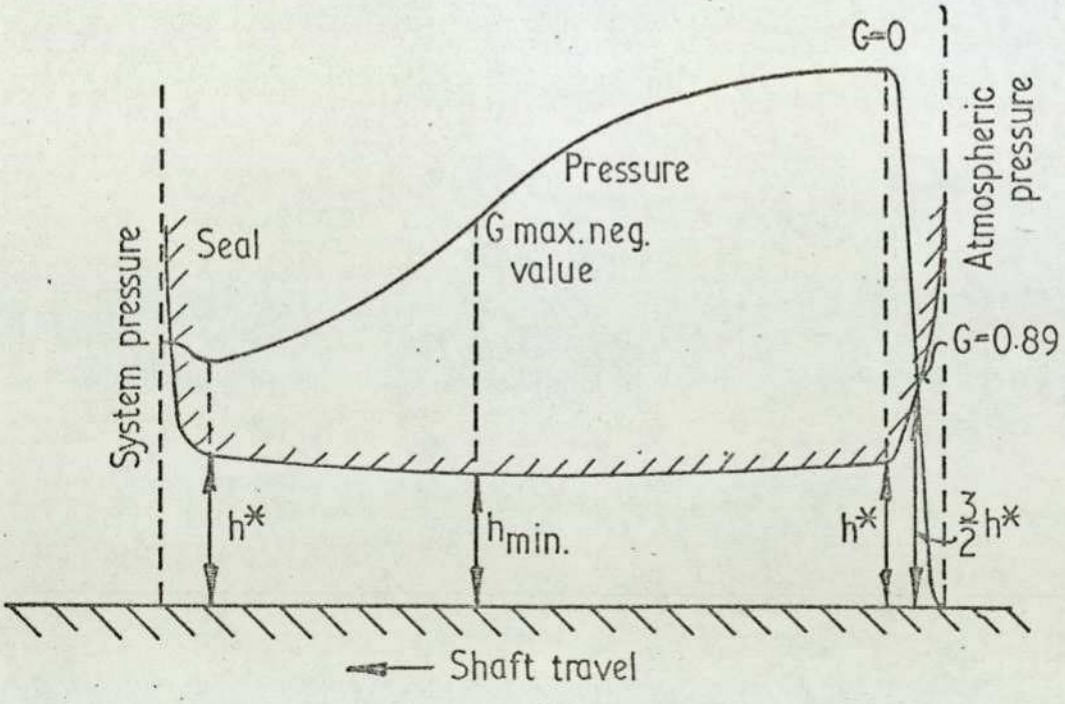


Fig. 5.10. Derivation of the outlet film profile for an instroke.



(a)



(b)

Fig. 5.11. General film profiles - negative leakage - instroke.

An approximate limit however can be derived in the following way: the leakage from the seal is positive, implying that the pressure flow must exceed the shear flow. From equation 5.6, the leakage can be written as:

$$q = \frac{-h^3}{12\zeta} \cdot \frac{dp}{dx} - \frac{Uh}{2}$$

which when equated to zero gives the limiting minimum value of the mean film thickness for those conditions, which is:

Minimum value of $h_{mean} = (6\zeta U/dp/dx)^{0.5}$

For typical values applicable to hydraulic seals this value of film thickness is approximately 100 to 300 micro inches. Below this leakage will become negative and the pressure profile must therefore assume a diatomic nature, that is a pressure maximum must exist, and the profile must revert to that suggested in figure 5.11. This implies that the film profile could have two stable shapes, one determined by the negative H part the other by the positive H part of the graph of figure 5.2.

Although the absolute values of film thickness are indeterminate for all seal profiles discussed in this section, it is possible to speculate on the relative values of the film thickness of the two profiles.

The film thickness at which the net flow is zero has been determined in Section 5.2 as:

$$h_{q=0} = (6\zeta U/dp/dx)^{0.5}$$

At the point where two stable films are possible, that is G = 0.89:

H = -3 or 3/2

The values of h can only be determined if h* is known for each film. Generally it is unknown, but for films slightly above or below $h_{q=0}$, the flow rate and hence h* can be assumed for purposes of this discussion to be the same, that is /+h*/ = /-h*/ Substitution of this value enables relative values of h to be determined:

For negative H: $h = /-3h^*/$

and for positive H values: $h = /\ 3/2h^*/$

It can be seen then that the stable film corresponding to positive values of H is half the thickness of that corresponding to negative values. This change should occur for a very small increase in pressure.

5.3. An elastohydrodynamic approach

The mathematical problem posed by a rubber seal under reciprocating motion is that of obtaining simultaneous solutions to:

(i) Reynold's lubrication equation which specifies the pressures in the lubricant film for a specified film profile and

(ii) the elasticity equation which describes the deflection of the seal surface for a given pressure at the surface.

Although the pressure developed in the film is not sufficient to cause significant changes in the fluid viscosity as is the case for 'hard' contacts the seal problem is complicated by the various stresses arising in the seal itself due to the initial interference and the transmission of the sealed pressure through the seal material. There is also the stress caused by the deflection of the seal surface but this is automatically taken into account by the elasticity equation. The main difficulty is in determining the stresses in the seal due to the interference and the sealed pressure.

Fisher (22) formulated an elasticity equation, which included the radial shear stresses in the seal, to enable the deflections of the seal surface to be evaluated for a given pressure at the surface. This method circumvented the problem of obtaining a complete axisymmetric solution to the elasticity equation providing the pressure in the fluid film and the radial stresses in the seal were known. At that time they were not and a solution to the problem could not be obtained.

Nau at a later date reformulated the problem using the elasticity equation of Fisher(22) and developed a computer program involving this and Reynold's equation in an attempt to obtain a solution by numerical means using an iterative technique. At this stage the present author became involved in research into the elastohydrodynamic behaviour of reciprocating seals and assisted in the further development of the program to the stage where stable solutions to the equations could be obtained.

The deflection of the seal surface is caused by the stress, S, the difference between the pressure, P, in the fluid film and the radial contact stress, Q, in the seal surface created by the interference and the sealed pressure which is transmitted through the seal, thus $S = (Q - P)$. The situation illustrated in figure 5.12. In general the quantities Q and P and hence S are unknown. However as a result of the success of the instrumentation discussed in Chapter 4, it was possible to obtain measured pressure and film

thickness profiles. This enabled the stress, S, necessary to deflect the seal the measured amount to be calculated using Hooke's Law, and this subtracted from the measured value of P gave the seal contact stress Q. This then provided at least an approximate solution which was used as input data for the theoretical evaluation of the problem.

5.3.1. Mathematical formulation of the problem

Lubrication equation

The lubrication equation is derived in Appendix J and is a standard form of the pseudo two-dimensional equation widely used in bearings. The equation is used in the form:

$$P(x) - P_1 = a_1 I_1(x) - a_2 I_2(x) \qquad (5.9.)$$

where $a_1 = 6\eta U$ and $a_2 = \left[a_1 I_1(\ell) - (P_o - P_1)\right] / I_2(\ell)$,

$$I_1(x) = \int_o^x h(x)^{-2} \cdot dx \quad \text{and} \quad I_2(x) = \int_o^x h(x)^{-3} \cdot dx$$

The boundary conditions $x = 0$, $P = P_1$; $x = 1$, $P = P_o$ are incorporated.

Elasticity equation

For the derivation of this equation it is assumed that the full axisymmetric treatment is unnecessary and can be approximated by a two-dimensional analysis as in Appendix K. It is assumed that the internal stress distribution is known at the sealing surface, the only other important internal stresses being the shear stresses and the compression stresses in the y-direction. This leads to the equation:

$$\frac{d^2h}{dx^2} - Ah = B \cdot S(x) \qquad (5.10)$$

The boundary conditions are (i) $\frac{dh}{dx} = 0$ at $x = 0$, that is, no shear stress on the inner end of the seal and (ii) $\frac{dh}{dx}$ = constant at $x = \ell$, this non-zero shear is not, in general known in practice. For much of the early work these shear boundary conditions were not actually used but values were

taken from a measured film profile obtained in the associated experimental work of Chapter 4.

Non-dimensionalisation

The following non-dimensionalisation scheme was applied to equation 5.9 and 5.10:

$$h=b\bar{H},\quad x=\ell X,\quad Q=\bar{Q}\ /(A\ell^2/E),\quad P=\bar{P}\ /(A\ell^2/E),\quad A=R/\ell^2,$$

$$L_1 = 6\zeta U\ell R/(Eb^2),\quad L_2 = \ell Ra_2/b^3E.$$

where $\bar{H}$, X, L_1, L_2, R, $\bar{P}$ and $\bar{Q}$ are dimensionless.

Equations 5.9 and 5.10 then become:

$$\bar{P}\ (X) - \bar{P}_o = L_1\ \bar{I}_1\ (X) - L_2\ \bar{I}_2\ (X) \qquad (5.11.)$$

and $$\frac{d^2}{dX^2}\bar{H} - R\,\bar{H} = S \qquad (5.12.)$$

where $\bar{I}_1\ (X) = \int_o^x \bar{H}^{-2}\ dX$ and $\bar{I}_2\ (X) = \int_o^x \bar{H}^{-3}\ dX,$

and $S = \bar{Q} - \bar{P}$

5.3.2. Numerical Solution

The solution of the overall elasto-hydrodynamic problem was carried out numerically using an ICL 1905 digital computer. For this purpose the elasticity equation was written in finite difference form and the resulting set of linear equations were solved by the Gauss-Seidel iterative method. The lubrication equation was integrated numerically.

By repeated iteration of the coupled elastic and lubrication equations it proved possible to obtain compatible solutions for the outstrokes over a range of speeds and rubber hardness. No solution was obtained for the instroke although this was attempted. In the light of experimentally obtained instroke seal film profiles it is possible that the lubrication process is somewhat different on the two strokes.

Finite difference schemes

It was expected that the seal film thickness and pressure would be relatively uniform over most of the seal length but would change rapidly near the ends. For this reason it seemed desirable to arrange for a finer finite difference mesh at each end of the seal than in the middle. The mesh selected varied continuously according to the relation:

$$d_n = d_1 \left\{ 1 + 2 \left[\frac{\ell}{(Z-1)\, d_1} - 1 \right] \mathrm{Sin}^2 \left(\frac{n \cdot \pi}{Z-1} \right) \right\} \qquad 5.13$$

The maximum spacing occurs at the middle of the seal, the value being:

$$d_{max} = \frac{2\ell}{(Z-1)\, d_1} - 1$$

The values chosen for the constants were as follows:

$$Z = 21, \qquad d_1 = 0.001$$

giving a maximum step size of 0.0998 and an overall length of 1.008. The length was arranged to be slightly greater than unity so that an 'extrusion profile' could be introduced between X = 1.000 and X = 1.008.

Runge Kutta methods with automatic mesh sizing were also considered for the integration of the lubrication equation, but this would have involved interpolation of the film thickness profile between the nodes used for the elasticity equation requiring an appreciable amount of extra compilation. This was not considered to be worthwhile at the time.

In the course of the work it became evident that greater accuracy was required in the integration of the lubrication equation, at the time the trapezoidal integration method was in use. However, in order to use conventional numerical integration schemes of higher order it was necessary to revert to a constant mesh spacing and this was therefore used in all the later work. The variable mesh formulation in Appendix L reduces to the constant mesh formulation when the constants d_n are set to a single value, equations L7 and L8 are therefore still valid with appropriate changes of coefficients a_{1n}, a_{2n}, a_{3n}.

Solution of the elasticity equation

The elasticity equation was reformulated in terms of finite differences as already described, the resulting set of linear recurrence equations were then solved by the Gauss-Seidel iterative method. However, the rate of convergence to the solution was very slow. The reason for this can be understood by examining the convergence criterion for the Gauss-Seidel method, a sufficient condition for convergence is:

$$\max_i \left[\frac{1}{|a_{ii}|} \sum_{j=i} |a_{ij}| \right] < 1 \qquad (5.14.)$$

where a_{ij} are the coefficients in equation. L7 (Appendix L)

From the computed values of a_{ij} this expression was evaluated and found to lie in the range 0.9900 - 0.9997. Clearly the sufficient condition was barely satisfied.

This problem was overcome by introducing 'over-relaxation', thus instead of replacing the 'old'film thickness value $h_n^{(k-1)}$ by the 'new' value $h_n^{(k)}$ it is replaced by

$$h_n^{(k)} = h_n^{(k-1)} + \omega (h_n^{(k)} - h_n^{(k-1)} \quad \text{where } \omega > 1 \qquad (5.15)$$

In practice the optimum value of the over-relaxation factor, ω, is determined by the quantity λ which is the limiting value of the ratio of the difference of successive Gauss-Seidel approximations:

$$\omega_{opt.} = 1 + \frac{\lambda}{(1 + \sqrt{1 - \lambda})^2} \qquad (5.16)$$

In the present case a value $\omega = 1.9$ was chosen and produced a great improvement in the convergence rate, reducing the number of iterations to about 25% of the original value.

Integration of the lubrication equation

For the solution of the lubrication equation two integrals have to be evaluated for each mesh node:

$$\bar{I}_1 (X) = \int_0^X \bar{H}^{-2} \, dX \quad , \quad X = 2, 3 \ldots Z \qquad (5.17)$$

$$\bar{I}_2 \cdot (X) = \int_0^X \bar{H}^{-3} \, dX \quad , \; X = 2, 3 \ldots Z \qquad (5.18)$$

In earlier versions of the program these integrals were evaluated by the trapezoidal rule but there was evidence that the resulting errors were a factor in causing instability of the main elasto-hydrodynamic iteration. To improve this situation Boole's rule for integration was incorporated in all later work; this is a five-point formula (4)

The main iteration loop

The basic scheme adopted for the solution of the lubrication and elasticity equations had to be further modified in order to obtain convergence to the solution. One essential modification was the incorporation of under-relaxation, that is the new P(X) obtained from the lubrication equation was modified before it was used to replace the old P(X) as input data to the elasticity equation:

$$\bar{P}(X)_{\text{modified}} = \bar{P}(X)_{\text{old}} + \omega \left\{ \bar{P}(X)_{\text{old}} - \bar{P}(X)_{\text{new}} \right\} , \; 0 < \omega < 1 \qquad (5.19)$$

The effect of this can be understood from figure 5.13. which simulates the present problem by a curve (a) representing the dependence of film pressure on $\bar{H}^{-2}$, and hence net compressive stress S, and a curve (b) representing the Hooke's Law surface deflection as a function of S. The point of intersection of the curves is the required solution of this simplified problem. If one commences with the value of S at A then the seal deflection is given by point B. The next estimate of film pressure is C and the next deflection is D. This sequence ABCD is clearly diverging from the solution. However, if instead of moving from B to C one goes part way only, to E, and so for subsequent approximations then the path followed is ABEFGH -- root. The method leads to convergence on the solution.

The optimisation of the under-relaxation factor, ω, presents a problem. To obtain an initial value of ω an experiment was conducted using a pair of functions to simulate the elastohydro-dynamic problem.

$$S = 100h \quad \text{and} \quad S = \frac{1}{h^3}$$

The solution to these equations was known and a range of under-relaxation values were tested to investigate the rate of convergence. It was concluded that $\omega = 0.25$ was the best value for rapid convergence of the above

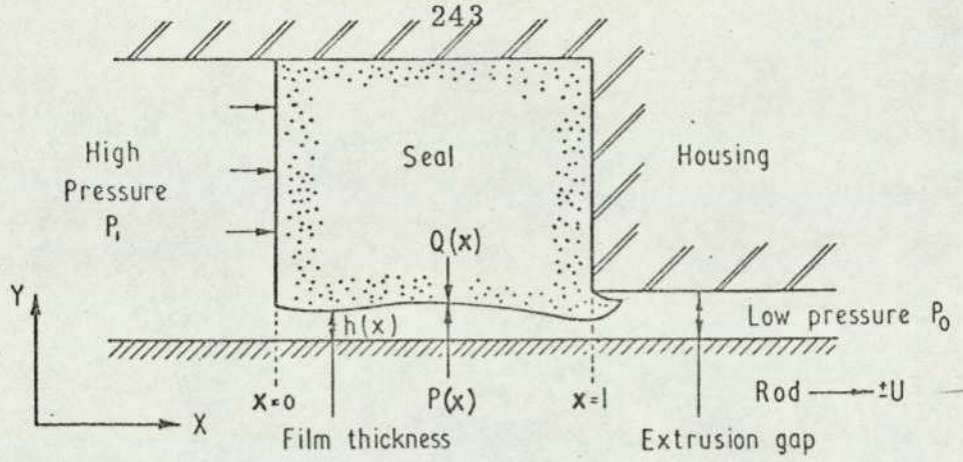


Fig. 5.12 Cross section through the seal illustrating the problem to be solved

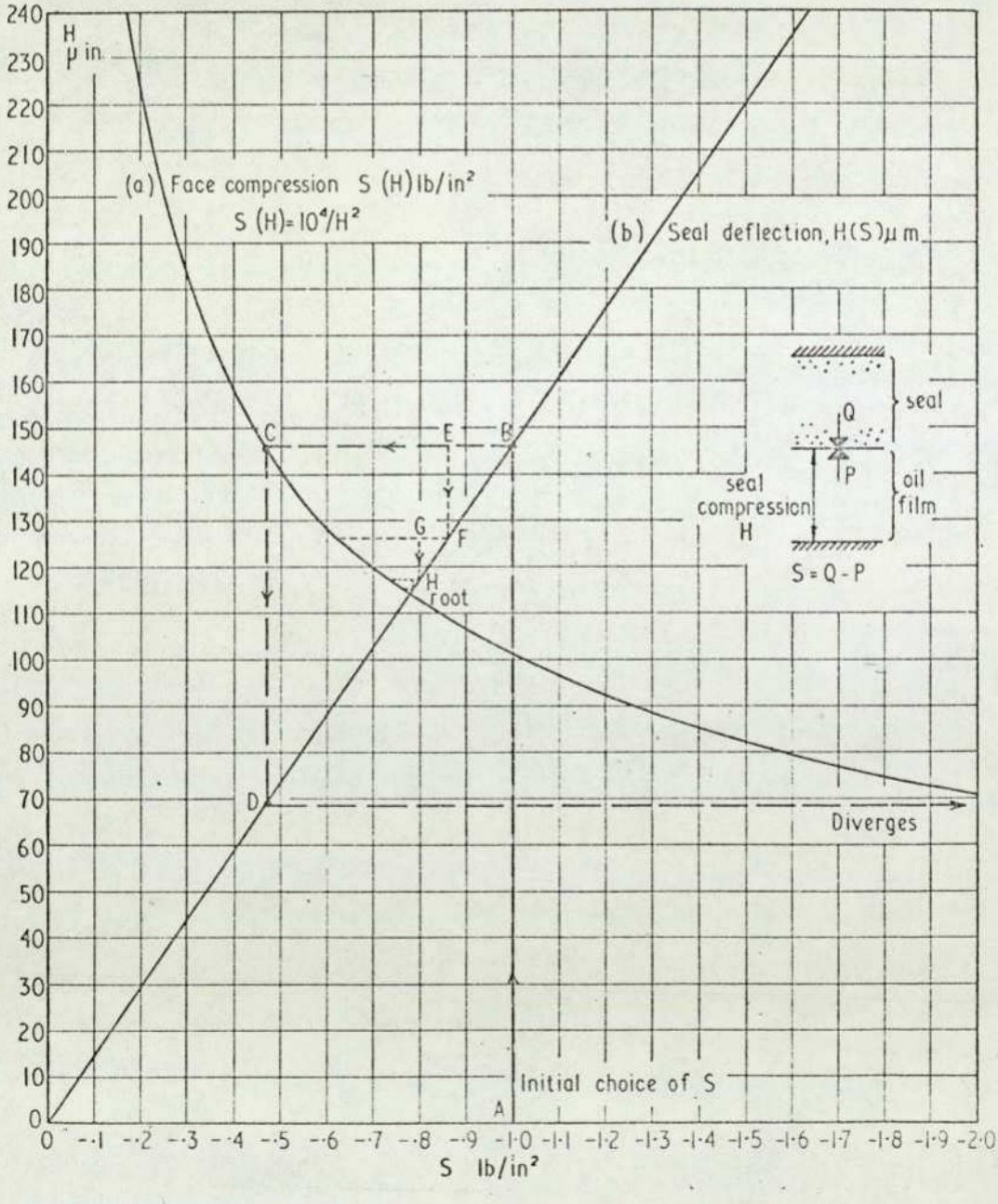


Fig. 5.13 The effect of under relaxation on the elastohydrodynamic equations as illustrated by a simplified model

simplified situation but this had to be considerably reduced to obtain a solution for the actual equations.

During program development it was found that the seal deflections were so sensitive to small changes in P(x), and hence in S(x), that the main iteration loop would not converge. To deal with this problem a number of alternatives were tried in conjunction with the above under-relaxation factor. These included restricting values of S to the range -4 to 0lbf/in^2; linking the change in the value of S, to the values in adjacent nodes; and the use of a variable under-relaxation coefficient, ω, dependent on the magnitude of S - increasing at smaller absolute values of S. However, none of these actions produced a sufficient improvement in the convergence rate.

It was realised early in the development of the program that the 'nip' at the low pressure edge of the seal was of critical importance in determining the overall pressure profile. Initially the shear stress at this edge had been set to that of the measured film profile for the initial pressure profile used and gave a calculated pressure profile very close to the value of contact stress. However, several values of shear stress were tried to see if an optimum value could be obtained. The results of this exercise are shown in figure 5.14., where the calculated pressure profiles are shown corresponding to the various outlet boundary conditions (a), (b), (c) and (d), the rest of the film remaining constant. For the remainder of the program development, boundary condition (c) was used, this value resulting in a pressure profile most closely related to the measured profile.

The above attempts to control S to sensible values became extremely complex and were, in the event, unsuccessful. However, once it was realised that the profile of the 'nip' could significantly affect the pressure profile, as described above, this could be used as an indirect method of controlling S. This was achieved through a subroutine TILTin which the three nodes at the lower pressure end of the seal were either multiplied or divided by the factors 0.950 (n = 20), 0.975 (n= 19) and 0.990 (n= 18) according to whether the pressure profile was too low or too high with respect to Q(x). In practice if the pressure was too high, the three nodes were tilted up in steps, and the pressure profile recalculated via the lubrication equation until the pressure was sufficiently close to the contact

stress. The value of S was thus indirectly controlled and the correct under relaxation formula could be used. The tilt procedure was in an iterative sub-loop about the lubrication equation figure 5.15 and did not therefore affect the shear stress boundary condition of the elasticity equation.

Experience with this tilting procedure showed that it was only required to control the very large excursions of pressure occurring during the first few iterations of the main loop. It was therefore used for the first five iterations and the program was then usually stable enough to allow the correct under relaxation equation, with a merely reduced value of ω, to control any tendency to instability over most of the range of the variables used.

Experiments were carried out with values of under-relaxation coefficient ω in the range 0.001 to 0.25 to examine the effect on convergence rate. It was found that for values above 0.025 convergence was not achieved and the best results were obtained with values of 0.01 to 0.02.

For the first solution obtained, the input data for which is given in Appendix M, the rate of convergence was particularly slow, about 400 main loop iterations were required. Subsequent solutions for new values of seal parameters were obtained in about 120 iterations, using known solutions as input data.

Figure 5.16 illustrates the rate of convergence for several speeds. Although the absolute magnitude of the film thickness oscillation about the solution is less at low speeds the pressure oscillation is worse because the absolute film thickness is less at low speed and pressure is related to this by a power law.

Whilst the convergence was acceptable in most cases, requiring 120 - 200 iterations, a number of runs exhibited complete instability. It was noticed however that this instability occurred under conditions in which the hydrodynamic component of the pressure profile was predominant. Thus, for high speeds, in this case greater than 5 ins/sec., or very thin films, such as those calculated for high hardness rubbers, the main loop was unstable because the inherent errors in the calculation of the hydrodynamic pressure component are magnified, creating in turn large fluctuations in the value of S(x) and hence H(x). Elimination of these fluctuations may

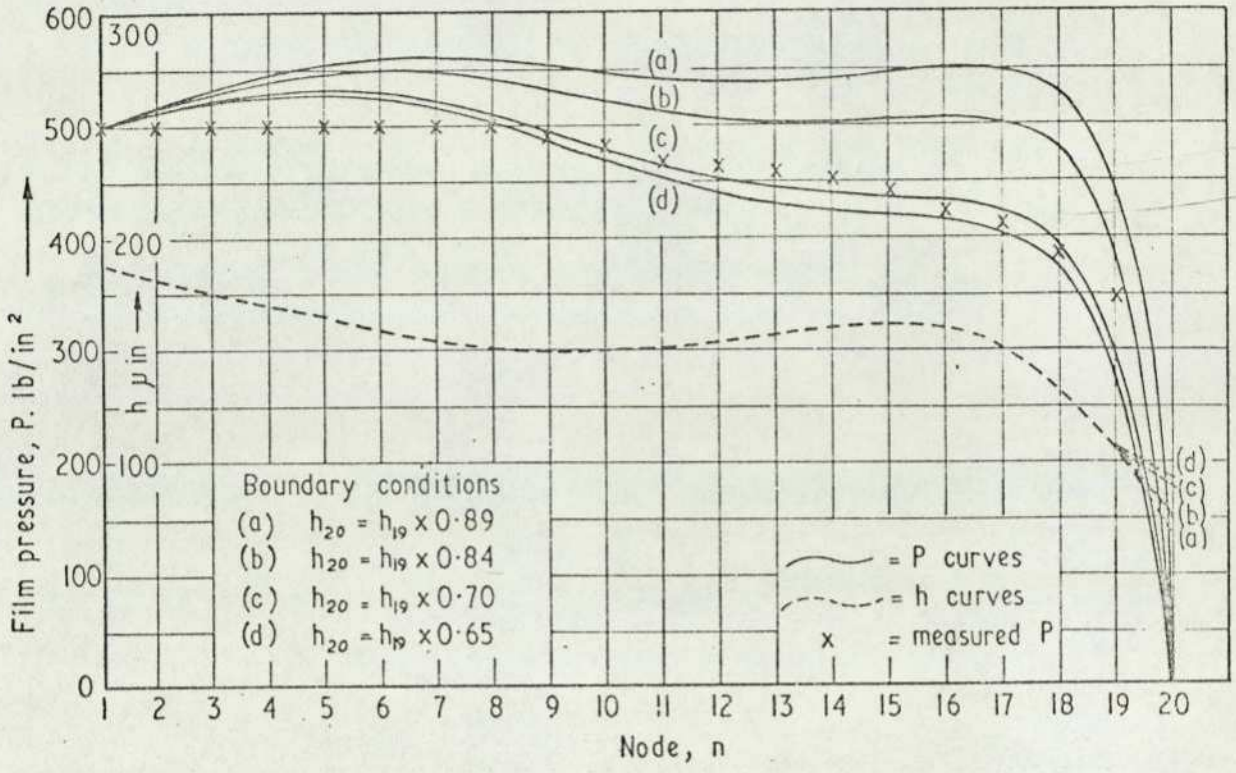


Fig. 5.14 The effect of shear strain at the low pressure edge of the seal on the pressure profile

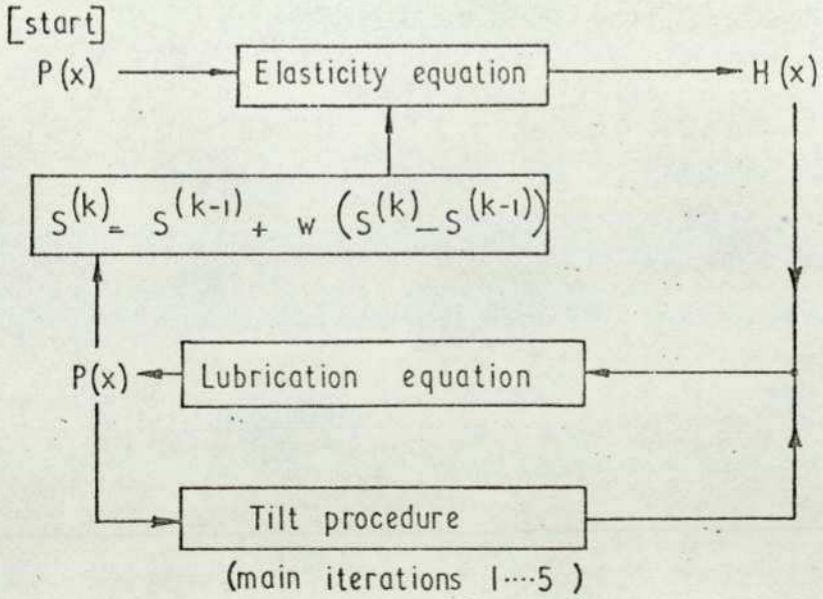


Fig. 5.15 Iteration procedure incorporating under relaxation and the TILT procedure to damp out instabilities in the main iteration loop

be achieved by improved techniques in the integration of Reynold's equation but at present this has not been attempted.

In an attempt to reduce the number of main iterations required a procedure was devised wherein the undulating values of S(x) were monitored to enable the corresponding maxima and minima at nodes 1 to 20 to be picked out, these values of S were then averaged to obtain values closer to the solution about which P(x) and S(x) oscillates. This procedure had only a marginal effect because the oscillation is over so many iterations that the reduction achieved was not worthwhile. A simplified version was then tried. For this only S(10) was monitored and the values of S at all nodes were averaged between their values when S(10) had reached its maximum and minimum. This worked better and was retained in the program figure 5.17, illustrates the effect on H(10).

The flow chart for the final version of the computer program master segment "Recipseal EHD Mk 2" is given in Appendix N, together with an annotated list of the subroutines.

5.3.3. Results.

All the results obtained from the elastohydrodynamic analysis have used the same contact stress distribution, Q(x), as specified in Appendix M. This distribution referred to a sealed pressure of 500 lbf/in^2 and this value has therefore been used throughout except where the pressure was explicitly changed. In this case the difference between contact stress and pressure, S(x),was increased or decreased in the same ratio as the old and new pressures. The rubber hardness was also kept constant at 85IRHD except where it was explicitly changed and conversions between hardness and Young's Modulus have been based on the values of Payne and Scott (43).

The fluid viscosity has not been varied as it is evident from equation 5.9 that viscosity and speed have identical effects. Thus where results are plotted for different speeds at constant viscosity they can equally be interpreted as being at constant speed for different viscosities.

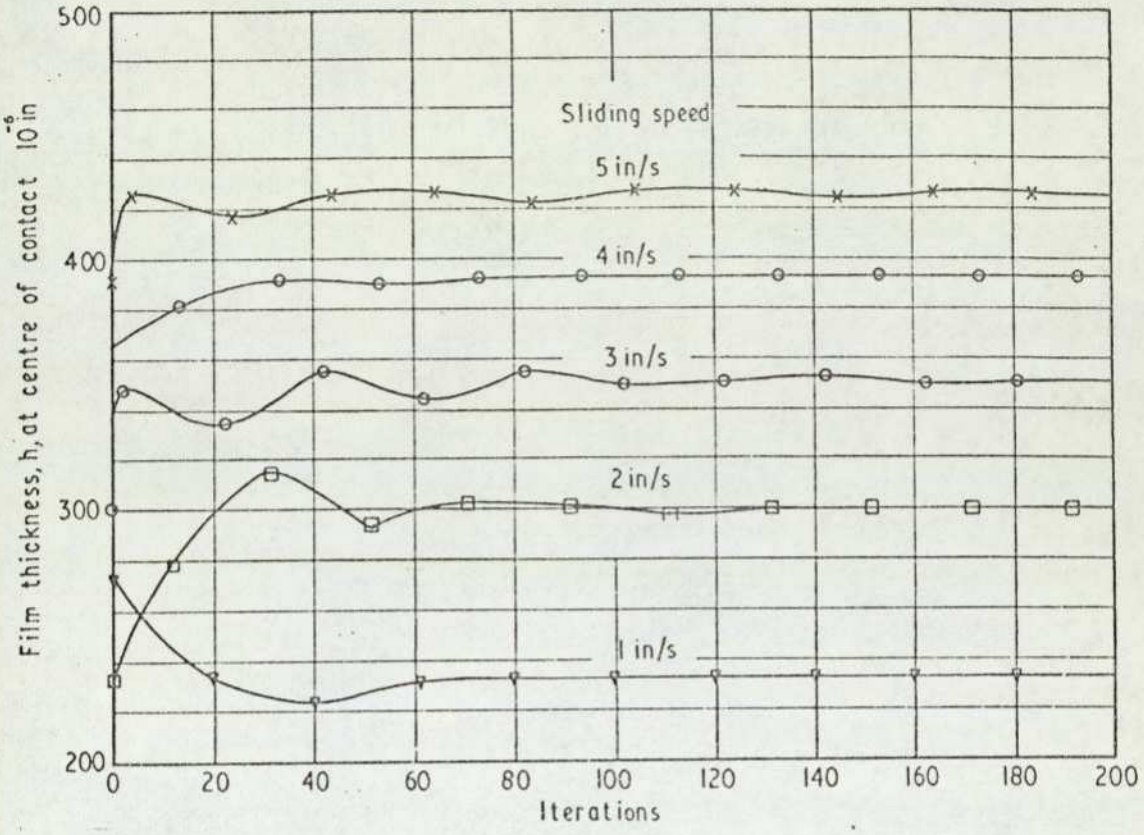


Fig. 5.16 Illustration of film thickness convergence behaviour at several values of speed

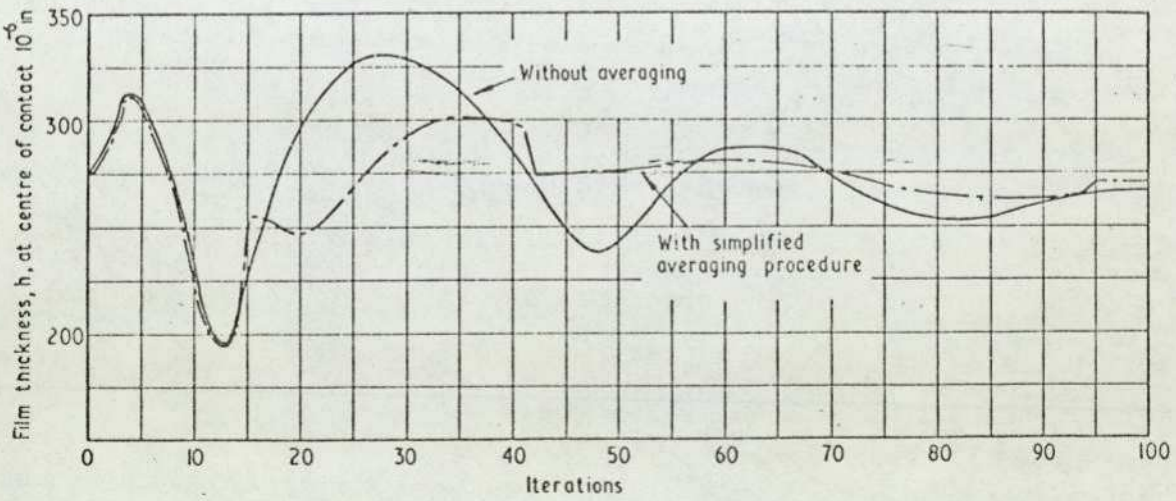


Fig. 5.17 The effect of the AVERAGING procedure on the convergence rate.

Film profiles, leakage and friction

The computed seal film profiles are shown in figures 5.18, 5.19 and 5.20, and indicate the effects of sliding speed, system fluid pressure and rubber hardness. The detailed shapes of these profiles clearly reflect the undulating nature of the seal contact stress Q(x), but the main feature of note is the relatively gradual reduction in film thickness over most of the contact with a rapid decrease in the film near the low pressure end. Most of the pressure gradient across the seal occurs at this 'nip' which is therefore important in controlling the leakage. The profile is of a typical form expected of elastohydrodynamic lubrication and furthermore agrees at least qualitatively with many of the measured profiles ofChapter 4. It is of interest to note that extrapolation of the graph of Hmax against seal hardness shown in figure 5.23 to the hardness of the 90 IRHD seals used in Chapter 4 does give reasonable quantitative agreement with the measured value of film thickness. Unfortunately the program was always unstable for values of Young's Modulus greater than 2000 lbf/in^2 and a calculated value of film thickness could not be obtained.

The shape of the profiles seems to change little with speed, but does so significantly with sealed pressue and seal hardness. Thus increasing the hardness of the rubber tends to diminish the undulations in the profile and the hardest value used shows an almost parallel profile over 90% of the contact the 'nip' only extending over the remaining 10%. Speed does not have this effect as here 90% of the contact retains the un dulations throughout the speed range, whilst the size of the 'nip' increases with speed. The effect of pressure appears to be of similar form to that measured in Chapter 4, that is the film thickness at the high pressure end of the seal increases whilst that at the low pressure end decreases as the sealed pressure increases. The shape thus changes significantly with pressure.

The above data can be summized by plotting the maximum and minimum values of film thickness, leakage and friction against the values of speed, pressure and seal hardness. Figures 5.21., 5.22 and 5.23. It can be seen that the maximum and minimum film thicknesses increase rapidly with speed and this is reflected in the rapid rise of leakage with speed. It must be borne in mind here that the leakage is only that due to a

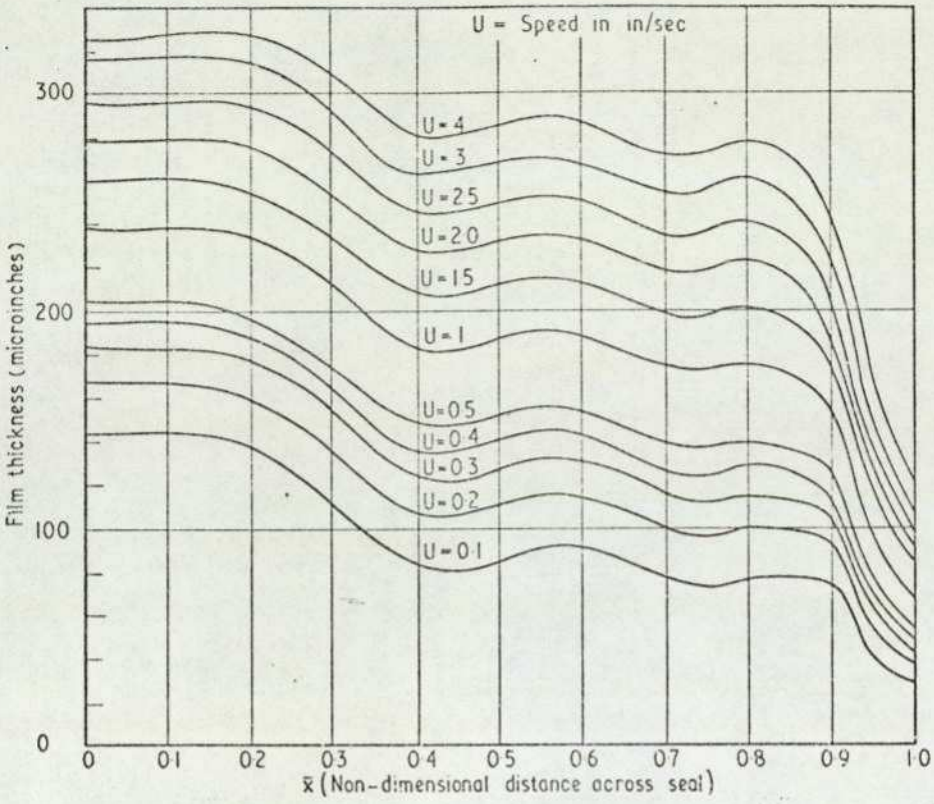


Fig. 5.18 The effect of seal sliding speed on the calculated film profile. (P = 500 lbf/in^2, rubber hardness = 85 IRHD)

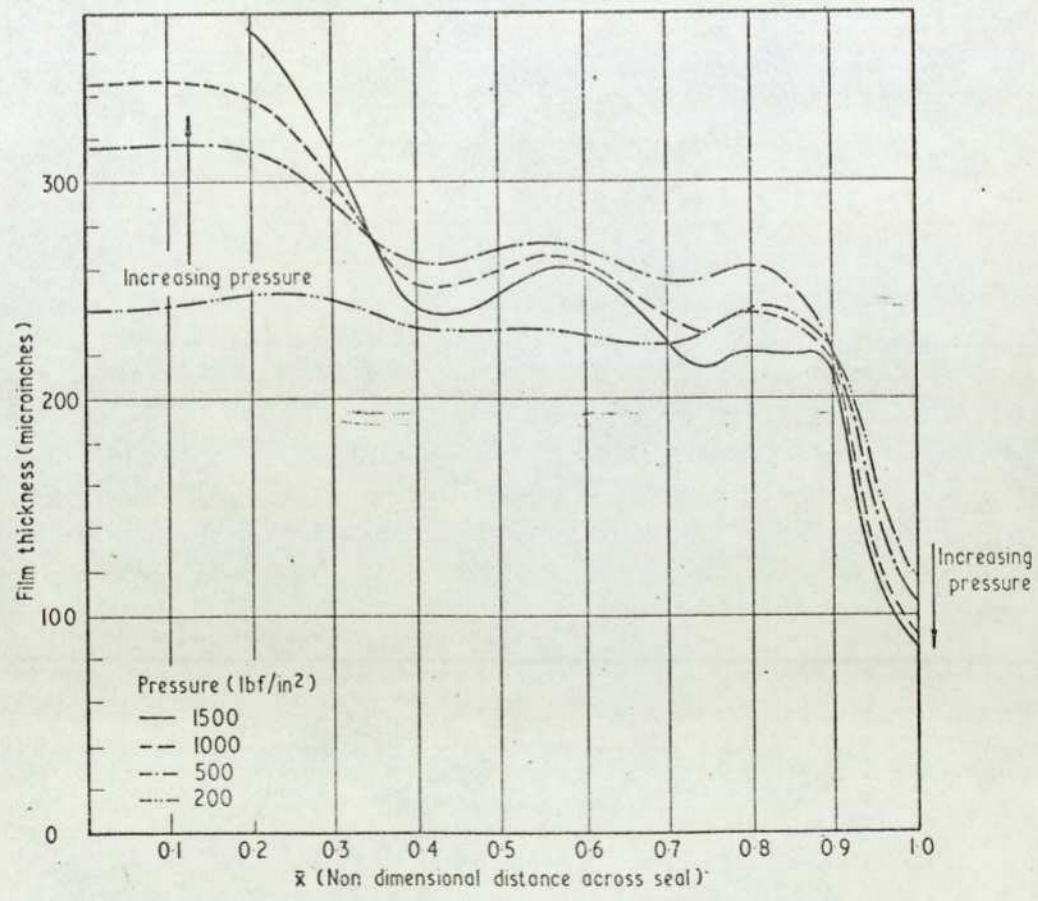


Fig. 5.19 The effect of system pressure on the calculated film profile. (U = 3 ins/sec, rubber hardness = 85 IRHD)

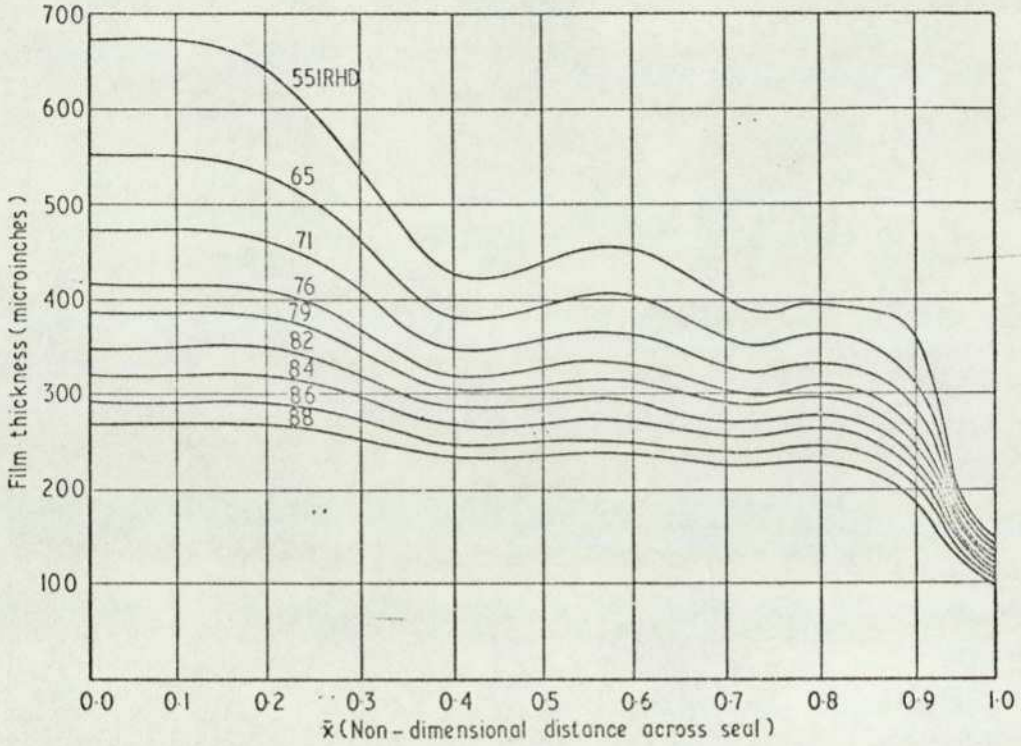


Fig. 5.20 The effect of rubber hardness on the calculated film profile. ($P = 500$ lbf/in^2, $U = 3$ ins/sec.)

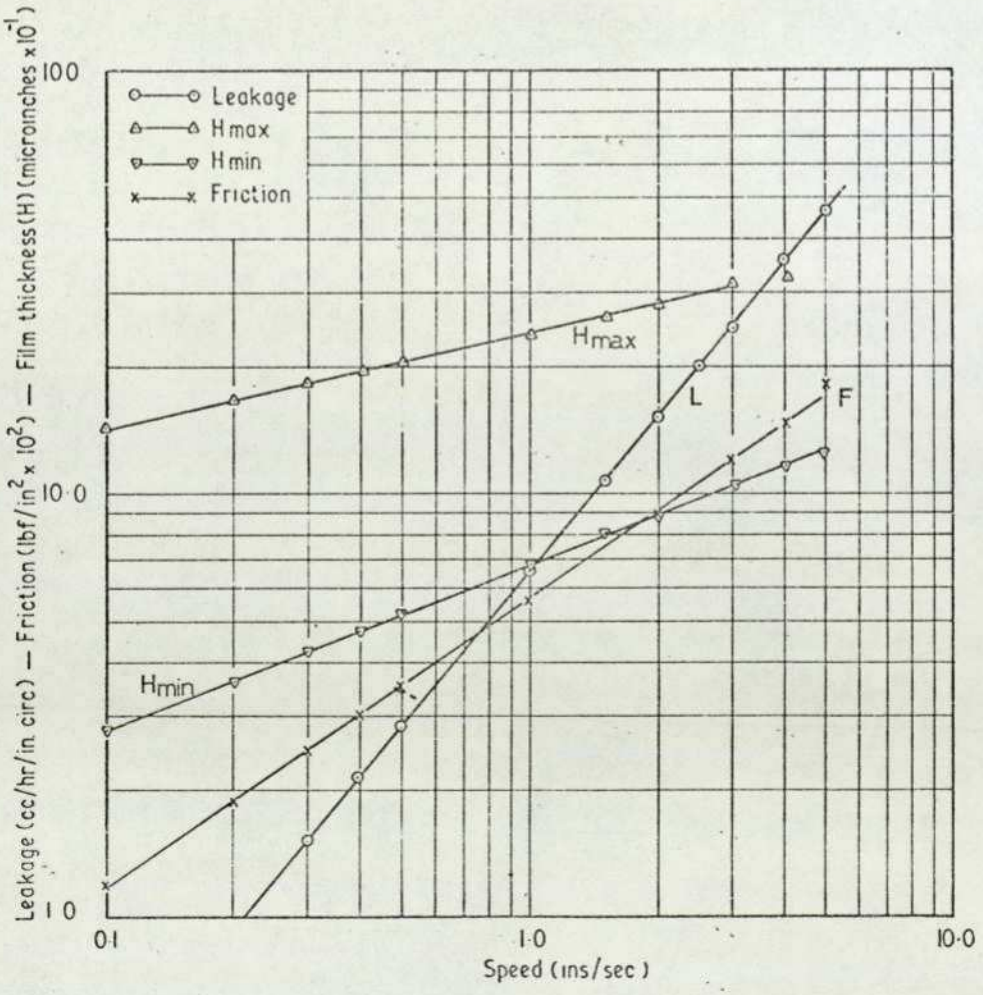


Fig. 5.21 Effect of speed on leakage L; friction F; and the film thickness at the ends of the film Hmax and Hmin. ($P = 500$ lbf/in^2, rubber hardness = 85 IRHD)

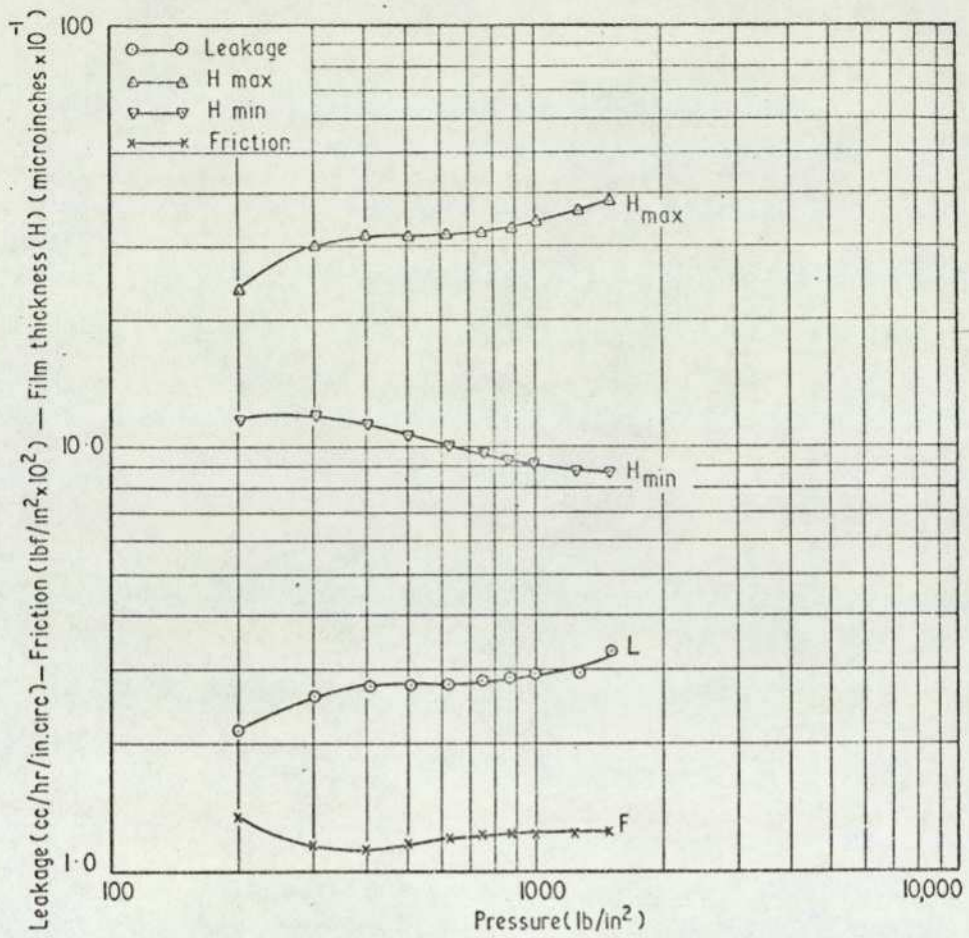


Fig. 5.22 Effect of pressure on leakage L; friction F; and the film thickness at the ends of the film Hmax and Hmin. (U = 3 ins/sec, rubber hardness = 85 IRHD)

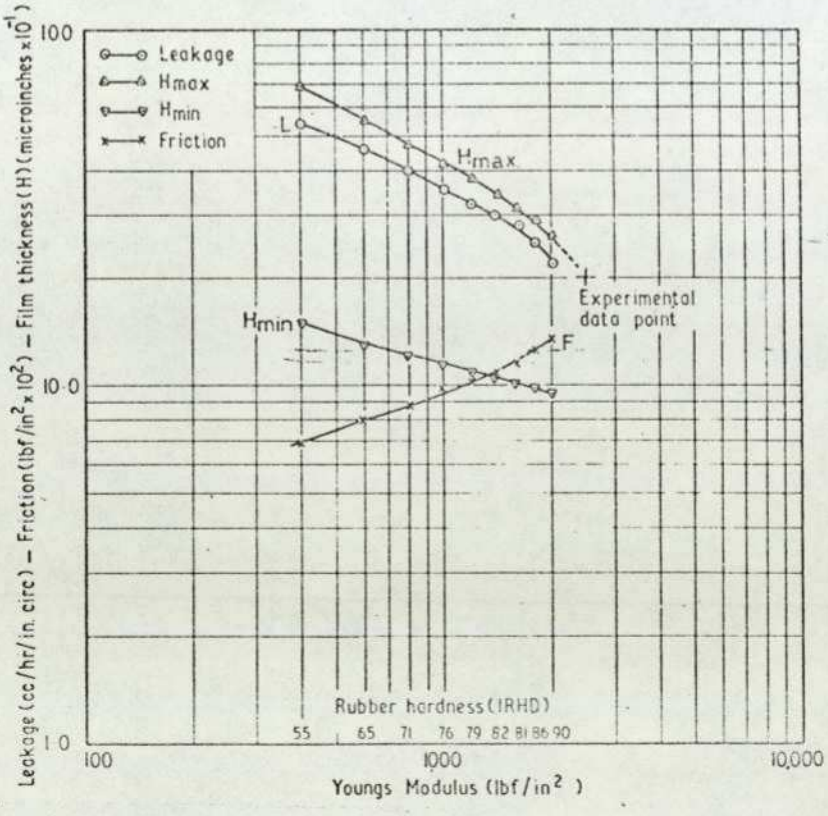


Fig. 5.23 Effect of rubber hardness on leakage L; friction F; and the film thickness at the ends of the seal Hmax and Hmin

continuous outstroke, and in practice some proportion of the total operating time of a jack will be spent on an instroke. This in itself will reduce the net leakage, but in addition some leaked oil would be expected to be returned to the system during the instroke periods. The friction of the seal is also shown to increase with speed as would be expected for a hydrodynamic film.

The sealed pressure appears to have relatively little effect on the leakage and friction of the seal, but the effect on the film thickness is to increase the maximum but decrease the minimum value of film thickness.

The rubber hardness as expected reduces the maximum and minimum film thickness values although the maximum value is reduced at a faster rate. The reduction in the film is reflected in the leakage rate and the friction which decrease and increase respectively.

It will be noticed in the data presented above that the actual values of friction are much lower than the values measured experimentally under similar conditions.

Film pressures

The deviations in pressure for different operating conditions are too small to show up when plotted in the normal way. The reason for this is clear when it is considered that for a seal of hardness 86 IRHD, a deflection of 10^{-4} ins can be achieved for a pressure change of only 0.3 lbf/in^2. The effects on the film pressure can be illustrated more clearly however by plotting S(x) (= Q(x) - P(x)) and this is shown in figures 5.24, 5.25 and 5.26

Over the ranges of variableswhich have been investigated pressure has the biggest effect on S, and hence P, although the effect of speed is also quite significant and if the range of speed was extended this could become almost as important as pressure. The effect of rubber hardness is much less pronounced and, as these already cover the range of useful values, this does not appear to be one of the important variables affecting seal behaviour.

The smaller undulations in the pressure profile may be due to the undulations present in the originally selected contact stress distribution, Q(x) but the large excursions near the low pressure end of the seal are probably more fundamental since they apply the necessary forces to produce the outlet 'nip' in the film profile. This is necessary to maintain the hydro-

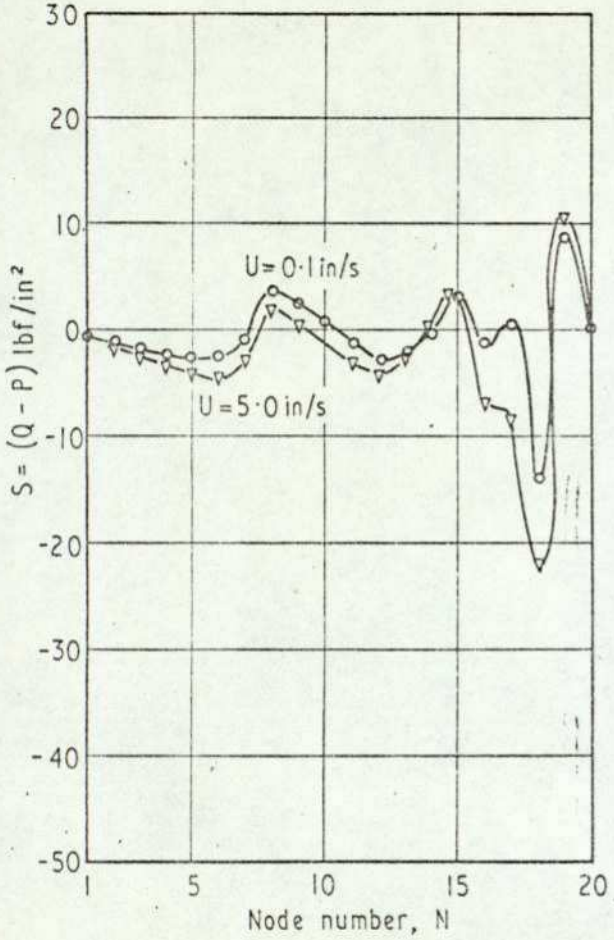


Fig. 5.24 The effect of sliding speed on the film pressure as indicated by S. (P = 500 lbf/in^2, rubber hardness = 85 IRHD)

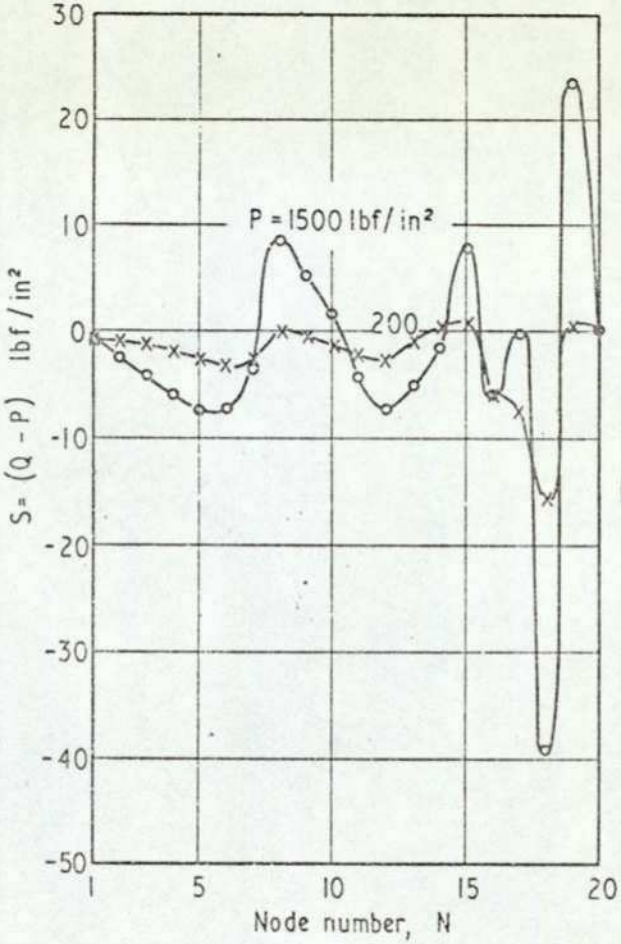


Fig. 5.25 The effect of system pressure on the film pressure as indicated by S. (U = 3 ins/sec, rubber hardness = 85 IRHD)

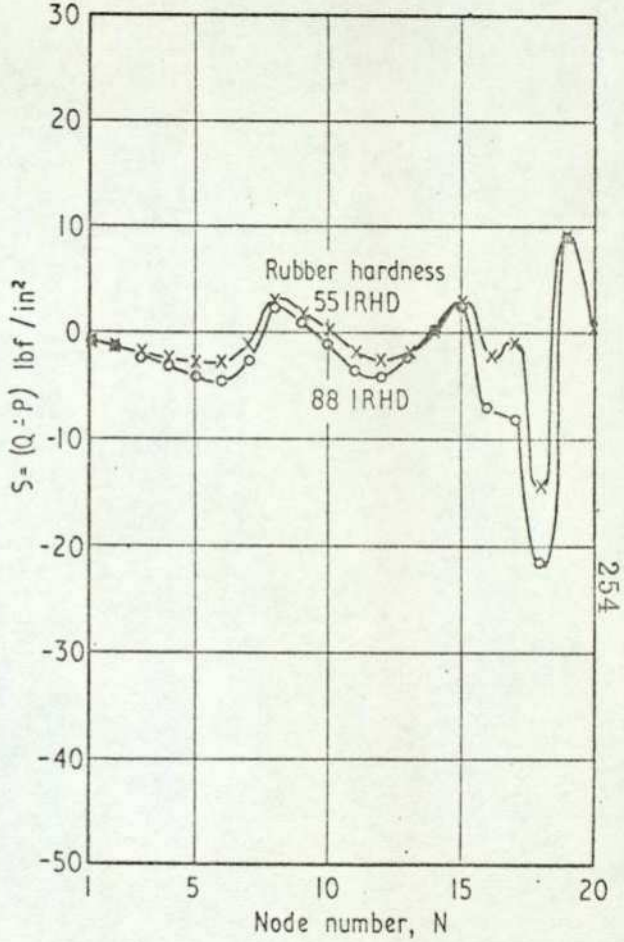


Fig. 5.26 The effect of rubber hardness on the film pressure as indicated by S. (U = 3 ins/sec, P = 500 lbf/in^2)

static pressure at a high level, close to Q, over most of the length of the seal. Without this the film cannot exist in its present form.

Step bearing analogy

When the seal operates dynamically and in addition has a pressure gradient across it, the pressure developed in the fluid film is comprised of two components: (i) that due to the relative motion of shaft and seal, the hydrodynamic component and (ii) that due to the sealed pressure, the hydrostatic component. It is interesting to evaluate the form of these two components; this has been done in figure 5.27. This reveals that the hydrostatic component predominates at the high pressure end of the seal, the hydrodynamic component here being zero. Near the 'nip' both components have similar magnitudes (in this particular example, but this is not essential). The hydrodynamic pressure profile has a triangular character resembling that of a Rayleigh step bearing which in fact the film profile resembles since it has a fairly uniform section followed by a sudden contraction. This analagous situation between the seal and a step bearing has been used in Appendix G to examine the effect of seal interference on the film thickness.

Effects of inlet boundary assumptions

The initial film thickness data corresponding to the pressure profile used for the first estimate of Q(x) appeared to have a finite shear value at the inlet edge, and this value was therefore incorporated into the boundary conditions for the early stages of the development of the numerical analysis. However, once stable solutions were obtained it was of interest to re-examine this boundary condition since one would expect the shear stress at the inlet to be zero in most practical situations. Various values of shear stress were therefore tried and stable answers were obtained. The shear was finally reduced to zero and a stable answer still obtained. Some of these are illustrated in figure 5.28. Note that the effect of reducing the shear stress was simply to reduce the general film profile down to a value nearer to that obtained experimentally. In view of the stability obtained, the zero shear stress condition was retained and used for all later calculations.

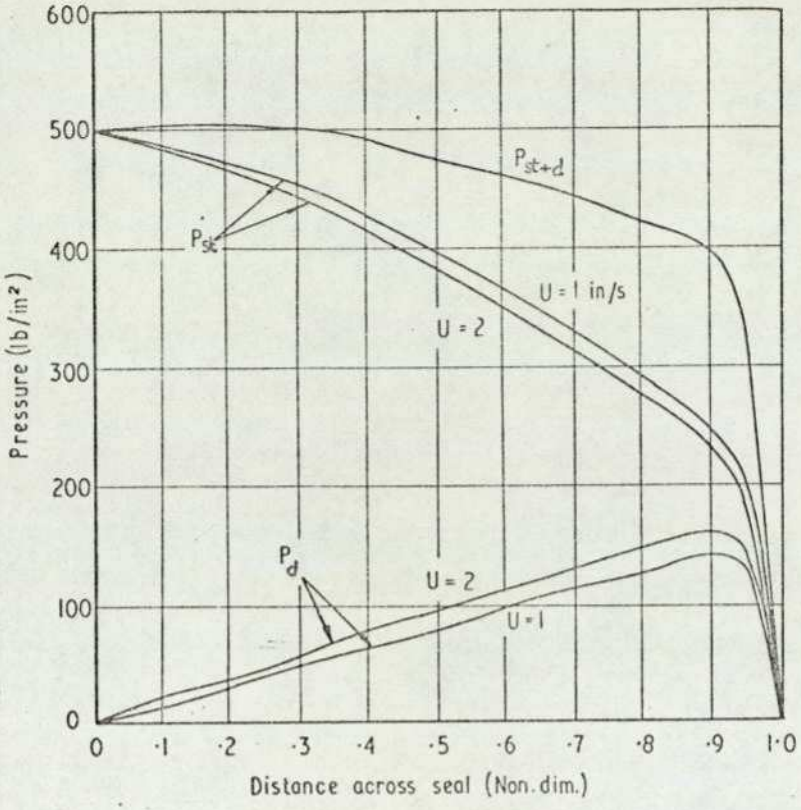


Fig. 5.27 The distribution of hydrostatic P_{st} and hydrodynamic P_d components of film pressure along the length of the seal.

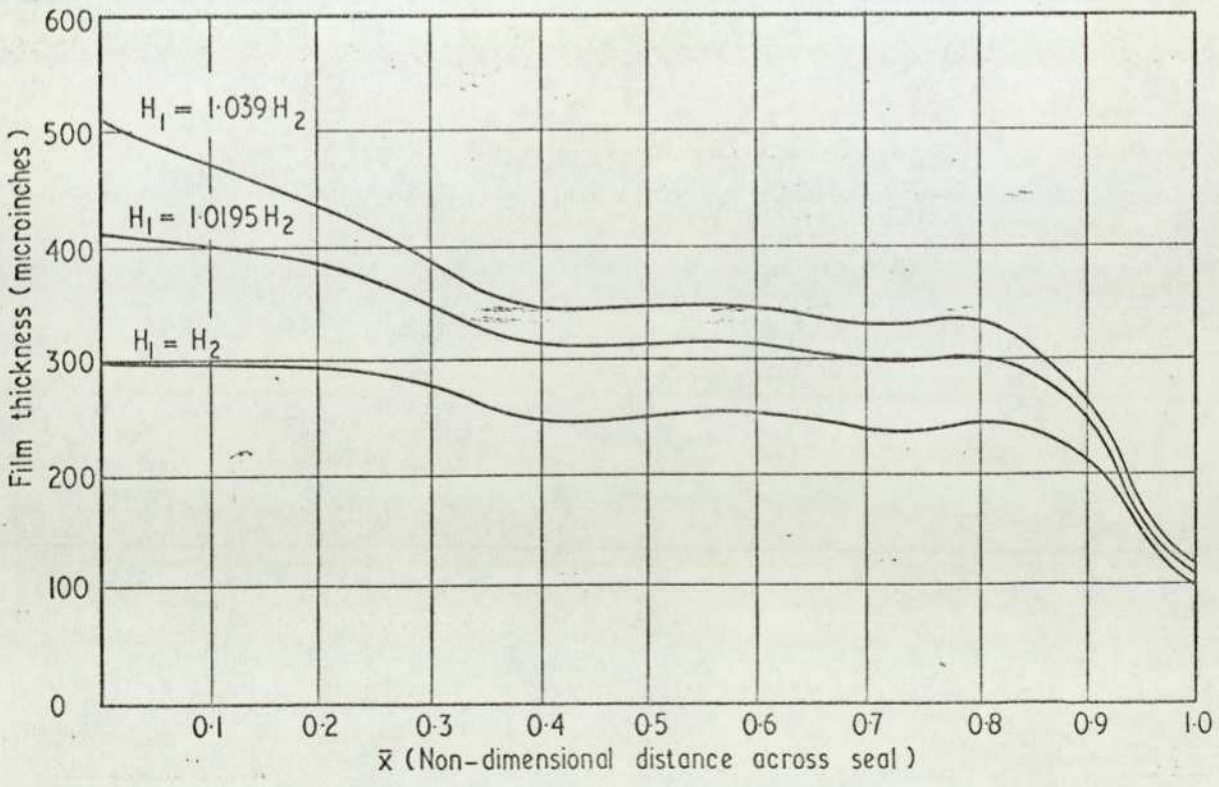


Fig. 5.28 The effect of inlet shear stress on the film profile.
(U = 3 ins/sec, P = 500 lbf/in^2, rubber hardness = 85 IRHD)

Also, during early attempts to overcome stability problems, the values of S(x) were calculated using Hooke's Law and the known film profile. This resulted in a small negative value for S(1), which was retained through most of the computer runs, the value of P(1) at the inlet being 500.62 lbf/in^2., for a corresponding contact stress Q(1) of 500.00 lbf/in^2. In a practical situation, S(1) should be zero at the inlet edge of the seal, and the program was run using this value; a stable solution was obtained. The result is shown in figure 5.29 and the effect of reducing S(1) to zero has been to reduce the film thickness throughout the seal contact, the effect being greater at the pressurised end of the seal. This boundary condition was therefore also incorporated into the program.

5.4. Discussion

Two theoretical methods have been used to analyse the elastohydrodynamic behaviour of reciprocating seals: both have advantages and disadvantages. Both methods have only successfully dealt with the problem as related to the outstroke, the instroke being difficult to deal with, and both have relied on measured film thickness and pressure profiles obtained in the instrumented rig study (Chapter 4).

The 'inverse' method, whilst allowing a rapid estimate of the film profile for a given pressure profile, does not give a film thickness in absolute terms. However, from the measured pressure profile, a basic film profile was obtained and considerable variations in this could be obtained by slight modifications of the pressure profile. The modifications are only of a very small order and the measured values of pressure were not sufficiently accurate or sensitive enough to allow the pressure gradient through the film to be determined. However, by slight modification of the pressure profile, film profiles which were typical of those measured could be obtained, including those having a double 'nip' condition. Although the interference stress has not been shown to influence the pressure in the fluid film directly, it has been shown to considerably affect the film thickness. This in turn would be expected to influence both the hydrodynamic and the hydrostatic pressure in the fluid film. The interference stress would therefore affect the pressure in the film, to cause considerable changes in the film profile and is therefore a variable of considerable importance in determining the elasto-

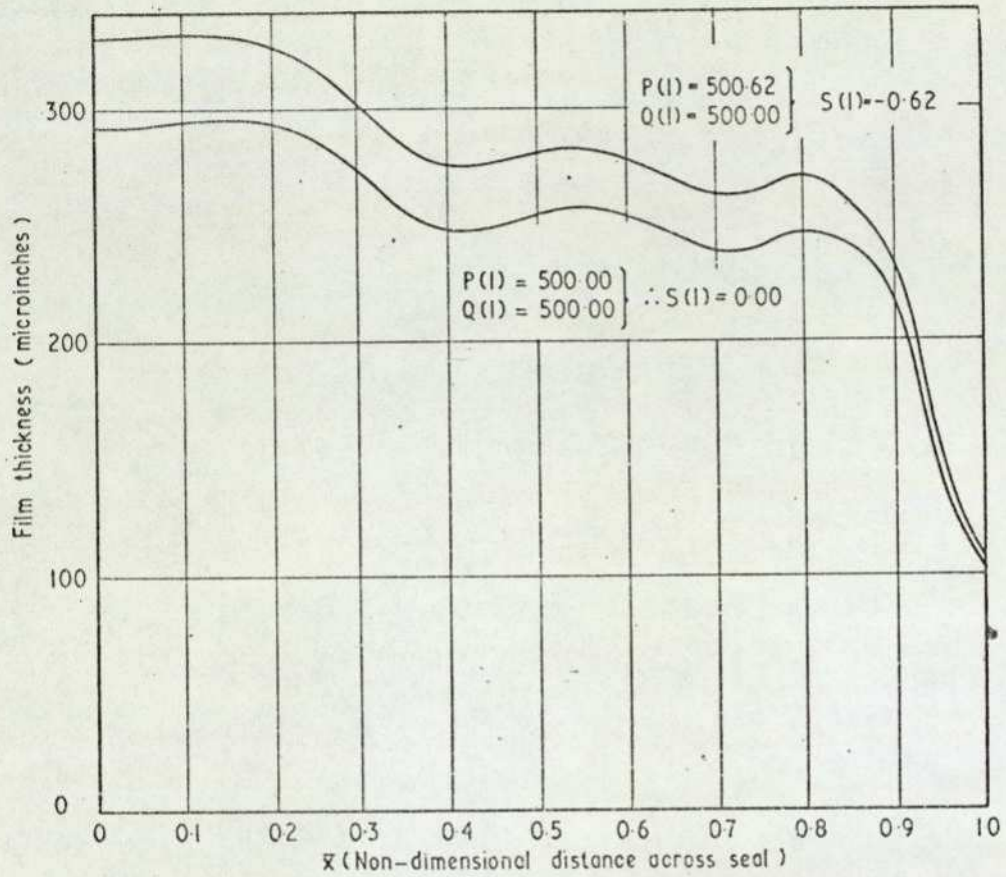


Fig. 5.29 The effect of inlet seal contact stress on the film profile. (U = 3 ins/sec, P = 500 lbf/in^2, rubber hardness = 85 IRHD)

hydrodynamic behaviour of the seal.

The elastohydrodynamic approach does enable the film thickness to be determined in absolute terms but at present state cannot deal adequately with significant changes in the interference stress. The measured pressure and film thickness profiles were also used for this approach to provide initial data for the program. However in spite of this advantage considerable effort was necessarily concentrated on the technical difficulties of obtaining a solution to the two equations arising from the physical nature of the problem. This is that the oil film is of the order of 0 to 200 micro inches thick and the rubbers used have a very low value of Young's Modulus between 1000 and 2000 lbf/in^2 for most seal materials. These two factors infer that the oil film pressure need only exceed the seal contact stress by a very small amount to create the necessary seal deflection. If the sealed pressure is 1500 lbf/in^2 the difference between the sealed pressur and the contact stress for a film thickness of 50 micro inches would be of the order of 0.02% of the sealed pressure. It is obvious that small pressure changes can cause large seal deflection and therefore small errors in calculating the pressure are magnified in solving the elasticity equation. It was for these reasons that such complicated iterati on procedures had to be developed. In spite of the above problems the iteration procedures enabled stable solutions to be obtained, at least for a part of the ranges of variables tested.

The results obtained are encouraging in that they agree qualitatively with those obtained experimentally. It was unfortunate that the values for Young's Modulus could not be extended to that of the 90 IRHD seals used, but at least extrapolation of one point has shown quantitative agreement.

The calculated relationship between leakage and speed has taken the form:

$$q \propto (\zeta . U)^{1.23} \qquad (5.20)$$

which is at variance with the results of Denny and Nau that

$$q \propto \zeta U^2 . \qquad (5.21)$$

However it has been shown that other relationships have been found by other workers with which the calculated relationship is much closer and will depend on many factors not included in the analysis.

The leakage can also be simply calculated if the variation of h* with speed is known. In the present case it is not, but it is known from the form of the pressure profile that it must be near the high pressure end of the seal, and Hmax would be more representative than Hmin. Thus the relationship between Hmax and speed is:

$$Hmax \propto U^{0.23} \qquad (5.22)$$

Substitution in the formula for Couette flow:

$$q = \frac{Uh^*}{2} \qquad (5.23)$$

gives:

$$q \propto U^{1.23} \qquad (5.24)$$

which agrees precisely with the calculated leakage relationship. The complete agreement infers that h* does in fact follow the same relationship with speed as Hmax and as the relationship between Hmin and speed is similar, the major part of the leakage must be Couette flow.

The theoretical friction data, as mentioned in the experimental sections, differs from that measured experimentally in that they are an order of magnitude too low. A further discrepancy is evident in the relationshi between friction and speed. Thus the experimental results indicate that

$$\text{specific friction} \propto U^{-0.5} \qquad (5.25)$$

whereas the theoretical result indicates

$$\text{specific friction} \propto U^{0.9} \qquad (5.26)$$

If the relationship for Hmax is substituted in the Newtonian friction formula:

$$\text{specific friction} = \frac{2U}{h} \qquad (5.27)$$

the relationship:

$$\text{specific friction} \propto U^{0.77} \qquad (5.28)$$

is formed to compare with equation 5·26. The agreement is not precise but both indicate a hydrodynamic mode of lubrication whereas relationship 5.25 indicates a boundary mode. There are thus two problems yet to be solved:

(i) The measured frictions are an order of magnitude or more greater than those calculated.

(ii) The measured values decrease with speed whereas the calculated values increase.

Pressure is shown not to affect the leakage greatly although the

seal hardness does. Thus the results indicate that:

$$q \propto (E)^{-0.5} \qquad (5.29)$$

a relationship also found experimentally by Nau (39)

The friction is shown to be related to Young's Modulus as follows:

$$\text{Specific friction} \propto (E)^{0.43} \qquad (5.30)$$

Thus the theoretical friction increases at a slightly lower rate than the leakage decreases, although this information cannot be used practically unless the discrepancy between measured and theoretical friction values is solved.

Finally it has been found that the film profiles obtained for an outstroke develop similar hydrodynamic and hydrostatic pressure profiles to those found for a Rayleigh step bearing, a geometry readily amenable to an analytic solution. This analogy has been used in Appendix G in an attempt to evaluate the effect of interference on the film thickness, with some success.

CHAPTER 6

DISCUSSION

The experimental and theoretical work Chapters, 3, 4 and 5 have brought to light many phenomena associated with the elasto-hydrodynamic behaviour of reciprocating seals, of which some have been discussed in the relevant chapters. The phenomena have shown that the behaviour of the seal is considerably more complex than envisaged, particularly in relation to the outstroke film profiles. The interferometric study, although operating with only a pad specimen and without a pressure differential has also revealed possible types of seal behaviour which could not have been recorded easily in any other way and has, therefore, significantly supplemented the results of the instrumented seal study.

The film profiles envisaged by previous workers (53)(34) and (29) were of a uniformly tapered form and many calculations were based on this. Rarely however was mention made of the effect of the two different strokes on the film thickness. These are of considerable importance in that on the outstroke the direction of motion of the shaft is the same as the direction of the sealed pressure, for the instroke they are opposites. If this affects the film profile and thickness, it will also affect the friction of the seal on the two strokes and this again has only been referred to in a few cases, but could be exceedingly important, particularly in the case of the rod seal.

The development of the instrumented seal rig and the subsequent results has enabled the above two points to be clarified by actual measurement of film thickness and friction for individual strokes.

The present results have shown a wide difference between the two strokes, with the outstroke films being much thicker than those of the instroke. In view of the results for the square edged specimen of the interferometric study, it is of interest to understand how a fluid film forms with a square edged seal. On the instroke the leading edge of the seal is that at the atmospheric pressure side of the seal and under pressurised conditions, the seal extrudes into the back-up clearance and forms a smoothly convergent inlet profile. (see figure 2.3). This is particularly the case where the seal edge is initially square and the microgeometry of the seal edge is not of great importance. The formation of the film on the outstroke where the leading edge is on the pressurised side of the seal is however less clear. The conditions at this edge are considerably

different from those prevailing at the edge of the specimens in the interferometric study in that the speed of sliding is higher, there is a large pressure force acting parallel to the sliding motion and the rubber is filled with carbon black particles. These particles agglomerate together during the vulcanisation process and would create variation in the microgeometry of the seal edge which would therefore be less 'square' than the specimens of unfilled rubber. It was emphasised in Chapter 3 that it is the microgeometry of the edge which is important and if the seal had only a very small radius caused by the carbon particles in the material or any moulding grinding or trimming operations which was combined with the higher speed and the pressure differential, a fluid film would form. Once formed, the hydrostatic pressure in the film would modify the seal profile into something approaching a step bearing in which hydrodynamic pressures would be generated. The seal edge then would be important during the initial stages of movement of the seal, but under steady state conditions other factors such as the seal shape, and interference, would determine the behaviour of the seal. In spite of the square edges therefore a fluid film is almost certain to form for both instrokes and outstrokes.

The difference in film thickness between the two strokes is due to the change in the relative motion of the shaft. Consider an outstroke having a parallel film over the majority of the contact with a pronounced'nip' at the atmospheric end. During this stroke the seal acts as a Rayleigh step bearing and therefore generates a positive hydrodynamic pressure assisting the hydrostatic pressure to form a thick film profile. During the instroke the film profile generates negative pressures and the film collapses leading to a thin almost parallel film profile.

The inherent leakage of seals is clearly explained by the form of the film profiles. Denny (10) had already proposed that leakage was due to the relative film thicknesses of the two strokes but his proposal required that the pressure differential across the seal alternated between zero for the outstroke and the system pressure on the instroke, a situation arising at the rod seal of a normally operated jack. The present work has shown that the same condition can occur for a constant pressure differential, and is a function of the stroke direction.

Because the behaviour of the seals is different for each stroke, it is essential that they are treated separately as both are affected by speed, pressure and other seal variables in different ways. Thus the net seal leakage is the result of the outstroke leakage less that returned to the system on the instroke and both depend on the film thickness, which on the outstroke is increased by both speed and pressure but is increased by speed and decreased by pressure on the instroke. These results are upheld to some extent by Nau(39) in practical measurements of seal leakage. However negative leakage, that is transference of oil across the seal against the pressure differential can occur under some conditions (19, 20) and (21) for seals operating under constant speed and pressure. This result infers that the film thickness is such that the Poiseuille component of leakage is negligibly small, Couette flow being predominant and the film thickness is thickest on the instroke.

The seal leakage then can be positive or negative and as the film thickness has been shown to be effected by variables such as the back-up clearance, seal edge profile and seal interference it may be possible to arrange the seal/groove geometry such that the variation in the film thickness between the two strokes was minimised. In a continuously stroking jack therefore the leakage would be a minimum. However this would not apply to jacks operating intermittently where the leakage would depend on many other factors not related to the seal/groove geometry. Each seal application therefore requires ideally a different seal/groove geometry.

The specific friction values recorded in the instrumented seal study for separate in and outstrokes correspond qualitatively in many instances with the measured values of film thickness. However quantitatively the measured values are an order of magnitude or more greater than predicted from the measured film thickness or those calculated in Chapter 5. Compared to the elastohydrodynamic lubrication system in 'hard' rolling or sliding contacts the present results are the reverse for in that case the measured frictions are an order of magnitude too low when compared with the calculated values. The discrepancy can however be explained by the increase in viscosity of the fluid in the contact caused by the exceedingly high pressures existing there. This cannot however be applied to the present case. Because of the poor thermal conductivity of the rubber frictional heating of the fluid

is likely to be considerable, particularly in view of the high measured values of friction, but this would tend to increase the discrepancy by reducing the actual fluid viscosity for the calculation of the friction.

Because the capacitance transducer only measured the film at one point on the circumference of the seal circumferential variation in the film could result in the measured values of friction, but measurements of film thickness around the circumference albeit at only eight points did not confirm this. In addition, friction measurements in the interferometric study, a situation where the complete contact can be seen to be lubricated under hydrodynamic conditions, also indicated the discrepancy mentioned above. Further possible explanations are:

(i) The carbon particles in the rubber of the seal may be situated some way below the actual surface of the rubber, and hence the measured film thickness would be greater than the actual value. A similar argument applies to the light reflected at the oil/rubber interface of the interferometric study. However both systems have measured films of the order of 5 micro inches and even if all measured films were reduced by this amount the calculated friction would still be considerably less than those measured.

(ii) If the surface of the rubber were assumed to contain many micro-asperities, these could penetrate the fluid film and the flattened tips of such asperirites could create high friction values. However no such phenomena were seen during the interferometric study even at the highest magnification. They would not of course have been detected with the capacitance transducer.

(iii) In dry sliding on very rough surfaces, hysteresis makes a large contribution to the total friction, but as the surface finish of the steel bore and the glass plate were better than 5 micro inches CLA, this does not seem to be a possibility here.

(iv) It has been reported by Cameron (6) that the viscosity of fluids increases as the film thins but the film in this case is usually thinner than the thinnest film measured during the present tests.

None of the explanations above solve the dilemma and the discrepancy between the two values of friction appears to be of a fundamental nature which requires further study.

Of the geometrical variables tested, the interference of the seal appears to be the most significant in affecting the film profile and the thickness.

Comparison of the results for seals of hardness 70 IRHD and 90 IRHD suggests that it is the interference stress which is the critical factor, not the linear radial interference of the seal, and seals having the same interference stress profile, although of different hardness would be expected to operate with similar film profiles.

Because of the complexities involved, a full theoretical treatment of the effect of interference on the film profile has yet to be achieved. However, the theoretical analysis of the elastohydrodynamic equations of Chapter 5 has revealed that the Rayleigh Step bearing is in some cases analogous to the seal film profile. Appendix G gives details of an analytical analysis of such a bearing which revealed that under certain conditions the bearing could exhibit very low stiffness and small changes in the applied load, which is analogous to the seal interference stress could cause large changes in the film thickness. In addition changes in the interference stress at any point through the contact would result in changes to the film profile. In particular, the double 'nip' profile obtained for the seal of hardness 70 IRHD could be caused in this way. The 'inverse' approach of Chapter 5 revealed that small fluctuations in the pressure profile are responsible for the double 'nip' profile and these are a result of variations in the interference stress superimposed on the contact stress created by the sealed pressure.

Such small changes in interference stress could also account for much of the poor repeatability of the results from seal to seal. The interference stress of any particular seal could also be affected by a number of variables leading to poor repeatability even in tests on the same seals. Such variables are as follows:

(i) the effect on the seal of increasing and decreasing the pressure

(ii) wear of the seal

(iii) stress relaxation of the seal with time

(iv) swell of the rubber caused by absorption of the sealed fluid

(v) the temperature of the seal would affect the Young's Modulus particularly at low and high temperatures. Variations in stress would also be caused by expansion and contraction of the seal itself.

(vi) anisotropy in the seal material

In the present tests, the calculation of interference stress from the measured strain and Young's Modulus is also open to doubt as it has been noted before (38) that apart from the difficulty of measuring the modulus of rubbers, the method of measurement can have considerable effect on the value obtained. The present method is based on measurements of the seal hardness using a Wallace Microhardness Tester and relating this to a theoretical relationship between the two variables. There is also some doubt as to the measured hardness value as specimen shape can also affect the result.

Due to the significant dependence of the film profile on the interference stress and the variation of stress with many of the above factors it can be seen that this factor could be responsible for many of the apparently inexplicable results obtained from seal to seal. The measurements of the film pressure were unfortunately not sufficiently sensitive to detect small changes in interference stress envisaged. Other workers (34)and (38) have measured the contact stress using a balanced pressure technique but the method is not ideally suited to measure the small changes in stress expected.

The 'breakout friction' of rubber seals has been shown by Nau (39) to increase with time at rest to a maximum value equivalent to that of a dry contact. The time at rest may be due to the dwell time between operations or the storage period of the equipment. It was previously thought that the friction increased because the oil was gradually squeezed out of the contact, but the study of the 'bubbles' of oil in a stationary contact in the interferometric study suggests that the oil is absorbed into the rubber. This would cause an increase in the contact area between the seal on the shaft and a proportionate increase in the friction force. It follows also from this study that a new and a presoaked seal should behave differently as far as the breakout friction is concerned and this allows the possibility of controlling the breakout friction by studying the absorption characteristics of rubber fluid combinations in more detail. The 'bubble' phenomena could also be used as an extremely precise tool for studying the absorption characteristics of rubbers and fluids as unlike standard swell tests, accurate weighings of rubber samples are not required and the bubble system could be used to measure quantities of

absorbed liquid as small as 10 micrograms. Providing certain optical requirements are fulfilled by the fluid and the rubber, there does not seem to be any special difficulties in using this technique.

CHAPTER 7

CONCLUSIONS

The aim of the research program was to examine the elasto-hydrodynamic behaviour of rubber seals under conditions of reciprocating motion and considerable success has been achieved, both experimentally and theoretically, in this aim.

The experimental results of Chapter 4 have shown that, in general, a thick fluid film forms on the outstroke but on the instroke the film is very thin: the seal therefore inherently leaks. The friction of such seals agrees qualitatively with the film thickness in that a low friction is associated with a thick film, and a high friction with a thin film. Quantitatively, however, the measured values of friction are an order of magnitude higher than those expected from the measured film thickness. This conclusion is confirmed by the friction measurements of the interferometric study of Chapter 3 in which the complete contact area can be seen to be lubricated. The phenomena is apparently of a fundamental nature and requires further study.

It is apparent that there is a wide range of outstroke film profiles, but these can be explained to some extent by proposing three seal lubrication regimes in which (a) boundary lubrication is dominant, (b) hydrodynamic lubrication is dominant and (c) hydrostatic lubrication is dominant. The two forms of film profile instability can be explained in terms of the transition regions between each regime.

Speed and sealed pressure have the greatest effect on the film profile, the speed increasing the film on both strokes whilst the pressure in general increased the outstroke film but decreases the instroke film. The results show that increasing the fluid viscosity also increases the film, the effect being more pronounced on the instroke. Of the seal geometrical variables, the linear interference has a marked effect, an increase in interference decreasing the film thickness. Although the softer seals resulted in a thicker film than the hard seals, this may be largely a result of the difference in interference stress. The friction did not appear to be greatly affected by the seal hardness. Other geometrical variables also affected the film profile but the effects were slight. In particular, the seal edge profile was exceedingly important in the interferometric study of Chapter 3 in which only very thin fluid films were formed, but was of much less importance in the instrumented study of Chapter 4, where the films were much thicker.

It was found that disturbances in the fluid film created by changes of direction, speed or pressure, propogated through the contact at half the speed of sliding. A movement at least two seal lengths was thus required before the fluid film became fully established. Under cyclic operating conditions where the stroke length is less than two contact widths, a full fluid film will never be formed and rapid seal failure could result. This phenomenon has been demonstrated in both experimental studies.

The poor repeatability of the test results is a feature common to much experimental work associated with seals but in this instance is believed to be a result of changes in the interference stress distribution combined with seal extrusion and edge profile effects. It is thought that further study in this area could lead to more consistent seal performance.

The 'bubble' experiments of Chapter 3 have shown that the breakout friction of seals is caused by the absorption of the fluid in the contact into the rubber and not as previously thought by the gradual squeezing out of the fluid. This occurs rapidly for previously unsoaked seals but more slowly for saturated seals. Control of the absorption characteristics could provide seals in which the breakout friction did not increase with time.

Both experimental approaches required considerable development, but in the event have proved to be exceedingly valuable tools in the study of a lubricated rubber contact.

The theoretical evaluation also consisted of two approaches. The 'inverse' solution of Reynold's equation has been used to examine qualitatively the effect of various pressure profiles on the film profile and the results have shown film profiles of the type obtained experimentally. The elastohydrodynamic approach has shown that it is possible to obtain a simultaneous solution to the elasticity and Reynold's equations, for the outstroke at least, in spite of the highly unstable nature of the situation. The results have shown stable films having an almost parallel section over most of the contact with a rapidly decreasing film at the atmospheric edge. Evaluation of the hydrodynamic and hydrostatic components of the film pressure revealed that the outstroke seal shape is analogous to the

Rayleigh step bearing, an analogy used to determine the effect of seal interference on the film thickness. The calculated film shapes are qualitatively and quantitatively similar to actual measured profiles.

The results obtained, whilst only of a preliminary nature, cover ranges of speed, pressure and rubber hardness, but only related to one contact stress distribution which may not be valid for all rectangular section seals. Whilst the effect of speed and rubber hardness is straightforward, an increase in speed increasing the film, an increase in hardness decreasing the film, the effect of pressure is more complex and an increase in pressure increased the film over the inner third of the seal but decreased it over the outer third. This effect was also recorded experimentally although agreement was only qualitative.

Both theoretical approaches have been of some value but due to the complex and unstable nature of the situation are not yet sufficiently developed to enable general seal behaviour to be predicted. The present results do however illustrate that solutions to these equations can be obtained.

CHAPTER 8

FUTURE REQUIREMENTS

Whilst the knowledge gained during the present work has explained to some extent the lubrication mechanism of reciprocating rubber seals, it is by no means conclusive and several further phenomena need to be explored.

Two particular immediate requirements for further research are as follows:

(i) There is evidence to suggest that the seal interference is much more important than previously assumed and the seal contact stress exerted by the seal determines to a greater extent the film thickness and hence the behaviour of the seal itself. It is also possible that the unpredictable behaviour and general non-repeatability of the measurements may also be due to changes in the contact stress. These variations could be caused in many ways, but in particular by stress relaxation. Rubber is a viscoelastic material and under a given strain the generated stress decreases with time. Its properties also change with temperature and the amount of fluid absorbed by the material. If the contact stress is important then all the above factors would be expected to cause changes in the behaviour of the seal as a whole. The effect of the contact stress could be evaluated in three ways: (i) A complete axisymmetric stress analysis of the seal, (ii) performance and film measurements of a seal, after development of suitable means for detecting small changes in the contact stress, and (iii) determining the effect of load on the film thickness, using a pad specimen and optical interferometry. It is realised that (ii) is difficult but a method similar to that used by Müller (34) could be used.

(ii) It is noticeable that throughout the test program the measured values of friction have been considerably higher than that expected from the measured film profile, both on the seal testrig and in the optical study. This discrepancy needs to be resolved, an understanding of it may lead to methods of modifying the seal shape or material to minimise the friction.

The seals tested so far have all been of rectangular section, a shape not generally used by industry. It would obviously be an advantage to extend the measurements to those available commercially. Once the film and pressure profile of these seals is known they could be optimised for use in particular applications.

In addition to the above needs, the effect of the hydrostatic pressure in the fluid films needs to be evaluated using optical interferometry. Results from Chapter 4 indicate that this hydrostatic pressure component could be very important in the lubrication process: the attempts in the present work did not go far enough in this direction.

There is also a further major objection to the present optical rig design in that the method is limited to particular combinations of fluid and rubber. However this problem is surmountable by suitable modification of the optical arrangements. Achievement of this and the application of a pressure gradient would make the optical method extremely attractive not only for the study of reciprocating seals but also for rotary lip seals. This method of studying the oil film could also be used to accurately determine rubber/fluid compatibility, using the 'bubbles' of Chapter 3, and would allow the absorption of micrograms of fluid to be easily detected.

On the theoretical evaluation, it is obvious that the present analysis is not developed sufficiently to allow the complete calculation of seal behaviour to be achieved. In particular the program requires an initial experimental determination of the pressure profile and an intuitive guess at the contact stress profile. This is obviously not ideal and extensions to the program are needed to obtain an axisymmetric stress analysis of the seal, which would allow changes of seal shape and interference on the behaviour of the seal to be evaluated.

REFERENCES

1. Anon. "21st progress report to Committee D". BHRA Progress Report No. PR 820, 22pp. (August, 1964).

2. Blok, H. "Inverse hydrodynamics". Proc. of the Int. Symp. on Lubrication and Wear, held at Houston Univ., pp. 7-151. (June, 1963). Publ. by McCutchen Publishing Co., Berkeley, U.S.A. (1965).

3. Blok, H. and Koens, H. J. "The breathing film between a flexible seal and a reciprocating rod". I. Mech. E. Proc., 180, Pt. 3B, pp. 221-3. (1965/66).

4. Buckingham, R. A. "Numerical methods". Book: publ. by Sir Isaac Pitman & Sons Ltd., London, 605pp. (1962).

5. Cameron, A. and Gohar, R. "Theoretical and experimental studies of the oil film in lubricated point contact". Proc. Roy. Soc., Series A 291, 1427, pp. 520-36. (April, 1966).

6. Cameron, A. "Principles of lubrication". Book publ. by Longmans Green & Co. Ltd., London, 591pp. (1966).

7. Cheyney, L. E., Mueller, W. J. and Duval, R. E. "Frictional characteristics of 'O' rings with a typical hydraulic fluid". Trans. ASME, 72, pp. 291-297. (1950).

8. Cnops, R. F. "The friction of elastomeric seals". Proc. 2nd Int. Conf. on Fluid Sealing, organised by BHRA Fluid Engng., Paper B7. (1964).

9. Denny, D. F. "The stiction of rubber seal rings". BHRA Fluid Engng. Res. Report No. RR 458. (1953).

10. Denny, D. F. "Leakage and friction of U seals". BHRA Fluid Engng. Res. Report No. RR 595. (1958).

11. Denny, D. F. "Sealing characteristics of multiple lip seals fitted to reciprocating shafts". BHRA Fluid Engng. Res. Report No. RR 614. (1959).

12. Denny, D. F. "Leakage characteristics of seals fitted to reciprocating shafts". Proc. I. Mech. E. Conf. Paper 22. (1961).

13. Dowson, D. and Jones, D. A. "An optical-interference method of measurement of time dependent elast-hydrodynamic film profiles". Report 3 I. Mech. E. Sym. on Experimental Methods in Tribology, held in London (Pub. in. I. Mech. E. 182, Pt 3G, 1967-68)

14. Dowson, D. and Swales, P. "Elastohydrodynamic lubrication of reciprocating seals". Proc. 3rd Int. Conf. on Fluid Sealing, organised by BHRA Fluid Engng., Paper F3. (1967).

15. Dowson, D. and Swales, P. "Development of elastohydrodynamic lubrication in reciprocating seals". Proc. 4th Int. Conf. on Fluid Sealing, organised by BHRA Fluid Engng., Paper A1. (1969).

16. Dyson, A., Naylor, H. and Wilson, A. R. "The measurement of oil film thickness in EHL contacts". Proc. I. Mech. E. EHL Symposium held in Leeds, pp. 76-91. (1965).

17. Edwards, W. H. (editor) "Problems in sealing aircraft fluid and hydraulic systems". Proc. of D. Mat. Conference. Publ. as D. Mat. Report No. 142. (May, 1967).

18. Eshel, A. "The propagation of disturbances in an infinitely wide foil bearing". Trans. ASME, Series F, 91, 1, pp. 120-125. (January, 1969).

19. Field, G. J., and Nau, B. S. "Interseal pressure between reciprocating rectangular rubber seals". BHRA Fluid Engng. Res. Report No. RR 978. (January, 1969).

20. Field, G. J. and Nau, B. S. "Interseal pressure between reciprocating rectangular rubber seals with back-up rings". BHRA Fluid Engng. Res. Report No. RR 1075. (September, 1970).

21. Field, G. J. and Nau, B. S. "Interseal pressure of piston seals in thin walled jacks". BHRA Fluid Engng. Res. Report No. RR 1088. (June, 1971).

22. Fisher, M. J. and Turnbull, D. E. "13th progress report to Committee D". BHRA Fluid Engng. Publication PR 674. (October, 1960).

23. Gibson, I. A., Hooke, C. and O'Donoghue, J. "Elastohydrodynamic lubrication of 'O' ring seals". I. Mech. E. Proc., 184, Pt. 3L. (1969).

24. Hirano, F. "Dynamic inverse problems in hydrodynamic lubrication". Proc. 3rd Int. Conf. on Fluid Sealing, organised by BHRA Fluid Engng. Paper F1. (1967).

25. Hirano, F. and Kaneta, M. "Dynamic behaviour of flexible seals for reciprocating motion". Proc. 4th Int. Conf. on Fluid Sealing, organised by BHRA Fluid Engng., BHRA Paper A2. (1969).

26. Hooke, C., Lines, D. and O'Donoghue. "Elastohydrodynamic lubrication of 'O' ring seals". I. Mech. E. Proc., 181, Pt. 1. (1966-67).

27. Hooke, C., Lines, D. and O'Donoghue, J. "A theoretical study of the lubrication of reciprocating 'O' ring seals". Proc. 3rd. Int. Conf. on Fluid Sealing, organised by BHRA Fluid Engng., Paper F4. (1967).

28. Iwanami, S. and Tikamori, N. "Oil leakage from an 'O' ring packing". Proc. 1st Int. Conf. on Fluid Sealing, organised by BHRA Fluid Engng., Paper B2. (1961).

29. Kambayashi, H. and Ishiwata, H. "A study of oil seals for reciprocating motion". Proc. 2nd Int. Conf. on Fluid Sealing, organised by BHRA Fluid Engng., Paper B3. (1964).

30. Kirk, M. T., "Hydrodynamic lubrication of perspex". Nature, 194, 4832, pp. 966-967. (June 9th, 1962).

31. Koens, Hammerschlog and Liem. Experimental work referred to by Theyse (51).

32. Lang, C. M. "Friction of flexible seals for hydraulic cylinders". BHRA Fluid Engng. Report No. TN 932. (1968).

33. Lang, C. M. " 'O' ring friction and leakage in hydraulic systems". BHRA Fluid Engng. Report No. TN 974. (1968).

34. Müller, H. "Leakage and friction of reciprocating flexible packings". Proc. 2nd Int. Conf. on Fluid Sealing, organised by BHRA Fluid Engng., Paper B2. (1964).

35. Müller, H. Ph. D. Thesis. Stuttgart.

36. Nau, B. S. "Water leakage and friction measurements on some moulded U-seals for reciprocating shafts". BHRA Fluid Engng. Res. Report No. RR 819. (1964).

37. Nau, B. S. "22nd progress report to Committee D". BHRA Fluid Engng. Publication PR 837. (February, 1965).

38. Nau, B. S. "Leakage and friction measurements on reciprocating square section seals". BHRA Fluid Engng. Res. Report No. RR 938. (1968).

39. Nau, B. S. "Friction and leakage of sliding rubber seals". BHRA Fluid Engng. Res. Report No. RR 973. (December, 1968).

40. Nau, B. S. "Friction of oil-lubricated sliding rubber seals". Proc. of the 5th Int. Conf. on Fluid Sealing, organised by BHRA Fluid Engng. held at Warwick Univ. (1971).

41. Nau, B. S. and Turnbull, D. E. "A simplified analysis of the characteristics of fabric rubber seals for reciprocating shafts". BHRA Fluid Engng. Res. Report No. RR 648. (February, 1960).

42. O'Donoghue, J. and Lawrie, J. M. "The mechanism of lubrication in a reciprocating seal". Proc. 2nd. Int. Conf. on Fluid Sealing, organised by BHRA Fluid Engng., Paper B6. (1964).

43. Payne and Scott. "Engineering design with rubber". Fig. 5.1 - McLaren, London. (1960).

44. Pinkus, O. and Sternlicht, B. "Theory of hydrodynamic lubrication". Book: publ. by McGraw Hill Book Co. Inc., 465pp. (1961).

45. Proc. I. Mech. E. (Discussion of reference 26), 181, Pt. 1, p. 185 (1966/1967).

46. Reynold's O. "On the theory of lubrication and its application to Mr. Beauchamp Towers experiments". Phil. Trans. Roy. Soc., London, 177, part 1. (1886)

47. Roberts, D. and Swales, P. "Elastohydrodynamic lubrication of highly elastic cylinders". Brit. Jnl. of Applied Physics. (J. Physics D.) Ser. 2, Vol. 2, pp. 1317-1326. (1969).

48. Roberts, A. D and Tabor, D. "Fluid film lubrication of rubber an interferometric study". Wear, 11, pp. 103-106. (1968).

49. Schallamach, A. "How does 'rubber slide' ". Wear, 17, pp. 301-302. (1971).

50. Southern, E. and Thomas, A. G. "Diffusion of liquids in crosslinked polymers". Trans of the Faraday Society, 163, Part 8, No. 536. pp. 1913-1921. (August, 1967).

51. Theyse, I. "The inverse hydrodynamic theory and its application to the design of controlled leakage between moving parts". Proc. 3rd. Int. Conf. on Fluid Sealing, organised by BHRA Fluid Engng., Paper F2. (1967).

52. Timoshenko, S. and Goodier, J. N. "Theory of elasticity". Book publ. by McGraw Hill Book Co., p362. (1951).

53. White, C. M. and Denny, D. F. "The sealing mechanism of flexible packings". M. O. S. Scientific and Tech. Memo No. 3/47. (1947). (Re-published by BHRA Fluid Engng., 1972).

APPENDICES

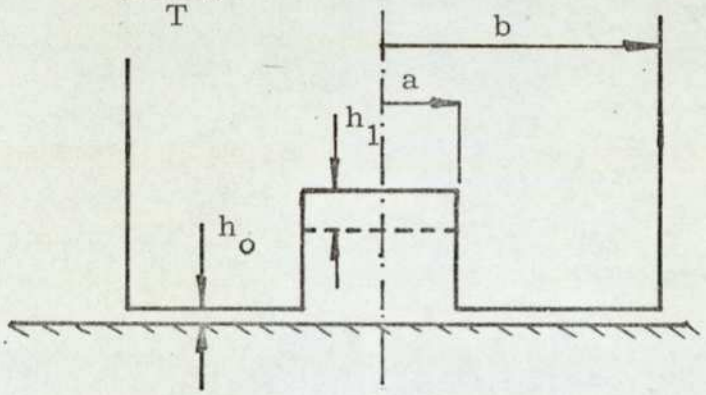
APPENDIX A

Escape of Liquid from a Trapped Bubble via a Thin Film

Consider an idealised situation comprising a cylindrical liquid bubble of radius a, surrounded by an annular thin film ofthickness h_o and outside radius b, let the depth of the bubble decrease by h_1 in time T, the liquid assumedto flow radially out to atmosphere at r = b under the action of a pressure differential P_s, see below.

The mean flow rate during time T is:

$$L = \frac{\pi a^2 h_1}{T} \qquad (A.1)$$



Also for an annular film Reynold's equation leads to:

$$L = \frac{h_o^3}{12\zeta} \frac{dp}{dr} \cdot 2\pi r \qquad (A.2)$$

or on integration:

$$L = \frac{h_o^3}{6\zeta} \frac{P_s}{\log_e b/a} \qquad (A.3)$$

Therefore:

$$\frac{\pi a^2 h_1}{T} = \frac{h_o^3 P_s}{6\zeta \log_e b/a} \qquad (A4)$$

hence the pressure differential required to obtain a flow L o' this value is:

$$P_s = \frac{6\zeta a^2 h_1 \log_e b/a}{T h_o^3} \qquad (A.5)$$

The following values aretypical for observed bubbles with mineral oil and silicone rubber:

$\zeta = 10^{-5}$ lb$_f$sec/in^2, a = 0.12 in., b = 0.2 in., $h_o = 3 \times 10^{-6}$ in., $h_1 = 10^{-4}$ in., T = 1200 sec.

inserting these in the expression for P_s gives:

$$P_s = 1360 \text{ lb}_f/\text{in}^2.$$

APPENDIX B

Absorption equation for a Trapped Liquid Bubble

For a diffusion process, the following equation is well established (50):

$$M = 2CA \left\{ \frac{Dt}{\pi} \right\}^{0.5} \qquad (B.1)$$

where M is the mass of liquid diffusing through area A up to time t, D being the diffusion coefficient and C the concentration at the surface A.

If the trapped liquid bubble under the seal has volumes V and V_o at times t and t_o respectively then:

$M = \rho (V_o - V)$ where ρ is the density of the fluid. (B.2)

Provided C and D are constant, the two equations can be combined to give:

$$V_o - V = bA(t)^{0.5} \quad \text{where } b = \frac{2C}{\rho} (D/\pi)^{0.5} \qquad (B.3)$$

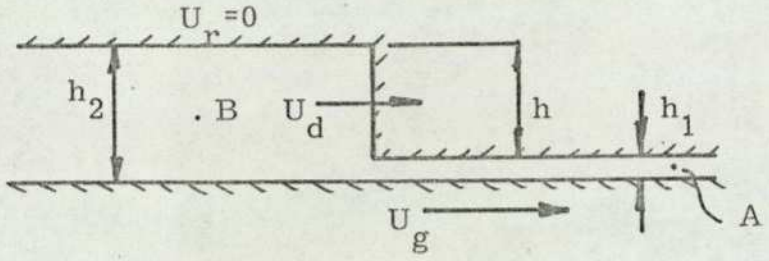
Thus a plot of $(V_o - V)$ against $A(t)^{0.5}$ should give a straight line of slope b.

For the usual specimens used in swell tests A is constant but for the present work A is proportional to the bubble size and is therefore a variable.

APPENDIX C

The Speed of Propogation of Disturbances.

Consider the follwing situation:



where U_r = speed of the rubber surface

U_d = speed of the disturbance

U_g = speed of the glass

h_1 and h_2 are the film thicknesses before and after the passing of the disturbance. Therefore $h = h_2 - h_1$.

If the Pouiseuille flow is assumed to be zero:

$$q = \frac{Uh}{2} \qquad \text{(C. 1)}$$

At A:
$$q_A = \frac{U_g h_1}{2} \qquad \text{(C. 2)}$$

At B:
$$q_B = \frac{U_g h_2}{2} \qquad \text{(C. 3)}$$

The volume necessary to increase the film thickness is:

$$q_I = U_d h \qquad \text{(C. 4)}$$

which must be equal to the difference in the flow rate before and after the disturbance:

$$q_I = q_B - q_A \qquad \text{(C.5)}$$

$$\therefore \quad U_d = \frac{U_g}{2}(h_2 - h_1) = \frac{U_g h}{2} \qquad \text{(C. 6)}$$

$$\therefore \quad U_d = \frac{U_g}{2} \qquad \text{(C. 7)}$$

APPENDIX D

Physical Properties of the Seal Materials.

Physical Properties.	X732JC	X724BD
Hardness IRHD	74	86
Specific gravity	1.24	1.28
Tensile strength lb_f/in^2	3050	3000
Elongation at break %	320	270
Tear lb_f/in	892	383
Compression set %		
24 hrs @ 70°C	13.0	15.0
Heat age		
168 hrs at 70°C		
Tensile strength change %	+1.6	+6.7
Elongation at break change %	-6.2	-7.4
Hardness change IRHD	+4	+5
Fluid resistance		
%volume change after:		
96 hrs @ 100°C in ASTMI	-3.9	-7.0
96 hrs @100°C in ASTMIII	+5.9	+2.0
48 hrs @ 40°C in RFB	+21.5	+15.8
Volume resistivity ohm.cm	476	278
Surface resistivity ohms	1000	500

APPENDIX E

Capacitance Method of Film Thickness Measurement

E. 1 Theory of Capacitance Measurement

It is well known that if two conducting surfaces are maintained at a fixed separation and a potential difference applied across them, a capacitance or storage of electric charge will be built up between them. The magnitude of the charge is proportional to the dielectric constant of the fluid between the plates, the projected area of one plate onto the other and inversely proportional to the distance between them. If one plate is in the form of a fixed area , and the fluid is not changed, the capacitance of the system can be varied by moving the plates normal to each other. The variation of capacitance can then be monitored and hence the separation of the plates can be simply calculated. This method can be used to measure the seperation of two surfaces such as those forming a bearing, or those forming a sliding seal, providing that the material of the seal is electrically conducting. In practice a small probe forms one of the plates of the capacitance and is mounted into a housing or shaft such that the probe is flush with the neighbouring surface and electrically insulated from it. The seal can then be used as the second plate of the capacitance.

It can be shown that the capacitance of such a probe can be calculated from the following equation:

$$C = \frac{KA}{4\pi h} \qquad \text{(E. 1)}$$

where K = dielectric constant of the fluid
A = area of the probe
h = separation of the two surfaces

Converting this to more practical units:

$$C = \frac{348.5\ K\ A}{h} \qquad \text{(E. 2)}$$

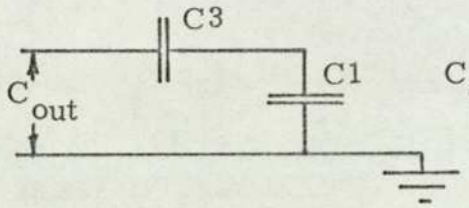
in which: A is in mm^2
C in picofarads $= 9 \times 10^{-1}$ e. s. u.

By rearrangement:

$$h = \frac{348.5\ K\ A}{C} \qquad \text{(E. 3)}$$

E. 2 The Practical Use of Capacitance Transducers.

In practice it is not possible to measure the capacitance of the probe directly as assumed above for simply mounting the probe in the housing and the various cables required add capacitance to the system. Also any measuring instrument is limited in its range and the range of the transducer must be limited. This is acheived by incorporating in the circuit a capacitance in series with the probe capacitance.



$$C_{out} = \frac{C \times C3}{C + C3}$$

At a film thickness near to zero C will be very large and the denominato of the equation will not be much affected by C3.

$$\therefore \quad C_{out} = C3 \qquad \text{(E. 4)}$$

The capacitance C3 can therefore be used to limit the maximum capacitance of the circuit.

The minimum capacitance is fixed by the stray capacitance of the transducer and the cables required. However, the minimum can be increased by the addition of a capacitance in parallel to the transducer capacitance.

The dielectric constant of the fluid must also be considered and although this is probably constant for any one fluid, factors such as temperature, water content and film cavitation may cause variations giving erroneous results.

The area of the probe is the final variable and needs to be chosen such that the capacitance of the probe and the associated circuitry attains sensible values when used over the range of film thickness of interest. Because the transducer measures over a finite area it needs to be as small as possible in order to obtain sufficiently detailed resolution of the variations in the film thickness across the seal. There is however a limit to the minimum practicable area, the sensitivity of the measuring instrument. The available equipment limited this to 0. 004 in^2.

Commercial capacitance transducers are usually fitted with a 'guard ring' around the actual transducer area in order to eliminate the effect of the capacitance field at the edge of the probe which would lead to some non-

linearity in the results. The present transducer did not have such a ring as the transducer length to film thickness ratio was approximately 100 which implied that any errors due to the capacitance field around the transducer would be slight and considerably less than other sources of error in the complete circuit.

E. 3 The Capacitance Circuit Used

The original circuit, in block diagram form was as shown in figure E. 2.

The capacitance of the lead from the oscillator to the demodulator was compensated for by the demodulator. Therefore, the system measured all capacitances up to the oscillator socket, figure E. 3

Of the four capacitances in the circuit only C4 and C3 could be directly measured. The capacitance C1 obviously depended on the film thickness and C2 contained an unknown capacitance between the probe and the housing. However, evaluation of these unknowns was possible as follows:

1. The probe was arranged to read infinite film thickness, that is the seal was not present and C1 zero.

2. The resulting capacitance $Cout_s$ was measured.

3 C2 was calculated from $Cout_s$, knowing C4 and C3, from the following equation:

$$C2 = \frac{C3(C4 - Cout_s)}{(Cout_s - C3 - C4)} \qquad (E.5)$$

Capacitance C2 was then known and measurement of Cout could be used to calculate C1 with a seal present from equation E. 2.

$$C1 = \frac{348.5\,K\,A}{h} = \frac{f}{h} \quad \text{where } f = 348.5\,K\,A \qquad (E.6)$$

For the complete circuit:

$$Cout = \frac{C1(C3 + C4) + C3(C2 + C4) + C2.C4}{(C1 + C2 + C3)} \qquad (E.7)$$

From which by rearrangement:

$$C1 = \frac{Cout(C2 + C3) - C3(C2 + C4) - C2.C4}{(C4 + C3 - Cout)} \qquad (E.8)$$

and substitution in equation E. 6 and rearrangement gives:

$$h = \frac{f(C3 + C4 - Cout)}{(Cout(C2 + C3) - C3(C2 + C4) - C2.C4)} \qquad (E.9)$$

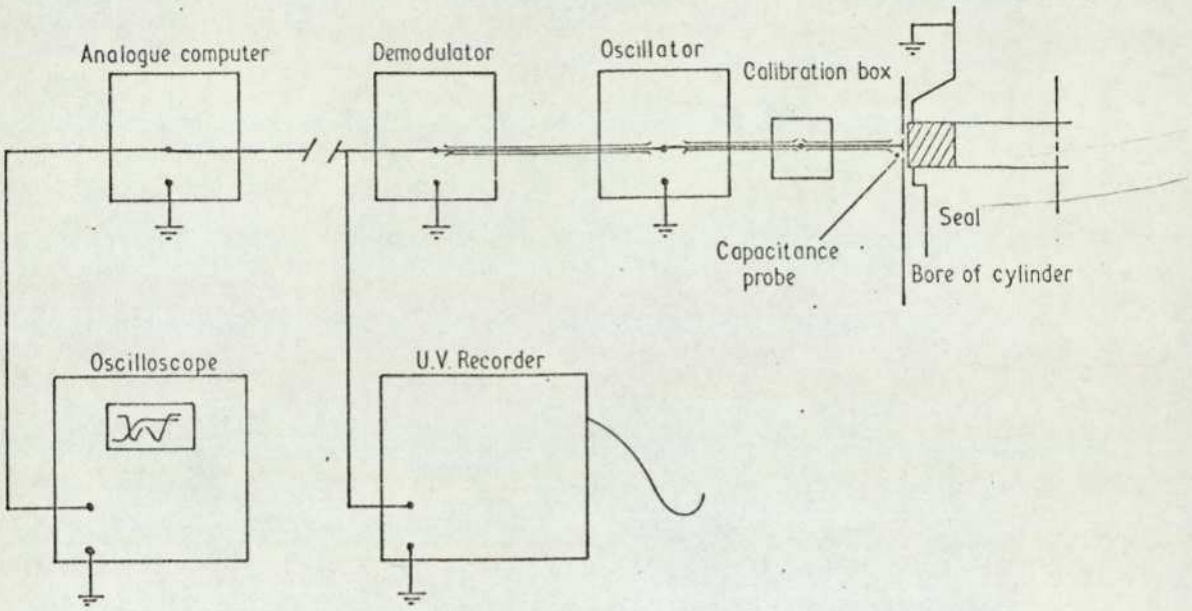


Fig. E2 Instrumentation for the measurement of film thickness

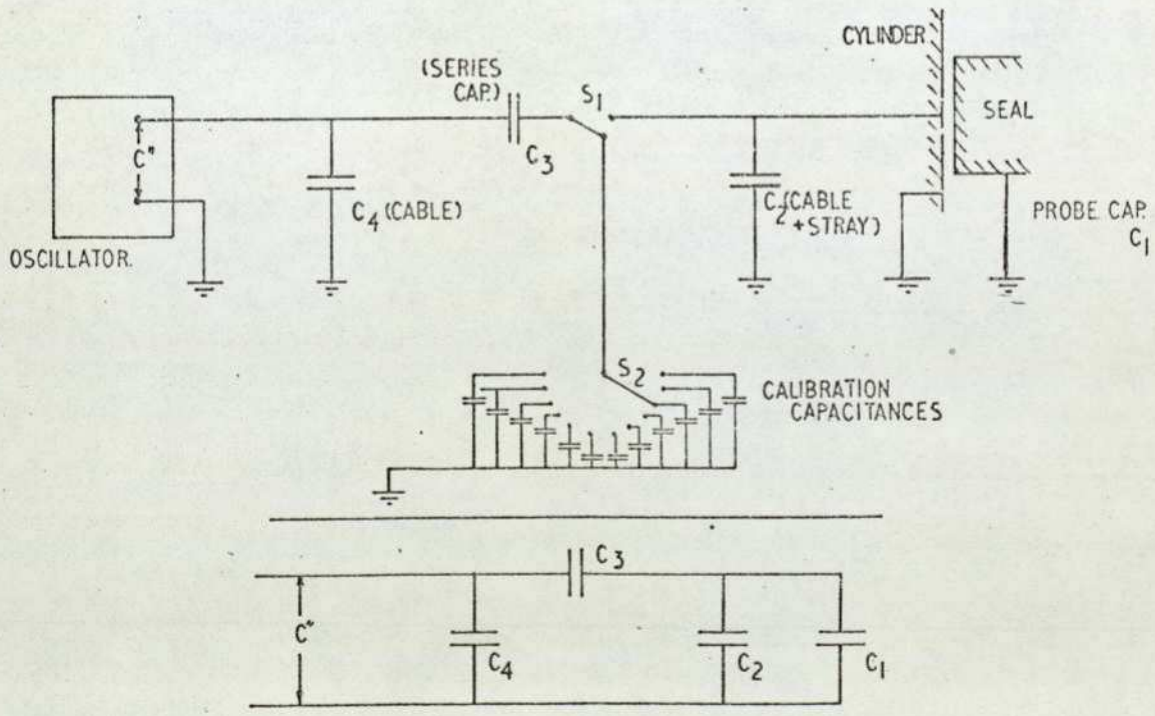


Fig. E3 Capacitance circuit for the measurement of film thickness

E. 4 Calibration of the System.

The calibration needed to be carried out by measurement of the capacitances and calculation. Two points for calibration presented themselves immediately. An infinite film thickness could be formed by moving the seal away from the transducer and zero film thickness could be formed by shorting the transducer to earth.

In order that a number of more practical points were available the transducer capacitance could be replaced by various other known capacitances. Measurement of Cout then enabled the equivalent film thickness of each calibration capacitance to be readily calculated.

In practice fixed capacitances were not ideal as they could rarely be arranged to represent particular values of film thickness and the circuitwas subsequently modified by replacing the calibration capacitances of figure E. 3 by an accurate variable capacitance. Suitable calculations allowed any value of film thickness to be represented simply by adjustment of the variable capacitance.

E. 5 Measurement of Capacitance

Frequency demodulator unit

The principle of operation is frequency modulation of an oscillator signal operating at approximately 2MHz which has as part of the external circuit the varying capacitance of the transducer. In effect the variation in the capacity of the transducer caused by the changing film thickness varies the frequency of the signal which is then applied to a frequency discriminator circuit, the output voltage of which is proportional to the change in the frequency and hence the measured capacitance. The unit operated between a range of $\pm$ 5 volts over the range of capacitance of approximately 30 - 110 pf.

The output voltage, however, was highly non-linear with film thickness and covered a range from zero to infinite film thickness.

Relationship between demodulator voltage, V, and film thickness.

Agraph of demodulator voltage, V, against the circuit capacitance is shown in figure E. 4. The straight line can be represented by the equation:

$$C = e + mV \qquad \text{(E. 11)}$$

where e = intercept on the Y axis for V=0

m = slope of the line

The film thickness could therefore be related to the demodulator voltage, V, by combining equations E. 9 and E. 11, thus:

$$h = \frac{f(C3 + C4 - (e + mV))}{(e+mV)(C2+C3)-C3(C2+C4)-C2.C4} \qquad \text{(E. 12)}$$

Analogue computer network

Equation E. 12 is obviously non-linear and considerable effort was required to convert the value of V to an equivalent film thickness. In order to reduce this an analogue network was built to linearise the demodulator voltage with respect to the film thickness. This was achieved as follows:

By defining:

$$a = (C3 + C4) \qquad \text{(E. 13)}$$

$$b = C3(C2 + C4) + C2.C4 \qquad \text{(E. 14)}$$

$$d = (C2 + C3) \qquad \text{(E. 15)}$$

and substituting in equation E. 12

$$h = \frac{f(a - e + mV)}{(e + mV)d - b} \qquad \text{(E. 16)}$$

which by rearrangement gives:

$$h = \frac{f(V + (e-a)/m)}{-(V - (b-ed)/md)} \qquad \text{(E. 17)}$$

Defining:

$$a' = (e-a)/m \qquad \text{(E. 18)}$$

$$b' = (b-ed)/md \qquad \text{(E. 19)}$$

We get:

$$h = \frac{f(V + a')}{-(V-b')} \qquad \text{(E. 20)}$$

If v = analogue output voltage with an input voltage V

$$v = \frac{-const(V + a')}{(V - b')} \qquad \text{(E. 21)}$$

a' and b' are of the same magnitude but of opposite sign to the demodulator voltage, V, for zero and infinite values of film thickness and can therefore be easily measured. The value of the constant is not important as the voltage, v, can be directly calibrated in terms of the film thickness using the variable capacitance. A diagram of the network is shown in figure E. 5

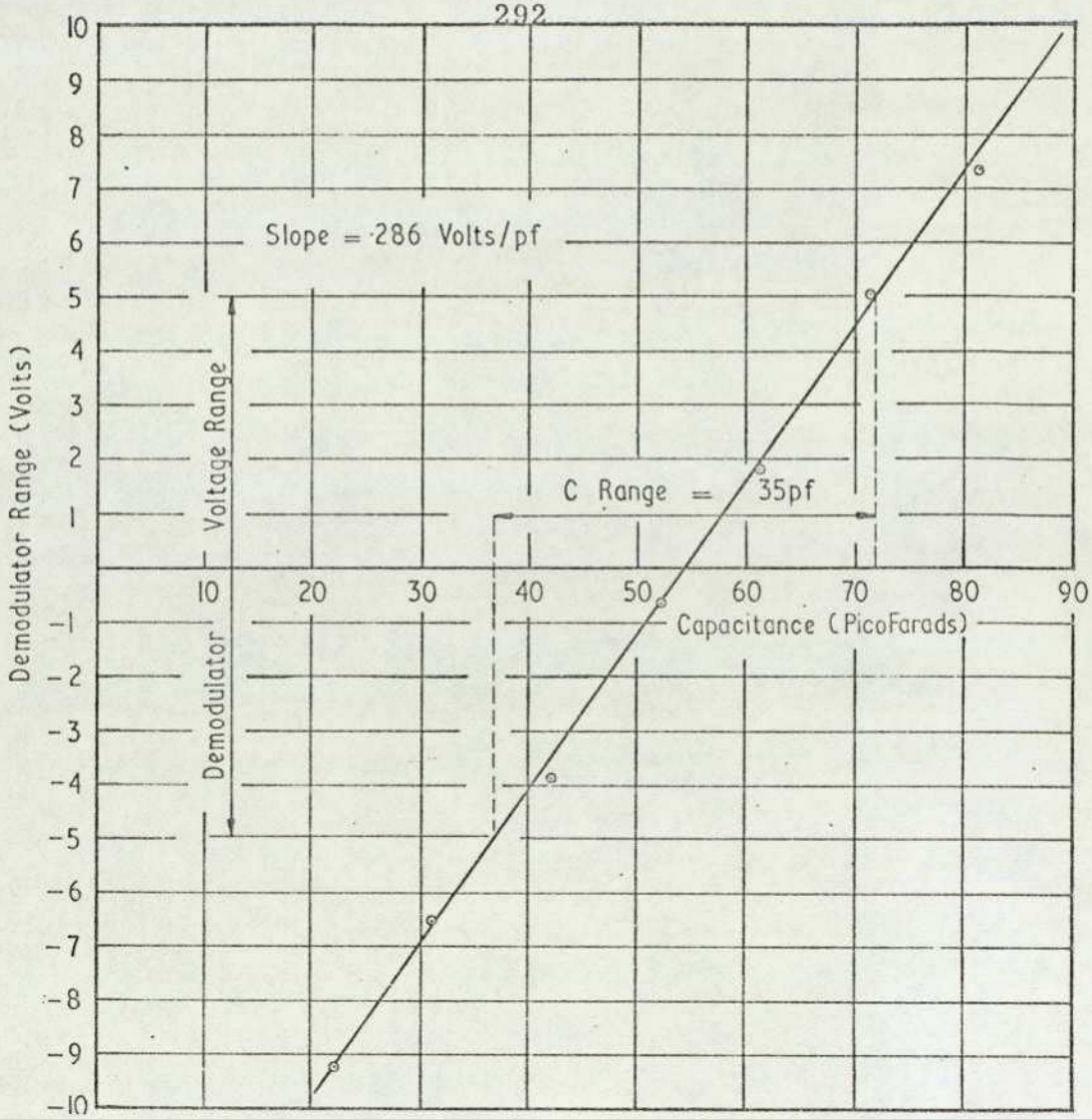


Fig. E4 Demodulator voltage against capacitance of the film measuring circuit

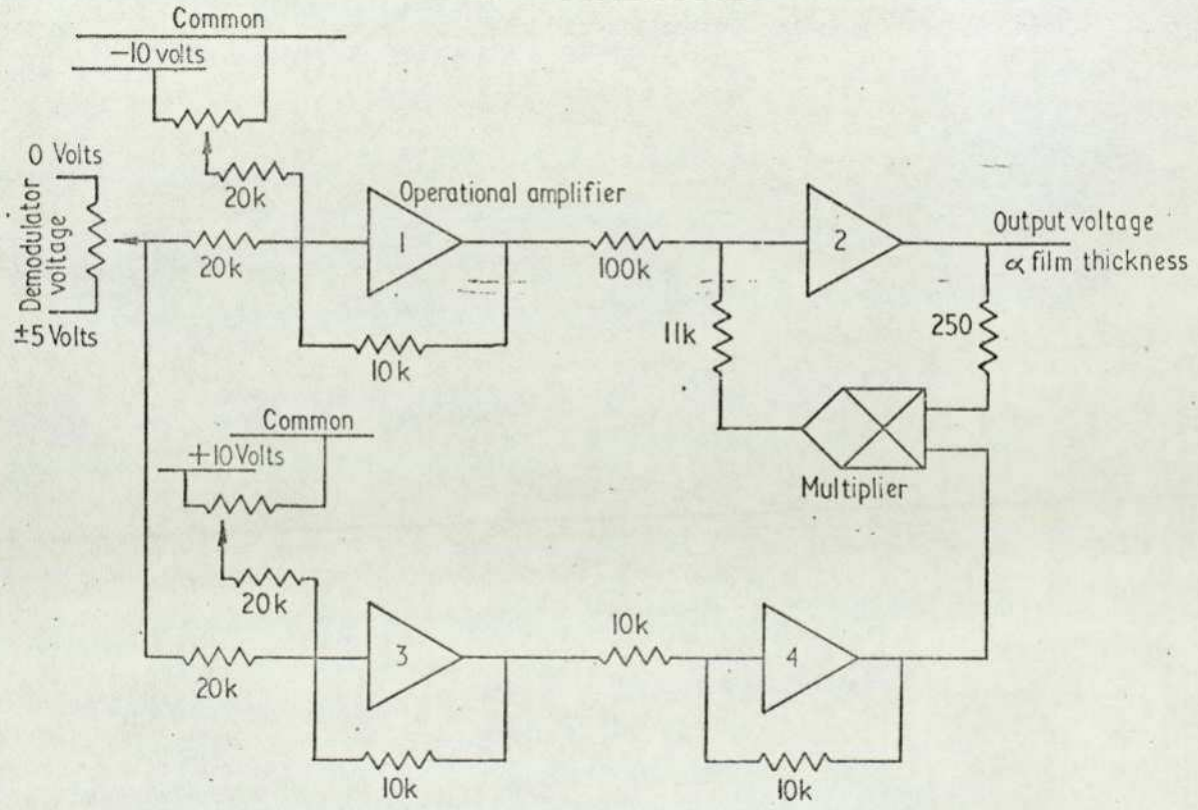


Fig. E5 Analogue network circuit

APPENDIX F.

Error Analysis of Film Thickness Measurement

F. 1. Errors due to the measurement of capacitance

The capacitance of the transducer can be calculated from equation E. 2 of Appendix E in which both K and A will be sources of possible error.

The dielectric constant is affected by water and air in the oil and by cavitation if it occurs. Cavitation although found to exist in low pressure face seals as a releasing of dissolved air would not be expected to occur during the present testsconducted at appreciable pressures, except very close to the atmospheric edge of the seal.

From (16) it was estimated that, over the temperature and pressure range envisaged in these tests, the dielectric constant of the oil to be used would be:

$$K = 2.3 \pm 0.015 \qquad (F.1)$$

The area of the transducer was calculated from measurements of the circumferential length and axial thickness to an accuracy of $\pm$ 0. 01mm. These were:

$$\text{Axial thickness} = 0.45 \text{ mm} \pm 0.01\text{mm}. \qquad (F.2)$$

$$\text{Circumferential length} = 4.62 \text{ mm} \pm 0.01 \text{ mm} \qquad (F.3)$$

$$\text{Area} = 2.079 \pm 0.050 \text{ mm}^2 \qquad (F.4)$$

From the above values the errors associated with the capacitance of the transducer were calculated.

The oscillator frequency is modulated by the changes in the capacitance of the complete circuit and errors in the measurement of the fixed capacitances, C3 and C4 of figure E. 3 will lead to errors in the calculated value of C2, (equation E. 5).

The accuracy of measurement of the capacitances was taken as the accuracy of the measuring instrument (Wayne Kerr Bridge Type B221) which was 0. 10% of the full scale deflection.

These measurement errors were taken to be 0. 25% before being used to calculate the errors in C2 and finally the overall capacitance of the circuit to take account of possible reading errors.

Using the above errors in the measurement of the capacitance, the errors in the final film thickness values were calculated to be as follows:

TABLE F1

h(microinches)	C1 pf	Cout pf	e_h(microinches)	$\%e_h$
0		113.9	0.0	0.0
10	166.6	90.3	0.5×10^{-1}	0.5
20	83.3	79.9	0.16	0.8
50	33.3	67.6	1.00	2.0
100	16.7	61.2	4.00	4.0
150	11.1	58.7	9.00	6.0
200	8.3	57.3	16.00	8.0
300	5.6	55.9	36.00	12.0

F. 2 Sources of error due to the seal mounting

The seal forms the second plate of the probe capacitance, and three sources of error arise due to the mounting of the seal onto the shaft and the seal itself. These are:

(i) Failure to provide a good earth return path.

(ii) The capacitance between the seal and the groove.

(iii) The resistance of the conducting rubber.

Earthing of the seal.

The earthing of the seal to the demodulator unit occurs through the seal contacting the groove, and the rod running through the linear bushings. Ideally the seal needs to be earthed directly to the demodulator, but experiments with and without an earth lead did not show any measurable variations in the result and the lead was dispensed with.

The effect of capacitance between the seal and the groove.

This can be calculated by assuming that the two capcitances are in series. The measured value of the seal groove capacitance was 50, 000 pf and assuming a transducer capacitance of 300 pf (representing a film thickness of 5 microinches) the resultant capacitance would be:

$$C = 298.5 \text{ pf}$$

giving an error of 1.5 pf or 0.5%. For thicker films the probe capacitance was smaller and lead to much lower errors. These were therefore considered negligible.

The effect of resistance of the seal material

In order for the capacitance circuit to be complete the seal must be electrically conducting. As rubber is usually classed as an insulator conductivity can only be increased by excessive loading of the rubber with carbon black and the conductivity is thus limited to values 50 - 500 ohm cm which may produce error in the measured capacitance of the transducer.

It can be shown that the error in the transducer capacitance due to a resistance in series with it is:

$$\text{Error in C1} = \frac{Z_T - Z_C}{Z_C} \times 100\%$$

where Z_T is the total impedance
Z_C is the impedance of the transducer.

This can be related to the resultant error in the measurement of the film thickness and analysis shows that the percentage error, for a seal resistance of 200 ohms, increases rapidly for values of film thickness below 10 micro inches although the absolute errors are small and can be ignored.

F. 3. Errors due to deflection of the transducer under pressure

The design of the transducer is described in section 4. 2. 7., and calculations during the design indicated that at pressures up to 1, 000 lb/in^2, deflection of the copper probe in its holder and of holder in the pressure vessel would be zero at 0 lbf/in^2 to 10 micro inches at 1, 000 lbf/in^2.

F. 4. Other sources of error

Limiting circuit ot the analogue network

To prevent overloading of the analogue network amplifiers, a limiting circuit was used on the output stage which caused the film thickness to be underestimated for values over 150 micro inches. The underestimation was found to be zero at 150 micro inches, increasing to 20 micro inches for a film thickness of 200 micro inches.

Measurement of oscilloscope trace deflection

At the lower film thickness values, errors could arise due to the physical measurement of the small deflections of the oscilloscope trace. These are small in absolute terms, 1 - 2 micro inches, and only occur for values of film thickness below 10 micro inches.

APPENDIX G

Pressurised Rayleigh Step Analogy

The theoretical study of the seal lubrication problem has shown that in general there are five stresses or pressures operating to form the film profile, which are:

(i) hydrostatic contact stress Q_s (sealed pressure transmitted through the seal)

(ii) interference stress, Q_i

(iii) hydrostatic film pressure, P_{st}

(iv) hydrodynamic film pressure, P_d

(v) pressure necessary to deflect the seal, S

These five terms are utilised in the elasticity equation of the theoretical study to calculate the deflection of the seal.

Thus equation (K7) of Appendix K can be written

$$\frac{d^2h}{dx^2} - Ah = B(Q - P) \qquad \text{(G1)}$$

where h = film thickness

x = distance along seal

Q = stress in seal

P = film pressure

A & B = constants

$$\text{and } S = B\left\{(Q_s + Q_i) - (P_{st} + P_d)\right\} \qquad \text{(G2)}$$

A study of the orders of magnitude of the above terms reaches the following conclusions:

(i) S is small of the order of 1-5 lbf/in^2

(ii) Q_i may be up to 100 lbf/in^2

(iii) $Q_s - (P_{st} + P_d)$ is of the same order as Q_i

Because S is small at all film displacements and Q_s and P_d are both related to the system pressure, $Q_s - (P_{st} + P_d)$ is always of the same order as Q_i and therefore Q_i assumes greater significance than if it is compared to the system pressure alone. For the true seal shape it is difficult, without considerable computing effort, to determine how P_{st} and P_d vary with the mean film thickness and therefore definite

conclusions about the effect of Q_i on the film thickness cannot be drawn. However, the theoretical study has shown that the outstroke film profile has the same basic form and properties as a Rayleigh step bearing which is considerably easier to analyse.

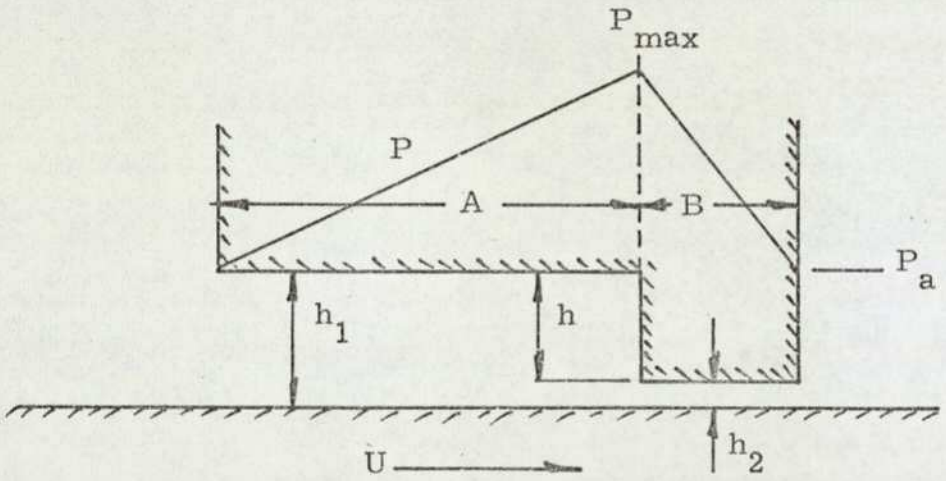
The following is the analysis of such a bearing having relative motion of the two surfaces and a pressure differential across it.

Assumptions

(i) The hydrostatic contact stress in a seal is assumed here to be the system pressure and acts across the length of the bearing.

(ii) The interference stress is an additional load on the bearing also constant across the bearing.

Hydrodynamic component of pressure P_d



For continuity

$$q_1 = q_2 \tag{G3}$$

Therefore from Reynold's equation:

$$-\frac{h_1^3}{12\zeta}\left\{\frac{dp}{dx}\right\}_1 + \frac{Uh_1}{2} = -\frac{h_2^3}{12\zeta}\left\{\frac{dp}{dx}\right\}_2 + \frac{Uh_2}{2} \tag{G4}$$

As the pressure distribution through the bearing is linear the pressure gradients can be written:

$$\left\{\frac{dp}{dx}\right\}_1 = \frac{Pmax}{A} \quad \text{and} \quad \left\{\frac{dp}{dx}\right\}_2 = -\frac{Pmax}{B} \tag{G5}$$

Substituting in equation (G4)

$$\frac{-h_1^3}{12\zeta} \frac{Pmax}{A} + \frac{Uh_1}{2} = \frac{h_2^3}{12\zeta} \frac{Pmax}{B} + \frac{Uh_2}{2} \qquad (G6)$$

from which on rearranging:

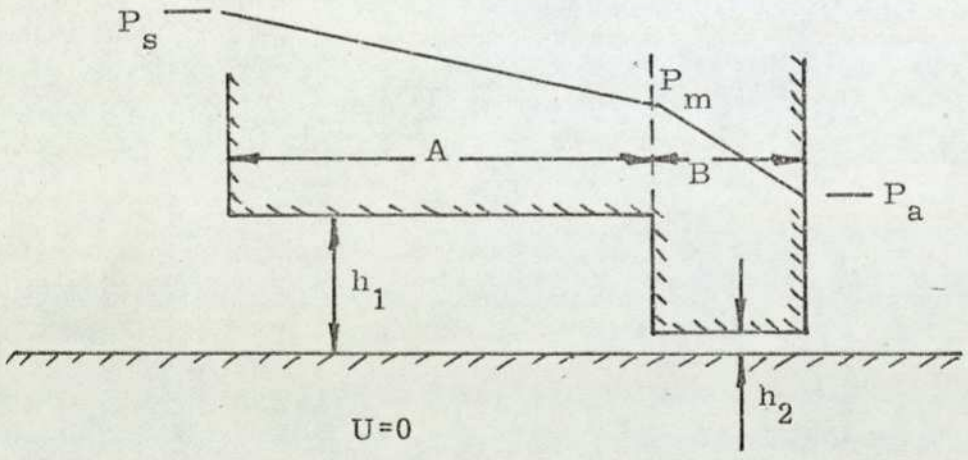
$$Pmax = \frac{6\zeta U (h_1 - h_2) AB}{(Ah_2^3 + Bh_1^3)} \qquad (G7)$$

Therefore the load capacity, W_d, provided by the pressure component P_d

$$= \frac{Pmax\ A}{2} + \frac{Pmax\ B}{2}$$

$$\therefore W_d = \frac{3\zeta U (h_1 - h_2) AB (A+B)}{(Ah_2^3 + Bh_1^3)} \qquad (G8)$$

Hydrostatic component of pressure, P_{st}



for continuity

$$q_1 = q_2 \qquad (G9)$$

∴ From Reynold's equation for U = 0,

$$\frac{-h_1^3}{12\zeta} \left\{\frac{dp}{dx}\right\}_1 = \frac{-h_2^3}{12\zeta} \left\{\frac{dp}{dx}\right\}_2 \qquad (G10)$$

from the above figure:

$$\left\{\frac{dp}{dx}\right\}_1 = \frac{(P_s - P_m)}{A} \quad \text{and} \quad \left\{\frac{dp}{dx}\right\}_2 = \frac{P_m}{B} \tag{G11}$$

Substitution in equation (G11) gives:

$$h_1^3 \cdot \frac{(P_s - P_m)}{A} = h_2^3 \cdot \frac{P_m}{B} \tag{G12}$$

which on rearranging gives:

$$P_m = \frac{P_s h_1^3 B}{(Ah_2^3 + Bh_1^3)} \tag{G13}$$

Therefore the load capacity W_{st}, provided by the pressure component P_{st}

$$= P_m A + \frac{(P_s - P_m)A}{2} + \frac{P_m B}{2} \tag{G14}$$

Which gives on rearrangement:

$$W_{st} = \frac{P_s}{2} \cdot A + \frac{Bh_1^3 (A + B)}{Ah_2^3 + Bh_1^3} \tag{G15}$$

The total load, W_T, carried by the bearing is thus:

$$W_T = W_d + W_{st} \tag{G16}$$

which must be equated to the contact stress load:

$$W_C = (A + B)(Q_i + Q_s) + S$$

In order that the bearing is stable:

$$W_T = W_C \tag{G17}$$

Figures G1 and G2 show the calculated performance data for two types of step bearing. In the first, figure G1, the step height is kept constant and it can be seen that as the film thickness decreases the hydrodynamic load increases rapidly for films below 100 microinches. The total load is shown as the sum of the hydrostatic and hydrodynamic loads and a solution to the problem is found where this line intersects the load due to the sealed pressure. For this particular bearing geometry, the stiffness is high and small changes in load due to increased interference would not decrease the film thickness significantly.

However, the seal profiles recorded rarely have a constant step height and figure G2 shows the calculated performance of a bearing in which the step height changes but h_2 remains constant. The behaviour in this case is completely different in that the assumed load line intersects the total load line in two places. At B the bearing has a negative stiffness. However, at A the stiffness is positive but very low and small changes in the net load, by increasing or decreasing the interference, will cause large changes in the film thickness.

The two above cases represent the two worst cases as far as an analogy to seal behaviour is concerned as the results have shown that in general h_1 and h_2 change independently and not in the fixed modes used above. The total load supported by the seal therefore lies somewhere between these cases and indicates that the stiffness of the seal surface will be quite low and small changes in load (interference stress) will therefore cause significant changes in the film thickness.

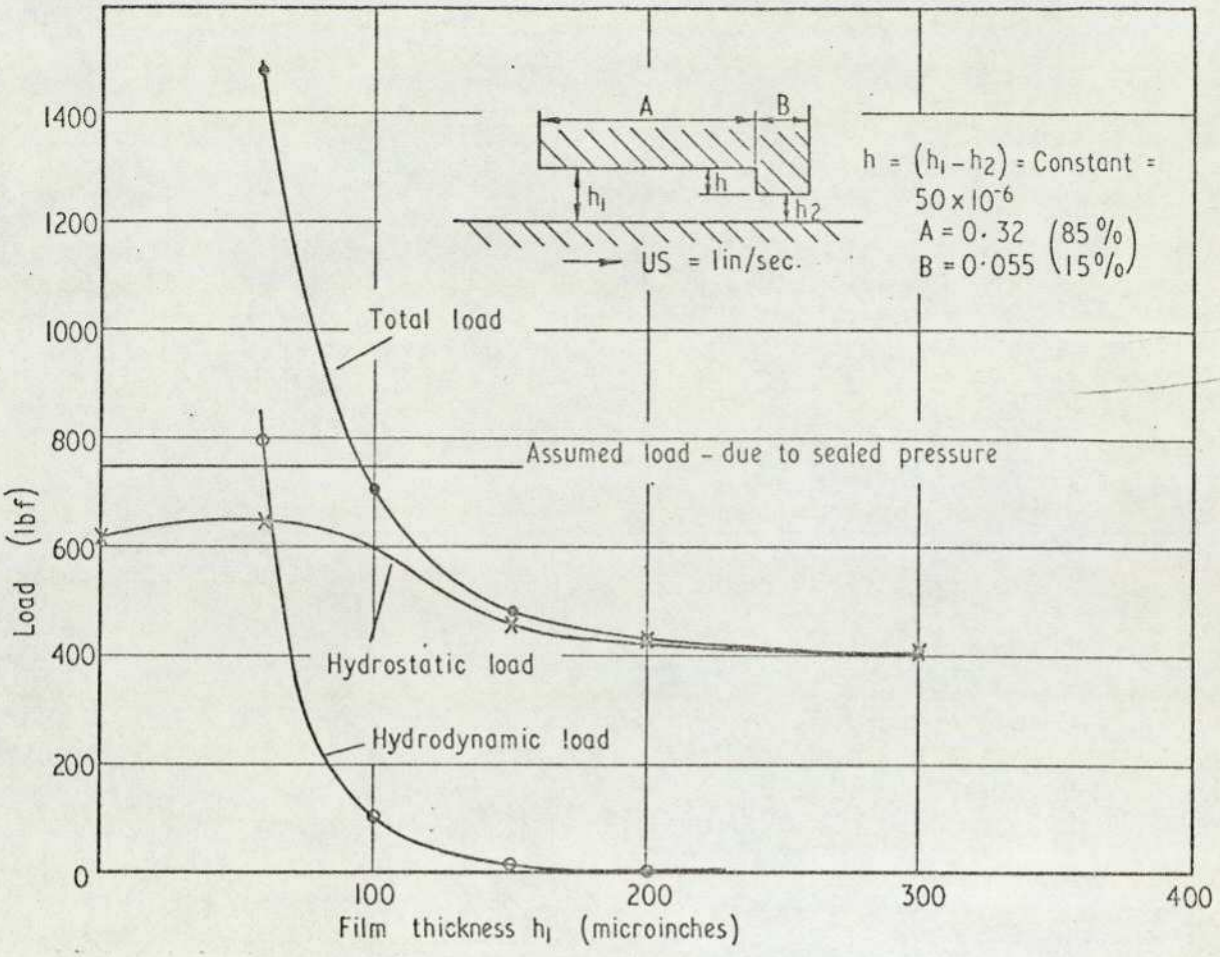


Fig. G1 Behaviour of Rayleigh step bearing with fixed step height

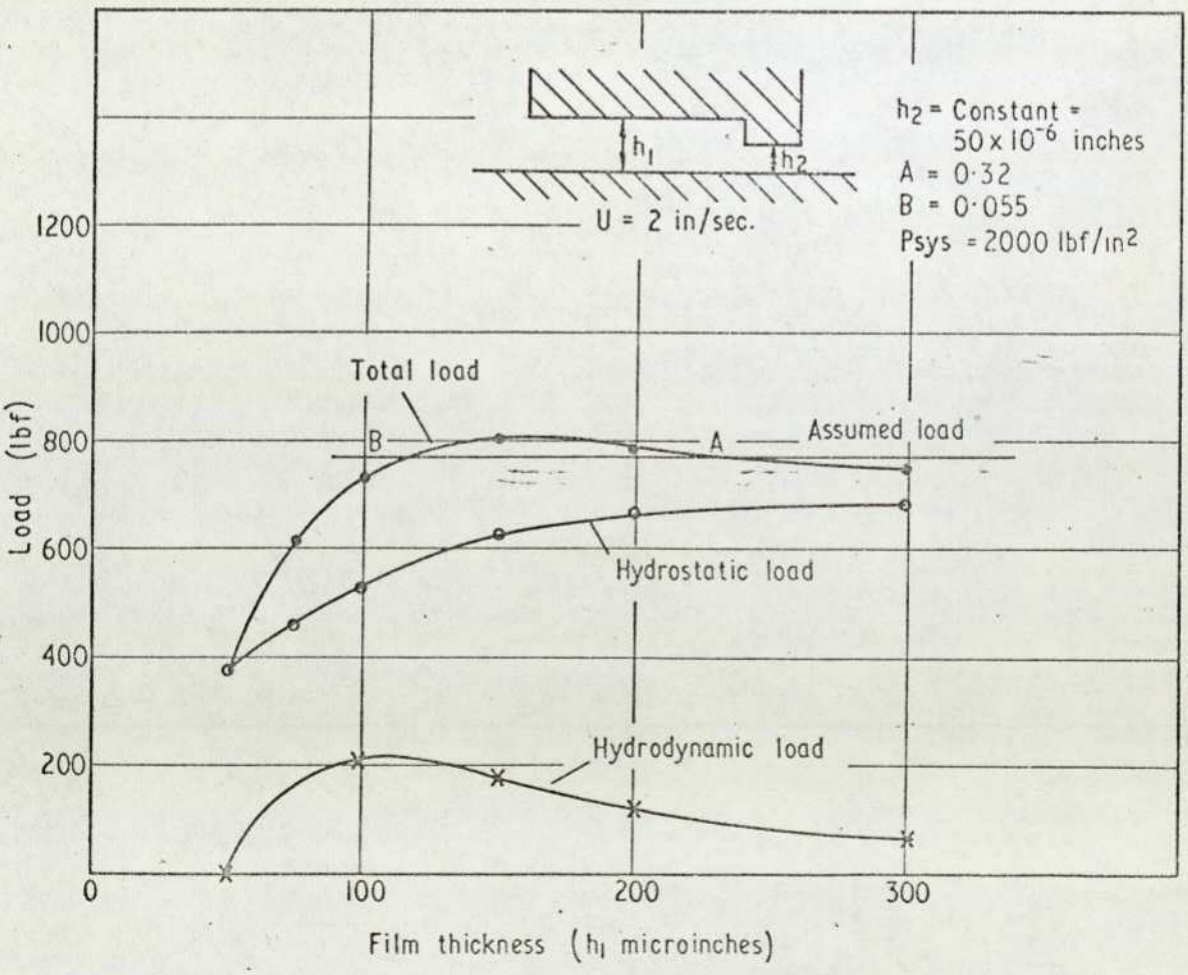
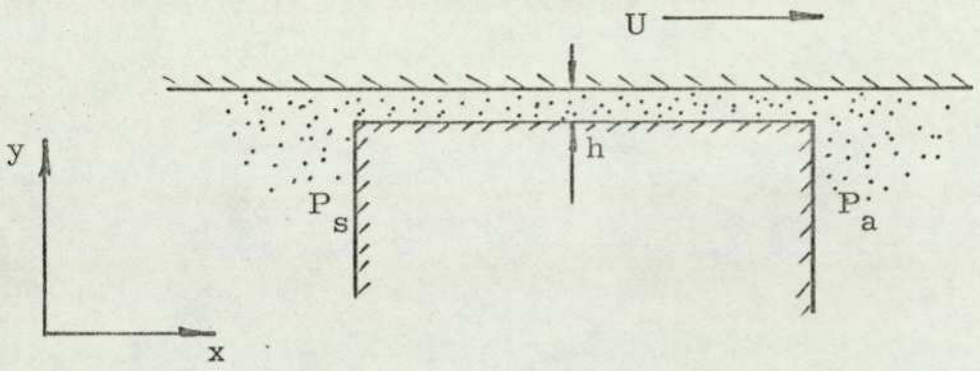


Fig. G2 Behaviour of Rayleigh step bearing with variable step height

APPENDIX H

Calculation of the Specific Friction for an Annular Clearance with Relative Motion of the Surfaces and a Pressure Differential.



The Newtonian definition of viscosity is:

$$F = \zeta \frac{du}{dy} \qquad \text{(H1)}$$

where F = force exerted by the shear of the fluid

ζ = fluid viscosity

$\frac{du}{dy}$ = velocity gradient through the film

For the point of the film where $\frac{dp}{dx} = 0$, $h = h^*$ and the velocity gradient is linear

$$\therefore \quad F = \frac{\zeta U}{h^*} \qquad \text{(H2)}$$

However, in general the velocity gradient is not linear and includes a component due to the Poiseuille flow through the clearance.

It can be shown that

$$\frac{dp}{dx} = \frac{\partial F}{\partial y} \qquad \text{(H3)}$$

and substitution in (H1) gives

$$\frac{dp}{dx} = \zeta \cdot \frac{\partial^2 u}{\partial y^2} \qquad \text{(H4)}$$

which on integration and rearrangement becomes

$$u = \frac{1}{2\zeta} \cdot \frac{dp}{dx} \cdot y^2 + y \cdot f1(x) + f2(x) \qquad \text{(H5)}$$

From the boundary conditions

$$u = U \text{ when } y = 0 \text{ and } u = 0 \text{ when } y = h$$

$$\therefore \quad u = \frac{1}{2\zeta} \cdot \frac{dp}{dx}(y - h)y + U\left\{\frac{h - y}{h}\right\} \qquad \text{(H6)}$$

Differentiation of (H5) and substitution into (H1) gives

$$F = \zeta\left\{\frac{1}{2\zeta} \cdot \frac{dp}{dx}(2y - h) + \frac{U}{h}\right\} \qquad \text{(H7)}$$

At the surface of the seal $y = 0$.

$$\therefore \quad F = -\frac{1}{2} \cdot \frac{dp}{dx} \cdot h + \frac{\zeta U}{h}$$

For conditions typical of seal operation:

$$\frac{dp}{dx} = -\frac{1000}{.375} \frac{\text{lbf}}{\text{in}^2}$$

$$h = 100 \times 10^{-6} \text{ inches}$$

$$\zeta = 10^{-5} \text{ reyns.}$$

$$U = 10 \text{ ins/sec.}$$

$$\therefore \quad F = +\frac{100 \times 10^{-6}}{2} \cdot \frac{1000}{.375} + \frac{10^{-5} \times 10}{100 \times 10^{-6}}$$

$$= 0.133 + 1.00$$

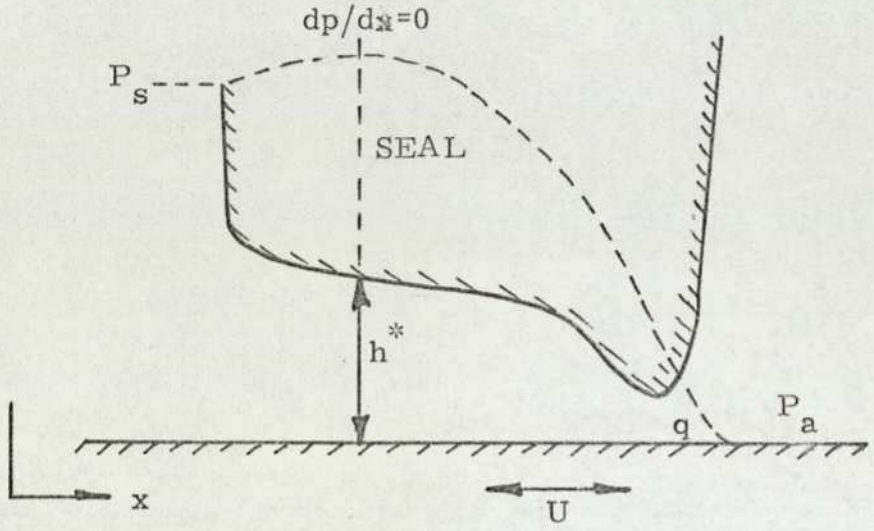
$$= 1.133 \text{ lbf/in}^2$$

The friction due to Poiseuille flow through the annulus is therefore only 11% of the total friction at the highest pressure differential used. The friction due to Couette flow predominates and over the pressure range used can be taken as approximately correct.

APPENDIX I

Derivation of Inverse Form of Reynold's Lubrication Equation

A seal having a lubricant film between the seal surface and the moving surface is shown below. The shaft motion can be out of, or into the high pressure region, but the pressure differential direction is always constant.



The leakage through such a clearance can be written:

$$q = \frac{-h^3}{12\eta} \cdot \frac{dp}{dx} + \frac{Uh}{2} \qquad \text{for an outstroke} \quad (I1)$$

At the position x^*, the pressure gradient is zero and the leakage is:

$$q^* = \frac{Uh^*}{2} \qquad (I2)$$

Continuity of flow must be maintained through the contact and therefore

$$q = q^* \qquad (I3)$$

Substitution of (I2) into (I1) gives:

$$\tfrac{1}{2}Uh^* = \frac{-h^3}{12\eta} \cdot \frac{dp}{dx} + \frac{Uh}{2} \qquad (I4)$$

$$\therefore \quad \frac{1}{6\eta U} \cdot \frac{dp}{dx} \cdot h^3 - h + h^* = 0 \qquad (I5)$$

Non-dimensionalising and rearranging using the following definitions:

$$H = {}^{h}/_{h^*} \quad , \quad G = \frac{h^{*2}}{6\eta U} \cdot \frac{dp}{dx}$$

gives:

$$G = \frac{(H - 1)}{H^3} \tag{16}$$

Rearrangement again gives the cubic equation:

$$GH^3 - H + 1 = 0 \tag{17}$$

the solution of which, for a given pressure distribution through the contact, constitutes the 'inverse' solution to Reynold's equation.

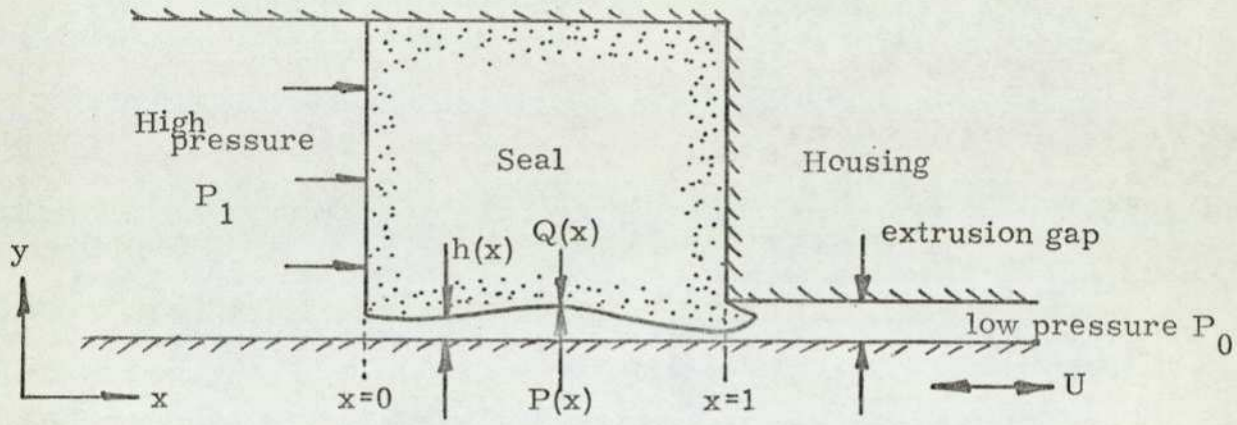
In general the above equation will have three roots which may be positive, negative or complex. The complex roots will have no physical meaning and neither in most cases will the negative root, therefore the positive root is used for most applications. However, where a pressure differential is applied to the contact a possibility of a negative root exists and this is discussed further in the relevant section.

Further discussion of the 'inverse' treatment of Reynold's equation can be found in Blok (2).

APPENDIX J

Derivation of the Lubrication Equation

The notation is that shown below for a pseudo two-dimensional fluid film



With the usual assumptions (44) for an incompressible, thin viscous film, the general Navier Stokes equations of the motion of the fluid can be reduced to:-

$$\frac{\partial p}{\partial x} = \frac{\partial}{\partial y}\left(\zeta \cdot \frac{\partial u}{\partial y}\right) \qquad \text{(J1)}$$

and, if the viscosity is constant across the thickness of the film, equation (J1) can be integrated twice with respect to y to give:

$$u = \frac{1}{2\zeta} \cdot \frac{\partial p}{\partial x}(y - h)y + \frac{h - y}{h} \cdot U \qquad \text{(J2)}$$

where the following boundary conditions have been applied:

$u = U$ at $y = 0$ and $u = 0$ at $y = h$.

If the flow across any section through the film is q per unit width then:

$$q = \int_{y=0}^{y=h} U\,dy \qquad \text{(J3)}$$

an combining equation (J2) and (J3):

$$q = \frac{-h^3}{12\zeta} \cdot \frac{\partial p}{\partial x} + \frac{Uh}{2} \qquad \text{(J4)}$$

Rearrangement of equation 4 gives:

$$\frac{\partial p}{\partial x} = \frac{6 \zeta U}{h^2} - \frac{12 \zeta q}{h^3} \qquad (J5)$$

and if ζ does not vary with x:

$$P - P_1 = 6 \zeta U \int_o^x \frac{1}{h^2}\, dx - 12 \zeta q \int_o^x \frac{1}{h^3}\, dx \qquad (J6)$$

Since in general q is not known the coefficient $12 \zeta q$ can be redefined in terms of known quantities by integrating equation (J6) from $x = 0$ to $x = \ell$, then:

$$\therefore \quad P_o - P_1 = 6 \zeta U \int_o^{\ell} \frac{1}{h^2}\, dx - 12 \zeta q \int_o^{\ell} \frac{1}{h^3}\, dx$$

and hence

$$12 \zeta q = \frac{6 \zeta U \int_o^{\ell} \frac{1}{h^2}\, dx - (P_o - P_1)}{\int_o^{\ell} \frac{1}{h^3}\, dx} \qquad (J7)$$

Defining the coefficients, $6 \zeta U$ and $12 \zeta q$ as a_1 and a_2 respectively and the functions $\int_o^x \frac{1}{h^2}\, dx$ and $\int_o^x \frac{1}{h^3}\, dx$ as $I_1(x)$ and $I_2(x)$ respectively equations (J6) and (J7) may be written:

$$P - P_1 = a_1 I_1(x) - a_2 I_2(x)$$

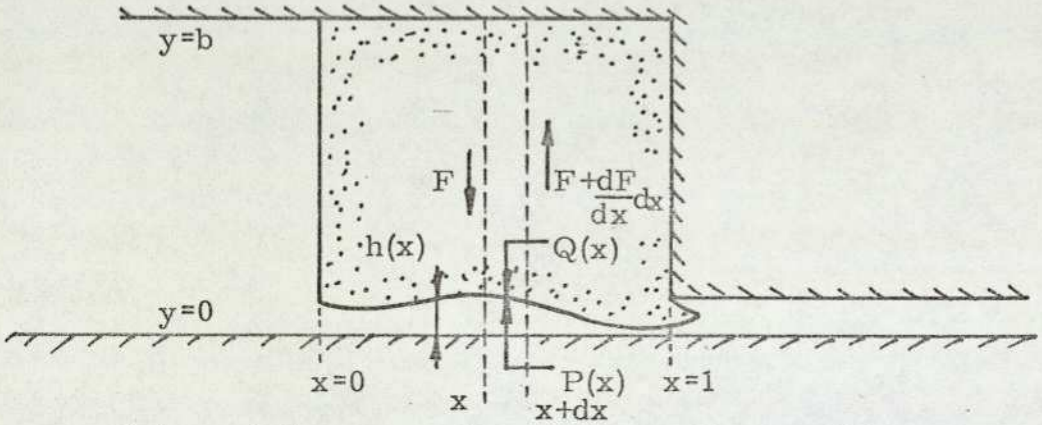
and $$a_2 = \frac{a_1 I_1(\ell) - (P_o - P_1)}{I_2(\ell)}$$

This is the form of the lubrication equation used in the program.

APPENDIX K

Derivation of the Elasticity Equation

The figure below shows the stresses acting in the y-direction on an element (x, dx) of the seal. These comprise (i) shear stress, F(x); (ii) internal stresses, Q(x), which comprise the stress due to initial interference in the housing and the effect of the pressure $(P_1 - P_o)$ acting on the end of the seal; and (iii) the fluid film pressure acting on the seal surface.



A force balance equation can be written as follows:

$$P\,dx + (F + \frac{dF}{dx}\,dx)\,b - F\,dx.\,b - Q\,dx = E\,h.\,dx/b \qquad (K1)$$

where the term on the right is the Hooke's Law term.

This reduces to:

$$\frac{dF}{dx} - \frac{E}{b^2} \cdot h = (Q - P)/b \qquad (K2)$$

The shear stress F is related to shear strain $\frac{dh}{dx}$ by:

$$F = G' \frac{dh}{dx} \qquad (K3)$$

where G' is the shear modulus.

Continuing K2 and K3 therefore gives:

$$\frac{d^2h}{dx^2} - \frac{E}{G'b^2}\,h = (Q - P)/bG' \qquad (K4)$$

where h, Q, and P are functions of x; h being the unknown.

The moduli E and G' are related by:

$$G' = \frac{E}{2(1+\nu)} \qquad \text{(K5)}$$

Thus equation K4 becomes:

$$\frac{d^2h}{dx^2} - 2\frac{(1+\nu)}{b^2} \cdot h = \frac{2(1+\nu)}{Eb}(Q - P) \qquad \text{K6}$$

or

$$\frac{d^2h}{dx^2} - A \cdot h = B.S(x) \qquad \text{(K7)}$$

where $A = 2(1+\nu)/b^2$, $B = Ab/E$. and $S(x) = Q(x) - P(x)$.

APPENDIX L

Variable Mesh Finite Difference Formulation of the Elasticity Equation

The mesh spacing, d, to the right of node n is defined as:

$$d_n = x_{n+1} - x_n \tag{L1}$$

The second derivation of h can then be written:

$$\left(\frac{d^2h}{dx^2}\right)_n = \frac{\dfrac{h_{n+1} - h_n}{d_n} - \dfrac{h_n - h_{n-1}}{d_{n-1}}}{(d_{n-1} + d_n)/2} \tag{L2}$$

$$= \frac{d_{n-1}}{D_n}(h_{n+1} - h_n) - \frac{d_n}{D_n}(h_n - h_{n-1}) \tag{L3}$$

where $D_n = d_n\, d_{n-1}\, (d_{n-1} + d_n)/2$ (L4)

The dimensionless elasticity equation from Chapter 5 is:

$$\frac{d^2H}{dX^2} - RH = S \tag{L5}$$

The substitution of L3 in L5 leads to:

$$h_n = \frac{h_{n+1} + \dfrac{d_n}{d_{n+1}} \cdot h_{n-1} - \dfrac{S_n D_n}{d_{n-1}}}{1 + \dfrac{d_n}{d_{n-1}} + R\dfrac{D_n}{d_{n-1}}} \tag{L6}$$

which can be written as:

$$h_n = a_{1n}\, h_{n+1} + a_{2n}\, h_{n-1} - a_{3n} \tag{L7}$$

where $a_{1n} = 1/\left(1 + \dfrac{d_n}{d_{n-1}} + \dfrac{RD_n}{d_{n-1}}\right)$

$$a_{2n} = a_{1n}\, d_n/d_{n-1}$$

$$a_{3n} = a_{1n}\, S_n\, D_n/d_{n-1}$$

The set of equations like L7 can be solved by the Gauss-Seidel method, in which case the k^{th} approximation to h_n is:

$$h_n^{(k)} = a_{1n} h_{n+1}^{(k-1)} + a_{2n} h_{n-1}^{(k)} - a_{3n} \qquad \text{(L8)}$$

APPENDIX M

Input Data used for Program Development

Seal length = 0.375 in. Seal thickness = 0.25 in.

Young's modulus of rubber, E = 1700 lbf/in^2 (i.e. hardness 85 IRHD approx.)

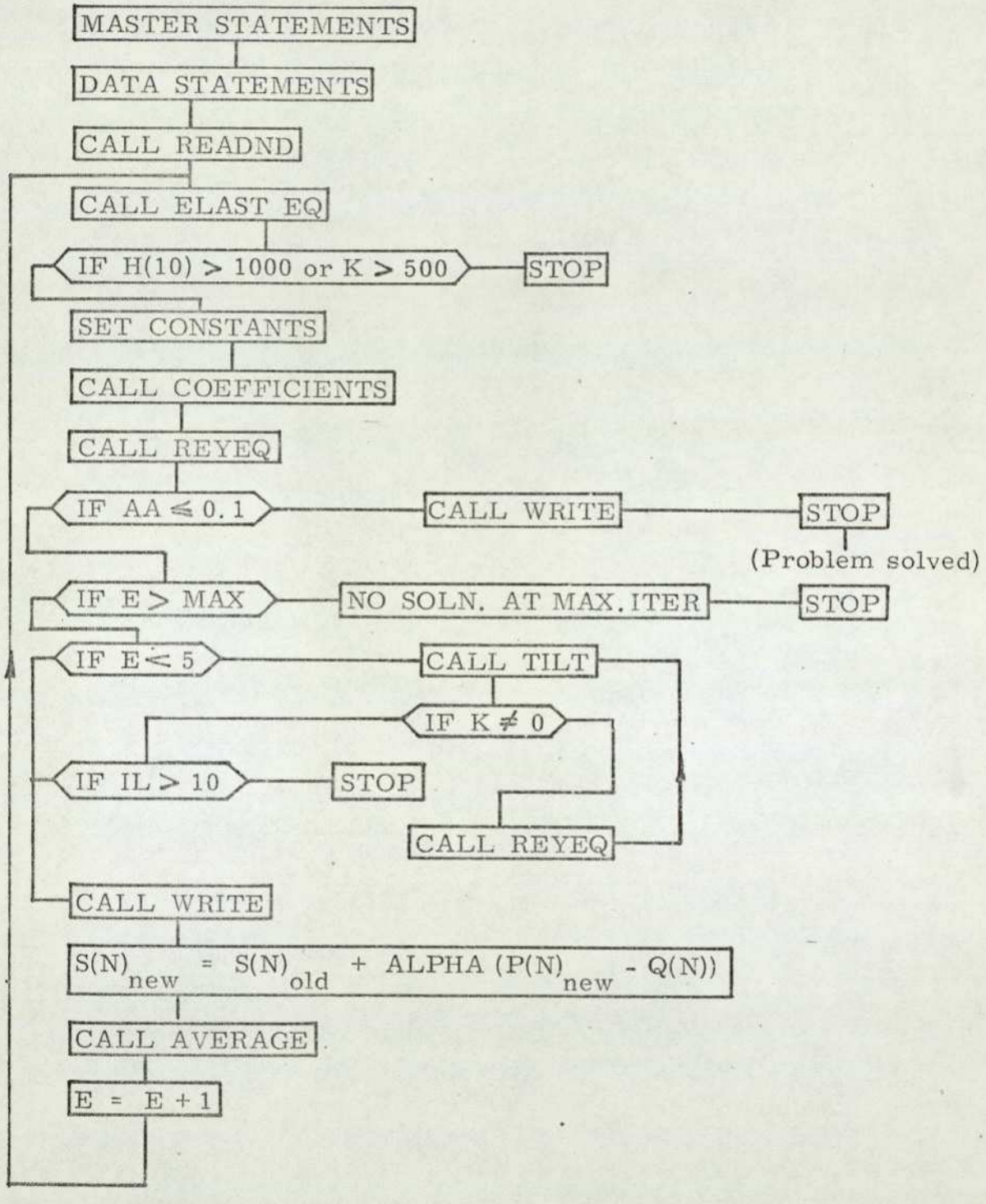
Poisson's ratio of rubber, ν = 0.5. Sliding velocity = 3 in/sec.

Fluid viscosity = 0.00001 lbf. sec./in^2.

Node no. n	Film pres. P_n	Contact stress Q_n	Film thickness H_n
1	501.50	500.00	192.0
2	501.40	500.00	185.0
3	501.30	500.00	178.0
4	501.20	500.00	172.0
5	501.10	500.00	169.0
6	501.00	500.00	165.0
7	501.00	500.00	160.0
8	501.00	500.00	159.0
9	491.00	490.00	154.0
10	481.00	480.00	152.0
11	471.00	470.00	151.0
12	464.00	463.00	151.0
13	458.00	457.00	153.0
14	451.00	450.00	160.0
15	441.50	440.00	170.0
16	422.00	420.00	186.0
17	411.00	410.00	180.0
18	380.60	380.00	160.0
19	345.20	345.00	110.0
20	0.00	0.00	86.0
	(lbf/in^2)	(lbf/in^2)	(10^{-6}in)

APPENDIX N

Flow Chart and Notation for "EHD Mk II" Program



NOMENCLATURE FOR FLOW CHART

P(N)	pressure at node N
Q(N)	seal contact stress at node N
S(N)	Q(N) - P(N)
K	number of iterations of elasticity equation
E	number of iterations of complete loop
AA	convergence criteria for program, set in subroutine 'REYEQ'
ALPHA	under relaxation factor

Subroutines

READND	This routine reads in constants such as number of nodes, seal sizes and physical properties and oil viscosity It also reads Z values of P(N), H(N) and Q(N) and non-dimensionalises them
ELASTEQ	Calculates the seal deflections from the current values of P(N) and Q(N)
COEFFICIENTS	Calculates new value of P(N) also leakage, friction and dynamic and static pressures
TILT	Used to tilt the film profile at the low pressure end of the seal and acts as a coarse control for the pressure distribution
WRITE	Writes out complete set of data for current iteration when called
AVERAGE	Monitors the value S(10) for successive iterations. When a maximum and a minimum have been reached, these values of S(10) are averaged before the recalculation of H(N) in the elasticity equation.

PUBLISHED PAPERS

External Publications

Field, G. J.	"Fluid Sealing". Food Manufacture, 47 7, pp. 22-24 + 30. (July, 1972).
Austin, R. M., Field, G. J.	"Use and selection of elastomeric seals and soft gland packings". Process Engineering,
Field, G. J.	"The cause and cure of interseal pressure" Fluid Power International, 36, 428, pp. 29-32 + 55. (Nov. 1971).
Field, G. J.	"Hydraulics R and D is down to earth". Engineering, 210, 5447, pp. 352-354. (Oct. 1970).
*Field, G. J., Nau, B. S.	"An experimental study of reciprocating rubber seals" Paper C5/72. Elastohydrodynamic Lubrication Symposium organised by the I. Mech. E., and held at Leeds University, April 1972.
*Field, G. J., Nau, B. S.	"Film thickness and friction measurements during reciprocation of a rectangular section rubber seal ring". Paper C5. 6th Int. Conf. on Fluid Sealing organised by BHRA Fluid Engineering, Munich G. F. R., Feb/March. 1973.
Field, G. J., Nau, B. S.	"Interseal pressure between reciprocating rectangular rubber seals". Paper D2. 5th Int. Conf. on Fluid Sealing organised by BHRA Fluid Engineering, Coventry, England 1971.
*Field, G. J., Nau, B. S.	"Interseal pressure between tandem reciprocating rubber seals with back-up rings". ASLE Trans. Vol. 16, 1, pp. 10-15. Presented at 27th ASLE Annual Meeting, Houston, May 1972.

* These papers presented in the thesis.

Internal Publications

Field, G. J. — "An introduction to the fractional factorial design of experiments". BHRA Fluid Engineering publication TN1044 (March, 1970).

Field, G. J., Nau, B. S. — "Interseal pressure between reciprocating rectangular rubber seals". BHRA Fluid Engineering Publication RR978, Jan. 1969.

Field, G. J., Nau, B. S. — "Interseal pressure between reciprocating rectangular rubber seals with back-up rings". BHRA Fluid Engineering Publication RR1075, Sept. 1970.

Field, G. J., Nau, B. S. — "Interseal pressure of piston seals in thin walled jacks". BHRA Fluid Engineering Publication RR1088, Jan. 1971.

† Field, G. J., Nau, B. S. — "The lubrication of rectangular rubber seals under conditions of reciprocating motion. Part 1 - A theoretical stydy". BHRA Fluid Engineering Research Report RR1189, June 1973.

† Field, G. J., Nau, B. S. — "The lubrication of rectangular rubber seals under conditions of reciprocating motion. Part 2 - An interferometric study". BHRA Fluid Engineering Research Report RR1199, June 1973.

† Field, G. J., Nau, B. S. — "The lubrication of rectangular rubber seals under conditions of reciprocating motion. Part 3 - An instrumented seal study". BHRA Fluid Engineering Research Report RR1200, June 1973.

† available to members of BHRA Fluid Engineering only.